

---

Doctoral

Science

---

2014-1

## Investigation of the Cellular and Molecular Mechanisms of Radiation-induced Bystander Effects

Hayley Furlong

Technological University Dublin, hayley.furlong@tudublin.ie

Follow this and additional works at: <https://arrow.tudublin.ie/sciendoc>



Part of the [Biochemistry, Biophysics, and Structural Biology Commons](#)

---

### Recommended Citation

Furlong, H. (2014). *Investigation of the Cellular and Molecular Mechanisms of Radiation-induced Bystander Effects*. Doctoral Thesis. Technological University Dublin. doi:10.21427/D7XW29

This Theses, Ph.D is brought to you for free and open access by the Science at ARROW@TU Dublin. It has been accepted for inclusion in Doctoral by an authorized administrator of ARROW@TU Dublin. For more information, please contact [arrow.admin@tudublin.ie](mailto:arrow.admin@tudublin.ie), [aisling.coyne@tudublin.ie](mailto:aisling.coyne@tudublin.ie), [vera.kilshaw@tudublin.ie](mailto:vera.kilshaw@tudublin.ie).



# **Investigation of the Cellular and Molecular Mechanisms of Radiation-induced Bystander Effects**

Submitted by

Hayley Furlong, BSc.

**For the award of, PhD**

Radiation and Environmental Science Centre  
(RESC)/ School of Biological Sciences  
Focas Research Institute, Dublin Institute of  
Technology

**Supervisors:**

**Dr. Orla Howe and Prof. Carmel Mothersill**

January, 2014

## **Abstract**

The overall aim of this study was to investigate the cellular and molecular mechanisms involved in radiation-induced bystander effects in HaCaT cells, predominantly at low-doses of irradiation. They do not follow the original dose-response theory and exhibit a unique cascade of signalling events, which are under intense investigation for radiation risk purposes. An *in vitro* system was first used to observe the bystander effect, comparing two cell viability assays while measuring apoptotic cell death in these known reporter HaCaT cells and established the most sensitive assay for bystander responses

Downstream bystander signalling events were then investigated through gene expression studies of apoptotic genes over a complex time-course with different low doses to reveal very specific changes in bystander responses. The expression pattern profile revealed novel unique bystander-induced apoptotic signalling pathways in different low doses of irradiation. Proteomic methods using 2D gel electrophoresis and mass spectroscopy further revealed novel proteins which were significantly over or under-expressed in the bystander reporter cells but using an *ex-vivo* fish model. These results revealed an induction of protection of the cells in response to oxidative stress and modulation of cell death processes.

The data generated in this thesis has led to the proposal of two distinct and comparative signalling pathways of a cellular radiation induced bystander response for 0.05 Gy and 0.5 Gy ionising radiation. These novel pathways have expanded our knowledge in the cellular and molecular mechanisms which occur when a cell receives a bystander signal and may have future clinical considerations and implications for patients undergoing radiotherapy treatment plans.















## Abbreviations

$\Delta\Psi_{\text{mito}}$	Mitochondrial Membrane Potential
AB	Alamar Blue
ANOVA	Analysis of Variance
APAF-1	Apoptotic Protease Activating Factor
CARD	Caspase Activation and Recruitment Domain
cDNA	Complementary DNA
CO <sub>2</sub>	Carbon Dioxide
DMEM	Dulbecco's Modified Essential Medium
DMSO	Dimethyl Sulfoxide
DNA	Deoxyribonucleic Acid
DSB	Double Strand Break
ER	Endoplasmic Reticulum
FBS	Foetal Bovine Serum
GTPases	Guanosine Triphosphate (GTP) Hydrolase
HaCaT	Normal Human Keratinocyte Cell Line
HSP	Heat Shock Protein
IAP	Inhibitor of Apoptotic Protein
ICCM	Irradiated Cell Conditioned Medium
IR	Ionising Radiation
Kb	Kilobase
MN	Micronucleus
MOMP	Mitochondrial Outer Membrane Permeabilisation
MPT	Mitochondrial Permeability Transition
mRNA	Messenger RNA
MTT	3-(4,5-Dimethylthiazol-2-yl)-2,5-diphenyltetrazoliumbromide
NADH	Nicotinamide Adenine Dinucleotide Dehydrogenase
NO	Nitric Oxide
NTE	Non Targeted Effects
TP53	Tumour Suppressor Gene
PBS	Phosphate Buffered Saline
PCR	Polymerase Chain Reaction
PIDD	P53-Inducible Death Domain
PMA	Phorbol Myristate Acid

PTPC	Permeability Transition Pore Complex
RIBE	Radiation-Induced Bystander Effects
RIGI	Radiation-Induced Genomic Instability
RNA	Ribonucleic Acid
RNS	Reactive Nitrogen Species
ROS	Reactive Oxygen Species
RT-PCR	Real Time Polymerase Chain Reaction
SCE	Sister Chromatid Exchange
SD	Standard Deviation
SDS	Sodium Dodecylsulphate
SOD	Superoxide Dismutase
SSB	Single Strand Break
UPR	Unfolded Protein Response
UV	Ultraviolet
HPV-G	Human Papillomavirus
Annexin II	ANXA2



# Table of Contents

Abstract.....	II
Declaration.....	III
Acknowledgments.....	IV
Research Outputs.....	VII
Abbreviations.....	IX
Chapter 1: Introduction.....	10
1.1 History of Radiation.....	10
1.2 Introduction to Clinical Radiation Types and Doses.....	14
1.3 Biological Interaction of Radiation with the Cell.....	19
1.4 Non-targeted Effects of Radiation.....	24
1.5 The Bystander Response-Overview.....	27
1.5.1 History of Bystander Response.....	29
1.5.2 Bystander Response Signalling Mechanisms in Cells.....	33
1.5.3 Intercellular Signalling of the Bystander Effect.....	34
1.5.4 Intracellular Signalling of the Bystander Effect.....	37
1.5.5 Potential Candidates for the Bystander Factor(s).....	44
1.5.6. Radiobiological Studies of Bystander Responses.....	45
1.5.6.1 Evidence <i>In vivo</i> .....	46
1.5.6.2 Evidence <i>In vitro</i> .....	48
1.5.6.2.1 Immortal Human Keratinocyte Cell Line- Bystander Reporter Model.....	50

1.6 Cell Death Mechanisms – Overview .....	51
1.6.1 Non-apoptotic Modes of Cell Death .....	52
1.6.1.1 Mitotic Catastrophe .....	52
1.6.1.2 Necrosis .....	53
1.6.1.3 Autophagic Cell Death .....	54
1.7 Apoptosis .....	55
1.7.1 Extrinsic Apoptosis .....	58
1.7.2 Intrinsic Apoptosis .....	60
1.7.3 Mitochondria and Bcl-2 Signalling .....	63
1.8 The Caspases – Overview .....	67
1.8.1 Initiator Caspase Signalling .....	70
1.8.2 Effector Caspase Signalling .....	73
1.8.3 Tumour Suppressor p53 Signalling .....	75
1.9 Thesis Overview .....	78
Chapter 2: Evaluation of Two Viability Assays to Measure Radiation-Induced Bystander Effects in Reporter Cells (MTT and Alamar Blue) .....	80
2.1 Introduction .....	81
2.2 Materials and Methods .....	86
2.3 Results .....	93
2.4 Discussion .....	115

Chapter 3: Apoptosis is Signalled Early by Low Doses of Ionising Radiation in a Radiation-Induced Bystander Effect.....	118
3.1 Introduction.....	121
3.2 Materials and Methods.....	125
3.3 Results.....	131
3.4 Discussion.....	137
Chapter 4: Radiation-Induced Bystander Mediated Apoptosis via the Intrinsic Pathway in HaCaT Cells Exposed to Low Doses.....	148
4.1. Introduction.....	149
4.2 Materials and Methods.....	151
4.3 Results.....	155
4.4 Discussion.....	162
Chapter 5: Identification of Key Proteins Signalled in Response to Radiation-Induced Bystander Effects in Human Skin Cells and a Gene Expression Investigation.....	165
5.1 Introduction.....	166
5.2 Materials and Methods.....	169
5.3 Results.....	177
5.4 Discussion.....	187

Chapter 6: General discussion.....	196
References.....	201
Appendices.....	246
Appendix A (Reagents).....	246
Appendix B (Working Protocols).....	251
Appendix C (Additional Raw Data).....	262



## List of Tables

**Table 2.1:** Percentage difference of viability between 0 Gy and 0.5 Gy and between 0 Gy and 5 Gy, for each cell line and cell viability assay, MTT or Alamar Blue (AB).

**Table 3.1** (*Table 1*) List of Forward and reverse oligo sequences of genes used in this study

**Table 3.2** (*Table 2*) Statistical values for Real-Time PCR gene expression analysis data presented in Figures 1 - 5.

**Table 4.1:** List of Forward and reverse oligo sequences of genes used in this study

**Table 4.2** Overview of the individual fold-changes of expression for each apoptotic gene analysed over 72 hr time-course for 0.005, 0.05 and 0.5 Gy doses

**Table 4.3** Statistical values for Real-Time PCR gene expression analysis data.

**Table 5.1:** Peptide ion identification information for proteins indicated in spot volumes

**Table 5.2** List of forward and reverse oligo sequences of ANXA2 and Actin

## List of Figures

**Figure 1.1** The average annual dose to a person in Ireland. The Radiological Protection Institute of Ireland (RPII) Annual Report and Accounts in 2012

**Figure 1.2** The electromagnetic spectrum.

**Figure 1.3** Various ionising radiation penetration ranges.

**Figure 1.4** Radiation exposures trigger a variety of complex responses at different levels of biological organisation.

**Figure 1.5** A schematic representation of how radiation can directly damage DNA in cells

**Figure 1.6** Free radicals generated during radiolysis of water

**Figure 1.7** Linear relationship of total dose response to ionising radiation.

**Figure 1.8** The model demonstrates how low-dose bystander effects do not fit into the linear no-threshold (LNT) model

**Figure 1.9** Signalling pathways mediating bystander responses in cells

**Figure 1.10** An illustration of the role of calcium as a mediator of intracellular bystander signalling in cells

**Figure 1.11** An illustration of calcium released from the endoplasmic reticulum that is concentrated in the matrix of the mitochondria and causes depolarisation of the inner mitochondrial membrane, disrupting electron transport and increasing ROS production.

**Figure 1.12** Intracellular oxidative stress and induction of DNA lesions.

**Figure 1.13** Schematic representations of apoptotic events.

**Figure 1.14** A schematic description of the intrinsic and extrinsic pathways of apoptosis.

**Figure 1.15** Mechanisms of release of intermembrane-space proteins from mitochondria.

**Figure 1.16 (a)** A schematic representation of the structural features of mammalian Caspases

**Figure 1.16 (b)** Schematic diagram of caspase activation.

**Figure 1.17** A schematic representation of the differential impact of p53 on cellular fate in response to DNA damage

**Figure 2.1** Viability of HaCaT cells after 24 hr exposure to 0, 0.5 and 5 Gy ICCM (1 and 24 hr) determined by the Alamar Blue assay

**Figure 2.2** Viability of HaCaT cells after 48 hr exposure to 0, 0.5 and 5 Gy ICCM (1 and 24 hr) determined by the Alamar Blue assay

**Figure 2.3** Viability of HT29 cells after 24 hr exposure to 0, 0.5 and 5 Gy ICCM (1 and 24 hr) determined by the Alamar Blue assay

**Figure 2.4** Viability of HT29 cells after 48 hr exposure to 0, 0.5 and 5 Gy ICCM (1 and 24 hr) determined by the Alamar Blue assay

**Figure 2.5** Viability of SW480 cells after 24 hr exposure to 0, 0.5 and 5 Gy ICCM (1 and 24 hr) determined by the Alamar Blue assay.

**Figure 2.6** Viability of SW480 cells after 48 hr exposure to 0, 0.5 and 5 Gy ICCM (1 and 24 hr) determined by the Alamar Blue assay

**Figure 2.7** Viability of HaCaT cells after 24 hr exposure to 0, 0.5 and 5 Gy ICCM (1 and 24 hr) determined by the MTT assay.

**Figure 2.8** Viability of HaCaT cells after 48 hr exposure to 0, 0.5 and 5 Gy ICCM (1 and 24 hr) determined by the MTT assay

**Figure 2.9** Viability of HT29 cells after 24 hr exposure to 0, 0.5 and 5 Gy ICCM (1 and 24 hr) determined by the MTT assay.

**Figure 2.10** Viability of HT29 cells after 48 hr exposure to 0, 0.5 and 5 Gy ICCM (1 and 24 hr) determined by the MTT assay

**Figure 2.11** Viability of SW480 cells after 24 hr exposure to 0, 0.5 and 5 Gy ICCM (1 and 24 hr) determined by the MTT assay.

**Figure 2.12** Viability of SW480 cells after 48 hr exposure to 0, 0.5 and 5 Gy ICCM (1 and 24 hr) determined by the MTT assay.

**Figure 2.13** Radiation-induced bystander effects of 19 different colorectal cancer patient samples, CRC-1- to CRC-38, determined by the MTT cell viability assay.

**Figure 2.14** Radiation-induced bystander effects expressed in percentage difference of determined by the MTT cell viability assay. The results displayed are the colorectal cancer patient samples coded CRC -1 to CRC38

**Figure 3.1 A-B:** (*Figure 1 A-B*) Comparison of relative fold-changes in gene expression levels of tumour suppressor gene TP53

**Figure 3.2 A-D:** (*Figure 2 A-D*) Comparison of relative fold-changes in gene expression levels of Pro-apoptotic Bax and anti-apoptotic Bcl-2

**Figure 3.3 A-D:** (*Figure 3 A-D*) Comparison of relative fold-changes in gene expression levels of synergistic JNK and ERK

**Figure 3.4 A-D:** (*Figure 4 A-D*) Comparison of relative fold-changes in gene expression levels of Initiator caspases 2 and 9

**Figure 3.5 A-F:** (*Figure 5 A-F*) Comparison of relative fold-changes in gene expression levels of executioner caspases 3, 6 and 7

**Figure 4.1:** Comparison of gene expression patterns of TP53, Bax, Bcl-2, ERK, caspase 2, caspase 9, caspase 6 and caspase 7 in HaCaT cells, following 1 hr, 6 hr, 12 hr, 24 hr, 48 hr and 72 hr exposures to 0.005 Gy indirect (bystander) gamma irradiation, presented as fold-changes of gene expression ( $*p < 0.05$ ).

**Figure 4.2:** Comparison of gene expression patterns of TP53, Bax, Bcl-2, ERK, caspase 2, caspase 9, caspase 6 and caspase 7 in HaCaT cells, following 1 hr, 6 hr, 12 hr, 24 hr, 48 hr and 72 hr exposures to 0.05 Gy indirect (bystander) gamma irradiation, presented as fold-changes of gene expression ( $*p < 0.05$ ).

**Figure 4.3:** Comparison of gene expression patterns of TP53, Bax, Bcl-2, ERK, caspase 2, caspase 9, caspase 6 and caspase 7 in HaCaT cells, following 1 hr, 6 hr, 12 hr, 24 hr, 48 hr and 72 hr exposures to 0.5 Gy indirect (bystander) gamma irradiation, presented as fold-changes of gene expression ( $*p < 0.05$ ).

**Figure 5.1** Representative 2D gel from HaCaT cells: Protein ID's are identified with an arrow on the gel.

**Figure 5.2:** (A - H) Increased and decreased expression of proteins (revealed through MS) by HaCaT cells exposed to media borne signals from directly irradiated fish skin.

**Figure 5.3** The mean-fold changes of ANXA2 expression in HaCaT cells directly and indirectly exposed to 0.05 Gy and 0.5 Gy irradiation for 1, 4, 8 and 24 hr.

**Figure 6.1:** The proposed radiation-induced bystander apoptotic signalling pathway response for HaCaT cells exposed to irradiated cell-conditioned medium at a dose of 0.05 Gy.

**Figure 6.2:** The proposed radiation-induced bystander apoptotic signalling pathway response for HaCaT cells exposed to irradiated cell-conditioned medium at a dose of 0.5 Gy.

# Chapter 1

## Introduction

### 1. Introduction

#### 1.1 History of Radiation

The field of radiobiology began in 1895 with the discovery of X-rays by Wilhelm Conrad Roentgen, followed by the first clinical use of X-radiation for treatment of a hairy mole by Leopold Freund in 1896 (Beyzadeoglu 2011). In the same year, Henri Becquerel engaged in experiments utilising the radioactive element uranium to determine the associated effects of radiation. Becquerel demonstrated that radiation seemed to arise spontaneously from the uranium as opposed to an external energy source. The term radioactivity was later used by Marie Sklodowska Curie and Pierre Curie for their discoveries of the radioactive elements polonium and radium in 1898 (Bernier *et al.* 2004). Marie Curie, whose work initially involved investigations into uranium rays, hypothesised that radiation came from the actual atom itself and not an interaction of molecules. Marie and Pierre attempted to isolate polonium and radium in their pure forms and published many papers (Feinendegen *et al.* 2008). At that time, the risks of radiation exposure were not well known but, in 1927, Hermann Joseph Muller revealed that humans exposed to radiation were at risk of developing physiological and genetic effects. Muller's early work as a geneticist involved *Drosophila*, through which he discovered mechanisms of crossing-over of genes. He later formulated the chief

principles of gene mutation and discussed how most mutations are detrimental and recessive. Muller's discovery that a quantitative relationship existed between radiation and lethal mutations sparked huge publicity, as it was the first time radiation risks had been recognised. Other researchers went on to repeat his experiments and expanded to other model organisms such as wasps (Whiting 1929). In 1930, Muller publicised the dangers of radiation exposure in humans, particularly for X-ray operators (Muller 1930). At the time, the use of radium-containing medicinal products was widespread, but they were removed from the market in the 1930s due to the emerging reports of hazardous effects posed to humans. By the 1940s, the growth of nuclear reactors and nuclear weapons was evolving, culminating in the devastating 1945 atomic bombings of Hiroshima and Nagasaki in Japan by the United States.

Radiation is found in our natural environment. Sources of natural background radiation include cosmic rays from outer space, natural radioactive materials in the ground and radionuclides naturally occurring in the body or in food. Gamma-ray and X-ray equipment used in hospitals and industry are also sources of exposure. Exposure to natural and man-made sources has increased due to an increase in human activities such as air travel, mining and medical practice. In Ireland on average, a person receives an annual dose of 3950 $\mu$ Sv from all sources of radiation. About 86% of radiation comes from the natural sources, mainly due to the accumulation of radon gas beneath houses. Man-made radiation contributes 14% (550 $\mu$ Sv), which is greatly dominated by the use of radiation in medicine (540 $\mu$ Sv). Other man-made sources make up about 1% (15 $\mu$ Sv) of radiation exposures (Radiological Protection Institute of Ireland, RPII, 2012). The

contribution from all these sources of radiation expressed as the average annual dose to a person in Ireland is displayed in Figure 1.1.

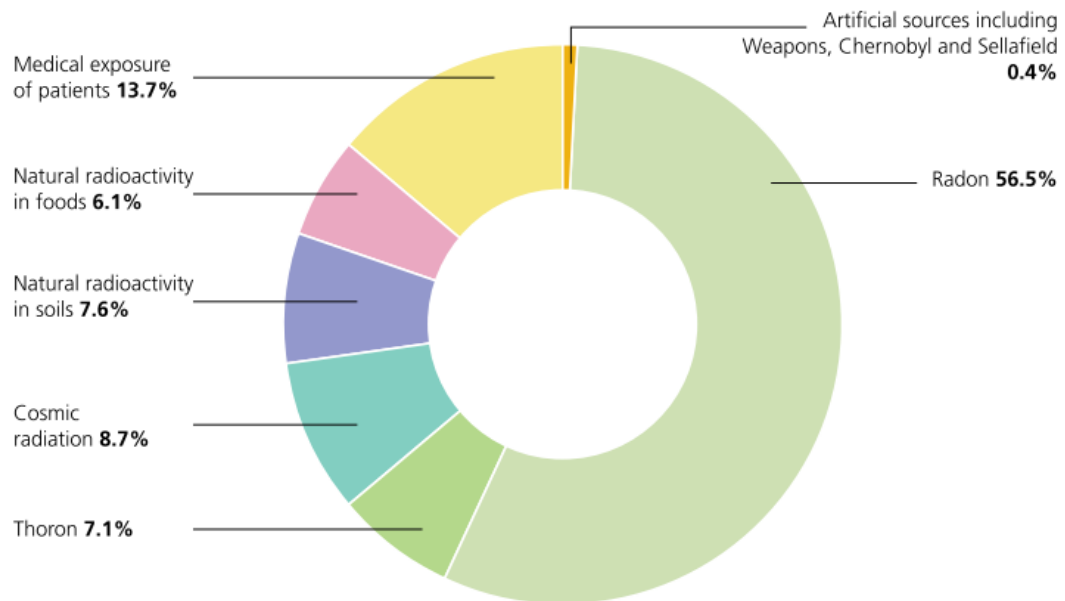


Figure 1.1 The average annual dose to a person in Ireland. The Radiological Protection Institute of Ireland (RPII) Annual Report and Accounts in 2012, “ *To ensure that people in Ireland are protected from the harmful effects of radiation*”. The figure above displays a breakdown of the percentage radiation exposures that each person in Ireland is exposed to annually (RPII, 2012).



Radiation has become a very important tool in modern clinical practice for both diagnostic and therapeutic purposes, such as cancer therapy. The use of radiation in clinical tissues or cells is based on the concept that it will selectively kill tumour cells while minimising the detrimental effect to normal surrounding cells and tissues (Baskar *et al.* 2012). However, radiation is frequently described as a ‘double-edged sword’ as it is an important tool for treatment of malignant tumors but it can also be a potential genotoxic agent causing genome instability and carcinogenesis (Hall & Giaccia 2012). In 1896, Emil Grubbe treated a breast cancer patient with radiation therapy (radiotherapy) for 1 hr each day for a total of 18 days and discovered palliative effects (Vujosevic & Bokorov 2010). Although Grubbe was a medical student at the time and did not actually publish this work until 1946 and 1947 (Grubbe 1946, 1947), he was in fact responsible for the introduction of the term “radiotherapy” in the late 1800’s. While the evolution of radiotherapy has undoubtedly resulted in increased patient survival rates, it must be noted that radiation-treatment-related complications can also occur. Human radiation-mediated responses have been thoroughly investigated at the molecular, cellular and tissue levels to better understand these complications for subsequent patients undergoing radiotherapy. Furthermore, delayed responses to IR for months to years post treatment have also been the subject of intense investigations because of the clinical implications of this phenomenon.

## 1.2 Introduction to Clinical Radiation Types and Doses

Radiation transmits energy in the form of either waves or particles and is classified as either ionising or non-ionising radiation types. IR is classified as electromagnetic radiation (X-rays and gamma-rays) and particulate radiation (electrons, protons,  $\alpha$ -particles, neutrons and heavy charged particles). Figure 1.2 shows the electromagnetic spectrum for both ionising and non-ionising radiation. Non-ionising radiations include ultraviolet (UV) radiation, microwave and infrared (Internal Atomic Energy Agency Publications, IAEA 2004). Protons, neutrons and  $\alpha$ -particles lose their energies over shorter distances than X-rays and gamma-rays with the same energy (Beyzadeoglu, 2011). Ionising radiation (IR) has higher frequencies and shorter wavelengths, and while non-ionising radiations have a lower frequency with longer wavelengths.

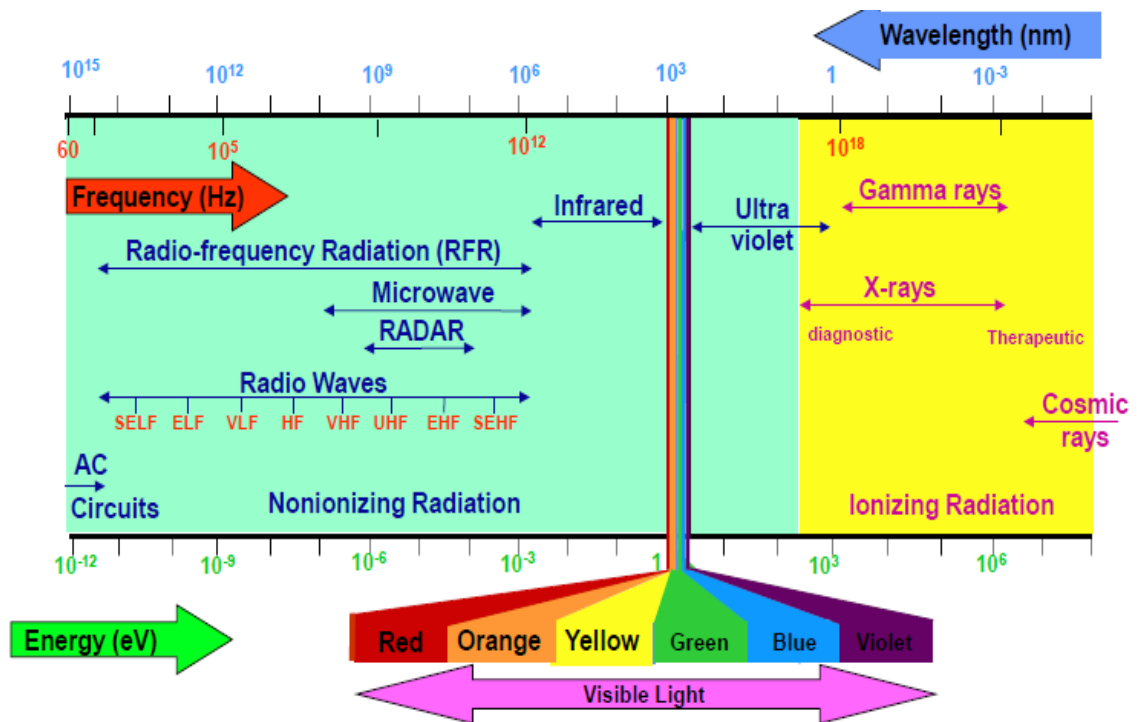


Figure 1.2 The electromagnetic spectrum. The electromagnetic radiation is characterised by the wavelength, frequency and energy per photon. It has no mass and can pass through matter. Ionising and non-ionising radiations are described above.

Ionising radiations that are commonly used in radiotherapy are described by the International Atomic Energy Agency in their 2004 publication “Radiation, People and the Environment” (IAEA, 2004). Alpha ( $\alpha$ ) radiation is a positively charged helium nucleus emitted by a large unstable nucleus. It has a short range of about 1-2cm and can be absorbed completely by paper or skin. If  $\alpha$ -radiation enters the body it can be quite harmful, as high energy depositions can result in nearby tissues. Beta ( $\beta$ ) radiation is composed of electron particles emitted by an unstable nucleus and are much smaller particles than  $\alpha$ -particles.  $\beta$ -radiation can be absorbed completely by plastic, glass or metal and cannot usually penetrate further than the top layer of skin, but very large exposures can induce skin burns. Gamma ( $\gamma$ ) radiation is a very high energy photon

emitted from an unstable nucleus that is usually emitting a  $\beta$ -particle at the same time. Gamma-radiation passes through materials, ionising the atoms as it is transmitted. It is very penetrating to skin and therefore only very dense materials such as lead can shield  $\gamma$ -radiations (see Figure 1.3). X-rays are very similar to gamma but are produced artificially by a rapid slowing down an electron beam. Likewise they are very penetrating and can transport high doses to internal organs in the body. Neutron (n) radiation is produced when nuclear fission causes neutrons to be ejected from the nucleus of an atom, these can be absorbed by a variety of materials, specifically with many Hydrogen atoms. They are usually produced artificially. If they interact with materials, they cause emissions of  $\beta$  and  $\gamma$  radiations. Exposures can be managed with the aid of heavy shielding.



Figure 1.3 Various ionising radiation penetration ranges. Electrons have smaller ranges and travel shorter distances than gamma and X-rays, and they can be absorbed by plastics, glass and metal layers (Internal Atomic Energy Agency Publications, IAEA 2004).

Living cells directly absorb IR (energy) which in turn disrupts atomic structures, generating chemical and biological changes in the cell, initiating a series of processes which can cause permanent physiological changes (Hall & Giaccia, 2012). Patterns of radiation tend to be localised along tracks of the charged particles. Different sources of radiation will determine the pattern of radiation. X-ray and gamma-radiation occur in well-separated tracks and  $\alpha$ -particles and HZE-particles (high energy) occur in dense columns along the path (Jain *et al.*, 2012). The amount of radiation delivered to a patient must be known in order to determine the ultimate damaging biological effects, referred to as biological effectiveness. The amount of energy absorbed is called dose, it is quantified as the 'absorbed dose, 'equivalent dose' and 'effective dose. Absorbed dose refers to the amount of radiation absorbed by tissue and the unit of measurement is Gray (Gy). 1 Gy represents one unit of energy (joule) in one kilogram (kg) of tissues. Radiation types differ in the way that they interact with biological material and therefore the absorbed doses do not always represent equal biological effects. So, another quantity takes into consideration the differences between the types of radiation administered. The unit for quantification of this dose unit is Sievert (Sv) and is referred to as the equivalent dose. Most often the unit is expressed as milli Sievert (mSv) and micro Sievert ( $\mu$ Sv) (Seltzer, 2011). Each major tissue and organ in the body has their own unique equivalent dose, when this is multiplied by a weighting factor it relates the risk associated with the specific tissue or organ. These doses are referred to as effective doses. Dosimetry measures dose and dose rates for patients undergoing radiotherapy using equipment called dosimeters or detectors (Beyzadeoglu, 2011).

Diagnostic and therapeutic radiation fields encouraged the development of radiation oncology, in which radiation types and energies have been established for the treatment of malignant tumors. There are three main divisions of radiotherapy that exist and

which differ based on the position of the radiation source, such as, external beam radiotherapy or teletherapy, brachytherapy (sealed source/internal radiotherapy) and systemic radioisotope (unsealed source) radiotherapy. External radiotherapy is in fact the most common type used. Kilovoltage X-rays are administered for the treatment of skin cancers and superficial tumors and include contact therapy machines, superficial therapy machines and supervoltage machines. Megavoltage X-rays are used for the treatment of more deeply seated tumours and are administered through Van Graaf generators, Cobalt-60 teletherapy units, Betatrons, Microtrons and Cyclotrons. The first Cobalt-60 teletherapy machine was developed in London, Ontario, in Canada in 1951 (Hall & Giaccia, 2012) and is used specifically to treat tumors < 10cm in depth, through the production of gamma-rays from Co-60 radioisotopes. Gamma rays have well-defined energies and are emitted during the decay of Co-60. The Linear Accelerator (Linac) was developed at Hammersmith Hospital in the United Kingdom and is used for more deeply placed tumors. The Linac involves the emission of free electrons and acceleration in an electromagnetic field, thereby increasing the energy (Beyzadeoglu 2011). Both technologies have led the way for external beam radiotherapy today followed by the use of IR and radioactivity as internal therapeutic agents, for example, brachytherapy. It is common for radiotherapy to be administered in a combined therapy approach, in conjunction with surgery and chemotherapy to treat malignant tumors. Radiation can be used before surgical removal of a tumour in an attempt to shrink the size of the tumour, and this is referred to as neo-adjuvant therapy. Radiation administered post-surgery is referred to as adjuvant therapy and can destroy any remaining tumour cells not removed surgically (Baskar *et al.*, 2012).

### 1.3 Biological Interaction of Radiation with Cells

The effect of ionising radiation (IR) is due to the geometry of physical energy deposition events in cells and tissues known as track structure, and is referred to as linear energy transfer (LET) (Muroya *et al.*, 2006). LET describes the energy transferred to the cell through IR per unit track length. Biological effectiveness of radiation is influenced by the LET, total dose administered, fractionation rate and radiosensitivity of the targeted cells or tissues (Hall, 2007). The effect of radiation damage on biological material greatly depends on the characteristic of radiation administered and increases as LET increases (measured in KeV/ $\mu\text{m}$ ). Low-LET radiations such as X-rays,  $\gamma$ -rays and  $\beta$ -particles deposit small quantities of energy on cells. High LET radiations, neutrons and  $\alpha$ -particles deposits more energy on the targeted areas causing more biological effects (Baskar 2010). This is because high-LET is capable of transferring a larger amount of energy per unit length and is likely to instigate DNA damage over a short period of time. Consequently it is more damaging than the same dose of electromagnetic radiation (low-LET radiation) (Baskar *et al.*, 2007). Exposure to high (-LET) particles have been shown to induce cell killing for the removal of dangerous cells (Jain *et al.*, 2012). Figure 1.4 shows the range of biological consequences of radiation. High doses can cause great physical damage to chromosomes and even low dose radiation can cause mutations and subsequent carcinogenesis.

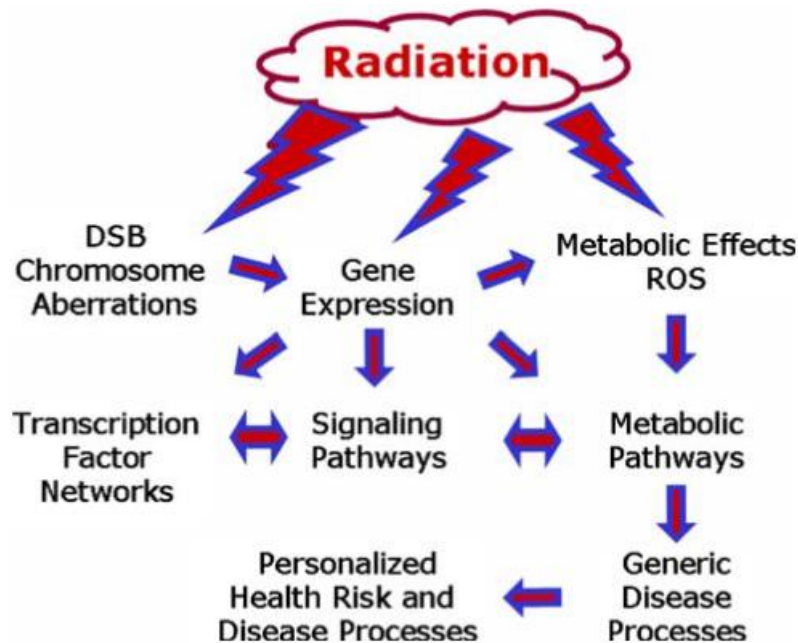


Figure 1.4 Radiation exposures trigger a variety of complex responses at different levels of biological organisation. The responses are part of a complex signalling network.

Radiation effects can occur either directly or indirectly in biological matter. The direct action of radiation involves the absorption of radiation energy and the direct interaction with cellular targets such as DNA, ionising or exciting molecules within a cell, instigating a series of signalling events leading to specific biological changes (see Figure 1.5). If the radiation is from a high -LET source then direct effects occur. Otherwise, radiation can interact with molecules other than DNA within the cell, most often water. This is due to the fact that mammalian cells are composed mainly of water and the radiation damage is indirectly induced through radiolysis of water in the cells (Hall & Giaccia, 2012).



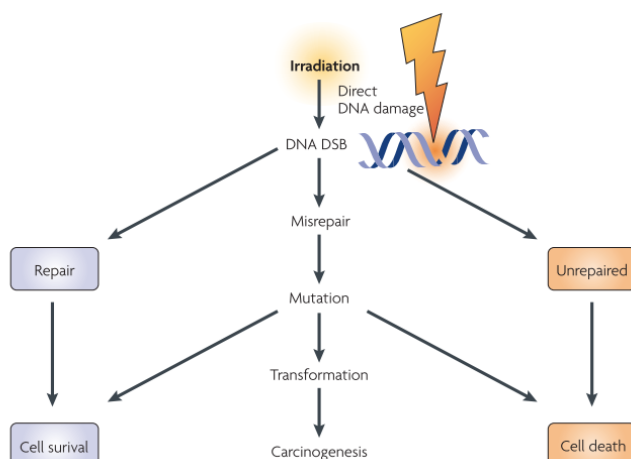


Figure 1.5 A schematic representation of how radiation can directly damage DNA in cells. If the damage is repaired then cells can survive, if the damage is not repaired that cell death is induced. Occasionally DNA double-strand breaks are misrepaired causing mutations and subsequent development of carcinogenesis (Prise & O’Sullivan 2009)

The radiation absorbed by biological materials results in either excitation or ionisation of atoms in a cell. Excitation occurs when an electron in an atom is elevated to a higher energy level without being actually ejected. Ionisation describes when radiation has enough energy to eject one or more electrons, creating an imbalance of electrons and protons and thus making an atom positively charged. These atoms are then referred to as ions and radiation is capable of producing ions (Joiner & Kogel 2009). The generation of free radicals cause oxidising changes that can damage nucleic acids, proteins and lipids (Hall & Giaccia, 2012). A schematic representation is presented in Figure 1.6. The figure describes ionisation and excitation occurring in irradiated cells, and the generation of  $\text{H}_2\text{O}^+$  and an electron ( $\text{e}^-$ ) from the ionisation of  $\text{H}_2\text{O}$ , a hydrogen atom

( $\text{H}\cdot$ ) and a hydroxyl radical ( $\cdot\text{OH}$ ) from the excited  $\text{H}_2\text{O}$ .  $\cdot\text{OH}$  is a cytotoxic oxygen radical responsible for the cellular damage. Free radicals are capable of moving throughout the cell damaging important cellular targets. About one quarter of radiation damage occurs directly therefore most radiation damage must be a result of indirect radiation. Although the IR tracks in cells can occur randomly, the responses to random IR can become coordinated by controlled cellular responses.

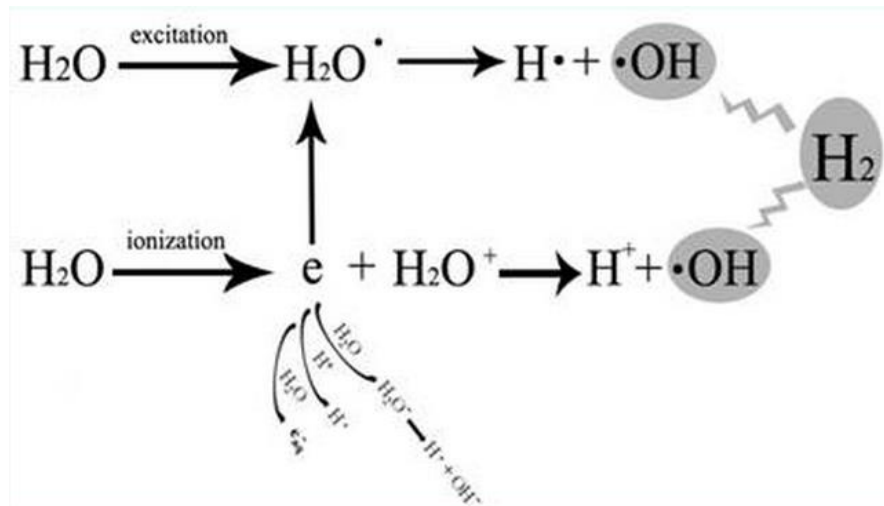


Figure 1.6 Free radicals generated during radiolysis of water (Qian *et al.*, 2013).

There are experimental methods to elicit a localised radiation exposure in cells enabling a more precise investigation of the associated cellular mechanisms. The use of radioactive elements has been successful for this purpose. Early studies show that subjecting DNA to a radioactive label such as  $^{125}\text{I}$  results in DNA double strand breaks (DSB) and can stimulate mutagenic and cytotoxic damage (Martin & Haseltine 1981). DNA molecules were constructed to contain a single  $^{125}\text{I}$  labelled deoxycytidine at a known position and sequence. Decay of  $^{125}\text{I}$  instigated DNA strand breaks. DNA damage can initiate cell death processes by means of apoptosis to remove damaged cells or DNA repair responses but occasionally the damage is incorrectly misrepaired resulting in chromosomal mutations, therefore increasing the possibility of survival and subsequent carcinogenesis, (reviewed by Prise & O'Sullivan 2009).

Earlier reports targeting and analysing cells individually, showed that the effects of radiation damage were exclusively dependent on direct irradiation of the nucleus and that cytoplasmic radiation caused very little cytotoxic effect (Zirkle & Bloom, 1953; Alexander & Bacq, 1961). The technology for micro-irradiations became available years later, in the 1990's, through the development of microbeams, which allow localised targeted radiation. They have become a very powerful radiobiological tool that facilitates targeting of single cells. They were originally designed to evaluate the biological effects of radiation specifically at very low doses. This enabled assessment of the environmental and occupational risks associated with low dose radiation exposure. In these circumstances, single cells are irradiated in occupational workers and the dose is spaced out over many years. Improved imaging, software and delivery of the beam have advanced the technology. Microbeams are capable of transferring charged particles, X-rays and electrons to the target cells. One of the major advantages of

targeting single cells is that key cell mechanisms signalled post exposure could be elucidated, thus revealing early radiation responses in cells.

The traditional concept of radiobiology was based on the target theory assuming that the primary target is DNA and that biological effects of exposure to radiation occur in the irradiated cell as a result of direct damage to DNA in the nucleus (Crowther 1924). In the 1970's DNA was uncovered as a sensitive target for radiation damage, (reviewed by Prise *et al*, 2003). Over the past two decades, the conventional radiobiology model has been challenged by the evolution of these biological consequences known as non-targeted effects (NTE) meaning that all previous assumptions have since been reconsidered. NTE will be discussed in detail in the next section, with particular emphasis on bystander effects.

#### **1.4 Non-targeted Effects of Radiation**

The non-targeted effect (NTE) concept emerged because of unusual cellular damage discovered in cells that did not depend on direct DNA damage. Non-irradiated cells were receiving damage signals from directly irradiated cells. In actual fact, there is very early evidence of non-targeted radiation effects from experiments dating back to 1915 (Murphy & Norton, 1915). Murphy and Norton performed partial body irradiations in mice (*Mus*), concluding that similar damaging effects could occur in distant non-irradiated parts of the body. The data was not fully acknowledged until other data emerged in from the work of Seymour and colleagues (1986) and then later by Nagasawa and Little in 1992 (1992) indicating the specific biological changes in response in non-targeted irradiations.

Four major manifestations significantly challenged the original radiobiology paradigm and led to the discovery of two important classifications of NTE. Firstly, in 1986 *de novo* lethal mutations were found to occur in cells surviving radiation and these cells even successfully divided for several generations post exposure (Seymour *et al.* 1986). Therefore, even after radiation treatment the effects of the initial dose persisted throughout the lifetime and progeny of cells. Secondly, bone marrow stem cell lineages derived from irradiated stem cells were explored for similar damaging effects, and delayed appearances of *de novo* chromosome aberrations in cells were discovered (Kadhim *et al.* 1992). It is not possible that these lethal mutations or aberrations could have been present at the time of irradiation. Therefore, the effect must have been a result of a communicated damage signal from directly exposed cells. Thirdly, in 1992 Nagasawa and Little (1992) discovered that very low dose  $\alpha$ -particle radiation resulted in more cells showing chromosome damage than were originally hit by the original ionising particles. Finally, media transfer experiments in bystander studies were developed and enabled the exploration of how NTE was signalled. Filter sterilised media was transferred from directly irradiated cells (donor cells) onto non-irradiated cells (recipient cells). Media from the directly irradiated cells was capable of triggering similar levels of clonogenic cell death and genomic instability in non-irradiated cells (Mothersill & Seymour 1997). These innovative discoveries established that this effect can cause both delayed and non-targeted chromosomal aberrations and gene expression changes Aypar *et al.*, 2011). The genetic changes induced in cells which are not irradiated but in receipt of signals from the irradiated cells are currently referred to as ‘radiation-induced bystander effects’ (RIBE) and will be described as RIBE throughout the rest of this study. This term was first used by Nagasawa and Little based on their findings in 1992. Kadhim and colleagues (1992) showed that genetic changes can

manifest in the progeny of an irradiated cell after many generations of cell division, and is better understood today as radiation-induced genomic instability (RIGI) (Aypar *et al.* 2011).

Genomic instability is reviewed in detail by Morgan and colleagues (Morgan, 2003). It is best described as the “instability events” that can occur in the progeny of an irradiated cell. A cell that survives irradiation has the ability to clonally expand, meaning that the progeny of the irradiated cell may undergo cell death. Otherwise, the instability events will occur in the progeny of the irradiated cell, resulting in chromosomal aberrations, mutations, micronuclei formation (MN) and gene amplifications. Bystander effects can occur in distant ‘out of field’ bystander cells and their progeny. Although the route by which both genomic instability and bystander effects occur can be different, the mechanisms are similar in nature. It is believed that genomic instability is a direct consequence of bystander signalling induced in response to radiation (Coates *et al.* 2004). In addition to RIBE and RIGI, there are other types of NTE that exist such as low-dose radio-hypersensitivity and abscopal effects. Reports show that cell lines demonstrating a large bystander effect do not show hyper-radiosensitivity (Joiner *et al.* 2001; Mothersill *et al.* 2002). Nevertheless, the molecular mechanisms are not very well understood and so the following study exclusively explores the molecular and biochemical effects of RIBE in a human skin model. The discovery of NTE has created greater uncertainty in radiation risk and health protection issues than previously predicted. It is clear that radiation not only poses a threat to exposed individuals but also to their progeny.

## 1.5 The Bystander Response – Overview

Radiation induced bystander effects (RIBE) have been shown to occur when an irradiated cell communicates with non-irradiated cells via secreted factors and or via gap-junctional intercellular communication.

These bystander effects have challenged the original target theory (that was mentioned earlier) as they do not follow the original concept. Figure 1.7 shows the linear relationship of total-dose responses to IR without bystander effects added in, as the figure just shows a general shape of the bystander effect. Bystander responses do not demonstrate a linear dose-response relationship as the classical target theory does (Belyakov, 2005).

The non-irradiated cells exhibit biological responses that are normally characteristic of irradiated cells. Bystander effects seem to be primarily a low dose phenomenon and saturation of the bystander response is said to occur at a threshold dose (0.2 Gy), but bystander effects have been found at higher doses (0.5 Gy) (Nagasawa & Little, 1992; Prise *et al.* 2005). Increasing the dose does not increase the number of affected cells in a population (Liu *et al.*, 2006) and the response is independent of dose in the range of 0.5–5 Gy (Sowa *et al.*, 2010). Reports show that exposure to very low doses (1 cGy-5 Gy) of <sup>60</sup>Co gamma radiation, initiates an increase in the development of cell death via apoptosis or necrosis as well as evidence of reduced cell cloning efficiency in the cells that were never exposed to radiation (Mothersill *et al.*, 2000; Mothersill & Seymour, 2002).

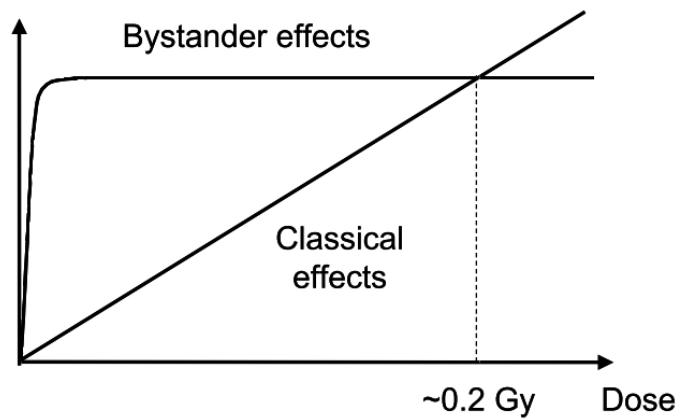


Figure 1.7 Linear relationship of total dose response to ionising radiation (Belyakov, 2005).

For these reason, the cellular communication of bystander responses has had to be re-considered in order to estimate the associated health-risks and consequential radiation protection issues. Data derived from high-dose epidemiological risk data contributes to the linear-no-threshold (LNT) model. So according to LNT, cancer-risk associated with low-dose exposure is derived from these data by extrapolation. It does not take into consideration that the risks of low doses may be different (See Figure 1.8). Bystander responses are induced at low doses, this suggests that a specific cellular mechanism may be responsible for ‘switching’ to direct effects at higher doses. So, the risks may be greater or less than what was previously predicted in the LNT model.



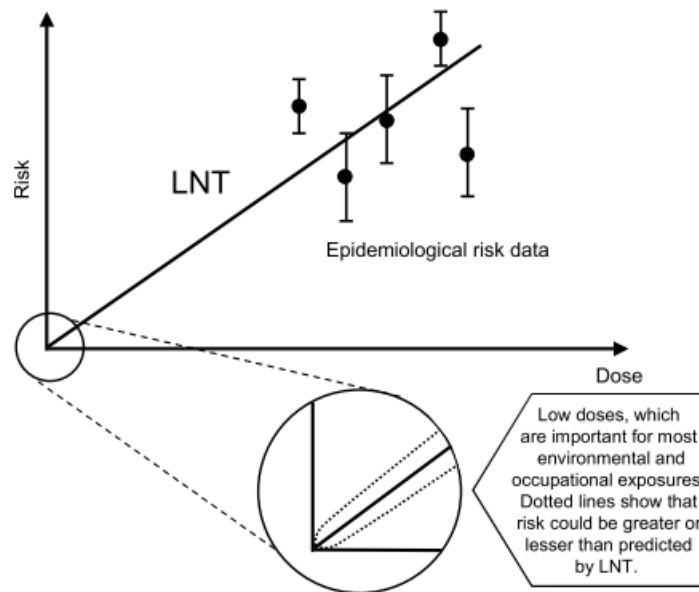


Figure 1.8 The model demonstrates how low-dose bystander effects do not fit into the linear no-threshold (LNT) model. The data for this model is derived from high-dose epidemiological data. As there is not any reliable epidemiological information in low dose region, there are uncertainties of the associated radiation risks. However, the figure shows that at low doses, the dotted lines are indicative of both beneficial or detrimental effects (Belyakov 2005).

### 1.5.1 History of Bystander Response

Prior to the recent interest in non-targeted effects of IR, there were numerous reports that a clastogenic factor capable of inducing chromosomal breaks in unirradiated lymphocytes was present in blood plasma after radiotherapy (Parsons *et al.*, 1954; Littlefield *et al.*, 1969; Faguet *et al.*, 1984). Clastogenic factors have been shown to be produced via superoxide and to induce the production of superoxide (Emerit, 1994).

Their clastogenic activity may be related to the formation of lipid peroxidation products (Emerit, Levy & Khan, 1991) and cytotoxic cytokines (Emerit *et al.*, 1995), which are currently candidates for mediating RIBE and will be discussed further in more detail. There is also a body of clinical and experimental radiotherapy data concerning so - called abscopal effects of radiation, whereby responses were observed in unrelated organs or tissues that were not irradiated (Nobler, 1969; Montour, 1971; Camphausen *et al.*, 2003). Abscopal effects have been previously referred to as the distant effects seen after local radiation therapy, however more recently the term has been used to relate to distant bystander effect. There is controversy surrounding the abscopal effect as there is data both supporting and contesting the concept (Kaminski *et al.*, 2005).

There are many definitions of radiation-induced bystander effects and here we define it as the ability of cells exposed to radiation to transmit indirect effects from targeted irradiated cells to non-irradiated neighbouring cells. There are very early reports of RIBE dating back to 1954. The report described the presence of bystander damage in bone marrow in the sternum of children that had previously received radiotherapy to their spleen for chronic granulocytic leukaemia (Parsons *et al.*, 1954). In the late 1960's, Hollowell and Littlefield further investigated what kind of bystander damage was associated with this response. They revealed that plasma from X-irradiated patients could induce chromosomal damage in non-irradiated lymphocytes held in culture and similarly plasma from high dose radiotherapy patients could stimulate chromosomal aberrations in non-irradiated cells (Hollowell & Littlefield, 1967; Hollowell & Littlefield, 1968). Another study reported that double the amount of chromosomal aberrations were generated in lymphocyte cultures exposed to irradiated plasma compared to non-irradiated plasma, suggesting that there was something in the plasma initiating damage in non-irradiated cells (Demoise & Conard, 1972).

Reports have shown that non-irradiated rats in receipt of blood plasma from irradiated rats displayed non-targeted damaging effects (Souto, 1962). The rate of mammary tumour development was increased in the rats indirectly exposed to radiation and quantified as the extent of damage induced. Littlefield and colleagues further investigated this type of damage and found that a variation exists between directly irradiated and non-targeted indirect radiation effects with regard to the range of chromosomal aberrations produced (Littlefield *et al.*, 1969). Their work was further validated by Scott (1969), however his data presented lower levels of aberrations consisting of the chromatid type only. In 1968 Goh & Sumner (1968) cultured normal leukocytes obtained from donor patients with irradiated patient plasma. They recorded that chromosome breaks were induced in the lymphocytes in receipt of the plasma. Remarkably, their study revealed that a transferable substance in the plasma was communicating the damage and so a specific signalling mechanism must be responsible, which had yet to be discovered.

Different patterns of genes expression occurs after low and high doses of irradiation in cells, suggestion that the gene changes are dose-dependent (Amundson, 2008). Bystander responses could be a result of differential gene expression, cell signalling and epigenetic changes prevailing at low doses of radiation. The differences in gene expression between low and high doses of irradiation could also be a result of time or tissue-dependent differences (Amundson *et al.*, 2000). An insight into the precise molecular mechanisms of RIBE in cells and tissues is essential to understanding the consequences of the bystander effect and any clinical implications.

There is uncertainty as to whether bystander effects are beneficial or detrimental. It is known that they induce stress effects instigating DNA repair mechanisms, indicative of

stimulated cellular damage. On the contrary, induction of adaptive responses and hormesis has occurred in cells indicating possible protective mechanisms (Calabrese *et al.*, 2011). It is believed that communication of a bystander factor may potentially act as a 'warning' to unirradiated cells, instructing or adapting the cells in case of subsequent exposures to damaging signals (Sawant *et al.*, 2001). Further to that, bystander cells are capable of becoming more radio-resistant than cells that have not been exposed to bystander signals (Rashi Iyer & Lehnert 2002; Mitchell *et al.* 2004; F. Lyng *et al.* 2006) and may possibly recognise the mutagen (IR) or perhaps protect the cell from further damage through initiation of specific cellular mechanisms. Interestingly, a study in 2008 demonstrated that ICCM harvested from radio-resistant cell lines (T98G, HT29 and SW480) transferred onto epithelial (HPV-G) cells did not show bystander effects (Ryan *et al.* 2008). Another study has shown that priming cells (U373, T98G, HGL21 and HT29) with 0.1 Gy irradiation 5 hr prior to exposure to 2 Gy and 5 Gy, demonstrates increased cloning efficiencies (Ryan *et al.* 2009).

Low dose radiation-induced protective responses are actually mediated in a bystander manner in cell culture indicative of shared signalling components between the responses. The distant molecular interactions leading to proliferation of either damaging or protective effects is dependent on cell type and the characteristics of the radiation.

Speculations have been made based on the specific biological endpoints associated with bystander effects. These appear to be common to both targeted and non-targeted radiation effects, including cell death, increased reactive oxygen species (ROS), enhanced cell growth, chromosome aberrations and mutations, altered gene expression and induction of genomic instability (Chaudhry 2006). Certain biological endpoints

such as the generation of free radicals acting on DNA depend on short-lived signals (Kashino *et al.* 2007).

### **1.5.2 Bystander Response Signalling Mechanisms in Cells**

The entire biological mechanism of the bystander cellular response is still not fully understood, but reports have shown that there are two fundamental mechanisms that transmit bystander signals. A) Cell – cell communication through cellular gap junctions has been considered to play a role when there is a high degree of cell to cell contact. A connexin-mediated gap-junction transfer of the bystander signal was also thought to be responsible for communicating the bystander signal (Azzam *et al.* 1998; Azzam *et al.* 2001). B) Other data revealed that production of the bystander factor does not always require cell to cell contact to transmit a signal to neighbouring cells (Mothersill & Seymour 1998). The main finding of this study was that the medium was taken from irradiated cells and put on cells in another flask caused bystander effects, so gap-junction communication could not be communicating. This was confirmed by inhibiting gap-junction communication with tumour promoter phorbol myristate acid (PMA) in epithelial cells prior to irradiation and the, which resulted in increased bystander death effects. It is clear that there is another mechanism responsible other than gap-junction communication. The hypothesis that the bystander signal can be secreted from directly-irradiated cells into the surrounding medium (Mothersill & Seymour 1997) was confirmed in other studies (Narayanan *et al.* 1997; Przybyszewski *et al.* 2004; Lehnert & Goodwin 1997). This is the primary course of signal transduction, particularly when there is no direct cell -to -cell contact or cells are located far apart.

The magnitude of the bystander effect ultimately depends on the number of cells initially irradiated and the concentration of the signal that they produce (Mothersill & Seymour 1998; Vines *et al.* 2008). Bystander signal generation and response to the signal have been acknowledged as separate processes. Production of a bystander signal seems to be more important than the number of non-irradiated cells receiving the signal to respond (Ryan *et al.* 2008). Signal generation is known to involve electrochemical processes similar to the nervous system, such as a reduction in mitochondrial membrane potential and induction of ion-flux and will be discussed later on (Poon *et al.* 2007).  $\text{Ca}^{2+}$  has been suggested as a 'death trigger' because of the influx of intracellular  $\text{Ca}^{2+}$  that lead to the cell demise (Fleckenstein *et al.* 1974) and for that reason it is said to be an intrinsic stress induced by cells as a result of an external stress such as IR (Cerella *et al.* 2010). It is important to emphasise that the RIBE pathway appears to be divided into two separate but connected events. The first being a signalling event between cells (intercellular) to communicate the bystander factor and the second being the events which are triggered within the cell (intracellular) when the signal is received.

### **1.5.3 Intercellular Signalling of Bystander Factor(s)**

Some of the key intercellular signalling mechanisms of bystander responses have been revealed but not fully elucidated. The initiating events in the bystander cascade in non-irradiated cells are from signals produced from the irradiated cells. Intercellular signalling molecules originating from directly-irradiated cells could have a significant role in transferring damage to non-irradiated bystander cells. Bystander responses have been compared to inflammatory type responses due to the activation of cytokines and activation of reactive oxygen species (ROS) and reactive nitrogen species (RNS) in

oxidative stress (Rastogi *et al.* 2013). Transcription factor NFK $\beta$ -dependent cytokines interleukin-6 and -8 (IL-6, IL-8), transforming growth factor- $\beta$  (TGF $\beta$ ) and tumour necrosis factor-  $\alpha$  (TNF $\alpha$ ) have all been implicated in bystander signalling (Gow *et al.*, 2010). TGF $\beta$ 1 is, a cytokine that mediates growth and differentiation and the activation of immune activity in cells and it, has been suggested to be a mediator of bystander responses (Lorimore *et al.* 2008; Shao *et al.* 2008). There is evidence of increases in the expression of TNF- $\alpha$  (Lorimore *et al.* 2008) and IL-8 cytokines (Narayanan *et al.* 1999) on the cell surface post-irradiation. A recent study measuring gene expression profiles and analysis of molecular signalling pathways, revealed that cytokine interleukin (IL)-1 $\alpha$  is released into serum of mice chronically exposed to high doses of gamma-radiation which is transferred to non-irradiated mice (Sugihara *et al.* 2013). Predominantly COX-2 signalling has been shown to be significant in inflammatory responses and an overexpression of COX-2 has been discovered in bystander cells suggesting that it mediates bystander signalling. Transcription factor NFK $\beta$  is known to control cyclooxygenase-2 (COX-2) expression which may be responsible for transmitting the bystander signal (Zhou *et al.* 2005; Hei *et al.* 2008). COX-2 is also a downstream target of mitogen-activated protein kinase (MAPK) pathways involved in radiation responses and may be linked to bystander responses. The MAPK pathway is essential for the activation of COX-2 and subsequent activation of RO and has been strongly implicated in bystander signalling (Ivanov *et al.* 2010; Lyng *et al.* 2006). Inhibition of these significant signalling events results in disabled bystander responses, and so they must play a role in signalling. A study in 2006 (Kaup *et al.* 2006) demonstrated how IR causes long-term changes in the DNA methylation in HPV-G cells and proposed that global dysregulation of genomic methylation is a possible mechanism by which non-targeted effects are transmitted. See Figure 1.9 for an illustrated description of some of

the signalling events that occur after irradiation and have been suggested as mediators of bystander signalling.

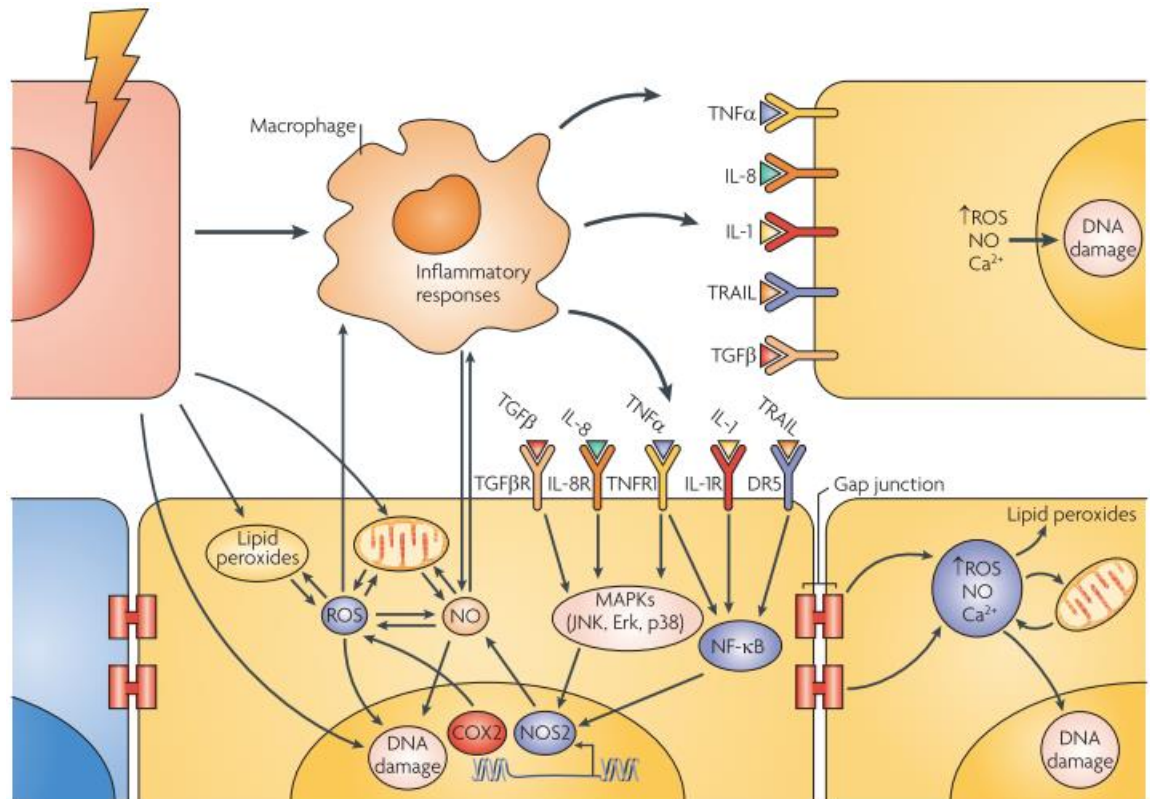


Figure 1.9 Signalling pathways mediating bystander responses in cells. External signals on the surface of the cell initiate bystander signalling as a result of indirect-irradiation either through gap-junction intercellular communication or by secretion of bystander factor(s) transmitted to neighbouring cells. Cytokines have been implicated in intercellular bystander signalling events (Prise & O’Sullivan 2009).



Intercellular signalling pathways are an important integrator of multicellular damage responses, they are essential in prevention of carcinogenesis development through the removal of damaged cells and inhibition of neoplastic transformation. Direct radiation exposures induce an imbalance of oxidative stress in human keratinocyte cells which participates and mediates cell death processes, in particular apoptosis.

#### **1.5.4 Intracellular Signalling of the Bystander Effect**

Directly irradiated cells produce bystander factor(s) via cell-cell communication or through the release of cytokines into the extracellular matrix (ECM). Cells indirectly exposed to ionising radiation are triggered by a localised stimulus on the cell membrane. The stimulus can be an influx of calcium through the plasma membrane (Lyng *et al.* 2006). Figure 1.10 shows a  $\text{Ca}^{2+}$  influx into the mitochondrion, inducing a permeability transition pore in the membrane of an adjacent mitochondrion. Cytochrome c is released from the mitochondria, which can diffuse to the nearby endoplasmic reticulum (ER) and bind to receptors which will instigate a release of  $\text{Ca}^{2+}$  from the ER. Cytoplasmic  $\text{Ca}^{2+}$  concentrations are increased and so the mitochondria take up the excess  $\text{Ca}^{2+}$ , again instigating the release of cytochrome c which then activates the formation of the apoptosome and caspases which are features of apoptosis (Mattson & Chan 2003). Lyng and colleagues (2002) demonstrated that transferring medium from irradiated human keratinocytes cells (0.5 or 5 Gy) to non-irradiated cells causes an increase in  $\text{Ca}^{2+}$  fluxes (within 30 s), loss of mitochondrial membrane potential (30 min – 2 hr) and an increase in reactive oxygen species (ROS) (after 6 hr of medium transfer). One study showed that a small number of cells in T98G and AGO populations had a  $\text{Ca}^{2+}$  response to ICCM harvested from the same cells and that the

time responses were different. They were able to conclude from this data that bystander factor(s) in the ICCM depend on the genotype of the irradiated cells (Shao *et al.* 2006).

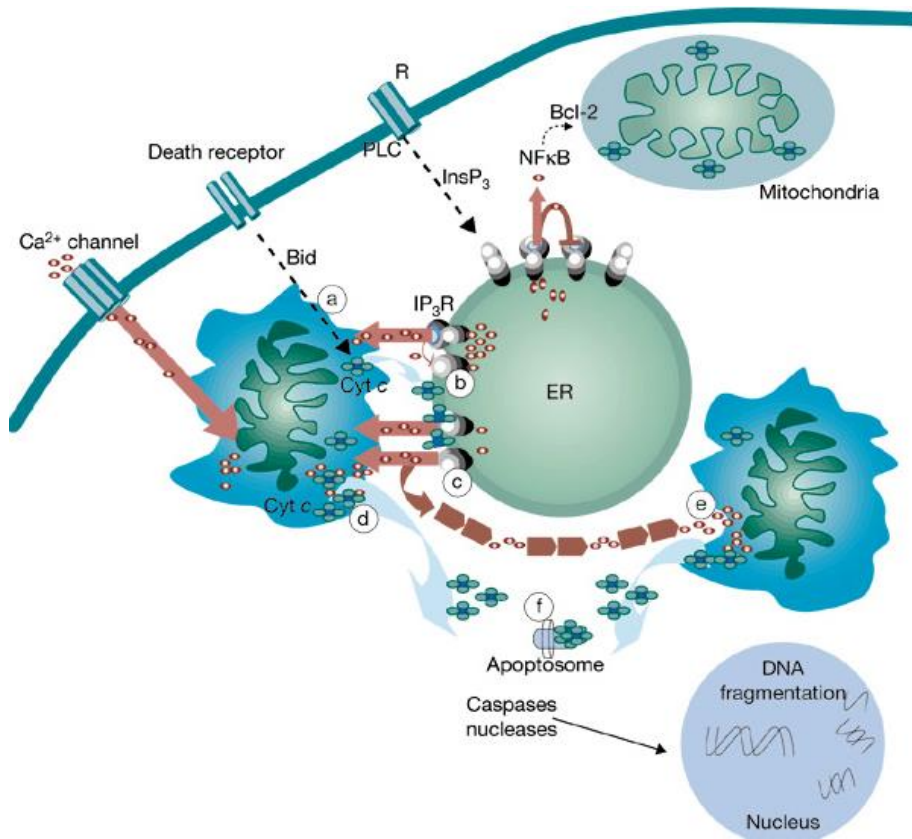


Figure 1.10 An illustration of the role of calcium as a mediator of intracellular bystander signalling in cells. An influx of  $\text{Ca}^{2+}$  triggers a series of biochemical processes upstream of apoptosis (Mattson & Chan 2003).

There is clear evidence advocating the extensive involvement of apoptotic mediated cell death in a bystander signalling cascade described in studies by Lyng and colleagues (Lyng *et al.* 2000; Lyng *et al.* 2002). The 2002 studies showed that apoptosis is initiated in non-irradiated cells receiving medium from directly irradiated cells, according to key apoptotic signalling events instigated including loss of mitochondrial membrane potential, influx of  $\text{Ca}^{2+}$  and an increase in ROS. Apoptosis is a tightly controlled and regulated process, necessary for the elimination of damaged cells that cannot be repaired. There are two important contributing factors to apoptosis; a loss of  $\text{Ca}^{2+}$  homeostatic control or very subtle changes in  $\text{Ca}^{2+}$  distribution within cells.  $\text{Ca}^{2+}$  overload can cause cytotoxicity and instigate apoptosis or necrotic cell death (Orrenius *et al.* 2003).  $\text{Ca}^{2+}$  induce changes in cell functions such as secretion, enzyme activation, and control of the cell cycle (Lyng *et al.* 2006). The slightest changes in  $\text{Ca}^{2+}$  signalling can have undesirable effects such as changes in cell proliferation and differentiation and modulation of apoptosis. Some reports have revealed a role for NADPH metabolism in bystander responses, associated with the mitochondrion (Deshpande *et al.* 1996). The increase in intracellular  $\text{Ca}^{2+}$  levels (Lyng *et al.* 2000; Lyng *et al.* 2002) and ROS (Lehnert *et al.* 1997; Shao *et al.* 2003; Azzam *et al.* 2002; Lyng *et al.* 2006; Lyng *et al.* 2006) have been highlighted by other reviewers as critical messengers in RIBE (Lyng *et al.* 2011).

The rise and decay of intracellular  $\text{Ca}^{2+}$  levels have been found to be similar to those of ROS indicating a close link between changes in  $\text{Ca}^{2+}$  and ROS production. Lyng and colleagues (Lyng *et al.* 2001) have demonstrated production of ROS and induction of apoptosis in human keratinocyte cells in response to radiation damage. Figure 1.11 shows how calcium is released from the endoplasmic reticulum (ER), the concentrated levels of  $\text{Ca}^{2+}$  in the mitochondria and the production of reactive oxygen species (ROS).

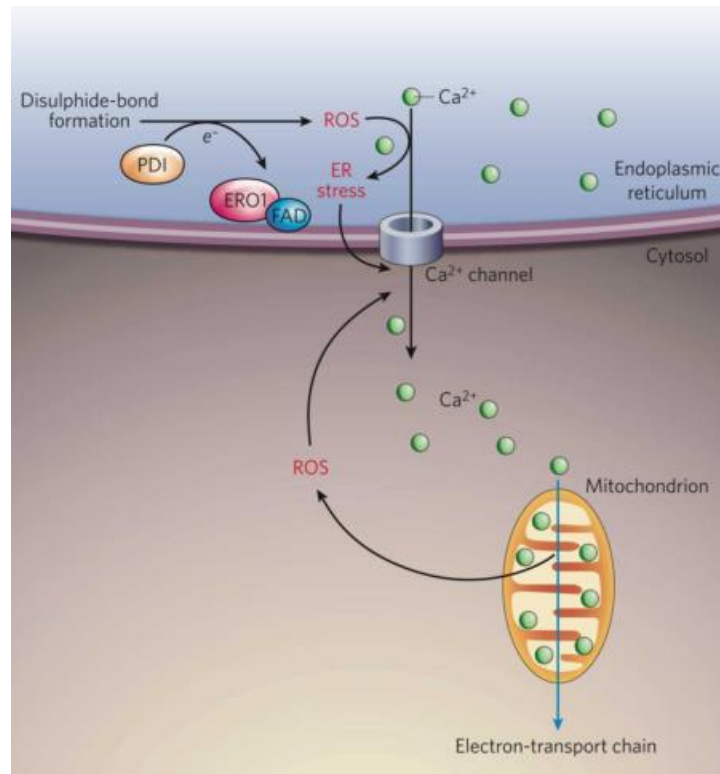


Figure 1.11 An illustration of calcium released from the endoplasmic reticulum that is concentrated in the matrix of the mitochondria and causes depolarisation of the inner mitochondrial membrane, disrupting electron transport and increasing ROS production. ROS produced in the mitochondria can instigate further release of calcium from the ER resulting in toxic amounts of ROS in the cell (Zhang & Kaufman 2008).

Normal cellular oxidative metabolism generates ROS and RNS and is responsible for control of cell growth pathways, which are effectively dependent on oxidants in cells. Disturbances to the balance of oxidant production and antioxidant defence modify the cellular redox environment inducing oxidative stress. In turn this encourages progression of diseases such as cancer.

Single energy deposition events from radiation instigate production of ROS in and around the radiation and in the intercellular matrix of the cell. ROS stimulate proliferation or cell death effects depending on their level of concentration. The contribution of free radicals such as ROS in bystander cells was first proposed by Clutton *et al.*, (1996). It is now known that production of ROS and NOS are key signalling events in bystander responses and thus central to many bystander investigations (Azzam *et al.* 2012). ROS travel from the directly-irradiated cell to a neighbouring non-irradiated bystander cell via redox-modulated intercellular communication mechanisms and has been extensively reviewed (Azzam *et al.* 2003; Mothersill & Seymour 2004; Prise & O'Sullivan 2009; Hei *et al.* 2011). Alpha-particle radiation has been shown to induce generation of ROS in cells, specifically superoxide anions and hydrogen peroxide (H<sub>2</sub>O<sub>2</sub>), causing indirect damage to DNA because of their toxicity (Narayanan *et al.* 1997). Studies have shown that nitric oxide (NO) production (Shao *et al.* 2003) and the presence of antioxidants and superoxide inhibitors and NO generators eliminate bystander effects (Narayanan *et al.* 1997; Azzam *et al.* 2002). Shao *et al.* (Shao *et al.* 2003) demonstrated that dimethyl sulfoxide (DMSO), a well-known ROS inhibitor, can decrease the number of MN produced in bystander cells thus reducing the bystander effect. The effectiveness of DMSO as a suppressor of the bystander signal in irradiated cells was further confirmed in a study that pre-treated cells to DMSO (Kashino *et al.* 2010) and showed reduced bystander effects.

Even though direct DNA damage is not required to induce RIBE, damage to DNA can be indirectly induced as a result of induction of these oxidative stress pathways such as ROS and NOS signalling in bystander responses previously described (Iyer *et al.* 2000; Shao *et al.* 2003). Exposure to IR causes a range of lesions in cellular DNA, including over 20 types of base damage, SSB's, DSB's and DNA–DNA and DNA–protein crosslinks (Prise *et al.* 2005). DNA DSB's have long been thought to be the most important factor for cell killing, with about 40 DSB's induced per 1 Gy in a typical cell (Olive 1998).

Many studies have focused on the DNA damage and repair processes in order to fully understand the mechanism and further implications of bystander effects (Mothersill *et al.* 2004). Mothersill *et al.*, studied mismatch repair (MMR) deficient cell lines exposed to ICCM to determine the bystander response from reduced clonogenicity. They demonstrated an increase in radiosensitivity in a panel of wild-type and mutant cells including DSB repair deficient cells and mismatch repair deficient cell lines. The overall bystander response is influenced by the repair phenotype of the cells receiving bystander signals as opposed to that of the cell producing the bystander signal (Kashino *et al.* 2010).

Mammalian cells provoke an integrated network of events in response to IR-mediated DNA damage. Figure 1.12 shows the complex signalling of oxidative stress and induction of DNA lesions in bystander cells. The measures taken involve functioning at both the protein and RNA levels to maintain genomic stability of the cells and to ensure consistency of genetic information (Jen & Cheung 2005). Non-irradiated cells receiving signals from low dose irradiated cells can exhibit a DNA damage response similar to the directly irradiated cells. At very low doses the DNA damage processes are responding

to the bystander factor, which must be shared between actual radiation energy and bystander signals. The bystander signal may be indirectly damaging nuclear DNA and initiating a transcriptional response, such as microRNA and regulating gene expression of bystander response pathways.

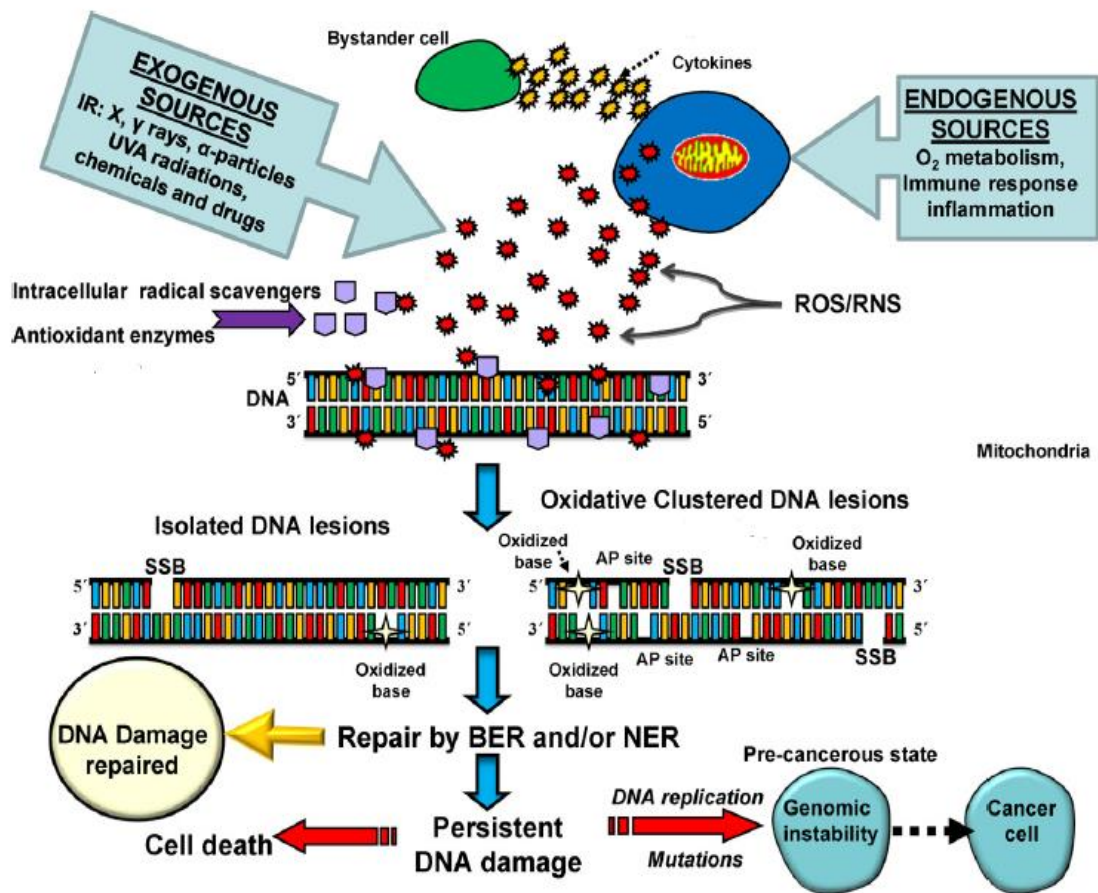


Figure 1.12 Intracellular oxidative stress and induction of DNA lesions. Intracellular communication in non-irradiated cells as well as oxidative metabolism, DNA repair mechanisms and cell death are the major mediators of responses to radiation (Kryston *et al.* 2011).

### **1.5.5 Potential Candidates for the Bystander Factor(s)**

Studies on the radiation induced bystander effect have hypothesised that a bystander factor is produced from cells directly irradiated and this factor is communicated to other cells causing the effects described previously. When medium is irradiated in the absence of cells, there is in fact no evidence of a bystander effect. In addition, bystander effects are dependent on the cell number present at the time of irradiation, suggestive of a cell derived factor involved in transmitting damaging signals (Mothersill & Seymour 1997).

Initially the factors were termed ‘clastogenic factors’ and believed to contribute to the development of carcinogenesis (Emerit 1994). Since then studies from Emerit and colleagues have revealed the presence of clastogenic factors in the plasma of patients undergoing radiotherapy (Emerit 1981; Khan & Emerit 1985; Emerit 1994; Emerit *et al.* 1995). Consequential biological and physiological changes can manifest shortly after or years after exposure signifying the persistence of the bystander response. Clastogenic factors have been found in plasma from atomic bomb survivors 31 years post-exposure (Pant & Kamada 1977). These clastogenic factors are now known to resemble the soluble bystander factors in media-transfer experiments. Cells in culture and tissue explants exposed to low doses of irradiation are capable of producing a bystander factor similar to clastogenic factors and have been explored by Mothersill, Seymour and colleagues (Seymour & Mothersill 2000; Lyng *et al.* 2000; Mothersill *et al.* 2001), including increased levels in cell death and reduced cloning efficiency. However, efforts to isolate the bystander factor(s) have been unsuccessful. Investigations have led to the discovery that the factor is small and transient and can travel over large distances through medium (600 – 700µm). The factor is also heat labile, denatures at 70°C and can survive freeze-thawing, suggestive that it is possibly a protein of some sort



(Mothersill & Seymour 1998). Candidate agents for the bystander factor include cytotoxic cytokines, mediators of ROS and/or RNS produced by low dose irradiated cells indirectly instigating DNA damage (Kashino *et al.* 2007; Chen *et al.* 2009; Lyng *et al.* 2011) and are implicated in the intercellular signalling of bystander responses (section 1.5.3). A recent study demonstrated an increase of apoptosis, TGF- $\beta$ , TNF- $\alpha$  in addition to induction of a Ca<sup>2+</sup> flux. This is comparable with the intercellular bystander signalling discussed (Irons *et al.* 2012). TGF $\beta$ , TNF- $\alpha$ , IL-8 and ROS are suggested intercellular signalling candidates reviewed by Blyth and Sykes (Blyth & Sykes 2011).

#### **1.5.6. Radiobiological Studies of Bystander Responses**

Studies of IR-induced non-targeted effect (NTE) responses *in vitro* and *in vivo* have been extensively investigated and reviewed (Matsumoto *et al.* 2007; Burdak-Rothkamm & Prise 2009; Wright 2010; Morgan 2012; Mothersill & Seymour 2012), with significant focus on the new challenges that have arisen in evaluating the potential hazards associated with low dose radiation exposures. Interestingly, both high and low LET radiations have been shown to induce a bystander effect in non-irradiated cells (Azzam *et al.* 2000). It has been suggested that low dose bystander effects may be the chief responses of low LET x-ray or gamma radiation (Seymour & Mothersill 2000) following  $\alpha$ -particles irradiations (Little *et al.* 2002).

### 1.5.6.1 Evidence *In vivo*

It was suggested that in a tissue environment, differentiation responds to irradiation as a means of protection from subsequent damage (Belyakov *et al.* 2006). In a study by Xue *et al.*, (2002) mice were injected with cells pre-labelled with the radioactive element  $^{125}\text{I}$  and distinct inhibition of growth was revealed. A bystander effect generated *in vivo* by the radio-labelled cells was most likely signalled to the non-targeted cells in the mice (Xue *et al.*, 2002).

Tissue models have unveiled bystander effects in distant tissues whole animals. For example, experiments employing partial body irradiations in mice revealed an induction of epigenetic changes (DNA methylation, histone modification and RNA-associated silencing) in unexposed bystander parts of mice (Koturbash *et al.* 2006). The same research group designed an *in vivo* model using the skin of rats and subjected the rats to half-body exposure by protecting the rest of the body with a thick lead shield (Koturbash *et al.* 2007). Data from the study revealed bystander effects occurred in distant non-irradiated spleen tissue. The study not only uncovered the spleen as an important target organ for the bystander effect but indicated the persistence of bystander signals in distant tissues. A follow-up study confirmed their findings and reported that direct cranial exposure in mice results in altered levels of cellular proliferation and apoptosis, as well as increased expression of tumour suppressor p53 protein in the bystander spleen tissue (Koturbash *et al.* 2008). There were significant different levels of DNA damage and sensitivity in bystander spleen tissue of the male and female mice, highlighting that bystander effects can be sex-specific coupled with the various sensitivities found between different strains of mice (Coates *et al.* 2008).

Lorimore *et al.*, (2008) investigated descendants of normal mouse hematopoietic clonogenic stem cells and exposed them to bone marrow-conditioned medium derived from gamma-irradiated mice. The normal stem cells exhibited chromosomal instability assessed by non-clonal cytogenetic aberrations in the clonal descendants of non-irradiated stem cells distinctly different to the descendants of gamma-irradiated cells. In a recent report Ilnytsky *et al.*, (2009) demonstrated that acute and fractionated exposure to IR induces epigenetic bystander effects within the same organism and are very distinct in different bystander organs. The report showed an induction of distinct DNA methylation changes in bystander spleen and the skin of mice subjected to single-dose (acute) or fractionated whole-body and cranial head X-ray exposure.

Transmission of bystander signals between organisms was first identified by Surinov and colleagues using mice (Surinov *et al.*, 2001). In their report they described the bystander phenomenon in which mice can produce bio-chemicals influential on the growth, survival and reproduction in the bystander mice. Since then, these effects have been discovered in other species such as rats, different species of fish (Mothersill *et al.* 2006) and tadpoles (Audette-Stuart *et al.* 2011) (reviewed by Mothersill & Seymour in 2012). Additionally, bystander effects have been found in different species of fish. There is clear evidence that bystander signals can be passed between species of freshwater rainbow trout (*Oncorhynchus mykiss*) (Mothersill *et al.*, 2006; Smith *et al.*, 2007). Transmission of the bystander signal occurs through the release of a messenger (bystander factor(s)) into the water. Studies have elucidated that bystander signals can be transmitted *in vivo* between freshwater rainbow trout gill but also the bystander signal has the ability to persist during the lifespan of the fish, further implicating issues surrounding whether or not bystander responses are protective (Mothersill *et al.*, 2010). The interesting data generated from these studies could be of relevance for human

health radiation protection issues and it is anticipated that further investigations into the specific bystander response signalling mechanisms will clarify this.

#### **1.5.6.2 Evidence *In vitro***

Both irradiated and non-irradiated cells can exhibit an up-regulation of stress inducible proteins, genetic changes, an induction of cell cycle checkpoints and cell death. John Little's research group at Harvard University in Boston (USA) were one of the first to report genetic alterations, such as sister-chromatid exchanges (SCE- the exchange of segments between sister chromatids during mitosis) and mutations induced by IR in the neighbours of cells that had received direct radiation (Nagasawa & Little, 1992). They examined the effect in Chinese hamster ovary cells post exposure to low fluences of high LET radiations ( $\alpha$ -particles) and revealed that the IR only traversed about 1% of cells *in vitro*, followed by an increase in sister chromatid exchange (SCE's) in 30% of the cells in culture. This was later confirmed in experiments using low LET radiation (Mothersill & Seymour, 1997). SCE's are frequently increased by IR and other damaging mutagens. Inhibition of stress inducible proteins and SCE's (Lehnert *et al.* 1997) is possible with antioxidant superoxide dismutase (SOD) and catalase and can terminate the bystander response (Azzam *et al.*, 2002). Antioxidant inhibitors such as SOD, catalase and N-acetylcysteine are particularly successful inhibitors of ICCM induced cell death (Lyng *et al.*, 2006).

The clonogenic technique developed by Puck & Marcus (Puck & Marcus 1956) has shown that cells are capable of responding to a bystander signal produced by the irradiated cell, and was the gold standard method in many bystander studies to report

bystander signalling in a variety of cell lines (Mothersill *et al.* 2000; R Iyer & Lehnert 2002) . The medium transfer technique developed by Mothersill and Seymour (Mothersill & Seymour 1997) was used to show a bystander response in HaCaT cells which revealed reduced cloning efficiencies. Bystander effects depend on the type of radiation distributed to the cell and appear to be cell- and genotype-specific (Baskar *et al.* 2007). Therefore, bystander effects have been observed in some cell systems but not others (Fournier *et al.*, 2009; Groesser *et al.*, 2008). Studies show that there is no evidence for a bystander response in a normal human fibroblast cell line, demonstrating how biological variation exists and creates issues for determining the risks associated with RIBE (Sowa *et al.* 2010). In 1997 Mothersill and Seymour investigated four cell lines for bystander effects: MSU-1 fibroblasts, PC-3 prostate carcinoma cells, SW48 colorectal cancer cells and HaCaT epithelial cells. Medium harvested from irradiated fibroblasts again showed no effect, with greater effects shown in the colorectal and epithelial cells. Therefore HaCaT's have been regarded as one of the most sensitive of cell lines reporting bystander effects (Mothersill & Seymour 1998).

A selection of fish cells and human keratinocyte HPV-G reporter cells receiving media from irradiated fish cells were used to assess which cells lines were good reporters of the bystander effects. HPV-G have a well-established bystander response (Liu *et al.* 2006) and showed increases in survival which was expected, whereas the fish cell lines did not respond. The study concluded that the fish cells may not be capable of producing a bystander factor and therefore signal production and response must be separate processes, which was described earlier in section 1.5.2 and 1.5.3 (O'Neill-Mehlenbacher *et al.*, 2007).

Bystander effects have been reported in partial-organ radiation exposure experiments (Khan *et al.*, 1998) whereby induction of DNA damage both in and out of the direct radiation field showed an increase in MN formation in the lung fibroblasts. Formation of MN is indicative of DNA damage or mutations in cells exposed to IR and subsequently increasing the risk of carcinogenesis. Alpha particle microbeam exposures have been employed to 3D human skin models ( Belyakov *et al.*, 2005) and show that the bystander effect can cause an induction of MN transmitting the effect for distances up to 1000 $\mu$ m from the original radiation site. The presentation of MN may represent a possible protective mechanism, removing damaged cells. Data from a ureter primary explant model study (Mothersill *et al.* 2001) revealed an induction of differentiation (the development of cells). Cells are not always killed in response to damage but can be removed from the clonogenic pool, so that the genetic stability of the system is maintained. The primary explant model developed by Mothersill *et al.*, (2001) allows tissue to be dissected and cultured *in vitro*. It specifically combines an investigation of the *ex vivo* effects while maintained *in vitro*. It is therefore a successful method for the investigation of bystander effects compared to *in vivo* methods exposing a whole animal while alive.

#### **1.5.6.3 Immortal Human Keratinocyte Cell Line- Bystander Reporter Model**

HaCaT cells are spontaneously immortalized non-tumorigenic human keratinocytes composed of a heterogeneous cell population with different proliferative abilities and differentiation grades, and are similar to primary keratinocytes (Boukamp *et al.* 1988; Balduzzi *et al.* 2010). HaCaT cell lines are commonly used in bystander media transfer experiments since they are well-established as reporters of the bystander response and

that is why they were chosen for the following study. A number of studies have successfully shown bystander effects in HaCaT cells and reported sensitivity of these cells to low doses of irradiation (Howe *et al.* 2009; Mothersill *et al.* 2009; Ryan *et al.* 2009; Lyng *et al.* 2012). Not only are HaCaT cells good reporters but they have also shown dose dependent responses to various low doses of IR and furthermore variation in response from ICCM generated from lymphocyte cultures from a cohort of patient blood samples (Howe *et al.*, 2009). These varied responses were either protective, due to a possible hormetic effect, or detrimental but patient variation in response to radiation is well known so HaCaT reporter cells were capable of showing this variation.

## **1.6 Cell Death Mechanisms – Overview**

Radiation-induced apoptosis is believed to be one of the major mechanisms of radiation-induced cell death (Prise *et al.*, 2005). Data has emerged describing evidence of changes in mitochondria, followed by caspase activation through either the intrinsic or extrinsic apoptotic pathway in response to radiation (Eriksson & Stigbrand, 2010; Prise *et al.*, 2007). Remarkably, reports have shown a considerable role for apoptosis-mediated cell death in non-irradiated cells ( Belyakov *et al.*, 2003; Belyakov *et al.*, 2001; Lyng *et al.*, 2000; Prise *et al.*, 1998). An increase of apoptotic cell death in the non-irradiated populations has been referred to now as one of the key hallmarks of radiation-induced bystander signalling, both *in vitro* and *in vivo* (Koturbash *et al.* 2008; Hamada *et al.* 2008; Asur *et al.* 2010).

Apoptosis is a well-defined cell death process and possibly the most frequent form of cell death. However there are other forms of cell death that can occur in response to

cellular damage depending on the stimuli. Other modes of cell death include mitotic catastrophe, necrosis and autophagic cell death and are collectively defined here as the non-apoptotic modes of cell death.

### **1.6.1 Non-apoptotic Modes of Cell Death**

Although apoptosis has been implicated in RIBE, other forms of cell death have been studied for their relationship to RIBE and are discussed below. It is possible that cross-talk between the different modes of cell death occurs in RIBE and so should be considered.

#### **1.6.1.1 Mitotic Catastrophe**

The relationship between radiation-induced apoptosis and clonogenic survival is complex because, after radiation, cells could die by apoptosis as a consequence of mitotic death as well as non-mitotic death, or by mitotic death without apoptosis. Mitotic catastrophe is thought to be a delayed form of cell death that is understood to occur during or as a result of irregular cell division, i.e. mitosis (Eriksson & Stigbrand 2010). Such irregularity would occur following DNA damage and deficient cell cycle checkpoints and a result of possible mutation of tumour suppressor P53. It has been shown in chromosomal aberration studies that cells in the absence of wild-type P53, are capable of a further cycle of division with increased numbers of aberrations, ultimately leading to a delayed form of apoptosis (Nitta *et al.* 2004). In 2005, Howe *et al.*, investigated whether there is a correlation between G2 chromosomal radiosensitivity



and specific aneuploid aberrations that are indicative of mitotic cell death in IR exposed patient prostate blood samples, and found a small and significant correlation (Howe *et al.* 2005). There is emerging evidence that mitotic catastrophe does not constitute a 'pure' cell death executioner pathway, but an onco-suppressive mechanism that precedes and is distinct from, yet operates through, cell death or senescence (Vakifahmetoglu *et al.*, 2008; Vitale *et al.*, 2011). More recently, our research group demonstrated increased mitotic cell death in HaCaT cells exposed to low doses of IR (Jella *et al.*, 2013).

#### **1.6.1.2 Necrosis**

For some time necrosis was thought to be an accidental cell death mechanism because it differs from apoptosis morphologically. An extensive amount of research has been invested into finding out exactly how this form of cell death is signalled and why it varies from other cell death modes. Studies conclude that necrosis is actually a highly controlled and regulated response pathway that is initiated in response to extreme physiological and pathological stress (Vandenabeele *et al.*, 2010). Necrosis is thought to be induced by death receptors, such as NF-kappa B-activating complexes and mediated by RIP1 and its homolog RIP3 dependent activity, which fully engage in functional interactions, ultimately activating the execution of necrotic cell death (Muñoz-Pinedo 2012). The presence of necrotic cells is frequently construed by the immune system as dangerous and therefore signals an immune response (Taylor *et al.*, 2008). Increased levels of necrosis have been found in shielded mega-colonies of human melanoma Me45 (Przybyszewski *et al.* 2004), whereas other bystander experiments have shown

larger increases of mitotic cell death (Jella *et al.* 2013), it is possible that the response is varied for different radiation types and doses.

### **1.6.1.3 Autophagic Cell Death**

The term ‘autophagic cell death’ has been widely used to indicate instances of cell death based on the specific morphological features, such as massive cytoplasmic vacuolisation (Galluzzi *et al.* 2012). Autophagy has been described as a survival mechanism, activated in cells subjected to nutrient or growth factor deprivation (Krysko *et al.* 2008). There is evidence to suggest that the mechanism of autophagy has similar features to necrosis, in that it can be mediated by RIP1. It can therefore be difficult to always distinguish between the two forms of cell death, although it is understood that there are clear morphological differences between autophagy and apoptotic cell death. The complex process of autophagic cell death has yet to be elucidated. Autophagy has been described as a form of cell death in cancer in response to radiation, and so could have implications in RIBE (Baskar *et al.* 2012). Negative regulation of autophagy has been shown to occur through the phosphatidylinositol 3-phosphate kinase (PI3K-Akt-mTOR) signalling pathway. The cascade is said to be the main signalling pathway in which autophagy is induced, and is activated in many types of cancer (Kondo *et al.* 2005).

## 1.7 Apoptosis

Apoptosis is a regulated process vital for the normal development and maintenance in tissue homeostasis, through regulation of cell numbers within a population (Wilson *et al.*, 2000). This form of apoptosis is well known as ‘programmed cell death’. Apoptosis can also be induced from uncontrolled cell cycle events and has been implicated in the development of many forms of carcinogenesis (Wilson *et al.*, 2000). The term ‘apoptosis’ was first introduced in 1972 by Kerr *et al.*, to describe a form of cell death that is morphologically different to other modes of cell death that exist (necrosis, mitotic catastrophe and autophagy). Characteristic morphological changes include cell shrinkage, membrane blebbing, nuclear and cytoplasmic condensation (Kerr *et al.*, 1972). However, it has been proposed that the presence of specific morphological features is not always sufficient to establish a causal link between a given process and cellular death.

The Nomenclature Committee on Cell Death (NCCD) is an international organisation that was set up in 2005 in an attempt to define international standards for the definition and classification of cell death. Prior to this, cell death definitions were based purely on morphological criteria. The first meeting in 2005 (Kroemer *et al.*, 2005) was to define different forms of cell death including apoptosis mostly focusing on how apoptosis can occur with and without caspase activation and that Autophagy represents a cell death mechanism but not necessarily via autophagic vacuolisation. Research progressed to next meeting in 2009 (Kroemer *et al.*, 2009) and revealed a ‘quantitative’ method of describing the biochemical features associated with cell death. Their most recent 2012 (Galluzzi *et al.*, 2012) meeting reported the molecular progression with appropriate

classifications and clear reference to the biochemical mechanisms involved in cell death.

In vertebrates, apoptosis typically proceeds through two central signalling cascades that lead to packaging the contents of dead cells into apoptotic bodies that can be recognised by neighbouring cells or macrophages and cleared by phagocytes (Elmore 2007). The pathways are tightly controlled processes maintaining a balance of pro-survival signals in the cell, but mutations of tumour suppressor P53 or overexpression of many anti-apoptotic proteins can induce tumourgenesis (Jin & El-Deiry 2005). Mutations of tumour suppressor P53 is common in many tumour cells consequently disabling apoptosis.

The first pathway of apoptosis is the extrinsic pathway, otherwise known as the death receptor pathway. The second is the intrinsic pathway also called the mitochondrial pathway. The two pathways converge at the apoptotic execution step where the executioner caspases, 3, 6 and 7 and other proteases and nucleases drive the final events to execute apoptosis. Therefore these two pathways are known as caspase-dependent signalling pathways. Caspase 3, 6 and 7 are more abundant and active than the upstream 'initiator' caspases 8 and 9 (Jin & El-Deiry 2005). Pro-caspase 3 and 7 can be activated by caspase 6, 8, 9 and 10. Remarkably, studies have shown that caspase 6 and 7 can compensate for the loss of caspase 3 (Zheng *et al.* 2000). Studies have shown that caspase-6 can be processed by caspase-7 in a caspase-3 independent manner in cells undergoing apoptosis (Inoue *et al.*, 2009). Radiation-induced apoptosis follows the intrinsic apoptotic route in particular as the bystander factor acts as the external stimulus entering the cell through membrane channels or gap junctions and initiating the intrinsic response via the mitochondria. Figure 1.13 describes three fundamental apoptotic events

initiated at the cellular membrane by different stimuli and the subsequent downstream events leading to the execution step where the three pathways converge using the same executioner caspase proteins.

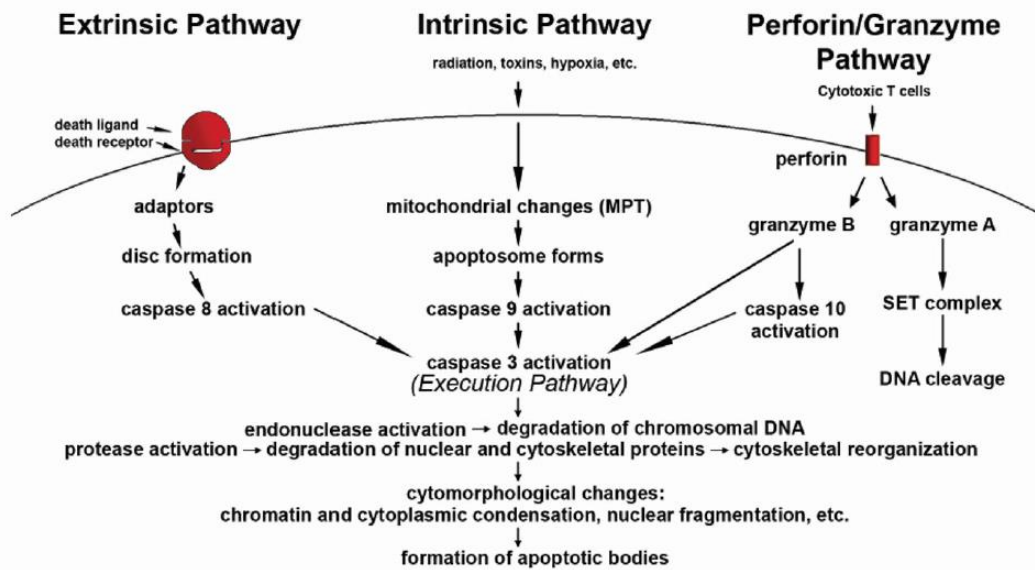


Figure 1.13 Schematic representations of apoptotic events. The two main pathways of apoptosis are illustrated, the extrinsic and intrinsic apoptotic pathways. Each pathway is independent from one another, and dependent on specific triggering signals to initiate activation. Each pathway activates their own specific initiator caspases and the two key pathways converge on the same executioner caspases for the final steps of apoptosis. However, the Granzyme/Perforin pathway is a caspase-independent process. The executioner caspases are responsible for the morphological features characteristic to apoptosis including membrane blebbing, chromatin condensation and the formation of apoptotic bodies that are then removed by nearby phagocytes (Elmore 2007).

Crosstalk at both the initiation and execution levels of the extrinsic and intrinsic pathway has been reviewed. The formation of multi-protein signalling complexes can either directly activate the caspase cascade or it can connect the extrinsic to intrinsic pathway through cleavage of BH3-only protein to Bid. This is directed through mitochondrial damage in the Fas pathway of apoptosis and mediated by caspase 8. caspase 8 can cleave and subsequently activate effector caspase 3 directly or it can activate the pro-apoptotic BH3-only protein Bid, triggering the release of cytochrome c from the mitochondria and activating effector caspases (Igney & Krammer 2002).

Apoptosis can be induced through a third pathway known as the Perforin Granzyme pathway. Granzymes are serine proteases that are released by perforin-containing cytoplasmic granules within cytotoxic T cells and natural killer cells. Their purpose is to induce apoptosis within virus-infected cells, thus it is less likely to be a route of cell death in cells damaged by IR. Granzyme can activate apoptosis by directly activating caspases, similar to the approach that initiator caspases activate effector caspases (Logue & Martin 2008). However, Granzymes can also induce apoptosis through the mitochondrial pathway, by cleaving the BH3-only protein Bid (Muñoz-Pinedo 2012).

### **1.7.1 Extrinsic Apoptosis**

The term extrinsic apoptosis has frequently been used to describe cell death that is induced by extracellular stresses, including anticancer chemotherapy inducing apoptotic stimuli (Fulda & Debatin 2006). Extrinsic signals are initiated at the plasma membrane through binding of death inducing ligands to cell surface receptors (Jin & El-Deiry 2005) such as Fas/CD95, tumour necrosis factor receptor (TNF-R1) and TRAIL

receptor. Receptors have a cysteine-rich extracellular domain and a cytoplasmic domain of about 80 amino acids, known as the death domain (DD). The DD transmits extracellular signals to the intracellular signalling pathways.

Stimulation of the death ligands leads to oligomerisation of the cell surface receptors, such as FasL to FasR1 and recruitment of the cytoplasmic adaptor protein Fas-associated death domain (FADD), which exhibits its DD binding to receptors. The receptor TNF- $\alpha$  is bound to TNFR1 following the same sequence of events and recruits an adaptor protein TRADD (Elmore 2007), which binds to another adaptor protein FADD. FADD can then associate with pro-caspase 8 through dimerisation of the death receptor domain. At this stage, death-inducing signalling complex DISC has been formed (Cain *et al.*, 2002), resulting in the activation of caspase 8, followed by activation of downstream effectors of the cell death program, caspase 3, 6 and 7, which effectively execute the final stages of apoptosis.

Most cancer cells are sensitive to death-ligand TRAIL whereas most normal cells are resistant. The relationship between the intrinsic and extrinsic pathways suggest the possibility that irradiated cells could eventually become sensitised to specific death ligand-induced apoptosis such as TNF-related apoptosis-inducing ligand (TRAIL). In addition, the TRAIL death ligand signalling occurs independently of tumour suppressor p53 (Jin & El-Deiry 2005).

Within white blood cells (lymphocytes) such as B cells, T cells and natural killer cells, caspase 8 activation is above the threshold and so can effectively activate the effector caspases, thus executing apoptosis. In hepatocytes, which are cells that make up most of the liver, the caspase 8 activation is below the threshold needed to fully execute apoptosis and so it requires contribution of the intrinsic pathway (Galluzzi *et al.* 2012).

Thus it is possible that the mitochondrial pathway is the most sensitive detector of apoptotic signals (Assefa *et al*, 2005).

### **1.7.2 Intrinsic Apoptosis**

The intrinsic pathway also referred to as the mitochondrial pathway is promoted by a diverse range of intracellular stimuli including radiation, influx of  $\text{Ca}^{2+}$ , growth factor deprivation and oxidative stress (Oberst *et al*, 2008). Radiation frequently prompts an intrinsic-apoptotic response. The process involves mitochondrial outer membrane permeabilisation (MOMP) and release of pro-apoptotic factors into the cytosol to initiate the cell death cascade. The signalling response stimulates release of cytochrome c from the mitochondria into the cytosol. Apaf-1 is a 130 kDa protein, and when in the presence of dATP and cytochrome c it forms a large apoptosome complex of around 700 – 1400 kDa (Cain *et al*. 2002). This wheel like structure is said to contain eight Apaf-1 subunits which in turn recruit and process caspase 9 to form a holoenzyme complex, and subsequent activation of effector caspases 3, 6 and 7 (Brentnall *et al*, 2013). There are factors responsible for the regulation in the formation and function of the apoptosome. These factors include intracellular levels of potassium ( $\text{K}^+$ ) inhibitors of apoptotic proteins (IAP), heatshock proteins (HSP) and Smac/Diablo which is a mitochondrial protein responsible for inhibition of IAP via mediation of caspases (Cain *et al*. 2002). The factors are responsible for correct assembly and functionality of the apoptosome as soon as the cell has reached the point in which it cannot recover from the fate of death.



Although the sources of apoptotic stimuli are heterogeneous, they are connected to a central mitochondrial control mechanism (Galluzzi *et al.* 2012). Other factors that can be released from the mitochondria are responsible for the morphological features of apoptosis. Both the mitochondria and the endoplasmic reticulum (ER) contribute to intrinsic apoptosis. Stress such as cellular radiation can burden the ER causing an increase of oxidative stress in the cell. Subsequent to the initial stress signal, the unfolded protein response (UPR) is instigated, a direct result of unfolded proteins in the ER. The UPR intends to restore normal cellular function and does so by resolving the unfolded protein issue via an increase of folded protein production and if this is not successful the response will persuade apoptotic cell death (Jimbo *et al.* 2003). The ER is known to be a major intracellular store of  $\text{Ca}^{2+}$  ions which are released into the cytosol in response to initiation of apoptosis. Remarkably, an influx of  $\text{Ca}^{2+}$  ions from the ER is often associated with uptake into the mitochondria. Pro-apoptotic Bax has been implicated in maintaining homeostatic concentrations of  $\text{Ca}^{2+}$  in the ER, and therefore possibly responsible for ER-induced intrinsic apoptosis (Jin & El-Deiry 2005). Figure 1.14 describes the apoptotic intrinsic and extrinsic signalling pathways. The extrinsic pathway followed is decided at the cell membrane where ligands bind to their specific receptors but other external stimulus interrupts the mitochondria and ER to execute the intrinsic pathway.

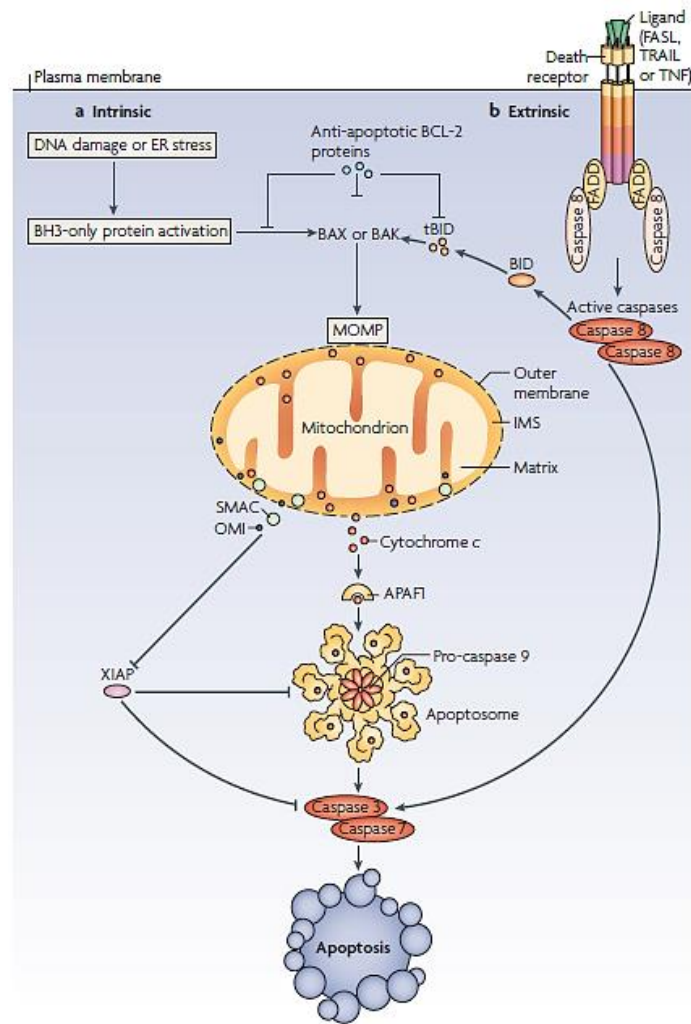


Figure 1.14 A schematic description of the intrinsic and extrinsic pathways of apoptosis. Specific ligands bind to their receptors at the cell membrane activating the extrinsic apoptotic pathway. Whereas, external stimulus such as ionising radiation can stimulate the endoplasmic reticulum and initiate activation of mitochondrial proteins in the cell. (Tait & Green 2010)

### 1.7.3 Mitochondria and Bcl-2 Signalling

Radiation-induced apoptosis appear to involve changes in mitochondria membrane permeability, followed by caspase activation (Prise *et al.* 2005). B cell lymphoma 2 (Bcl-2) family of proteins maintain mitochondrial membrane status and the balance of interactions between the members of the Bcl-2 protein family which in turn maintains regulation of  $\text{Ca}^{2+}$  homeostasis of the cell (Jin & El-Deiry 2005).

The Bcl-2 family of proteins are grouped into three sub-families centred on mutual BH (BCL-2 Homology) domains. The first are the anti-apoptotic proteins that include Bcl-2, Bcl-xL, Bcl-w, Mcl-1 and A1/Bfl-1. Then the Pro-apoptotic proteins are classified by BH (BH1-3) domains, Bcl-2 associated-X protein (Bax), Bcl-2 killer (Bak) and Bok and finally the BH3-only domain proteins (Lomonosova & Chinnadurai 2008). Damage to the cell will either antagonise anti-apoptotic proteins of the Bcl-2 family or activate multi-domain pro-apoptotic Bax and Bak. The events give rise to cell death through either the release of molecules involved in apoptosis or the loss of mitochondrial functions, essential for cell survival.

Mitochondria are critical regulators of the intrinsic pathway and when they undergo a loss of mitochondrial membrane potential ( $\Delta\Psi_{\text{mito}}$ ), the apoptotic pathway is activated. The process of MOMP is mediated and controlled through interactions of pro and anti-apoptotic Bcl-2 family members (Lyng *et al.*, 2000). Dominance by pro-apoptotic signalling instigates MOMP (Chipuk *et al.*, 2006). Subsequent to initial apoptotic stimuli, pro and anti-apoptotic Bcl-2 family of proteins begin to migrate and assemble on the mitochondrial membranes, anti-apoptotic signals are accountable for allowing the cell to cope with a certain level of stress (Galluzzi *et al.* 2012).

Pro-apoptotic Bax is a 21 kDa monomeric cytosolic Bcl-2 family protein and translocates to the mitochondria in the early stages of intrinsic apoptosis. Bax is activated as a result of conformational changes in its structure, oligomerisation and is inserted into the outer mitochondrial membrane (OMM), leading to MOMP (see Figure 1.15) which will be activated within the first five minutes of apoptosis (Oberst *et al.* 2008). Structural similarities have been observed between BCL-2 proteins such as Bax and Bcl-xL (Bcl2-L1) and bacterial pore-forming toxins and so it is possible that BAX and BAK might be capable of directly forming pores in the mitochondrial outer membrane (Suzuki *et al.* 2000). Alternatively, mitochondrial permeability transition (MPT) can occur on the inner mitochondrial membrane as a result of opening of the multi-protein complex, permeability transition pore complex (PTPC) (Galluzzi *et al.* 2012). Knockout studies have shown that cells lacking pro-apoptotic Bax or Bak will not undergo MOMP or subsequent apoptosis (Wei *et al.* 2001)

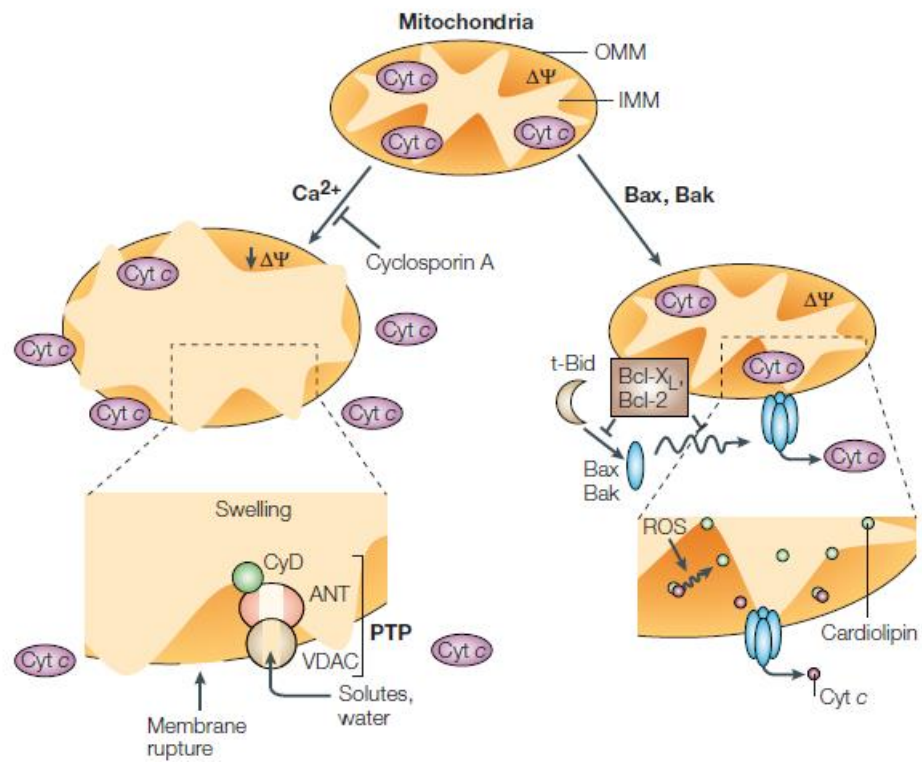


Figure 1.15 Mechanisms of release of intermembrane-space proteins from mitochondria. The two mechanisms for permeabilisation of the outer mitochondrial membrane (OMM) (Orrenius *et al.* 2003).

A cell death-associated biochemical process can develop in apoptosis and is deemed reversible until the irreversible phase the 'point of no return' is crossed, and until that point is reached, it may not lead to the cell demise. The permeabilisation of the mitochondrial outer membrane is implied as this irreversible point of no return stage of intrinsic apoptosis and it can trigger additional ROS production (Chipuk *et al.* 2006). A reduction in mitochondrial membrane potential ( $\Delta\Psi_{\text{mito}}$ ) is followed when the external mitochondrial membrane becomes permeabilised. Lethal proteins are released from the mitochondrial intermembrane space (IMS) into the cytosol through the pores formed and regulated by Bcl-2 family proteins. Cytochrome c is released in addition to the simultaneous release of other molecules to antagonise the inhibitory functions of IAP's on effector caspases. The release of cytochrome c in the presence of ATP triggers oligomerisation of apoptotic protease-activating factor 1 (APAF1). This instigates formation of the apoptosome, recruiting and activating initiator caspase 9 and possibly caspase 2, which in turn recruits effector caspases 3, 6 and 7 allowing for execution of apoptosis (Jin & El-Deiry 2005).

Reports show that Bax is capable of forming a channel allowing protein permeabilisation or it can act with another pro-apoptotic protein called Bak to form the pathway. Bax acts directly on ceramide channels formed in phospholipid membranes causing them to disassemble (Ganesan & Colombini 2010). Evidence has emerged for the association of ceramide with Bax activity. Cumulative mitochondrial ceramide provokes Bax translocation to mitochondria and subsequent activation. Thus it is possible that activated Bax and ceramide can synergistically induce MOMP (Ganesan & Colombini 2010) and that ceramide may be a secondary messenger that can activate apoptosis. A ceramide-mediated process is said to be generated by the activation of acid sphingomyelinase, leading to hydrolysis of sphingomyelin to ceramide. Ceramide might

also be released by direct activation of mitochondrial ceramide synthase through cellular exposure to radiation.

Anti-apoptotic Bcl-2 is a 26kDa protein that can be located in the mitochondria, ER and perinuclear membranes (Kang & Reynolds 2009). The permeabilisation of the mitochondrial membrane releasing cytochrome c can be inhibited by the addition of anti-apoptotic Bcl-2. Early studies examining cell death initiated by cell damage, such as IR, found that overexpression of Bcl-2, prevents cell death.

### **1.8 The Caspases – Overview**

Radiation-induced apoptosis has been described as a caspase-dependent process, although there are still uncertainties surrounding the sequence of caspase activation in response to non-targeted radiation. Caspases are a family of aspartic acid-specific proteases and the major effectors of intrinsic apoptosis (Chowdhury *et al*, 2008). Robert Horvitz first documented the importance of caspases in apoptosis through genetic studies of development of the nematode *Caenorhabditis elegans*, he discovered that *C. elegans* have at least four genes, ced-3, ced-4, ced-9 and egl-1 which are central to the execution of apoptotic cell death and caspases are homologous to the ced-3 gene (Graves *et al*. 1998).

Since then, a total of 12 proteases have been discovered in mammals including caspase 1 – 10 and caspase 12 and 14. Caspases are divided into two classes centred on their function, structure, length of their N-terminal prodomain, substrate specificity and abundance in cells. Caspases are expressed as single-chain pro-enzymes composed of three domains: an N-terminal pro-peptide, a large subunit and a small subunit (Logue &

Martin 2008) and are synthesised as inactive pro-caspases in cells (see Figure 1.16 a). The mechanism of caspase activation (see Figure 1.16 b) involves internal cleavage of the small and large subunits so that they separate and form a catalytic site (Markus G. Grütter 2000). It has been suggested that because caspase 3 and 7 are deficient of linker regions, the catalytic site cannot form in the absence of proteolytic cleavage between the subunits (Cain *et al.* 2002).

Since a variety of stimuli including radiation can activate caspases, the order in which caspases are activated is central to understanding the signalling events unique to the stimulus involved. Radiation-induced apoptosis occurs via activation of caspases through cleavage of cytosolic proteins, leading to the phagocytic engulfment of an apoptotic cell, and thus removing damaged cells from the body (Tait & Green 2010). Activation of caspases is fundamental to apoptotic cell death and is controlled by a balance of pro- and anti-apoptotic Bcl-2 family proteins, HSP and IAP's (Launay *et al.* 2005).



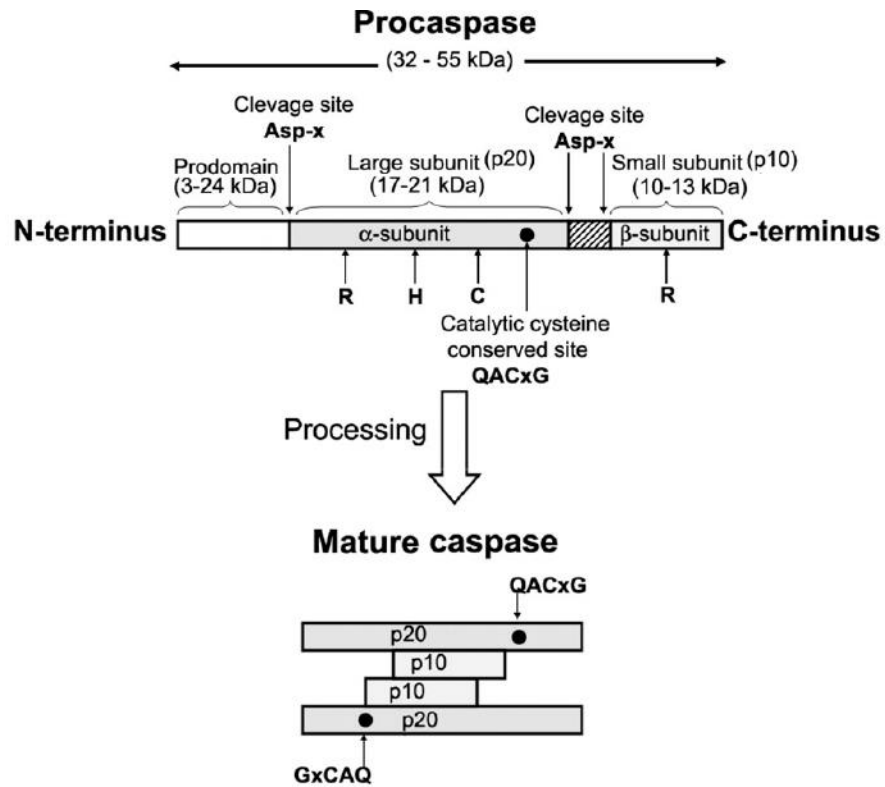


Figure 1.16 (a) A schematic representation of the structural features of mammalian caspases. C, H and R are the active site residues. Caspases are synthesised as a catalytically dormant tripartite proenzyme, which is a single polypeptide chain of 32-55 kDa in size representing three domains. The pro-caspases consists of a 17- 21 kDa large central internal domain (p20) containing a large catalytic subunit (active site), a 10-13 kDa small C-terminal domain (p10) also called a small catalytic subunit and a 3-24 kDa NH<sub>2</sub> terminus prodomain called a death domain (DD) (Chowdhury *et al.* 2008).

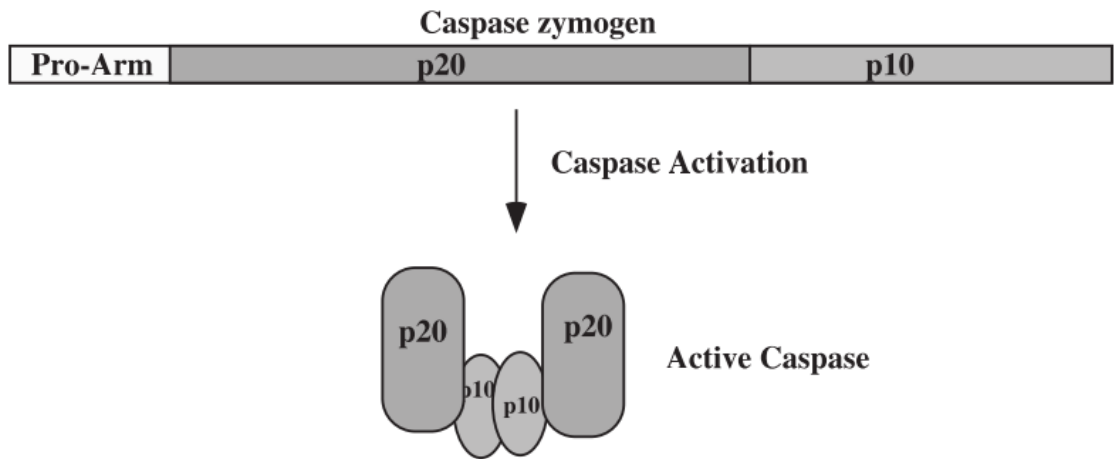


Figure 1.16 (b) Schematic diagram of caspase activation. Caspases exist as zymogens and are activated by proteolytic processing of the N-terminal fragment and by endo-proteolytic processing creating two fragments of approximately 10 (p10) and 20 (p20) kDa as described in Figure 1.16 a (LeBlanc 2003).

### 1.8.1 Initiator Caspase Signalling

Initiator pro-caspases 2, 8, 9 and 10 have a long domain and they exist in their inactive zymogen forms as monomers in the cytoplasm of cells. Initiator caspases require dimerisation or oligomerisation for activation and are responsible for the early initiating events of apoptosis (Launay *et al.* 2005). Activation of initiator caspases involves formation of protein complexes containing pro-caspase molecules. Inactive zymogen dimers within the cytoplasm are recruited to form complexes by specific adaptor proteins.

Caspase 2 has been classified as an initiator caspase due to the N-terminal caspase activation and recruitment domain (CARD) within its pro-domain (Logue & Martin 2008). Even though it was one of the first caspases to be discovered, its precise role remains unclear and somewhat controversial. Studies have shown that initiator caspase 2 is not capable of processing any other caspase member, but is able to cleave and process Bcl-3 family member Bid, assuming then that this initiates the release of cytochrome c from the mitochondria. Caspase 2 may be an initiator of apoptosis via the mitochondrial pathway (Guo *et al.*, 2002). Other reports mention that activation could occur after induction of heat-shock cell death (Vakifahmetoglu-Norberg & Zhivotovsky 2010). Even though caspase 2 and caspase 9 are both classified as initiators due to structure, there is no evidence of an overlap in functionality. However, knockout studies in mice null of caspase 2 exhibited a very similar phenotype to those that lack caspase 9 (Logue & Martin 2008). Caspase 2 has been described as caspase 3-dependent, suggesting it is only activated after the formation of the apoptosome (Logue & Martin 2008). Pro-caspase 2 interacts with other proteins through CARD and can form part of a complex known as the 'PIDDosome' which was first described in 2004 (Tinel & Tschopp 2004). It consists of a P53-inducible death domain-containing protein (PIDD), RIP-associated ICH-1 homologous protein with a death domain (RAID) and pro-caspase 2. Interestingly an increase of PIDD promotes p53 induced apoptosis and inhibition of PIDD can reduce the p53 mediated signalling (Vakifahmetoglu-Norberg & Zhivotovsky 2010). This suggests a relationship between caspase 2 and P53 signalling. It is possible that caspase 2 has very specific circumstantial criteria for functionality and may even be cell specific.

IR-induced apoptosis is mediated by the mitochondria, caspase 9 and is independent of caspase 8 activity (Hosokawa *et al.* 2005). Interestingly, the ability of caspase 9 is

increased in the presence of cytosolic APAF-1 and the formation of the apoptosome, suggesting that caspase 9 requires other cytosolic proteins to complete its conformational change and activity (Cain *et al.* 2002). It has been suggested that the active form of caspase 9 is actually the Apaf-1 complex (Rodriguez & Lazebnik 1999). caspase 8 is required for signalling of the death receptor (extrinsic) pathway. It is known for its mitochondrial remodelling ability through cleavage of Bcl-2 family member Bid into tBid. However, there is no evident role for caspase 8 in intrinsic apoptosis. Caspase 9 can hinder cytochrome c from accessing the complex III in the mitochondria and therefore increasing the production of ROS (Brentnall *et al.* 2013). Interestingly ROS production is increased if highly specific caspase 9 cleaves Bid into tBid. Nevertheless if effector caspases are activated ROS production is inhibited. This has been suggested to be a feedback loop occurring on the mitochondria after it has released cytochrome c and activated caspase 9 and possibly the exact 'point of no return' of intrinsic apoptosis (Brentnall *et al.* 2013). Cells derived from animals that are null of caspase 9 have demonstrated resistance to external stress agents, such as cytotoxic drugs and radiation. Caspase 2 cannot process any other member of the caspase family, but can cleave the BH3-only protein Bid, presumably to instigate cytochrome c release. Caspase 2 may initiate apoptosis by harnessing the mitochondrial pathway. Radiation-induced cytochrome c release including the subsequent caspase activation can be inhibited by anti-apoptotic Bcl-2 proteins. Therefore it is apparent that radiation-induced caspase activation is dependent on mitochondrial signalling.

### 1.8.2 Effector Caspase Signalling

Effector caspases of intrinsic apoptosis are often called executioner caspases and include pro-caspases 3, 6 and 7 which have a short pro-domain. The inactive effector caspases 6 and 7 zymogens exist in cells as dimers that require proteolytic cleavage at internal aspartate residues to generate two large and two small subunits and responsible for the final stages of apoptosis (Oliver & Vallette 2005). Heterodimerisation of these subunits separate the large and small subunits from each other causing a conformational change and then resulting in an active effector caspase (Kaufmann *et al.* 2008). Binding of caspase 3 and 7 may require the assistance of other proteins (Cain *et al.* 2002). In turn these caspases can activate effector caspase 6.

Activated effector caspase 3 cleaves substrates in the cytosol that are essential for structural functions of the cell associated with the characteristic features of apoptosis, including membrane blebbing, chromatin condensation and nuclear DNA fragmentation (Slee *et al.*, 2001) These effector caspases are capable of cleaving downstream pro-caspases and cellular proteins through dismantling of cellular machinery via destructive enzymes such as DNases, which are endonucleases that split nucleic acid chains at internal sites (Slee *et al.* 2001). Caspase 3 can also inhibit ROS production by inhibiting the transport of electrons and reducing the mitochondrial membrane potential, which therefore maintain the integrity of the cell undergoing apoptosis (Brentnall *et al.* 2013). Inhibition of caspases prevents the appearance of some morphological signs of apoptosis, including chromatin condensation and DNA fragmentation. In this case the cell death process will change from apoptosis to a combination of cell death morphology and may create a delay (Kroemer *et al.* 2009). Nevertheless, caspase-independent cell death can occur despite the efficient inhibition of caspases and can

exhibit some of the morphological signs of apoptosis, autophagy or necrosis (Pradelli *et al.* 2010).

Caspase activation is not always required for the execution of the cell death program but may be necessary for the development of characteristic apoptotic morphology, which can define the type of cell death occurring. Some studies suggest that cell death is a caspase-dependent process because the integration of caspase inhibitors will affect the process (Oberst *et al.* 2008).

As mentioned earlier, initiator caspase 9 is directly responsible for the activation of downstream effector caspases 3 and 7. Caspase 3 creates a positive-feedback amplification loop to promote further processing of caspase 9 (Logue & Martin 2008). Studies have shown that caspase 7 does not appear to drive any further caspase activation event, whereas caspase 3 propagates the cascade further by proteolytic processing and activation of caspases 2 and 6 downstream. It is widely accepted that caspase 9 cleaves caspase 3 and caspase 7, and that caspase 3 cleaves caspase 6 and caspase 2. In the final stage of this caspase cascade, caspase 6 catalyses the activation of caspase 8 and caspase 10. However, there are inconsistencies in some data involving knockout studies in mice, and so it is believed that caspase 7 is actually capable of cleaving caspase 6 and 2, assuming that caspase 2 is initiated further downstream. There is evidence that caspases can also exceed their apoptotic roles in responses such as inflammatory type responses and immune cell proliferation and differentiation (Launay *et al.* 2005).

### 1.8.3 Tumour Suppressor p53 Signalling

Radiation-induced DNA damage can trigger apoptosis via a p53-mediated pathway that can incorporate up-regulation of the pro-apoptotic protein Bax, cell-death ligands or receptors, or ceramide synthase. There is recent evidence to suggest that release of cytochrome c from the mitochondria may be a p53-dependent process in the bystander response and is cell line dependent (Hei *et al.*, 2011), although p53-independent pathways have also been characterised. The tumour suppressor gene p53 that encodes TP53 has frequently been referred to as the ‘guardian of the genome’ (Efeyan & Serrano 2007, p. 1006) as it manages a diverse set of pathways including DNA repair, cell cycle arrest, and apoptotic cell death (Jen & Cheung 2005). In particular TP53 is responsible for managing oncogenes. Oncogenes are altered versions of normal cellular genes responsible for controlled cell growth and differentiation. Over-expressed or mutated oncogenes are characteristic in cancer cells (Halazonetis *et al.* 2008). TP53 determines whether a cell exposed to IR will survive DNA damage and proliferative arrest by promoting minor DNA repair, or it can make such an arrest irreversible by activating cell death (Coleman *et al.* 2005). Hence, it plays a major role in determining the cell’s fate (see Figure 1.17). If the radiation-mediated damage is too extensive for cell survival, the tumour suppressor p53 is activated as a crucial transcription factor signalling cell death. Failure of the TP53 activated process may result in the development of carcinogenesis or genomic instability post irradiation. There is evidence that mutated TP53 gene is implicated in a range of human tumours (Efeyan & Serrano 2007). Studies involving epithelial cells from rat lungs revealed an increase of TP53 in a large number of cells, much more than was expected (Deshpande *et al.* 1996).

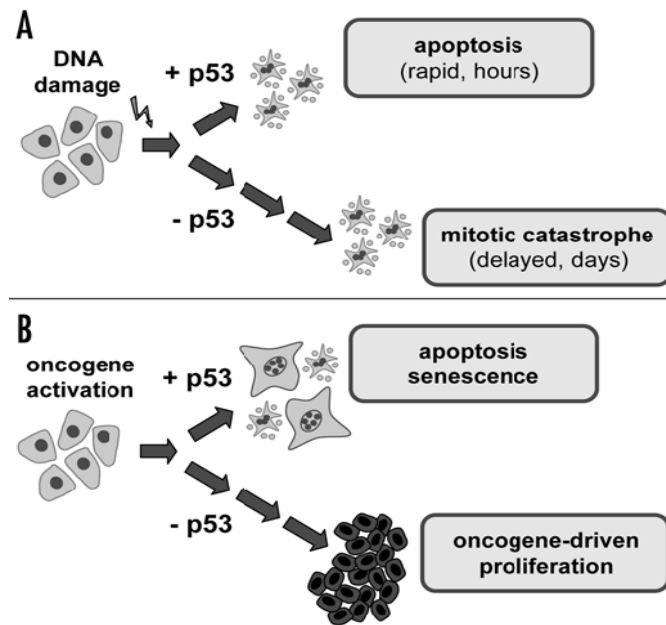


Figure 1.17 A schematic representation of the differential impact of p53 on cellular fate in response to DNA damage (A) or oncogenic signalling (B). Cells with active p53 will undergo apoptosis but cells deficient in p53 will undergo aberrant mitosis eventually leading to mitotic cell death (A). Oncogenic signalling in cells with p53 leads to an elimination of cells via apoptosis and cells lacking in p53 will continue to proliferate (B) (Efeyan & Serrano 2007).

TP53 employs its transcription regulatory activity mostly through direct binding to the regulatory sequences of its target genes (Rashi-Elkeles *et al.* 2011). p53 is a transcriptional regulator of Bcl-2, Bax and Bid and can represent an apoptogenic factor on the mitochondrial membrane surface. There is a developing range of p53 targets



which currently exceeds 100 genes and the biological roles of the p53-mediated network has been extensively reviewed (Harris & Levine 2005).

Cells directly exposed to IR have increased levels of TP53 and ROS. Bystander cells can exhibit decreased TP53 levels, higher levels of ROS and a DNA repair protein (Iyer & Lehnert, 2002b). HaCaT cell lines are non-transformed keratinocytes with mutant p53, however, the mutant p53 cells lines induce bystander responses. There is evidence that media transferred from p53-mutated tumour cells to bystander normal human cells induces NO signalling, and media transferred from normal cells to bystander p53-mutated tumour cells occurs via ROS. Both signalling pathways are characteristic to the bystander response (Ryan *et al.* 2008) as described previously. In (2011) Mothersill *et al.*, demonstrated that the p53 signalling pathway is involved in bystander responses and that signals can be produced by cells deficient in functional p53.

## Thesis Overview

The overall aim of this research study was to investigate the cellular and molecular mechanisms involved in radiation-induced bystander effects in cells. Bystander effects occur when directly irradiated cells communicate damaging signals to non-irradiated neighbouring (bystander) cells, predominantly at low-doses of irradiation. They do not follow the original dose-response theory and exhibit a unique cascade of signalling events, which are under intense investigation for radiation risk purposes.

Investigations *in vitro* and *in vivo* have been successful in better understanding bystander responses. The bystander reporter HaCaT cell line is well established and report the bystander effect very well. Some of the intercellular and intracellular signalling pathways and potential candidates for the bystander factor have been revealed to date. Cytokines may be important for the initial signalling of the bystander response and pathways involving oxidative stress, calcium and mitochondrial-apoptosis have been implicated.

However, the specific molecular signalling mechanisms that occur in a radiation induced bystander response are not well-understood. The first experiment conducted for research (described in chapter 2) was to demonstrate the classical radiation induced bystander effect in HaCaT reporter cells exposed to low doses of IR (0, 0.5 and 5 Gy). Different cells and viability assays were used to prove the hypothesis that HaCaT cells were sensitive and good reporters of the bystander effect compared to other cells *in vitro*. The classical bystander media transfer protocol was followed with generation of ICCM at an early (1hr) and late (24hr) timepoint as it has emerged that time is critical in the response. Reduction in viability of the HaCaT reporter cells indicated that apoptosis was a key event in the cellular mechanism of RIBE.

In chapter 3 and 4, the intracellular downstream events of RIBE were investigated by focusing on genes specifically involved in the intrinsic pathway of apoptosis. HaCaT reporter cells exposed to a range of low doses of ICCM with early to late timepoints were used to measure gene expression levels. The genes investigated included tumour suppressor TP53, mitochondrial pro-apoptotic Bax and anti-apoptotic Bcl-2, Mitogen-activated protein kinases (MAPK) genes ERK and JNK, initiator caspases 2 and 9 and effector (executioner) caspases 3, 6 and 7.

To obtain further information about the molecular mechanisms of the RIBE another biological test model using was incorporated. This involved using fish irradiated *in vivo* with similar low doses of IR but cultured *ex vivo* to generate irradiated cell conditioned medium (ICCM). This ICCM was then used to measure protein expression in the reliable reporter HaCaT cells.

The bystander reporter HaCaT cell model were used throughout all of the studies described in this thesis to ensure consistency throughout the investigation and obtain realistic and comparative data in an attempt to elucidate the RIBE pathways. Chapter 6 details a summary of the data generated including two cellular and molecular signalling RIBE pathways that have been proposed for 0.05 Gy and 0.5 Gy irradiations in HaCaT cells. It is anticipated that these pathways may have clinical considerations and implications for radiotherapy patients in the future.

## **Chapter 2**

### **Evaluation of Two Viability Assays to Measure Radiation-Induced Bystander Effects in Reporter Cells**

## 2.1 Introduction

There has been a lot of interest in the effects of irradiation that do not require direct DNA damage, known as non-targeted effects (NTE). Nagasawa and Little first described the ‘clastogenic effects’, now known as bystander effects with experiments using alpha-particle radiation that induced indirect damage effects (Nagasawa & Little 1992). The exact cellular and molecular responses are not very well known but are under intense investigation. There is data to support both concepts and are extensively discussed by Hei *et al.* (2011). The development of the media-transfer technique has enabled researchers to investigate radiation-induced bystander effects (RIBE) more specifically (Mothersill & Seymour 1997). The radiobiological effects observed in media transfer experiments include induced cell death mechanisms (Jella *et al.* 2013) or reduced cell viability (Seymour & Mothersill 2000) in the non-irradiated neighbouring cells.

One of the common *in vitro* biological endpoints used to investigate RIBE in cells is measurement of cell death (i.e. measuring their viability). The clonogenic assay created by Puck and Marcus (1956) has been a gold standard radiobiological tool in measuring the clonogenicity in bystander cells for some time. The disadvantage of this assay is that the setup is very time-consuming taking approximately 12-14 days for the colonies to grow. Furthermore, very large volumes of irradiated cell-conditioned medium (ICCM) are required for the clonogenic assay. Alternatives to this assay to measure RIBE are cell viability cytotoxicological assays, MTT and Alamar Blue, which can be done on 96 well microtitre plates for high throughput viability analysis. The advantages of these assays are that they require substantially less media than in a clonogenic assay (100µl compared to 5ml) and many test doses and timepoints can be tested with a high turn

over time. In the current study, both MTT and Alamar Blue assays were used to determine the RIBE in HaCaT cells compared to other potential ‘reporter’ cells of the bystander effect. Two parallel tests were used so that sensitivity of the test method for the three cell lines could also be confirmed and consolidate the data further. As mentioned in Chapter 1, bystander responses are induced at low doses and the risks may be greater or less than what was previously predicted in the linear non-threshold (LNT) model, and a reduction in viability is expected in HaCaT cells exposed to ICCM.

Human HaCaT cells (see Appendix A2.1 for an image of the HaCaT cell line) were used for this study as they have previously been shown to be good reporters of the radiation induced bystander response and are well-established (Howe *et al.* 2009; Lyng *et al.* 2012) comparable to the response of the HPV- G cell line used previously by our group (Lyng *et al.* 2011; Jella *et al.* 2013). HaCaT cells are an immortalised cell line derived from human keratinocytes that have either been infected with simian virus 40 (SV40) or transfected (Boukamp *et al.* 1988). The cell line thrives in both *in vitro* and *in vivo* conditions and has a high differentiation potential comparable to normal human keratinocytes (Lehman *et al.* 1993). A report in 2001 revealed that media from irradiated HaCaTs has the ability to kill recipient cells (Lewis *et al.* 2001), therefore supporting the bystander phenomena. A recent study also shows evidence of bystander effects in HaCaTs cells (Jella *et al.* 2014), and primarily a possible role for exosomes in the response in addition to a reduction in viability at low doses between 0.005 Gy and 0.5 Gy, which are pertinent doses to the current and proceeding chapters in this Thesis.

There are limitations to using the HaCaT cell line model due to evidence of their growth and differentiation properties which is greatly dependent on the type of cell culture media used (Wilson, 2014) and these limitations are acknowledged by the author.

Increased levels of calcium have been shown to induce changes to morphology and the normal cellular processes thus resulting in decreased proliferation and increased differentiation of HaCaT cells (Micallef *et al.*, 2009). The protein kinase C (PKC) system has been implicated in driving different cellular processes and is dependent on the roles of PKC sub-family isoforms that exist in HaCaT cells. The different isoforms, cPKC  $\alpha$  and  $\beta$ ; novel nPKC $\delta$  and  $\epsilon$ , are antagonistic in that they can regulate different processes such as proliferation, differentiation, cell death and tumourgenesis. It has been suggested that altered calcium levels could have a significant role in the overall PKC system (Papp *et al.*, 2004). For that reason, cell culture media with known low levels of calcium are favoured for *in vitro* HaCaT cell models. The current study could be improved by introducing low calcium level cell culture media to maintain preferred cell culture conditions (Deyrieux & Wilson, 2007) and thus reducing inconsistency and variability between data generated. Further to that, an additional real-time q-PCR study investigating already identified genes (Lemaître *et al.*, 2004) expressed in both proliferating and differentiating HaCaT cells, would establish the current state of the HaCaT cells used and could operate as an internal quality control method.

In the current study HaCaT cells were used to 'report' RIBE in ICCM harvested from HaCaT cells compared to two different colorectal cell lines at low doses of irradiation (0.5 Gy and 5 Gy), harvested at two different time points (1 hr and 24 hr) determined by the Alamar Blue and MTT cell viability assays. The two human colorectal cancer cell lines were selected for this study are HT29 cells, a human colorectal adenocarcinoma cell line originally isolated from a primary grade I-II tumor from a 44-year-old Caucasian female, they are radioresistant and have mutant TP53 status (see Appendix A2.2 for an image of HT29 cells). Secondly, SW480 cells were chosen, which are a human colorectal adenocarcinoma cell line isolated from a secondary grade III-IV

tumor, are highly radiosensitive and have wild-type TP53 (see Appendix A2.3 for an image of SW480 cells). Both of these colorectal cells were chosen for this study because Ryan *et al.*, (2009) showed bystander effects in SW480, HaCaT and HPV-G cells and HT29 cells which had increased cloning efficiency after the addition of ICCM (Ryan *et al.* 2009). An explanation for this is that SW480, HaCaT and HPV-G must be more sensitive to ICCM. Specifically for the HaCaT cells, they appear to reach a plateau at 5 Gy ICCM exposure and the SW480 cell line reach a plateau at 0.5 Gy. Reductions of viability have been shown in HaCaT cells exposed to 0.05 Gy and 0.5 Gy ICCM and very little differences were previously shown with 0.005 Gy doses (Lyng *et al.* 2011).

In a study in 2000, Seymour and Mothersill (Seymour & Mothersill 2000) reported bystander effects in human keratinocytes immortalised by transfection with the HPV 16 by a reduction in clonogenicity. HPV-G cells show on average a 40% reduction over a wide range of doses when exposed to ICCM (Mothersill *et al.* 2004). The authors discussed how doses between 0.01–0.5 Gy show clonogenic death by the bystander effect only and that bystander effects appears to saturate at doses in the range of 0.03–0.05 Gy. They suggest that for doses greater than 0.5 Gy clonogenic death is a result of a dose-dependent non-bystander effect. So, to summarise, bystander effects occur predominantly below 0.5 Gy and above 0.5 Gy a direct effect occurs. It is evident then that the cells have a specific mechanism in place for ‘switching’ from cell death to proliferation at the higher doses.

The first cell viability method used in this study as mentioned earlier was the Alamar Blue assay. The assay was fully standardized according to the method of O’Brien *et al.* (2000). Alamar Blue is a chromogenic dye and works as a redox indicator and measures cell viability and proliferation. Chemical reactions occur within cells producing



products such as cellular dehydrogenases; FMNH<sub>2</sub>, FADH<sub>2</sub>, NAHD, NADPH and cytochromes. These products reduce the Alamar Blue generating a fluorescent signal as a response. Reduced cell viability in an oxidised environment will generate a pink colour and increased cell viability in a reduced environment will generate a blue colour. Spectrophotometric measurement of the colour change generate data signifying cell viability (Anoopkumar-Dukie *et al.* 2005). The Alamar Blue assay is highly sensitive, inexpensive and a robust quantitative method. It is safe to handle, as it does not include any toxins or radioactive reagents. In contrast the MTT assay was used in parallel. The MTT assay (3-(4,5-dimethylthiazol-2-yl)-2,5-diphenyltetrazolium bromide) is a colorimetric method that measures the metabolic activation of the cells (Berridge & Tan 1993) resulting in measurement of the cells viability and proliferation (Jose *et al.*, 2011; Al- Rubeai, 1997). MTT is a yellow water-soluble substrate that is converted into a purple formazan crystal product by mitochondrial dehydrogenase enzymes. The enzymes reduce the tetrazolium salt are nicotinamide adenine dinucleotide dehydrogenase (NADH) and nicotinamide adenine dinucleotide phosphate dehydrogenase (NADPH). This chemical reaction shows the cell's proliferation and its absorbance is measured with a spectrophotometer. A linear relationship is shown between the formazan crystal product and the viable cell number in a variety of cell types (Doyle & Griffiths 1997). The assay is deemed to be highly reliable and sensitive and was incorporated into this study for this reason.

Howe *et al.*, (2009) described how over a three year period, collected, cultured and irradiated whole blood samples from colorectal cancer patients and the ICCM from these lymphocyte cultures was harvested and stored at -80°C for subsequent use. Recipient HaCaT cells were exposed to the harvested ICCM and measured for a bystander effect using the Alamar Blue viability assay. RIBE shown by the individual

colorectal cancer patient's samples varied using this assay. The patient samples revealed both decreased and increased viability, indicative of a radiation-induced bystander response. This also suggests that the RIBE responses were specific to each patient, perhaps some individuals respond and some do not. For this reason this current study measured the sensitivity of both Alamar blue and MTT assay to report RIBE for three chosen cell lines. The harvested colorectal patient ICCM from Howe *et al.*, (2009) were re-analysed to validate the sensitivity of the parallel assays for response to ICCM.

## **2.2 Materials and Methods**

### **2.2.1 Routine Cell Culture Maintenance, Sub-culturing and Counting**

An immortal human keratinocyte cell line, HaCaT, was kindly received from Dr Petra Boukamp's laboratory (Boukamp *et al.* 1990) and used for this study, in addition to two colorectal adenocarcinoma cell lines, HT29 and SW480, to compare the sensitivity of bystander responses, with both MTT and Alamar Blue cell viability assays. Both colorectal cell lines have previously shown to report bystander effects (Ryan *et al.* 2009).

The three cell lines were adapted to and routinely cultured in DMEM: F12 (Dulbeccos Modified Eagles Medium) medium (Sigma) supplemented with 10% fetal bovine serum (FBS, Gibco) and 2mM L-Glutamine (Gibco). Cells were maintained in an atmosphere of 37°C and 5% CO<sub>2</sub> and grown to approximately 70-80% confluency to ensure they were in the logarithmic phase of growth. Cells were removed from stock flasks using a 1:1 mix of EDTA:Trypsin, (EDTA: 0.1 g of EDTA in 500 ml PBS:Trypsin 2.5% 10X) and a 1:10 dilution of Trypsin then neutralised in EDTA.  $2 \times 10^5$  cells were counted

using a Coulter Counter and were plated into T25 flasks (see Appendix A1 and A12 for a list of materials and reagents and cell culture consumables used and for a full description of routine cell culture maintenance, counting and plating of cells see Appendix B1 and B2).

For the direct donor cell irradiations  $3 \times 10^5$  cells (HaCaT, HT29 and SW480) were counted and plated into T25 flasks in replicates of 8 per time and dose. The growth of each cell line was monitored for 2-3 days so that the cells were allowed to reach 70-80% confluency, to ensure the phase of growth of the cells.

### **2.2.2 Irradiations, Generation and Harvest of ICCM**

Once the cells reached 70-80% confluency they were transported to the Co<sup>60</sup> teletherapy Unit at St. Luke's Hospital (Rathgar, Dublin, Ireland) and irradiated at 0 Gy, 0.5 Gy and 5 Gy. For the 0.5 Gy and 5 Gy dose points the source to sample distance was 80 cm. The dose rate delivered was approximately 1.5 Gy/min during these experiments as evaluated at the 80 cm source to sample distance. Thermoluminescent dosimeters (TLD) were used to confirm that the appropriate dose was delivered. Cells were transported back to the laboratory and re-incubated at 37°C for 1 hr. ICCM was harvested from the HaCaT, HT29 and SW480 cells and pooled per replicate flasks at 1 hr and 24 hr time points for each of the three dose points (0, 0.5 and 5 Gy) for each cell line. The irradiated flasks were replaced with 5ml of fresh DMEM F12 media and re-incubated. The ICCM was filter sterilised with a 0.2µm filter (Nalgene) and stored at – 80°C for the subsequent viability assays.

### **2.2.3 Preparation of Bystander Reporter Cells in Microtitre Plates for Viability Assays**

HaCaT, HT29 and SW480 cells were maintained, sub-cultured and counted as described in Section 2.2.1.  $1 \times 10^4$  cells were plated into each well of 96-well plates (Invitrogen, see Appendix A1) for the 24 hr exposure and  $5 \times 10^3$  were plated into each well of a 96-well plate for the 48 hr exposure time, for each cell line.

Each test plate for both the MTT and Alamar Blue assay were set up in parallel to measure 1 hr and 24 hr harvested ICCM for 24 hr and 48 hr assay exposure times in triplicate for each cell line (see Appendix C1.1 for exact layout of 96-well microplates in the raw data). The plates were clearly labelled with the cell line name (HaCaT, HT29 and SW480), specific time points of 1 hr and 24 hr and doses 0, Gy, 0.5 Gy and 5 Gy. Fifteen replicate wells ( $n = 15$ ) were prepared in total per treatment (1 hr 0 Gy, 1 hr 0.5 Gy, 1 hr 5 Gy and 24 hr 0 Gy, 24 hr 0.5 Gy and 24 hr 5 Gy ICCM), 5 of the 15 replicate wells were set up on three plates separately. Plates were incubated for 24 hr at 37°C with an atmosphere of 5% CO<sub>2</sub> to allow cells to attach. After the incubation period, medium was poured off the cells. 100µl of ICCM (0 Gy, 0.5 Gy and 5 Gy) was added onto the cells in the labelled 96-well plates and 100µl of fresh DMEM was added to the control cells on each plate. The plates were re-incubated at 37°C with an atmosphere of 5% CO<sub>2</sub> for the assay exposure time points of 24 hr and 48 hr.

#### **2.2.4 Alamar Blue Cell Viability Assay**

The Alamar Blue cell viability assay was used to determine RIBE in un-irradiated HaCaT, HT29 and SW480 cell cultures exposed to ICCM from the irradiated cell cultures.

After the exposure times of either 24 hr or 48 hr, the control media and ICCM was poured off the cells and they were washed three times in sterile phosphate buffered saline (PBS). Residual PBS was pipetted out of the wells and 100µl of fresh Alamar Blue medium (5% [v/v] solution of Alamar Blue) was prepared in fresh media (without FBS or supplements) was added to each test well. Plates were incubated for 3 hrs at 37°C. Absorbance was read immediately after incubation on a GENios fluorescence microplate reader and fluorescence was quantified using excitation and emission wavelengths of 540 nm and 595 nm, respectively. Blank control wells contained medium and Alamar Blue dye only without cells. The data (in fluorescence units from the microplate reader) for the ICCM test wells were normalised to the assay control (DMEM medium only) and bystander effects were calculated as a change of viability in the irradiated group compared to the unirradiated group per sample. Refer to Appendix A3 for a list of reagents used for the Alamar Blue assay and Appendix B3, B4 and B5 for the complete Alamar Blue assay.

### **2.2.5 MTT Cell Viability Assay**

The 3-(4,5-dimethylthiazol-2-yl)-2,5-diphenyltetrazolium bromide (MTT) assay measures cell viability and it was used to determine radiation-induced bystander effects of HaCaT, HT29 and SW480 cell lines exposed to ICCM from the directly-irradiated cell cultures (Mosmann 1983). After the exposure time points (24 and 48 hr), control media (DMEM) and ICCM were poured off the cells in the 96-well plates and rinsed with PBS and 100µl of fresh DMEM medium (without FBS or supplements) was added to each well. 10µl of working MTT solution (5mg/ml) was prepared in PBS and added to each well and the plates were re-incubated for 3 hr at 37°C in an atmosphere of 5% CO<sub>2</sub>. After the incubation period, medium was discarded and cells were washed with 100µl of PBS and 100µl of DMSO was added to each well to resolve the formazan crystals and extract the dye. Plates were shaken at 240 rpm for 10 min and the reduction of MTT to a blue formazan product was measured at an absorbance of 595nm on a GENios fluorescence microplate reader. The data (in fluorescence units from the microplate reader) for the ICCM test wells were normalised to the assay control (DMEM medium only) and bystander effects were calculated as a change of viability in the irradiated group compared to the unirradiated group per sample. Refer to Appendix A4 for a list of MTT reagents used and Appendix B3, B4 and B6 for full details of the MTT assay.

### 2.2.6 Colorectal Patient ICCM Samples

The colorectal patient ICCM samples were generated by colleagues (Howe *et al.*, 2009) at the Focas Institute, Dublin Institute of Technology, as part of another research study and were provided for this pilot study to assess sensitivity of the MTT assay compared to the Alamar blue assay previously reported in Howe *et al.*, (2009) for the same patient ICCM samples. Blood samples from a number of colorectal patients (n=38) were cultured *in vitro* and irradiated with 0 Gy and 0.5 Gy of Co<sup>60</sup> irradiation using the same radiation source and protocol described above in section 2.2.2. Thirty minutes post exposure the ICCM was harvested, filter sterilised and stored at -80°C. Further information on the patients was not available.

Complete details of culture conditions and translational bystander experiments for this work are provided in Howe *et al.*, (2009). Briefly, the original lymphocyte cultures were routinely set up from fresh blood (stored at 4°C) within 24 hr of collection from the donor. The cultures were set up in four 25cm<sup>2</sup> flasks (Corning) through the addition of 2 ml of whole blood into 18 ml of pregassed (0.5% CO<sub>2</sub>) and prewarmed (37°C) RPMI 1640 cell culture medium (Sigma) supplemented with 12.5% fetal calf serum (Gibco) and 2 mM L-glutamine (Gibco). Then 0.2 ml of phytohemagglutinin (PHA) (RemelHA 15) was added to the cultures to stimulate the cells into mitosis. The cultures were grown in a mammalian cell culture environment at 37°C with 95% air/5%CO<sub>2</sub>. At exactly 48 hr of incubation, 15 ml of cell culture medium was replaced with fresh RPMI 1640 culture medium containing 0.15 ml PHA. At 72 hr incubation, the cultures were transported to the <sup>60</sup>Co irradiation facility in St. Luke's Hospital, Dublin, and two of the flasks were irradiated with 0.5 Gy  $\gamma$  radiation while the remaining two control flasks

were sham-irradiated. The lymphocyte cultures were re-incubated at 37°C for 30 min after irradiation to allow recovery of the cells.

Ten thousand HaCaT reporter cells were plated in 96-well microplates as described in Section 2.2.4 (preparation of bystander reporter cells) for a 24 hr exposure only. Cells were exposed to colorectal patient ICCM (0 Gy and 0.5 Gy) and the MTT assay (see Section 2.2.5 for full description of assay) was set up to measure RIBE in the samples. Radiation-induced bystander effects were measured with the GENios fluorescence microplate reader as described previously. Ethical approval for this part of the study was granted by the St. Vincent's Hospital Ethics and Medical Research Committee, and patients gave written informed consent prior to participation in this study

### **2.2.7 Statistical Analysis**

The GENios fluorescence microplate reader measures the fluorescence in each test well per plate and generates the final readings as fluorescent unit values. Once all of the plates for each Bioassay and exposure time (24 hr and 48 hr) had been measured, the fluorescent unit values were extrapolated for viability calculations and analysis. Radiation-induced bystander effects were measured for both MTT and Alamar Blue assay by calculating the mean (average) of fluorescent unit value from each test well per plate and then averaging the results for each set of triplicate plates per assay (n = 15).

Mean values were normalised to the non-treated assay controls, by subtracting the mean values from the non-treated internal assay controls to give a final result. Percentage viability was calculated relative to the assay control, which was set to 100%. Percentage viability of each bioassay (MTT and Alamar Blue) is graphically displayed as bar charts



with standard deviation error bars, and individual cell line responses are reported separately in the following Results section 2.3. Statistical analysis of the fluorescent values were carried out using GraphPad Prism statistical program, with a one-way Anova followed by Bonferroni's Multiple Comparison Tests, and are displayed in Table 2.1. See C1.14 in the Appendices for a figure showing percentage viability differences in HaCaT cells determined by MTT.

## **2.3 Results**

### **2.3.1 Radiation-Induced Bystander Effects in Cell Lines**

The results of Alamar Blue assay for HaCaT, HT29 and SW4980 are displayed in Figures 2.1 - 2.6 and the results of the MTT assay for the same cell lines respectively are displayed in Figures 2.7 - 2.12.

Cell Line	Assay	Exposure (hr)	ICCM sample	% Difference in Viability					
				0 Gy - 0.5 Gy		0 Gy - 5 Gy		0.5 Gy - 5 Gy	
HaCaT	AB	24	1 hr	-6.9	ns	-1.3	ns	5.6	ns
			24 hr	-8.3	ns	-1.4	ns	6.9	ns
HaCaT	AB	48	1 hr	-11.5	ns	5.4	ns	6.1	ns
			24 hr	2.4	ns	4.5	ns	6.9	ns
HT29	AB	24	1 hr	-3.2	ns	-3.8	ns	-0.6	ns
			24 hr	-2.8	ns	-3.6	ns	-0.8	ns
HT29	AB	48	1 hr	-0.4	ns	-1.6	ns	-1.2	ns
			24 hr	-1.1	ns	-1.6	ns	-0.5	ns
SW480	AB	24	1 hr	-0.8	ns	-3.1	ns	-2.2	ns
			24 hr	-1.9	ns	-1.9	ns	0.0	ns
SW480	AB	48	1 hr	-0.8	ns	-0.6	ns	0.2	ns
			24 hr	-0.6	ns	-1.3	ns	-0.7	ns
HaCaT	MTT	24	1 hr	-15.1	***	-12.6	**	2.5	ns
			24 hr	-18.2	***	-18.6	***	-0.4	ns
HaCaT	MTT	48	1 hr	0.3	ns	-0.4	ns	-0.7	ns
			24 hr	-23.5	**	-18.2	**	4.7	ns
HT29	MTT	24	1 hr	-17.0	ns	-46.5	**	-29.5	*
			24 hr	15.1	ns	0.2	ns	-14.8	ns
HT29	MTT	48	1 hr	-30.3	ns	-60.6	ns	-30.4	**
			24 hr	-21.6	ns	-38.1	ns	-59.9	**
SW480	MTT	24	1 hr	35.0	*	3.6	ns	-31.4	*
			24 hr	-18.0	ns	-20.2	ns	-2.2	ns
SW480	MTT	48	1 hr	0.3	ns	25.8	ns	25.5	ns
			24 hr	3.7	ns	-21.3	ns	-24.9	ns

Table 2.1: Percentage differences of viability between the 0 Gy and 0.5 Gy doses and between the 0 Gy and 5 Gy doses, for each cell line and cell viability assay. A positive value represents an increase of viability and a negative value represents a decrease of viability. Statistical analysis are represented as  $P > 0.05$  (ns),  $P \leq 0.001$  (\*\*\*),  $P \leq 0.01$  (\*\*), and  $P \leq 0.05$  (\*)

### **2.3.2 Alamar Blue Cell Viability Assay**

#### *HaCaT Cell line*

The results for the Alamar Blue assay in HaCaT cells after 24 hr exposure to 0 Gy, 0.5 Gy and 5 Gy ICCM (1 and 24 hr ICCM harvests) are shown in Figure 2.1. For the 24 hr exposures, HaCaT cells exhibited a non-significant decrease in viability from 0 Gy to 0.5 Gy, a non-significant decrease in viability from 0 Gy to 5 Gy and a non-significant increase in viability between 0.5 Gy and 5 Gy for both the 1 hr and 24 hr ICCM.

The results for HaCaT cells after 48 hr exposure to 0 Gy, 0.5 Gy and 5 Gy (1 and 24 hr ICCM) are shown in Figure 2.2. For the 1 hr ICCM samples there was a non-significant decrease in viability from 0 Gy to 0.5 Gy, followed by a non-significant increase of viability from 0 Gy to 5 Gy and a non-significant increase in viability between 0.5 Gy and 5 Gy. For the 24 hr ICCM samples, there was a non-significant increase of viability from 0 Gy to 0.5 Gy, a non-significant increase from 0 Gy to 5 Gy and a non-significant increase in viability between 0.5 Gy and 5 Gy.

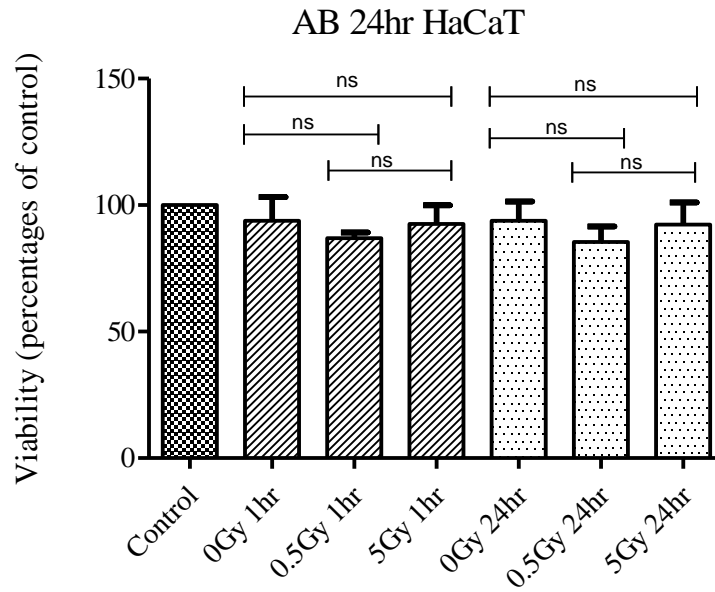


Figure 2.1 Viability of HaCaT cells after 24 hr exposure to 0, 0.5 and 5 Gy ICCM (1 and 24 hr) determined by the Alamar Blue assay. Data are expressed as mean percentage of control plus standard deviation (n = 15). Statistical analysis are represented as  $P > 0.05$  (ns),  $P \leq 0.001$  (\*\*\*),  $P \leq 0.01$  (\*\*) and  $P \leq 0.05$  (\*). See Appendix C1.1 for raw data.

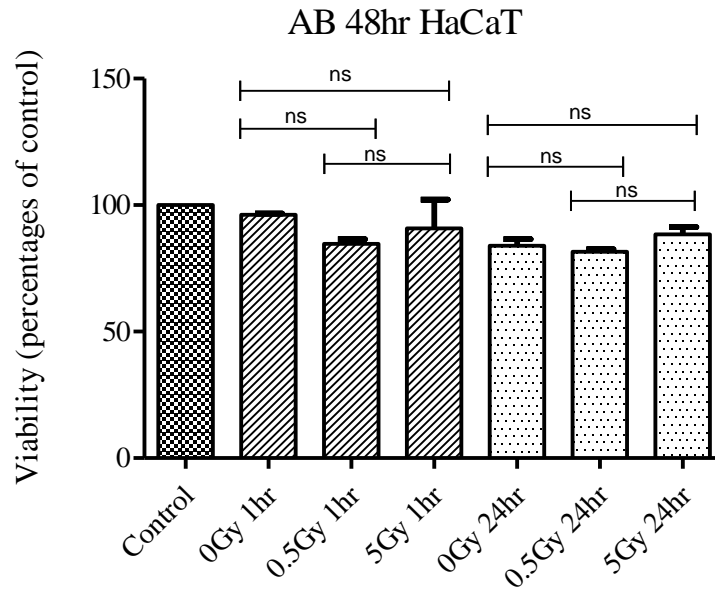


Figure 2.2 Viability of HaCaT cells after 48 hr exposure to 0, 0.5 and 5 Gy ICCM (1 and 24 hr) determined by the Alamar Blue assay. Data are expressed as mean percentage of control plus standard deviation (n = 15). Statistical analysis are represented as  $P > 0.05$  (ns),  $P \leq 0.001$  (\*\*\*),  $P \leq 0.01$  (\*\*) and  $P \leq 0.05$  (\*). See Appendix C1.2 for raw data

### *HT29 Cell line*

The results of the Alamar Blue assay for HT29 cells after 24 hr exposure to 0 Gy, 0.5 Gy and 5 Gy ICCM (1 and 24 hr ICCM harvests) are shown in Figure 2.3. There was a non-significant decrease in viability for 1 hr ICCM exposures from 0 Gy to 0.5 Gy, from 0 Gy to 5 Gy and between 0.5 Gy and 5 Gy. In the 24 hr ICCM samples, cell viability was non-significantly reduced from 0 Gy to 0.5 Gy, from 0 Gy to 5 Gy and between 0.5 Gy and 5 Gy.

For the 48 hr exposures there was a non-significant reduction of viability from the 0 Gy to 0.5 Gy, from 0 Gy to 5 Gy and between 0.5 Gy and 5 Gy for the 1 hr ICCM samples and this is shown in Figure 2.4. For the 24 hr ICCM samples, there was a non-significant reduction in cell viability between 0 Gy and 0.5 Gy, from 0 Gy to 5 Gy and between 0.5 Gy and 5 Gy.

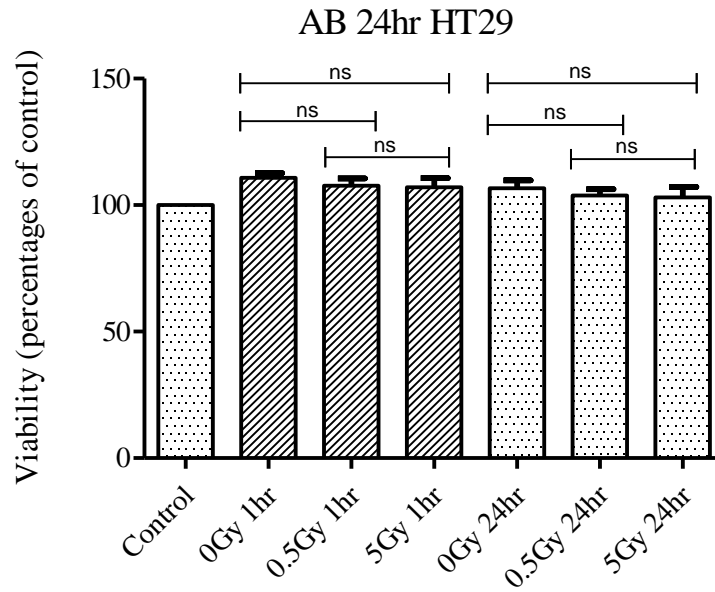


Figure 2.3 Viability of HT29 cells after 24 hr exposure to 0, 0.5 and 5 Gy ICCM (1 and 24 hr) determined by the Alamar Blue assay. Data are expressed as mean percentage of control plus standard deviation (n = 15). Statistical analysis are represented as  $P > 0.05$  (ns),  $P \leq 0.001$  (\*\*\*) ,  $P \leq 0.01$  (\*\*) and  $P \leq 0.05$  (\*). See Appendix C1.3 for raw data.

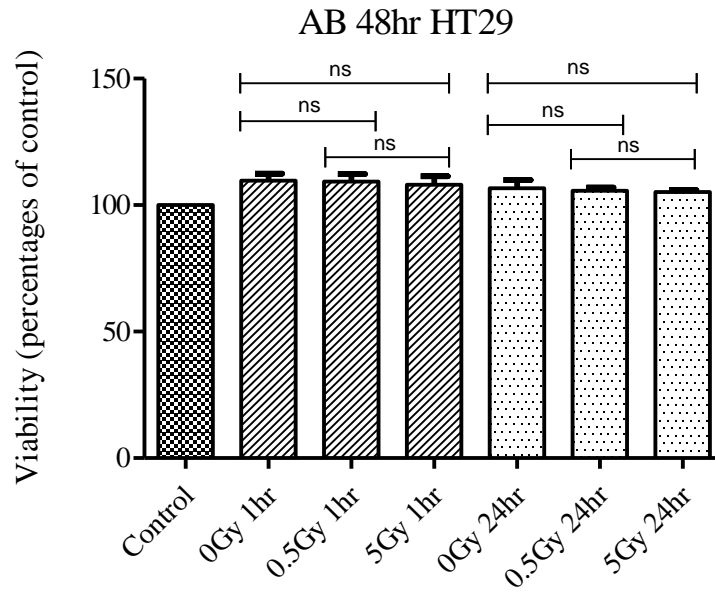


Figure 2.4 Viability of HT29 cells after 48 hr exposure to 0, 0.5 and 5 Gy ICCM (1 and 24 hr) determined by the Alamar Blue assay. Data are expressed as mean percentage of control plus standard deviation (n = 15). Statistical analysis are represented as  $P > 0.05$  (ns),  $P \leq 0.001$  (\*\*\*),  $P \leq 0.01$  (\*\*) and  $P \leq 0.05$  (\*). See Appendix C1.4 for raw data.



### *SW480 Cell line*

The results of the Alamar Blue assay for SW480 cells after 24 hr exposure to 0 Gy, 0.5 Gy and 5 Gy (1 and 24 hr ICCM) is shown in Figure 2.5. For the 1 hr and 24 hr ICCM samples, there was a non-significant reduction of viability between the 0 Gy and the 0.5 Gy, from 0 Gy to 5 Gy and between 0.5 Gy and 5 Gy.

The results of the SW480 48 hr exposures are shown in Figure 2.6. For the 1 hr ICCM samples, there was a non-significant decrease from 0 Gy to 0.5 Gy, from 0 Gy to 5 Gy and a non-significant increase between 0.5 Gy and 5 Gy. For the 24 hr ICCM samples, there was a non-significant decrease in viability from 0 Gy to 0.5 Gy, from 0 Gy to 5 Gy and between 0.5 Gy and 5 Gy.

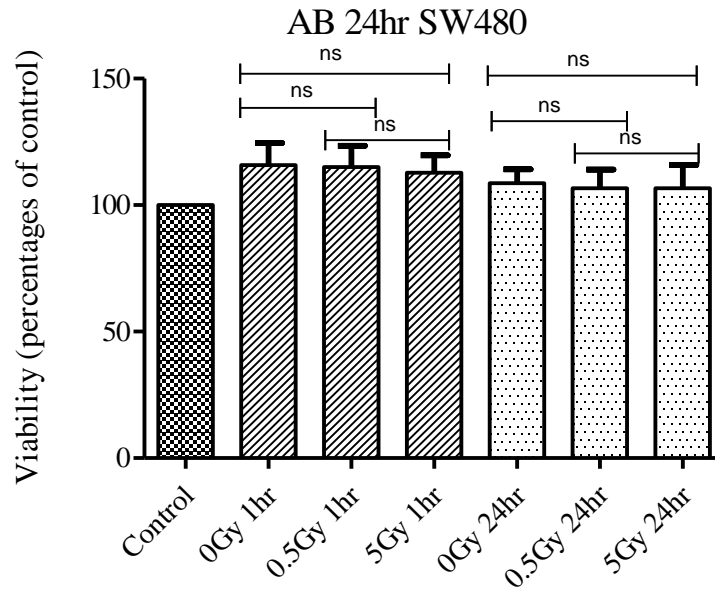


Figure 2.5 Viability of SW480 cells after 24 hr exposure to 0, 0.5 and 5 Gy ICCM (1 and 24 hr) determined by the Alamar Blue assay. Data are expressed as mean percentage of control plus standard deviation (n = 15). Statistical analysis are represented as  $P > 0.05$  (ns),  $P \leq 0.001$  (\*\*\*),  $P \leq 0.01$  (\*\*) and  $P \leq 0.05$  (\*). See Appendix C1.5 for raw data.

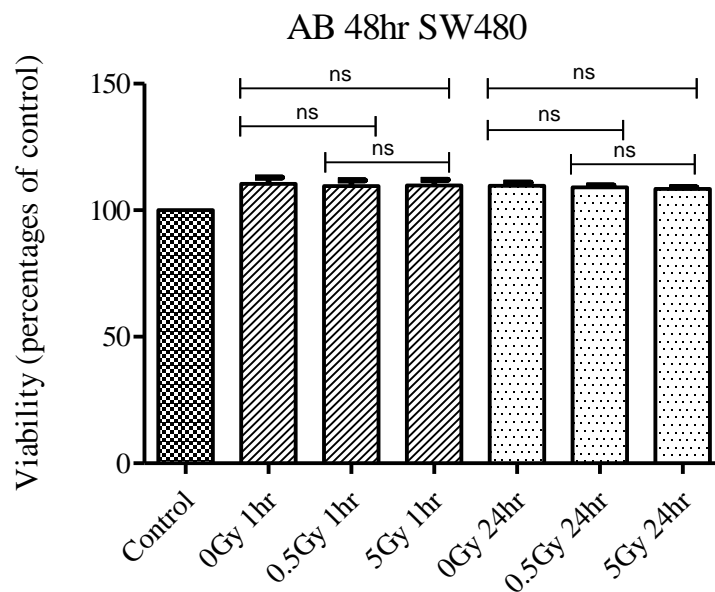


Figure 2.6 Viability of SW480 cells after 48 hr exposure to 0, 0.5 and 5 Gy ICCM (1 and 24 hr) determined by the Alamar Blue assay. Data are expressed as mean percentage of control plus standard deviation (n = 15). Statistical analysis are represented as  $P > 0.05$  (ns),  $P \leq 0.001$  (\*\*\*),  $P \leq 0.01$  (\*\*) and  $P \leq 0.05$  (\*). See Appendix C1.6 for raw data.

### 2.3.3 MTT Cell Viability Assay

#### *HaCaT Cell line*

Cell viability was measured with the MTT assay, and the results of the assay for HaCaT cells after 24 hr exposure to 0 Gy, 0.5 Gy and 5 Gy ICCM (1 and 24 hr ICCM harvests) are shown in Figure 2.7. For the 24 exposures with 1 hr ICCM, there was a significant decrease in viability from 0 Gy to 0.5 Gy, a significant decrease of viability from 0 Gy to 5 Gy and a non-significant between from 0.5 Gy to 5 Gy. For the 24 exposures with 24 hr ICCM there was a significant decrease in viability from 0 Gy to 0.5 Gy, a significant decrease from 0 Gy to 5 Gy and a non-significant increase between 0.5 Gy and 5 Gy.

The results for HaCaTs exposed for 48 hr are shown in Figure 2.8. For the 1 hr ICCM, there was a non-significant increase of viability from 0 Gy to 0.5 Gy, a non-significant decrease in viability from 0 Gy to 5 Gy and a non-significant decrease between 0.5 Gy and 5 Gy. For the 24 hr ICCM, there was a significant decrease in viability between 0 Gy and 0.5 Gy, a significant decrease in viability from 0 Gy to 5 Gy and a non-significant increase in viability between 0.5 Gy and 5 Gy.

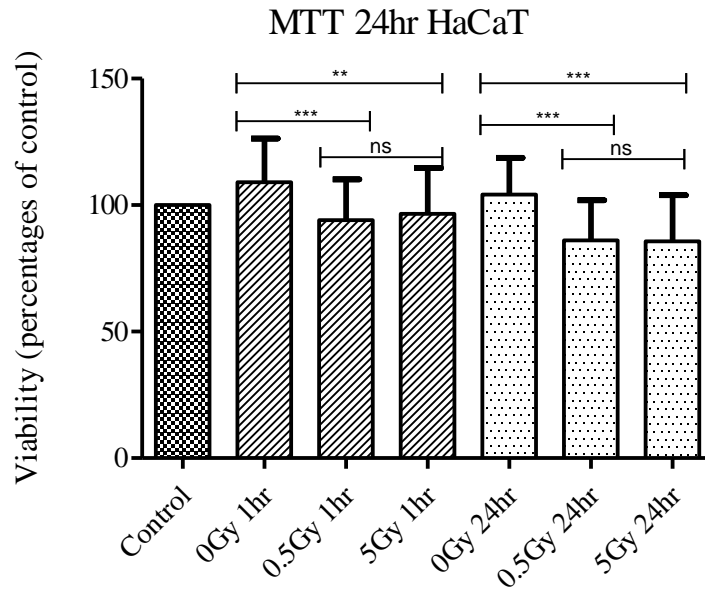


Figure 2.7 Viability of HaCaT cells after 24 hr exposure to 0, 0.5 and 5 Gy ICCM (1 and 24 hr) determined by the MTT assay. Data are expressed as mean percentage of control plus standard deviation (n = 15). Statistical analysis are represented as  $P > 0.05$  (ns),  $P \leq 0.001$  (\*\*\*),  $P \leq 0.01$  (\*\*) and  $P \leq 0.05$  (\*). See Appendix C1.7 for raw data.

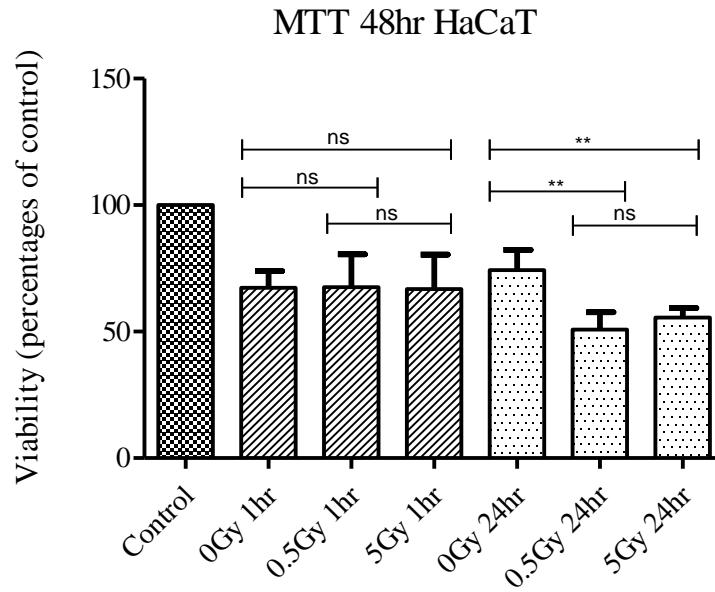


Figure 2.8 Viability of HaCaT cells after 48 hr exposure to 0, 0.5 and 5 Gy ICCM (1 and 24 hr) determined by the MTT assay. Data are expressed as mean percentage of control plus standard deviation (n = 15). Statistical analysis are represented as  $P > 0.05$  (ns),  $P \leq 0.001$  (\*\*\*) ,  $P \leq 0.01$  (\*\*) and  $P \leq 0.05$  (\*). See Appendix C1.8 for raw data.

### *HT29 Cell line*

The MTT assay results for HT29 24 hr exposures are shown in Figure 2.9. There was a non-significant decrease in cell viability for the 1 hr ICCM, from 0 Gy to 0.5 Gy, a significant decrease from 0 Gy to 5 Gy and a significant decrease between 0.5 Gy and 5 Gy. For the 24 hr ICCM, there was a non-significant increase of viability from 0 Gy to 0.5 Gy, a non-significant increase from 0 Gy to 5 Gy and a non-significant decrease between 0.5 Gy and 5 Gy.

The MTT assay results for HT29 48 hr exposures are shown in Figure 2.10. There was a non-significant decrease of cell viability for the 1 hr ICCM from 0 Gy to 0.5 Gy, a significant decrease in viability from 0 Gy to 5 Gy and a non-significant decrease between 0.5 Gy and 5 Gy. For the 24 hr ICCM, viability was non-significantly decreased from 0 Gy to 0.5 Gy, non-significantly decreased from 0 Gy to 5 Gy and significantly decreased between 0.5 Gy and 5 Gy.

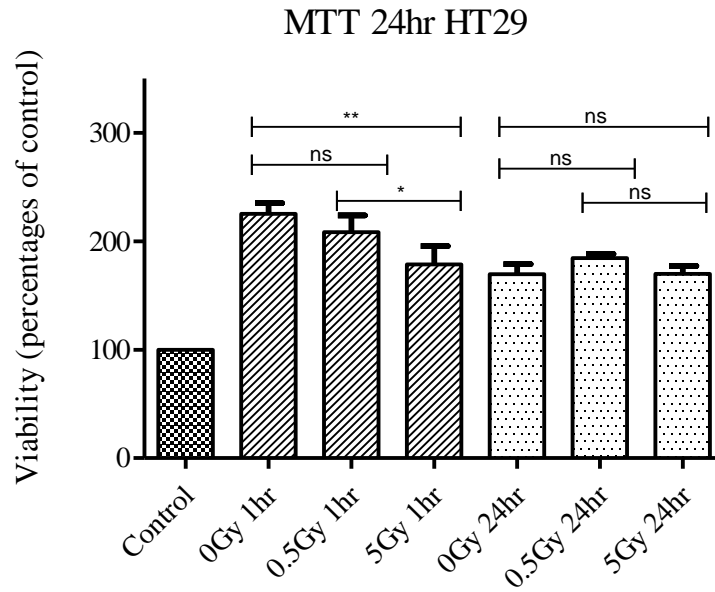


Figure 2.9 Viability of HT29 cells after 24 hr exposure to 0, 0.5 and 5 Gy ICCM (1 and 24 hr) determined by the MTT assay. Data are expressed as mean percentage of control plus standard deviation (n = 15). Statistical analysis are represented as  $P > 0.05$  (ns),  $P \leq 0.001$  (\*\*\*),  $P \leq 0.01$  (\*\*) and  $P \leq 0.05$  (\*). See Appendix C1.9 for raw data.

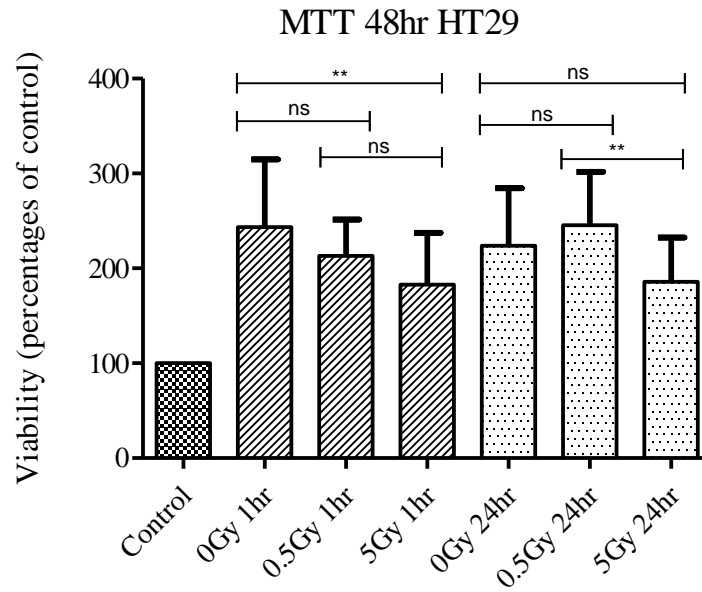


Figure 2.10 Viability of HT29 cells after 48 hr exposure to 0, 0.5 and 5 Gy ICCM (1 and 24 hr) determined by the MTT assay. Data are expressed as mean percentage of control plus standard deviation (n = 15). Statistical analysis are represented as  $P > 0.05$  (ns),  $P \leq 0.001$  (\*\*\*),  $P \leq 0.01$  (\*\*) and  $P \leq 0.05$  (\*). See Appendix C1.10 for raw data.



### *SW480 Cell line*

The MTT assay results for SW480 24 hr exposures are shown in Figure 2.11. Viability was significantly increased from 0 Gy to 0.5 Gy, non-significantly increased from 0 Gy to 5 Gy and significantly decreased between 0.5 Gy and 5 Gy, for the 1 hr ICCM samples. For the 24 ICCM samples, viability was non-significantly decreased from 0 Gy to 0.5 Gy, from 0 Gy to 5 Gy and between 0.5 Gy and 5 Gy.

The MTT assay results for SW480 48 hr exposures are shown in Figure 2.12. There was a non-significant increase of viability from 0 Gy to 0.5 Gy, from 0 Gy to 5 Gy and between 0.5 Gy and 5 Gy, for the 1 hr ICCM samples. For the 24 hr ICCM samples, there was a non-significant increase of viability between 0 Gy and 0.5 Gy and a non-significant decrease in viability from 0 Gy to 5 Gy and between 0.5 Gy and 5 Gy.

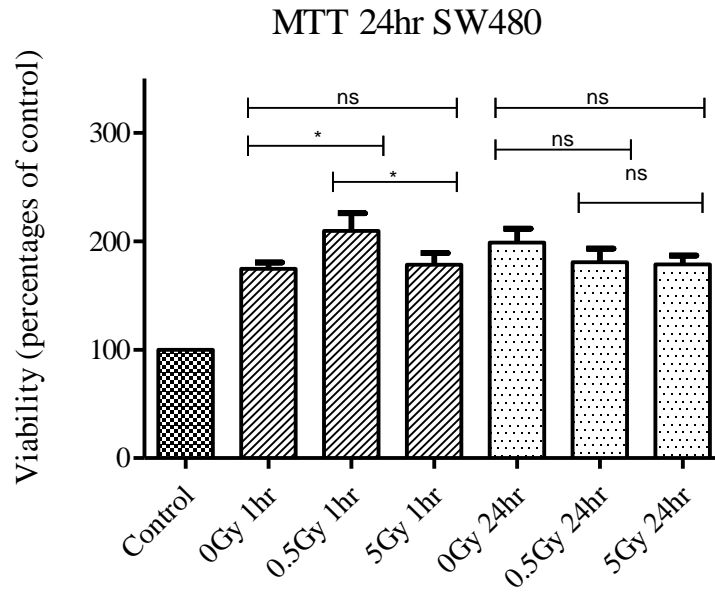


Figure 2.11 Viability of SW480 cells after 24 hr exposure to 0, 0.5 and 5 Gy ICCM (1 and 24 hr) determined by the MTT assay. Data are expressed as mean percentage of control plus standard deviation (n = 15). Statistical analysis are represented as  $P > 0.05$  (ns),  $P \leq 0.001$  (\*\*\*),  $P \leq 0.01$  (\*\*) and  $P \leq 0.05$  (\*). See Appendix C1.11 for raw data.

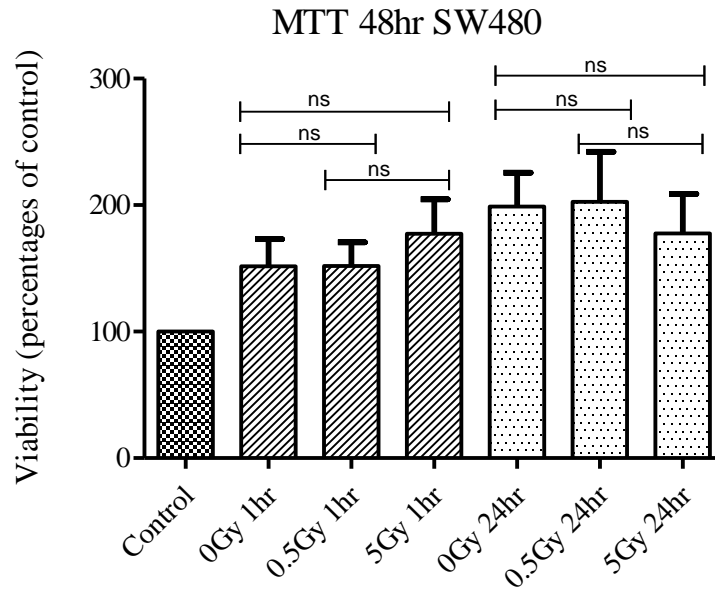


Figure 2.12 Viability of SW480 cells after 48 hr exposure to 0, 0.5 and 5 Gy ICCM (1 and 24 hr) determined by the MTT assay. Data are expressed as mean percentage of control plus standard deviation (n = 15). Statistical analysis are represented as  $P > 0.05$  (ns),  $P \leq 0.001$  (\*\*\*) ,  $P \leq 0.01$  (\*\*) and  $P \leq 0.05$  (\*). See Appendix C.12 for raw data.

### **2.3.4 Radiation-Induced Bystander Effects in Individual Colorectal Patient ICCM Samples**

The colorectal patient ICCM samples were generated by a colleague at our Institute and details are described above in Section 2.2.2. The MTT assays were set up with HaCaT reporter cells and incubated with the 0 Gy and 0.5 Gy ICCM samples per colorectal patient ICCM at a 24 hr exposure time point, details of the MTT assay were described in section 2.2.5. Figure 2.13 displays the 38 different donor samples coded CR1 - CR19 and CRC-20 – CRC38.

Variation of viability between the non-irradiated 0 Gy control and the irradiated 0.5 Gy sample (per patient) was indicative of a RIBE. Significant variation of viability response was evident between the non-irradiated samples and the irradiated samples at 0.5 Gy per patient. Figure 2.14 show RIBE and differences between the non-irradiated (0 Gy) samples and the irradiated (0.5 Gy) samples from each patient donor.

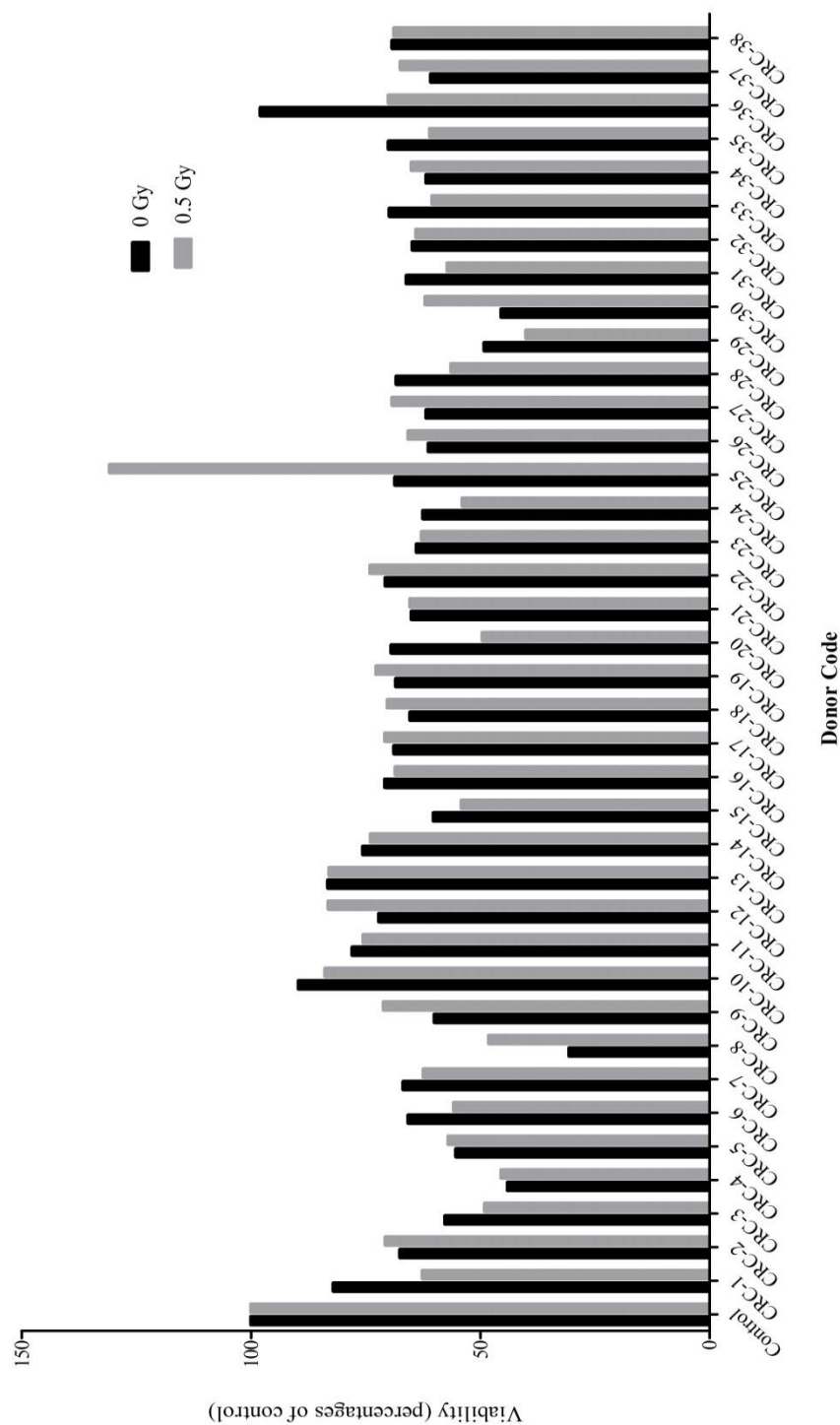


Figure 2.13 Radiation-induced bystander effects of 19 different colorectal cancer patient samples, CRC-1- CRC-19 and CRC-20- CRC-38, determined by the MTT cell viability assay. (See Appendix C1.13 for raw data) Experiment was carried out once, therefore n=1

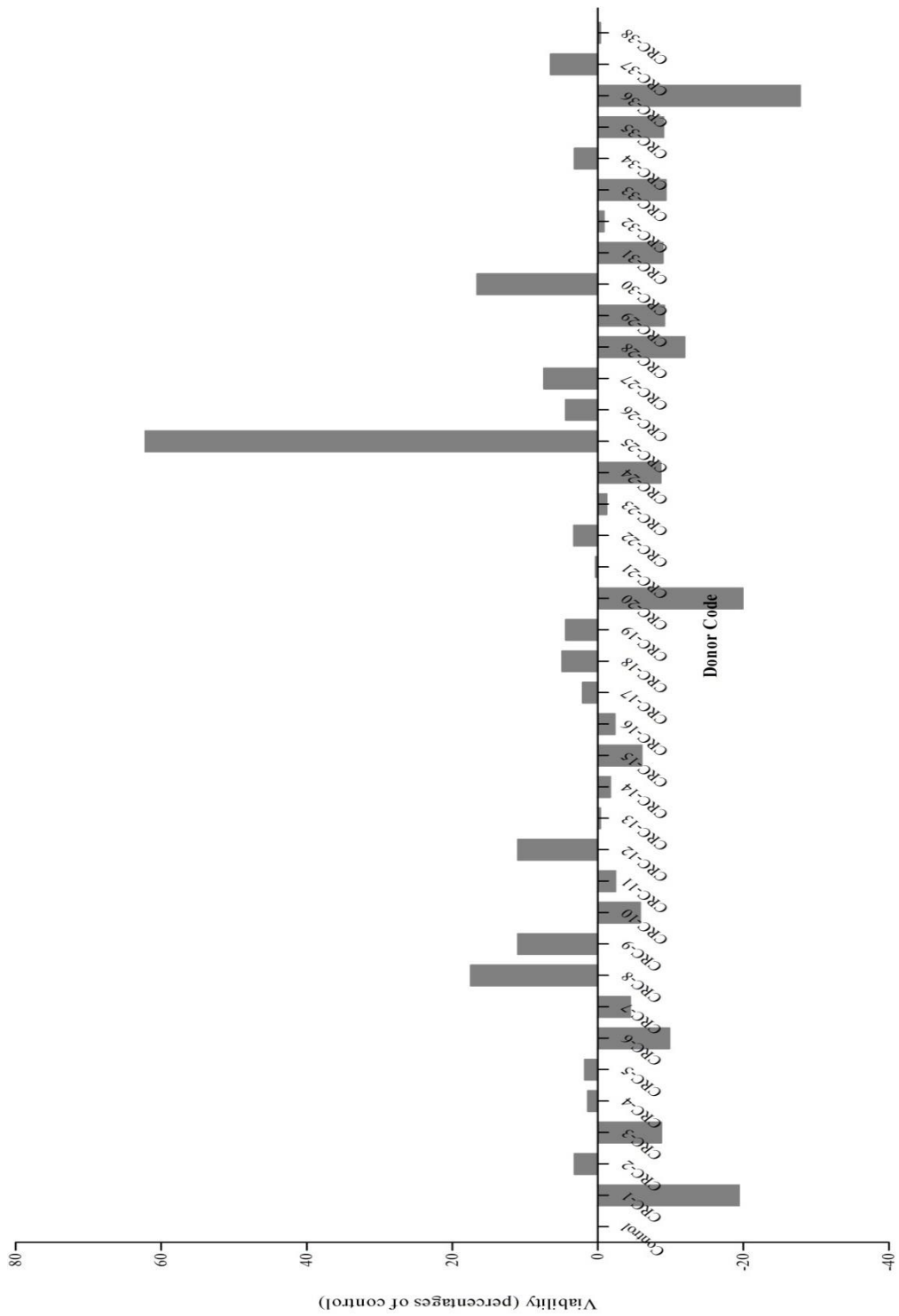


Figure 2.14 Radiation-induced bystander effects expressed in percentage difference of viability determined by the MTT cell viability assay. The results displayed are the colorectal cancer patient samples coded CRC -1 to CRC - 38. (See Appendix C1.13 for raw data)

## 2.4 Discussion

Mothersill and Seymour developed an *in vitro* medium transfer experiment to measure RIBE that is widely used in bystander studies today (1997). In the study, media from directly irradiated cells was harvested and transferred to cells that had not been irradiated and bystander effects were discovered such as decreased clonogenicity (reduced clonogenic survival in cells). The same study revealed that bystander responses are apparent in both epithelial cells and in fibroblasts; however, fibroblasts are not capable of producing a bystander effect themselves. A reason for this could be that cell and tissue architecture and cell-to-cell communication, play a role in the generation and signalling of the bystander response. The media transfer technique indicates that a signal transduction mechanism is responsible for the release of a bystander signal (bystander factor) from directly irradiated cells into their surrounding medium upon exposure.

The hypothesis of this study was to investigate RIBE in epithelial HaCaT cells and two colorectal cell lines, HT29 and SW480, in response to low doses of indirect irradiation (0.5 Gy and 5 Gy) by the addition of ICCM. Two fundamental viability assays (MTT and Alamar Blue assay) were chosen for the study, as they have been used for many research studies at our Institute and were deemed to be the most sensitive and reliable.

It was initially hypothesised that there would not be a significant difference between the HaCaT cells versus the colorectal cancer cell lines regarding the pattern of bystander effect. Surprisingly, the results of the two viability assays showed a consistent decrease of viability for the HaCaT cells compared to the assay control. The colorectal cell lines HT29 and SW480 showed a contrary increase of viability compared to the control. The results indicate that RIBE can vary depending on the cell line and possibly vary

between different tissues and tumor types which has been shown in other studies investigating different cell lines (Vines *et al.* 2008).

The Alamar Blue assay was also previously used at our Institute by Howe *et al.*, (2009) for a bystander translational study comparing intrinsic radiosensitivity and bystander responses in individual patients. Variation of response was observed between patients for both endpoints but no correlation between the two. It was suggested that the sensitivity of the Alamar blue assay may have played a role in the bystander data generated. Two ICCM exposure time points of 24 hr and 96 hr were compared and contrasted. RIBE was more pronounced in samples exposed for 24 hr in comparison to 96 hr. It is believed after 96 hr exposure, cells condition diminish due to a lack of nutrients, particularly in ICCM and the reduced survival is reflected in decreased viability. For that reason, time points of 24 and 48 hr were chosen for the current comparative study.

For the HaCaT, HT29 and SW480 cells, there were substantial differences of viability between ICCM harvest time points of 1hr and 24 hr, and between the incubation times, 24 hr and 48 hr determined by the MTT assay, which were not pronounced in the Alamar Blue assay. Furthermore, statistical analysis revealed more statistically significant differences in viability for the cell lines tested with MTT. This is suggestive that the MTT assay is more sensitive than the Alamar Blue assay. It was expected that the bystander signal would be higher in HaCaT cell cultures exposed to 24 hr ICCM compared to the 1hr exposures, generating a distinct change of viability and evident of the bystander response. Furthermore, for the individual colorectal carcinoma patient ICCM samples an expected variation in RIBE between individual patients was observed. However, a more pronounced RIBE was obtained compared to the Alamar



blue RIBE data generated for Howe *et al.*, (2009). Therefore, the data generated from both the MTT assay and Alamar Blue assay conclude that the MTT assay is more sensitive and consistent in reporting RIBE.

With regards to dose response, in both the viability assays, a reduction of viability (i.e. the bystander effect) was observed from 0 to 0.5 Gy followed by an increase of viability at 5 Gy in the HaCaT cells. A proposed bystander ‘dose-response’ curve from the calculated percentage difference of viability compared to the control in HaCaT cells for the most sensitive MTT assay is shown in Appendix C1.14. An increase of viability at 5 Gy could be due to the fact that a threshold exists in a linear dose response to radiation which is consistent with other low-dose bystander studies (Seymour & Mothersill 2000). The most sensitive dose appears to be 0.5 Gy for direct irradiation and ICCM and at higher doses the cells had a hard time to adapt due to possible cellular and molecular mechanisms triggered. At the lowest dose, 0.5 Gy the cells were capable of resisting apoptosis through adjustment of the cellular mechanisms of repair or carcinogenesis from the ICCM before they eventually became unhealthy and unable to proliferate encouraging apoptotic cell death. The radiation induced bystander response showed an interesting result, that varied, showing either a decrease or an increase of viability which also was found of Howe *et al.*, (2009) using the Alamar blue assay. The more sensitive assay (MTT assay) used for measuring RIBE *in vitro* represents either an increase or decrease of viability in bystander cells in different patient samples. Why this ‘change’ of viability in patient samples occurs is still unknown. One suggestion is that patients who undergo radiotherapy treatment may respond to the same doses differently, so are there harmful effects associated with the variability? Additional research to consider the associated molecular mechanisms is essential before any conclusions can be made.

## **Chapter 3**

**Apoptosis is signalled early by low doses of ionising radiation in a radiation-induced bystander effect**

**This chapter has been published in *Mutation Research: Fundamental and Molecular Mechanisms of Mutagenesis*.**

Furlong, H., Mothersill, C., Lyng, F. M., & Howe, O. (2013). Apoptosis is Signalled Early by Low Doses of Ionizing Radiation in a Radiation-Induced Bystander Effect. *Mutation Research/Fundamental and Molecular Mechanisms of Mutagenesis*, (741-742), 35-43.

Hayley Furlong<sup>a,b\*</sup>, Carmel Mothersill<sup>c</sup>, Fiona M Lyng<sup>a</sup>, Orla Howe<sup>a,b</sup>

<sup>a</sup>DIT Centre for Radiation and Environmental Science, Focas Research Institute, Dublin Institute of Technology, Kevin St, Dublin 8.

<sup>b</sup>School of Biological Sciences, College of Sciences and Health, Dublin Institute of Technology, Kevin St, Dublin 8.

<sup>c</sup>Medical Physics and Applied Radiation Sciences, Nuclear Research Building, 1280 Hamilton, Ontario L8S 4K1

\*Hayley Furlong was responsible for the experimental and written preparation of this document; all other authors were responsible for the original Bystander Research theory.

Person to whom all correspondence must be sent:

Ms. Hayley Furlong

DIT Centre for Radiation and Environmental Science

Focas Research Institute

Dublin Institute of Technology

Kevin St, Dublin 8, Ireland

Tel: +353-14027974

Fax: +353-14027904

Email: [hayley.furlong@dit.ie](mailto:hayley.furlong@dit.ie)

Keywords: Bystander, Apoptosis, Ionising radiation, Gene expression

## **Abstract**

It is known that ionising radiation (IR) induces a complex signalling apoptotic cascade post-exposure to low doses ultimately to remove damaged cells from a population, specifically via the intrinsic pathway. Therefore, it was hypothesised that bystander reporter cells may initiate a similar apoptotic response if exposed to low doses of IR (0.05 Gy and 0.5 Gy) and compared to directly irradiated cells. Key apoptotic genes were selected according to their role in the apoptotic cascade; tumour suppressor gene TP53, pro-apoptotic Bax and anti-apoptotic Bcl2, pro-apoptotic JNK and anti-apoptotic ERK, initiator caspase 2 and 9 and effector caspase 3, 6 and 7. The data generated consolidated the role of apoptosis following direct IR exposure for all doses and time points as pro-apoptotic genes such as Bax and JNK as well as initiator caspase 7 and

effector caspase 3 and 9 were up-regulated. However, the gene expression profile for the bystander response was quite different and more complex in comparison to the direct response. The 0.05 Gy dose point had a more significant apoptosis gene expression profile compared to the 0.5 Gy dose point and genes were not always expressed within 1 h but were sometimes expressed 24 h later. The bystander data clearly demonstrates initiation of the apoptotic cascade by the up-regulation of TP53, Bax, Bcl-2, initiator caspase 2 and effector caspase 6. The effector caspases 3 and 7 of the bystander samples demonstrated down-regulation in their gene expression levels at 0.05 Gy and 0.5 Gy at both time points therefore not fully executing the apoptotic pathway. Extensive analysis of the mean-fold gene expression changes of bystander data demonstrated that the apoptosis is initiated in the up-regulation of pro-apoptotic and initiator genes but may not very well be executed to final stages of cell death due to down-regulation of effector genes.

## **1. Introduction**

A 'bystander factor' can be produced in cells exposed to ionising radiation (IR) and can subsequently affect the function and survival of surrounding un-irradiated cells due to cellular communication of the bystander signals. This communication is either through gap junctions or by secreted factors in the surrounding medium that transmits a signal [1]. The importance of understanding altered gene expression in radiation induced bystander effects (RIBE) is apparent in the literature but has yet to be fully characterised. This study investigates gene expression changes in both directly irradiated and bystander human keratinocyte HaCaT cells.

A broad range of information regarding gene expression changes in directly irradiated cells is available, but less so for bystander cells. Human epithelial keratinocytes exposed to direct and indirect irradiation has been shown to induce initiating apoptotic events specifically on the mitochondrial related intrinsic pathway, with the increase of expression of anti-apoptotic Bcl-2 [2–5]. Mothersill et al. found that a threshold of approximately 1Gy exists to induce Bcl-2 in directly irradiated cells [6] but it is thought that there may be a different threshold for bystander irradiated cells [7]. It is important therefore to understand the signalling mechanisms involved on a molecular level. Expression levels of bystander factor induced-apoptosis related genes, in particular Bcl-2 and cytochrome c have been determined using fluorescent probes [5].

An attempt to establish cellular regulatory mechanisms in bystander cells was made in 2008, with measurement of global gene expression of alpha particle direct irradiated normal human lung fibroblasts 4 h after exposure compared to parallel bystander effects. Both direct and bystander effects were compared with the discovery that two major transcriptional centres, P53 and NfκB which regulate the direct response also have a role in the bystander cells but to a different extent [8]. P53 functions as a transcription factor in response to the stress of ionising radiation. Kuang et al investigated the genes that are targeted directly by P53 and this paper examined its role more thoroughly in response to indirect (bystander) radiation at very low doses [9]. The application of genome wide microarrays has been beneficial to determine changes in transcript profiles in human melanoma cells grown in conditioned medium from irradiated cells where they made the observation that factors transmitted from IR cells can affect transcript levels in non-IR cells [10]. The effect and involvement of chemicals in specific pathways in bystander responses has also been investigated with measurement of gene expression changes, in particular the MAPK downstream targets.

These results showed bystander induced changes in MAPK proteins and downstream targets [11].

Elmore [12] describes two distinct pathways of apoptosis in detail in her review of programmed cell death. These pathways are the extrinsic pathway which is associated with transmembrane receptor-mediated interactions involving death receptors which form multiprotein complexes. The second, intrinsic pathway involves a diverse array of non-receptor mediated stimuli which produce intracellular signals involving the mitochondria. The two described pathways have unique events initiating the pathway and unique signalling events, but there is evidence that the two pathways are linked due to molecules in one pathway influencing the other [13]. However, studies have shown that the intrinsic pathway is a more sensitive indicator of apoptotic signals when exposed to IR [14]. Subsequently only the intrinsic apoptotic cascade was considered for this bystander study to compare the gene expression response with directly irradiated cells at the same doses and time points. A group of 'intrinsic pathway' apoptotic genes were chosen for this study, dependent on their function, location and role in apoptosis.

It is known that ionising radiation in cells initiate changes in the intrinsic apoptotic pathway directly involving the mitochondria and the activation of a group of proteases known as caspases. Two groups exist according to function, initiator caspases (caspase 2, 8, 9, 10) and effector caspases (caspase 3, 6, 7). Initiator caspases cleave inactive pro-forms of effector caspases, thereby activating them. Effector caspases in turn cleave other protein substrates within the cell, to trigger the apoptotic process [15]. Caspases are the main effectors of apoptosis through cleavage of cellular substrates. Pro-caspases 8, 9 and 10 are the main initiators although the main function of some do not relate to

apoptosis. In this study, only selected initiator caspases related to the intrinsic pathway were studied (caspases 2 and 9) to capture their role in the cascade. The role of caspase 2 was included in the study because its precise role in apoptosis is still unclear, however it is thought to induce apoptosis in response to intrinsic and extrinsic signals [16]. All of the known effector caspases (caspase 3, 6 and 7) were selected to capture all mechanisms which result in the execution of apoptosis.

Different modes of cell killing such as apoptosis, necrosis, mitotic catastrophe, senescence and autophagy do exist. Cells that are exposed to IR may experience rapid or delayed cell death, such as mitotic cell death which has been investigated by Howe et al, [17]. Oncosis is the term more commonly used to describe the process of necrosis, as it is a mode of cell death that refers to the degradative processes that occur after cell death [12]. One particular paper showed a significant increase of necrosis in indirectly irradiated cells (bystander cells) in comparison to directly irradiated cells and also suppressed proliferation activity [18, 19]. Autophagy is thought to arise in damaged cells that cannot be removed by engulfment cells and is thought to lead to cell death through the process of cytoplasm destruction [20]. There may very well be other significant mechanisms responsible for the response of the bystander cells such as cross-talk to other cell death pathways. In a recent publication [19] our laboratory compared cell death pathways (apoptosis, necrosis and mitotic cell death) in directly irradiated and bystander HaCaT cells.

The bystander effect may be also be mediated by signalling pathways responsive to oxidative stress thus activating stress related kinases and their down-stream transcription factors, such as JNK and ERK. JNK is a member of the Mitogen-activated protein kinases (MAPK's), in which their pathways play an important role in



transportation of stress signals such as ionising radiation from the surface of the cell to the nucleus and responses are dependent on stimulus type [21]. Zhou et al, [22] showed that inhibition of ERK can lead to an increase in number of bystander cells.

Gene expression levels of these selected apoptotic genes were measured in directly irradiated and bystander HaCaT cells exposed to low doses of IR or ICCM respectively 1 h and 24 h after exposure. To our knowledge, this is the first report demonstrating the apoptotic gene expression levels in the intrinsic apoptotic pathway related to a radiation-induced bystander response and compared in parallel to the direct IR response *in vitro*.

## **2. Materials and methods**

### *2.1 Direct and bystander irradiation experiments in vitro*

An immortal human keratinocyte cell line, HaCaT, which was kindly received from Dr Petra Boukamp's laboratory [23] were used in these studies as they have previously been shown to be good reporters of the radiation induced bystander response [22, 23]. They were routinely cultured in DMEM: F12 (Dulbeccos Modified Eagles Medium) medium (Sigma) supplemented with 10% fetal bovine serum (FBS, Gibco) and 2mM L-Glutamine (Gibco) in DMEM medium. Cells were maintained in an atmosphere of 37°C and 5% CO<sub>2</sub> and grown to approximately 70-80% confluency to ensure they were in the logarithmic phase of growth. Cells were removed from stock flasks using a 1:1 mix of EDTA:Trypsin, EDTA: 0.1 g of EDTA in 500 ml PBS:Trypsin 2.5% 10X) and a 1:10 dilution of Trypsin then neutralised in EDTA. 200,000 cells were counted using a Coulter Counter and were plated into T25 flasks. A set of flasks were set up at 1 h and 24 h direct irradiation experiment and for harvesting of bystander media for each of the

dose points (0 Gy, 0.05 Gy 0.5 Gy) in triplicate. Another set of flasks were set up as bystander recipients at 1 h and 24 h for bystander irradiations for each of the dose points (0 Gy, 0.05 Gy 0.5 Gy) in triplicate. All flasks were incubated with a fresh media change after 1 day. The growth was monitored for 2-3 days so that the cells were allowed to reach 70-80% confluency, to ensure the phase of growth of the cells and to grow as many cells as possible per dose and time point. After 72 hours of culturing, cells (direct irradiation flasks only) were irradiated at room temperature using the cobalt 60 teletherapy unit in St. Luke's hospital (Rathgar, Dublin) with a distance from radiation source to flask of 80cm, and a field size of 25 x 25cm. All irradiated flasks were placed back into the incubator directly after irradiation until 1 h post exposure. Our group has shown that the bystander factor is produced from 30 seconds onwards from the rapid formation of calcium fluxes in similar HPV-G keratinocyte cells exposed to low doses of irradiated cell conditioned media (ICCM) [2]. The Media (ICCM) was harvested and pooled per triplicate flask for the directly irradiated flasks at 1 h and 24 h time points and each of the three dose points (0, 0.05 and 0.5 Gy). This was labelled ICCM. 5ml of fresh DMEM F12 media was replaced on the 24 h direct irradiation flasks and they were re-incubated for 24 h while an RNA extraction was conducted immediately on the 1 h direct irradiation flasks. The ICCM was filtered through a 0.22µm filter (Nalgene) to remove any dead cells or debris. The ICCM was then immediately transferred to the bystander parallel cultures of 1 h and 24 h time points at the three dose points (0, 0.05 and 0.5 Gy). For both the direct and bystander cell cultures, RNA was extracted at the relevant time points of 1 h and 24 h of each dose point. The Tri-Reagent (Sigma Aldrich) extraction technique [26] was used which briefly involves cell lysis, phase separation (with chloroform), Isopropanol precipitation and ethanol washing of the extracted RNA. The re-dissolved RNA in DEPC water

(Sigma-Aldrich 1 x ) was stored at -80°C for subsequent studies. The bystander ICCM experiment was set up according to the medium transfer technique developed by Mothersill and Seymour [1].

## *2.2 Gene expression studies*

### *2.2.1 Optimisation of apoptosis gene primers*

Apoptosis gene primers were first synthesised using the PRIMER3 programme. Caspase 3 and caspase 7 primer sequences were sourced from (Jooyeon Hwang) [27]. Bax and Bcl-2 primer sequences were sourced from (Hans-Peter Gerber) [28]. See Table 1 for individual gene primer sequences. All primer sets were obtained from Sigma Genosys, UK and were of Homosapien in origin, desalted and scaled to 0.05µmol. They were sent lyophilised and re-suspended to a concentration of 100µM, and further diluted depending on individual primer performances. Each primer set was optimised before experimentation for gene expression by assessing different primer annealing temperatures. A conventional PCR protocol using the enzyme TAQ Polymerase (Red TAQ, Sigma) was used. Each individual reaction consisted of 1µl H<sub>2</sub>O, 2µl template DNA (HaCaT), 10µl Red Taq polymerase (Sigma), and 2µl of each primer (Forward and Reverse) to a total volume of 20µl. The PCR program incorporated the following conditions; PCR initiation activation step for 2 minutes @ 94°C, Denaturation for 40seconds @ 94°C, Annealing for 1 minute @ 63°C, Extension for 40 seconds @ 72°C, Final extension for 2 minutes @ 72°C and then holding the samples at 8°C. The denaturing/melting temperatures ( $T_m$ ) and annealing temperature ( $T_a$ ) were calculated. The  $T_m$  of the primers is calculated by the following equation

$$T_m = 2 [A+T] + 4 [G+C]$$

Ranges of annealing temperatures ( $T_a$ ) were tried for each primer set until a pure PCR product/band was obtained with 1% agarose gel electrophoresis. The clearest largest band on the gel image indicated the optimum temperature for that specific primer set.

### *2.2.2 Expression of apoptosis genes in direct and bystander irradiation samples using real-time PCR and SYBR green technology*

RNA samples were quantified on a Helios  $\gamma$  spectrophotometer which measured the absorbance of the extracted RNA at 260nm and protein concentration at 280nm. A ratio of absorbance at different wavelengths (Absorbance 260:280) was calculated and samples were selected based on whether they fell in between the permitted ratio range of 1.8 – 2.0 which indicated high purity samples. All RNA samples were then reverse transcribed into a complementary DNA copy (cDNA) using the Quantitect reverse transcription kit (Qiagen, UK). According to the manufacturer's instructions, 1  $\mu$ g/ $\mu$ l of pure RNA was used in a final volume of 20  $\mu$ l. gDNA wipeout buffer was added to RNA template and RNase-free water, and incubated for 2 minutes on ice. In a separate tube Quantiscript Reverse Transcriptase, Quantiscript RT Buffer and RT primer Mix were mixed and placed on ice. The Reverse transcription mix was added to the Genomic DNA elimination mix and incubated for 15-30 min at 42°C, and then incubated for 3 minutes at 95°C to inactivate Quantiscript Reverse Transcriptase. The newly synthesised cDNA was stored at -20°C until subsequent gene expression studies were carried out by real time PCR.

Real time PCR experiments were carried out using Lightcycler® 480 (Roche Diagnostics) and SYBR Green technology (Roche). The formation of PCR products

was detected by measurement of SYBR Green fluorescence signals from each experiment. SYBR Green intercalates into the dsDNA helix and the increase in SYBR Green fluorescence is directly proportional to the amount of dsDNA generated.

The real-time PCR protocol used to calculate gene efficiency involved the addition of 2µl of cDNA product, 10µl SYBR Green (Roche), 6µl H<sub>2</sub>O and 2µl of each primer (forward and reverse) to a total volume of 20µl. This protocol was used to calculate the efficiency of each gene in the study, with an expected gene efficiency value of 2. The PCR programme consisted of the following steps; PCR initial activation step for 10 minutes @ 95°C, Denaturation for 10 seconds @ 95 °C, Annealing for 1 minute at 57, 60, 64 °C (depending on optimised temperature of primer involved) and extension for 1 minute @72°C. Each sample analysed were set up in triplicate, n = 3. And mean values were calculated.

### *2.2.3 Analysis of gene expression data*

Relative quantification analysis directly from the LC480 program (from the real-time PCR experiments using SYBR green fluorescence) was used to determine the apoptosis gene expression levels in target and reference genes. The reference gene (Tubulin) normalises sample to sample differences and was important to determine the changes in expression of different genes, according to dose and time. Two ratios were compared in each experiment, the ratio of target (gene of interest) to a reference (housekeeping gene) sequence, and the ratio of sequences within a calibrator (positive sample) sample. The result was expressed as a normalised ratio which is  $(\text{conc.target}):(\text{conc.target}) / (\text{conc.reference}):(\text{conc.reference})$

The quantitative endpoint for real-time PCR is the threshold cycle (CT). Schmittgen and Livak best define this value as ‘‘*The PCR cycle at which the fluorescent signal of the reporter dye crosses an arbitrarily placed threshold*’’[29]. A mathematical model widely used in the analysis of Real-time PCR data, the *delta delta CT method* [30] was subsequently applied to the raw CT data to give a ratio of target gene: reference genes to show the gene expression changes.

Mean-fold changes are calculated from mean normalised values of raw CT data between samples, dose/time. The *deltadelta CT* mathematical model normalises sample to sample differences. The aim was to determine the effect of both direct and indirect irradiation on the expression of the chosen target genes. This method enabled the measurement of gene expression changes of target genes normalised to Tubulin (housekeeper gene) monitored at 0.05 Gy and 0.5 Gy at 1 h and 24 h exposures and relative to the expression at 0 Gy (control). The value of the mean-fold change at 0 Gy (control) was 1. The mean-fold changes in gene expression of each target gene were plotted by Microsoft Excel, and the graphs present either up-regulation or down-regulation of samples (target genes) determined whether they reach above or below the control sample value of 1.

#### *2.2.4 Statistical data analysis*

Significance of variances between doses and time points were determined, for each specific gene targeted, by the statistical one-way ANOVA test with the aid of Microsoft excel and variances were considered significant if  $p < 0.05$ . The overall outcome on the statistical analysis recorded was a ‘NO’ for significance in table 2 compared to those

deemed significant with a 'YES'. Samples not considered statistically significant were still plotted.

### **3. Results**

#### *3.1 Optimised annealing temperatures for primers*

The set of primers which were designed with a PCR primer design tool programme online, PRIMER3, were analysed by conventional PCR to optimise the melting temperature prior to the gene expression experiments. Agarose gel electrophoresis provided strong bands which correlated to a temperature gradient used in the PCR programme, from this the best suited temperature was chosen for further RT-PCR experiments. Primer sequences for Bax, Bcl-2 and caspase 3, 7 were sourced from literature [23,24]. A list of forward and reverse sequences is shown in Table 1 and the optimum temperatures ( $T_m$  °C) for each primer set are also shown.

#### *3.2 RT-PCR gene expression study*

The expression levels of each gene will be discussed separately to unveil any emerging expression patterns of apoptosis in these HaCaT cells. Figures 1 to 5 display the direct in comparison to the bystander data of each target gene and highlight emerging changes in gene expression levels, be they up-regulated or down-regulated with respect to the control samples that have been set to one for each gene investigated.

### 3.2.1 TP53

Figure 1A-B displays a comparison of relative mean-fold changes in gene expression levels of tumour suppressor gene TP53 in HaCaT cells, following 1 h and 24 h exposures to 0.05 Gy and 0.5 Gy in direct and indirectly irradiated cells. TP53 is up-regulated in direct cells after 1 hr exposure to 0.5 Gy and down-regulated in all other direct samples. The bystander data shows that TP53 is up-regulated after 1 h in the lower dose of 0.05 Gy and down-regulated at other doses/time points. All TP53 data is statistically significant, direct  $p < 0.05$  and bystander  $p < 0.05$  and presented in Table 2.

The tumour suppressor gene responds to a range of stresses by inducing cell cycle arrest and/or apoptosis in damaged cells from IR. TP53 is a well described transcription factor that can induce the expression of multiple pro-apoptotic gene products such as caspase activators and pro-apoptotic members of the Bcl2- family such as Bax. It is known that TP53 has a critical role in regulating the bcl-2 family of proteins but the exact mechanisms have not yet been determined [31]. The direct and bystander data shows a role in the early initiation steps of apoptosis. As it is an initiator of further downstream apoptotic genes, the low dose may have implicated a response for the activation of TP53. The data illustrates a possible functional role for the initiation of the apoptotic process, at very low doses.

### 3.2.2 Bax and Bcl2

Pro-apoptotic Bax mean-fold gene expression changes are displayed in figure 2A-B. In the direct cells Bax is up-regulated in both doses which increases after 24 h and more so



in the higher dose of 0.5 Gy. In the bystander samples, Bax is up-regulated at the lower dose of 0.05 Gy after 24 h. This instigated a somewhat delayed response.

Figure 2C-D shows that anti-apoptotic Bcl-2 in direct cells is down-regulated with 0.05 Gy after 1 h and 24 h. It is then up-regulated with 0.5 Gy after 1 h and down-regulated after a further 24 h. The bystander cells displayed up-regulation after 1 h and then down-regulation after 24 h exposure to 0.5 Gy. However, one striking difference in Bcl-2 expression levels was for the 0.05 Gy bystander cells, where up-regulation was seen compared to direct cells. Table 2 revealed all gene expression changes of Bax and Bcl-2 to be statistically significant. Bax direct  $p < 0.05$  and Bax bystander  $p < 0.05$  and Bcl-2 direct  $p < 0.05$  and Bcl-2 bystander  $p < 0.05$

Bax and Bcl-2 are antagonistic to one another, in that pro-apoptotic Bax promotes the release of cytochrome c and other apoptotic factors whereas anti-apoptotic Bcl2 blocks the release of these factors [32]. The up-regulation of Bax shows that mitochondria have a role to play in the intrinsic apoptotic cascade of both direct and bystander cells at low doses. Comparing the Bax and Bcl-2 direct and bystander data it is clear that Bax up-regulation is greater so it possibly overrides the anti-apoptotic effects of Bcl-2, allowing apoptosis to continue. This is expected as it is usually in favour of inducing the apoptotic pathway.

### *3.3 JNK and ERK*

Pro-apoptotic JNK expression is displayed in figure 3A-B and is up-regulated in direct samples with 0.05 Gy after 24 h. JNK is up-regulated but not much greater than the control sample with 0.5 Gy after 1 h. All other samples are down-regulated. The

bystander samples showed very little expression of JNK with only down-regulation observed. All changes were statistically significant as seen in Table 2. Direct  $p < 0.05$  and bystander  $p < 0.05$

Anti-apoptotic ERK expression changes can be seen in figure 3C-D ERK is up-regulated in direct samples at 0.05 Gy at both time points but to a much greater extent after 1 h. The 0.5 Gy samples showed minor up-regulation of ERK after 1 h and down-regulation after 24 h. The bystander samples displayed down-regulation, so slight that expression cannot visually be observed in the graphical display of data. The bystander data showed no statistically significant changes in gene expression across the ERK samples displayed in Table 2, direct  $p < 0.05$  and bystander  $p > 0.05$

Multiple stress-inducible molecules such as c-jun N-terminal kinase (JNK) and mitogen-activated protein kinase MAPK/extracellular signal-regulated protein kinase (ERK) have been implied in transmitting the apoptotic signal [33–35]. JNK and ERK direct data had expected up-regulation, this is expected as JNK is pro-apoptotic and should respond to damaging signals. An unexpected response was detected in bystander samples, in that JNK and ERK were down-regulated in bystander conditions. This was remarkable as both genes were anticipated to have roles in the initiation process. This could possibly be due to the low doses administered, suggesting that the signal from direct cells is not strong enough to induce the pro-apoptotic function of JNK in bystander cells. Consequently there could be a threshold in existence for a response of both genes under these low dose circumstances

### 3.4 Initiator caspases (2, 9)

Initiator caspase 2 data is presented in figure 4A-B. The direct samples demonstrated down-regulation of caspase 2 with 0.05 Gy after 24 h and 0.5 Gy after 1 h. The bystander data varied to the direct in that caspase 2 was up-regulated with 0.05 Gy after 1 h and other bystander samples were down-regulated. Table 2 reveals clear statistical significance in both the direct and bystander data, direct  $p < 0.05$  and bystander  $p < 0.05$

Caspase 9 (Figure 4C-D) expression in direct samples was comparable to the bystander, in that caspase 9 was up-regulated with a low dose of 0.05 Gy after 1 h in both types of exposure, more so in the direct samples. Caspase 9 was down-regulated in all other direct and bystander samples. Statistical analysis as seen in Table 2 determined that caspase 9 direct data is statistically significant  $p < 0.05$  whereas bystander data is not statistically significant  $p > 0.05$  so may not be applicable to the overall response.

Caspase 9 seems to be switched on and up-regulated in response to direct irradiation which is expected as it is the key protein recruited in the intrinsic apoptotic pathway after cytochrome c has been released from the mitochondria. They bind along with apaf-1 to generate the apoptosome or otherwise called 'the wheel of death' which ultimately leads to downstream apoptotic events its established role associated with the formation of the apoptosome (wheel of death) in the apoptotic process. It was unusual therefore to see that both initiator caspases 2 and 9 up-regulated in response to indirect irradiation, suggesting a dual-role in both genes in a low dose bystander response and validates their role as initiators in this bystander response.

### 3.5 Effector caspases (3, 6, 7)

Figure 5A-F displays changes in gene expression of the effector caspases. Caspase 3 direct data was not statistically significant ( $p = 0.194$ ) specified in Table 2, but inspection of the data shows expression of the gene across all samples with an increase in up-regulation with 0.05 Gy and an increase of up-regulation in the 0.5 Gy samples. Caspase 3 was down-regulated in the bystander samples and statistically significant as  $p < 0.05$  for all doses and times and is presented in Table 2.

Caspase 6 is down-regulated in direct samples but the bystander data had a very different response in that caspase 6 was up-regulated after 1 h exposure to 0.05 Gy, and all other expression of the gene was down-regulated in the other doses and time points. Caspase 6 data was statistically significant in both direct and bystander data in Table 2, direct  $p < 0.05$  and bystander  $p < 0.05$ .

In the direct samples caspase 7 is up-regulated at 0.05 Gy after 1 h which decreased over the 24 h exposure. The 0.5 Gy dose induced up-regulation and a very slight increase after 24 h. The bystander data showed only down-regulation of the gene, and both direct and bystander data is statistically significant in Table 2, direct  $p < 0.05$  and bystander  $p < 0.05$ .

Caspase 3 is considered to be the most important of the effector caspases and is activated by any of the initiator caspases. Caspase 3 specifically activates the endonuclease CAD which subsequently degrades chromosomal DNA within the nuclei and causes chromatin condensation, one of the prominent cellular features of apoptosis that is detected microscopically [36]. In comparison to that, caspase 6 does not present up-regulation in direct data, so it has no role to play in this direct response. Although,

caspase 7 displays up-regulation in the direct samples across all doses/time points. This is quite interesting when in comparison to the bystander data. Uncharacteristically, caspase 3 and caspase 7 were not expressed in bystander data as up-regulators, but caspase 6 was. The expression of caspase 3 was expected to be up-regulated in the samples for all doses and time points since pro-apoptotic Bax and initiator caspase 2 and 9 were all consistently expressed. It's likely that caspase 6 has dual function (not yet elucidated) and it also may not be compelled to execute the final stages of the apoptotic pathway in the bystander cells, and so cell death be completed

#### **4. Discussion**

This study consolidates the role of apoptosis in directly irradiated cells *in vitro* with low doses of ionising radiation at 1 h and 24 h after exposure and also provides evidence for the role of the apoptotic cascade in a radiation induced bystander response at low doses of ionising radiation. As previously mentioned our laboratory [19] has compared cell death pathways (apoptosis, necrosis and mitotic cell death) in directly irradiated and bystander HaCaT cells and has been documented. Apoptosis, necrosis and mitotic cell death was observed at 24, 48 and 72 hours with higher levels in the directly irradiated cells. The induction of apoptosis in bystander cells has been shown previously by our laboratory [2, 3, 5].

Although the gene expression data was consistent and consolidated the role of apoptosis in the direct and bystander IR response, the picture for the role of apoptosis in the bystander response that emerged was more complex. It implies a different role for TP53 for the direct compared to the bystander response, which may be due to the multiple

functions of TP53 and perhaps even beyond cell cycle arrest and apoptosis. It was selected in this study because of its key importance in apoptosis and for interacting with several of the specific apoptosis inducers of the intrinsic pathway. Our data indicates a definite role for mitochondria in the bystander response. This is suggested from an immediate and prolonged role of Bax in the apoptotic response for both direct and bystander samples. So evidently the pathway has been initiated in the bystander cells. Possibly Bax is working in tandem with P53 in the bystander response.

JNK has pro-apoptotic properties and due to the high expression levels consistent with Bax in these samples consolidates the hypothesis that apoptosis is a key event in the direct IR response but perhaps not in the bystander response.

The role of caspase 2 is still under much investigation but it has been suggested to be an initiator caspase of both the intrinsic and extrinsic apoptotic pathways. For this reason, both caspase 2 and 9 were included in this study (and extrinsic pathway associated initiators excluded). The direct samples demonstrated that caspase 9 permitted the progression of the apoptotic initiation events. Bystander data reported caspase 2 and as the leading initiator of further down-stream caspases in the bystander response.

The role of effector caspase 3 and 7 are still unclear but their expression levels in this study was consistent for directly irradiated cells (at the same doses and time points) indicating a possible dual role in the execution of apoptosis. It is known that caspase 3 causes chromatin condensation in the execution of apoptosis, but considering that other processes such as cell shrinkage, membrane blebbing and apoptotic body formation, perhaps caspase 6 has a role to play in these apoptotic execution processes. For the bystander cells, it appeared that caspase 6 was the only one to be up-regulated as opposed to effector caspase 3 and 7 displaying down-regulation signifying a late

response. Maybe caspase 7 does not have a huge role to play in the overall apoptotic bystander response.

The data clearly indicated differences between the apoptotic events in the direct versus the bystander response for dose and time. The direct samples demonstrated up-regulation in gene expression in both doses and time points. However bystander data displayed a common trend in that evidence for up-regulation was more notably apparent at the lower dose of 0.05 Gy. It was suggested that perhaps this was due to the extent of the damage by the low doses analysed (0.05 Gy and 0.5 Gy) or the exposure time analysed in the study 1 and 24 h. Perhaps the full apoptotic cascade needs more than 24 hours to complete the process. To obtain a clearer pattern of the apoptotic gene expression profile bystander response, lower doses (0.005 Gy) would be required and additional time points at intervals between 1 to 24 h (6 h, 12 h ) would also be useful to indicate the changes in expression levels at specific times. The consideration of apoptosis genes from the other two known apoptosis pathways (extrinsic and Granzyme perforin pathway) would be beneficial to detect if the bystander response is a unique pathway with cross talk between genes of the apoptosis pathways. It is well known that there is cross-talk between all of the three types of apoptosis pathways and it is possible that the bystander response may be involved in this cross-talk.

Further to this study our group are currently analysing the post-translational effects of these genes, because protein expression doesn't always go hand in hand with gene up-regulation. It is possible to get post-translational modification of existing proteins, hence in their active form. Thus an RNA result showing no change does not necessarily mean no change in activity. It could suggest an alternative cell death mechanisms are in operation. From this study we can delineate that human keratinocyte bystander cells

exposed to low doses of ionising radiation have a different role of cell death than directly irradiated cells.

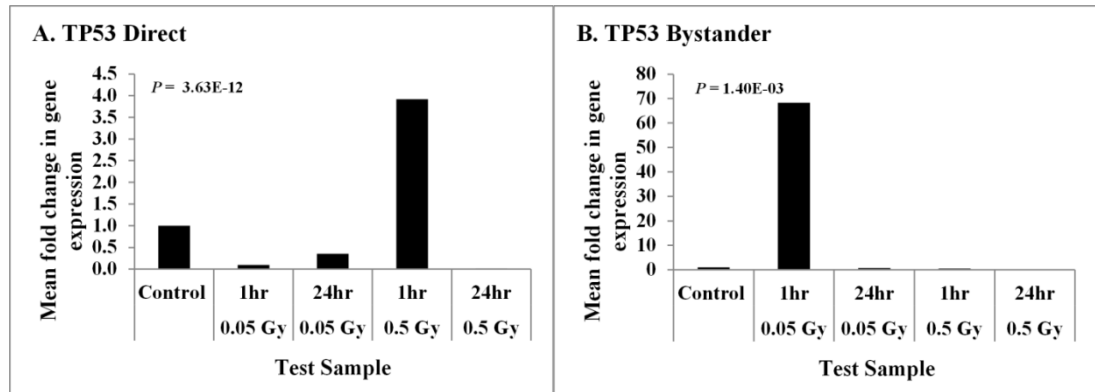


Figure 1 A-B: Comparison of relative fold-changes in gene expression levels of tumour suppressor gene TP53 in HaCaT cells, following 1 hr and 24 hrs exposures to 0.05 Gy and 0.5 Gy direct and indirect gamma irradiation.



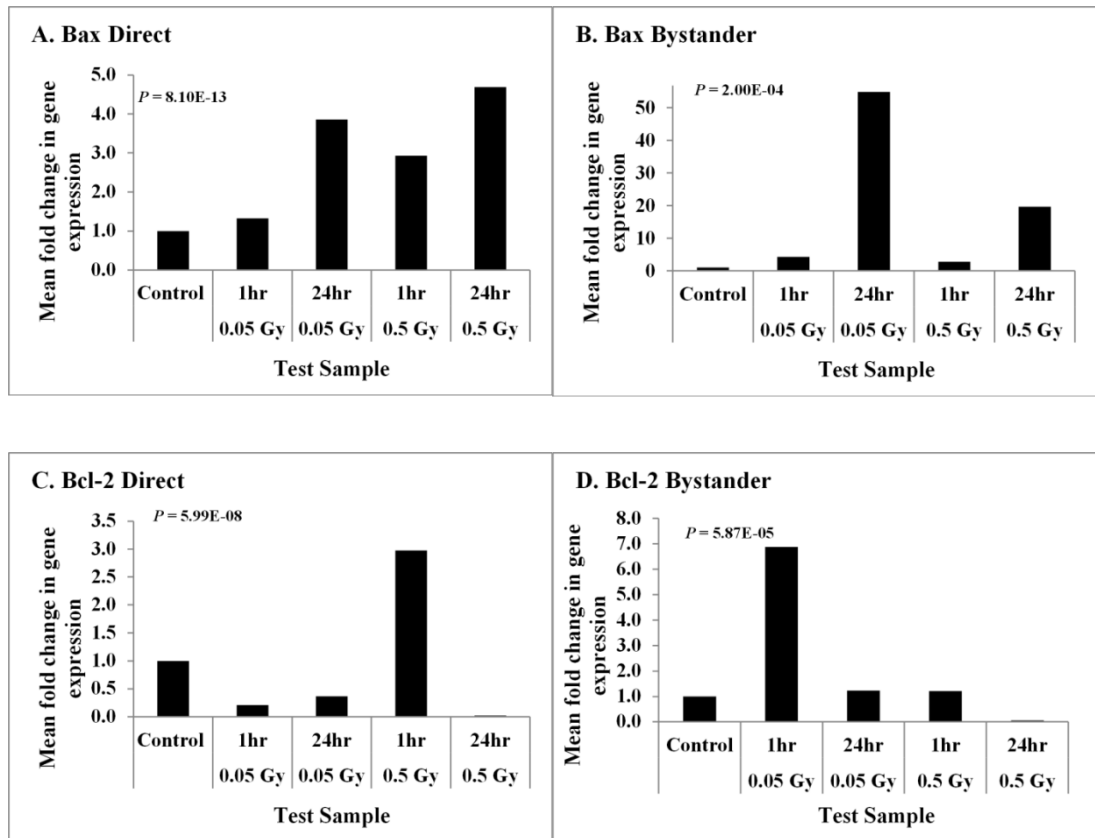


Figure 2 A-D: Comparison of relative fold-changes in gene expression levels of Pro-apoptotic Bax and anti-apoptotic Bcl-2 in HaCaT cells following 1 hr and 24 hrs exposures to 0.05 Gy and 0.5 Gy direct and indirect gamma irradiation.

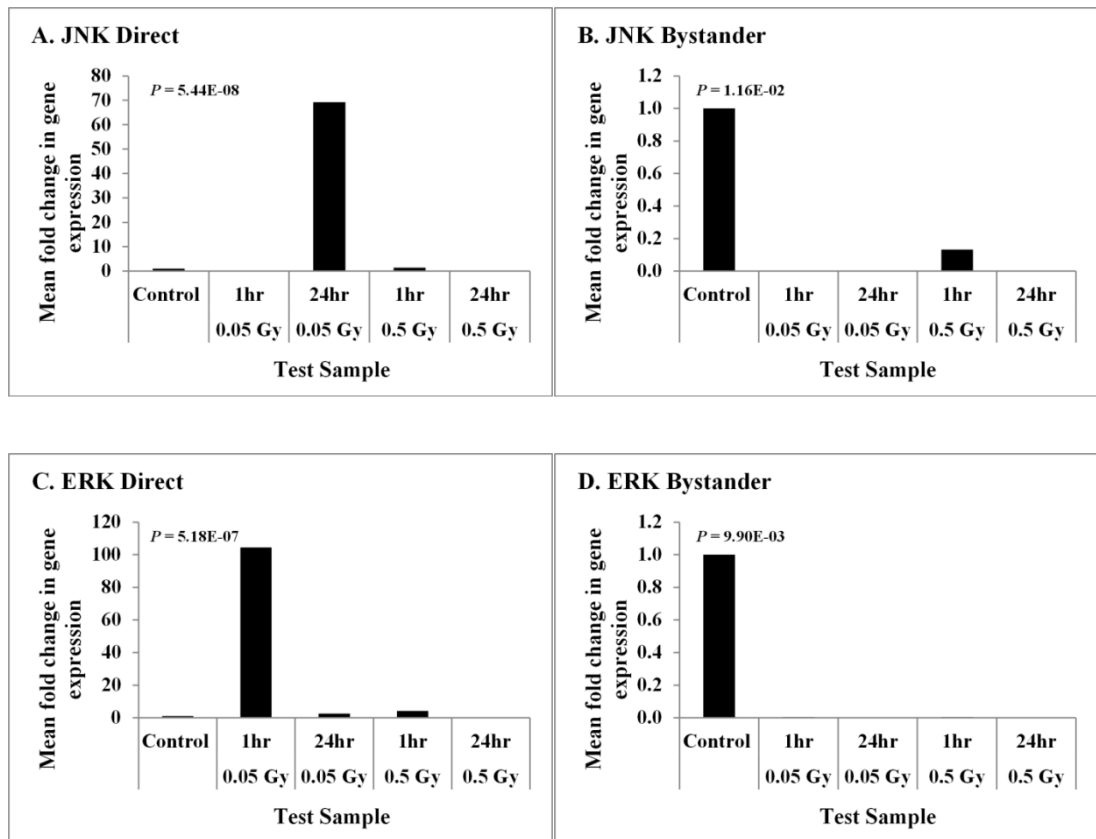


Figure 3 A-D: Comparison of relative fold-changes in gene expression levels of synergistic JNK and ERK in HaCaT cells following 1 hr and 24 hrs exposures to 0.05 Gy and 0.5 Gy direct and indirect gamma irradiation.

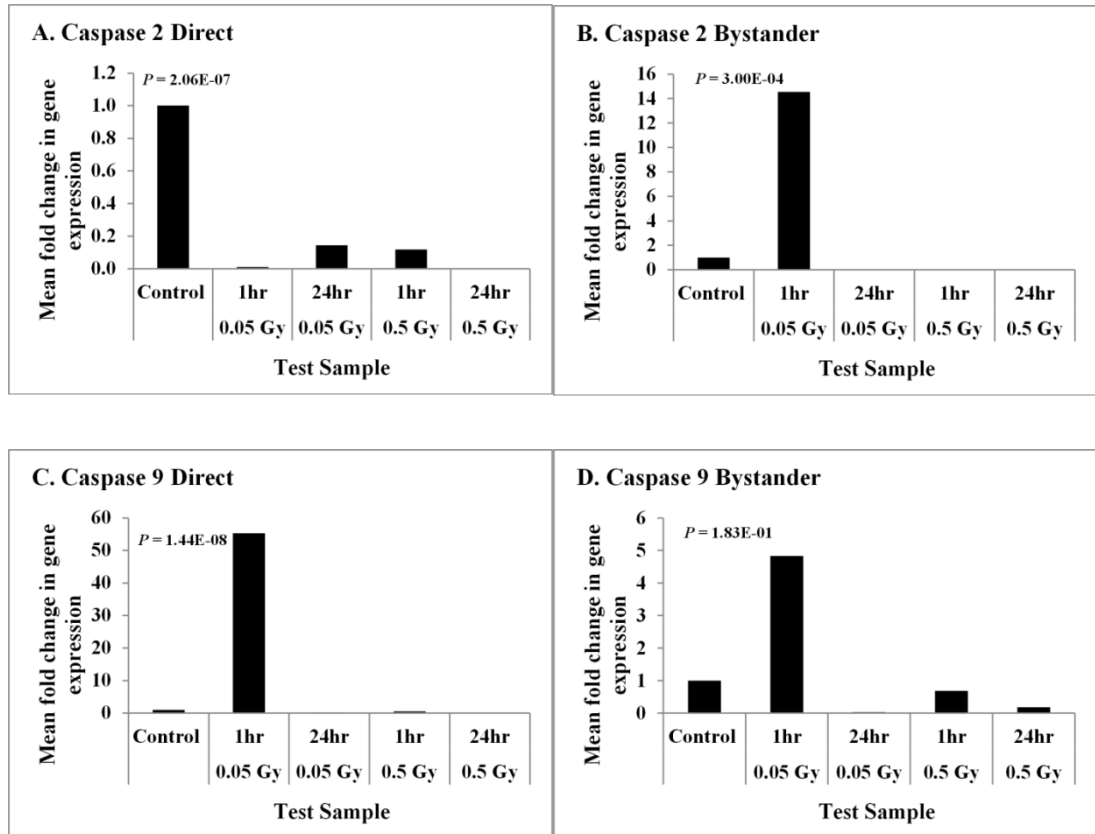


Figure 4 A-D: Comparison of relative fold-changes in gene expression levels of initiator caspases 2 and 9 in HaCaT cells following 1 hr and 24 hrs exposures to 0.05 Gy and 0.5 Gy direct and indirect gamma irradiation.

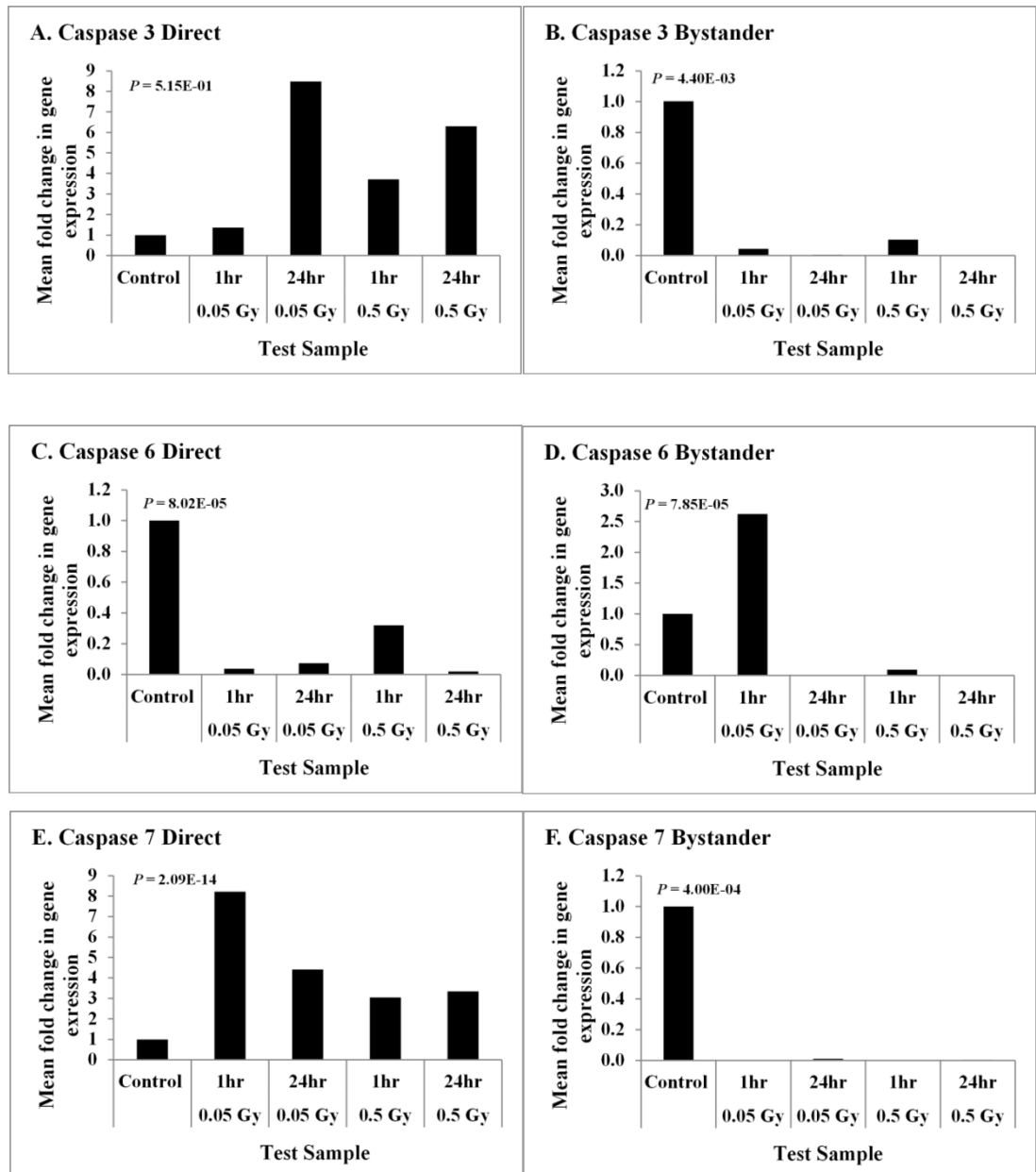


Figure 5 A-F: Comparison of relative fold-changes in gene expression levels of executioner caspases 3, 6 and 7 HaCaT cells following 1 hr and 24 hrs exposures to direct and indirect 0.05 Gy and 0.5 Gy gamma irradiation.

<b>Gene</b>	<b>Forward oligo sequence</b>	<b>Reverse oligo Sequence</b>
TP53	5'GTCTTTGAACCCTTGCTTGC'3	3'CCACAACAAAACACCAGTGC'5
Bax	5'AGGATGCGTCCACCAAGAAG'3	3'CCAGTTGAAGTTGCCGTCAGA'5
Bcl-2	5'AAGCGGTCCCGTGGATAGA'3	3'TCCGGTATTCGCAGAAGTCC'5
ERK	5'TTAGGGCTGTGAGCTGTTCC'3	3'TCAGGAGGATGAGGACATGG'5
JNK	5'TTAAAGCCAGTCAGGCAAGG'3	3'CATTGATGTACGGGTGTTGG'5
Caspase 2	5'CTACCTGTTCCCAGGACACC'3	3'AGAACAGAAACCGTGCATCC'5
Caspase 9	5'TCCAGATTGACGACAAGTGC'3	3'AGGGACAGTGCTGAACATCC'5
Caspase 3	5'TTTGTTTGTGTGCTTCTGAG'3	3'TGAATTTTCGCCAAGAATAT'5
Caspase 6	5'CCTGACCAACATGGAGAAGC'3	3'AGTGATTCTCCTGCCTCAGC'5
Caspase 7	5'AAGATCCCAGTGGAAGCTGA'3	3'TCTCATGGAAGTGTGGGTCA'5
Tubulin	5'GCTTCTTGGTTTTCCACAGC'3	3'CTCCAGCTTGGACTTCTTGC'5

**Table 1** List of Forward and reverse oligo sequences of genes used in this study

**Table 2** Statistical values for Real-Time PCR gene expression analysis data presented in Figures 1 to 5. Significant differences in gene expression changes were determined with One-Way Anova, whereby the mean values of target genes were compared for significant variability in data. A gene expression change was deemed statistically significant (denoted by a ‘YES’ in the table below) only if  $p < 0.05$  and values are displayed below.

Gene	Dose Gy	One Way Anova (Direct) $p =$	Significance Direct	One way Anova (Bystander) $p =$	Significance Bystander
TP53	Control	3.63E-12	YES	1.40E-03	YES
Bcl-2 Family Pro and Anti-apoptotic					
Bax	Control	8.10E-13	YES	2.00E-04	YES
Bcl-2	Control	5.99E-08	YES	5.87E-05	YES
Stress Activated Protein Kinases					
JNK	Control	5.44E-08	YES	1.16E-02	YES
ERK	Control	5.18E-07	YES	9.90E-03	NO
Initiator Caspases					
Casp 2	Control	2.06E-07	YES	3.00E-04	YES
Casp 9	Control	1.44E-08	YES	1.83E-01	NO
Effector Caspases					
Casp 3	Control	5.15E-01	NO	4.40E-03	YES
Casp 6	Control	8.02E-05	YES	7.85E-05	YES
Casp 7	Control	2.09E-14	YES	4.00E-04	YES

## Acknowledgement

The authors acknowledge financial support from the FP6 Integrated Project, *Non-targeted effects of ionising radiation (NOTE)* FI6R 036465.

### **Permission for reproduction of published work in a thesis (Chapter 3)**

“Apoptosis is Signalled Early by Low Doses of Ionising Radiation in a Radiation-Induced Bystander Effect”

Excerpt from the section of “Authors Rights” posted on Elsevier website.

<http://www.elsevier.com/journal-authors/author-rights-and-responsibilities>

Authors can use either their accepted author manuscript or final published article for:

- Use at a conference, meeting or for teaching purposes
- Internal training by their company
- Sharing individual articles with colleagues for their research use\* (also known as 'scholarly sharing')
- Use in a subsequent compilation of the author's works
- **Inclusion in a thesis or dissertation**
- Reuse of portions or extracts from the article in other works
- Preparation of derivative works (other than for [commercial purposes](#))

## **Chapter 4**

### **Radiation-Induced Bystander Mediated Apoptosis via the Intrinsic Pathway in HaCaT Cells Exposed to Low Doses**



## 4.1 Introduction

The biochemical and genetic changes that occur in a radiation induced bystander response are central to understanding the implications of the response on a cellular and potential clinical level. There is a lot of debate as to whether the bystander response is protective (Barcellos-Hoff & Brooks 2001; Portess *et al.* 2007) or detrimental (Chaudhry 2006; Belyakov *et al.* 2006; Lyng *et al.* 2005). Either way the signal produced by the directly targeted cell will determine the magnitude of the bystander effect and this is apparent in studies which demonstrated the difference between bystander signal generation and response to signals (Vines *et al.* 2008). Low dose bystander responses instigate enhanced radioresistance (Iyer & Lehnert 2002). Biological endpoints of bystander responses have been explored including activation of calcium signalling, intracellular reactive oxygen species activation and apoptosis/cell death mechanisms and have been reviewed by Blyth and Sykes in 2011 (2011).

Apoptosis, originally termed ‘‘interphase death’’ by Bacq & Alexander in 1961 (1961) was re-named apoptosis by Kerr *et al.*, (1972). *In vitro* studies have confirmed that cells of epithelial origin tend to undergo reproductive cell death and secondary apoptosis following IR (Aldridge *et al.* 1995). Induction of apoptosis is linked to a series of molecular events, including an induction of calcium flux, loss of mitochondrial membrane potential and a consequent increase of the number of apoptotic cells (Lyng *et al.* 2000). Increased cell death in cells exposed to low doses of IR can be analysed using either the clonogenic assay (Puck & Marcus 1956) or cytotoxicological cell viability assays as discussed in Chapter 2. In particular human keratinocyte cells are known to be good reporters of the bystander response, specifically HaCaT cells and which have been exploited in a number of *in vitro* experiments whereby the number of

apoptotic cells increases in response to indirect-irradiation (Mothersill *et al.* 2000; Mothersill & Seymour 2002).

Consequently, a comprehensive study of the role of apoptotic gene expression changes in directly irradiated versus bystander HaCaT cells was completed in Chapter 3 (Furlong *et al.* 2013). A selection of pro and anti-apoptotic genes from the intrinsic apoptotic pathway were chosen and analysed for significant changes in gene expression. Mitochondrial associated genes and caspases play a role in the apoptotic intrinsic pathway and have been considered as sensitive detectors of apoptotic signalling (Assefa *et al.* 2000; Sitailo *et al.* 2002; Assefa *et al.* 2003). Apoptosis is initiated through radiation exposure and activates caspases in human keratinocytes commonly through the intrinsic pathway which is regulated by mitochondrial genes Bax and Bcl-2 (Lindsay *et al.* 2011). The Bcl-2 family of genes located at the mitochondria promote release of cytochrome c which is required for activation of the caspases. In particular the initiator caspases drive the latter part of the response recruiting effector caspases to complete the cell death pathway. The bystander factor is produced from 30 seconds onwards from the rapid formation of calcium fluxes in human keratinocyte cells exposed to low doses of ICCM (Lyng *et al.* 2000) and may be occurring up-stream of apoptotic events. Chapter 3 (Furlong *et al.* 2013) revealed that the role of apoptosis in bystander cells takes a more complex course of action. The data revealed that initiator caspases responded immediately suggesting that the pathway was not fully executed by the effector caspases and the low-dose bystander responses varied from each other.

For that reason, the aim of the current study was to demonstrate more extensive effect of a radiation induced bystander response with gene expression changes of TP53, Bax, Bcl-2, ERK, caspase 2, caspase 9, caspase 6 and caspase 7, including a lower dose range of IR (0.005Gy, 0.05 Gy and 0.5Gy) because it was clear in Chapter 3 that something

interesting was occurring at the low doses in bystander cells. The genes were investigated over intervals within a broad timeframe (1, 6, 12, 24, 48 and 72 hr). This study did in fact deliver a more defined molecular insight into the mechanisms of bystander responses at very specific times and doses and an apoptotic signalling pathway is proposed in Chapter 6.

## **4.2 Materials and Methods**

### **4.2.1 Direct and Bystander Irradiation Experiments *in vitro***

HaCaT cells were routinely cultured, maintained and counted as described in Chapter 2 (section 2.2.1).  $2 \times 10^5$  HaCaT cells were plated into T25 flasks as follows; a set of flasks were set up for direct irradiation and for harvesting of bystander media for each of the dose points (0 Gy, 0.005 Gy, 0.05 Gy, and 0.5 Gy) in triplicate. Another set of flasks were set up as bystander recipients also in triplicate. Full experimental details of the direct irradiation exposure, the irradiated cell conditioned media (ICCM) harvest and exposure for bystander HaCaT cells are provided in detail in Chapter 3 (section 2.1). For the 0.5 Gy dose point the source to sample distance was 80 cm, for the 0.05 Gy and 0.005 Gy dose points, the source to sample distance was 191.5 cm. The dose rate delivered was approximately 1.5 Gy/min during these experiments as evaluated at the 80 cm source to sample distance. Thermoluminescent dosimeters (TLD) were used to confirm that the appropriate dose was delivered. The media (ICCM) was harvested and pooled per triplicate flask for the directly irradiated flasks at each of the time points (1, 6, 12, 24, 48 and 72 hr) and each of the dose points (0, 0.005, 0.05 and 0.5 Gy). Flasks were re-incubated until time for RNA harvest while an RNA extraction was conducted immediately on the 1 hr direct irradiation flasks (See Appendix A5, A6 and A7 for a list

of reagents used). RNA was extracted following the same method as described in Chapter 3 (section 2.1) and details of the RNA extraction, quantification and cDNA synthesis can be found in Appendix B7, Appendix B8 and Appendix B9.

#### **4.2.2 Gene Expression Study**

Apoptosis gene primers TP53, Bax, Bcl-2, ERK, caspase 2, caspase 9, caspase 6 and caspase 7 were designed and optimised following the same procedure as described in Chapter 3 (section 2.2.1) and a list of forward and reverse sequences for each gene are displayed in Table 4.1 (refer to Appendix B10 and Appendix B11 for primer design and optimisation details). Relative quantification analysis directly from the LC480 program (from the real-time PCR experiments using SYBR green fluorescence) was used to determine the apoptosis gene expression levels in target and reference genes (see Appendix B12 for full RT-PCR protocol and conditions) just as in Chapter 3. Mean-fold changes were calculated from mean normalised values of raw CT data between samples, dose/time (Schmittgen & Livak 2008) as described in Chapter 3 (section 2.2.3). Gene expression changes of target genes were normalised to Tubulin (housekeeper gene) exposed to 0.005 Gy, 0.05 Gy and 0.5 Gy at 1, 6, 12, 24, 48 and 72 hr and measured relative to the expression at 0 Gy (control). The value of the mean-fold change at 0 Gy (control) was fixed to zero by logging the gene expression values and mean-fold changes in gene expression of each target gene were plotted in GraphPad Prism.

### **Statistical data analysis**

Significance of variances was determined for each specific gene targeted with Two-way analysis of variance (ANOVA) tests using GraphPad Prism statistical program. For each target gene the control (0 Gy) samples were compared to each dose to determine overall significant changes. Variances were considered significant if  $p \leq 0.05$ . Statistical significance between time-points of each gene is marked on Figures 4.1 – 4.3 with,  $P > 0.05$  (ns),  $P \leq 0.01$  (\*\*) and  $P \leq 0.05$  (\*).

Table 4.1: List of Forward and reverse oligo sequences of genes used in this study

<b>Gene</b>	<b>Forward oligo sequence</b>	<b>Reverse oligo Sequence</b>
TP53	5'GTCTTTGAACCCTTGCTTGC'3	3'CCACAACAAAACACCAGTGC'5
Bax	5'AGGATGCGTCCACCAAGAAG'3	3'CCAGTTGAAGTTGCCGTCAGA'5
Bcl-2	5'AAGCGGTCCCGTGGATAGA'3	3'TCCGGTATTCGCAGAAGTCC'5
ERK	5'TTAGGGCTGTGAGCTGTTCC'3	3'TCAGGAGGATGAGGACATGG'5
Caspase 2	5'CTACCTGTTCCCAGGACACC'3	3'AGAACAGAAACCGTGCATCC'5
Caspase 9	5'TCCAGATTGACGACAAGTGC'3	3'AGGGACAGTGCTGAACATCC'5
Caspase 6	5'CCTGACCAACATGGAGAAGC'3	3'AGTGATTCTCCTGCCTCAGC'5
Caspase 7	5'AAGATCCCAGTGGAAGCTGA'3	3'TCTCATGGAAGTGTGGGTCA'5
Tubulin	5'GCTTCTTGGTTTTCCACAGC'3	3'CTCCAGCTTGGACTTCTTGC'5

## 4.3 Results

### RT-PCR Gene expression study

The bystander dose-specific responses are discussed separately to unveil any emerging apoptotic gene expression patterns in HaCaT cells that may be dose-specific. Figures 4.1 – 4.3 display the changes in expression of TP53, Bax, Bcl-2, ERK, caspase 2, caspase 9, caspase 6 and caspase 7 in response to indirect irradiations (0.005, 0.05 and 0.5 Gy). The results are presented in bar charts as the fold-change ( $\text{Log}_{10}$ ) of gene expression for each gene selected over a period of time (1, 6, 12, 24, 48 and 72 hr) per dose. The results are discussed as either significant or non-significant which relates to how significantly the expression of the target gene was altered with respect to the non-irradiated control samples, which have been set to zero. Refer to Appendix C.3.1 and C.3.2 for raw direct and bystander data for this chapter. Tubulin was chosen for this study as it was deemed the most suitable based on a similar radiobiological study showing that  $\beta$ -tubulin is a reliable reference gene (Li *et al.*, 2011). Although the study argued that  $\alpha$ -tubulin was not a suitable reference gene for radiation studies. Likewise, others have shown that  $\beta$ -tubulin is the more suitable reference gene for studies with HaCaT cells (Campos *et al.*, 2009; Kim *et al.*, 2010), mostly for Western Blot analysis, as there are very few real-time q-PCR studies that employ tubulin as the reference gene. It is clear from current data that there are changes in tubulin expression with treatment of ICCM. Therefore, due to the variability in expression, future studies should incorporate a thorough analysis of several potential housekeeper genes to validate the data.

Figure 4.1 shows that between 1 hr and 12 hr, TP53 was significantly up-regulated. Between 12 hr and 24 hr, 48 hr and 72 hr exposure TP53 was significantly down-regulated. Bax was significantly down-regulated between 6 hr and 24 hr, 48 hr and 72 hr. Bcl-2 was significantly down-regulated between 1 hr and 6 hr, 12 hr and 24 hr, and significantly up-regulated between 12 hr and 48 hr. ERK was significantly up-regulated between 1 hr and 12 hr, 1 hr and 72 hr and 6 hr and 72 hr exposure. ERK was significantly down-regulated between 12 hr and 48 hr exposure. Between 24 hr, 48 hr and 72 hr, ERK was significantly up-regulated. Caspase 2 was significantly up-regulated between 1 hr and 72 hr, 12 hr and 72 hr, 24 hr and 72 hr and between 48 hr and 72 hr exposure. Caspase 6 was significantly down-regulated between 12 hr and 48 hr exposure. Caspase 7 was significantly up-regulated between 1 hr and 6 hr exposure and significantly down-regulated between 6 hr and 12 hr exposure. All other changes in gene expression were deemed not statistically significant. Figure 4.2 shows the 0.05 Gy bystander response. TP53 was significantly down-regulated between 24 hr and 72 hr exposure. Bcl-2 was significantly down-regulated between 1 hr and 6 hr, 1 hr and 12 hr and between 1 hr and 24 hr exposure. ERK was significantly up-regulated between 1 hr and 12 hr exposure. Figure 4.3 shows the 0.5 Gy response, whereby all of the gene expression changes were not statistically significant.



Table 4.2: Overview of the individual fold-changes of expression for each apoptotic gene analysed over 72 hr time-course for 0.005, 0.05 and 0.5 Gy doses. Values over zero are said to be ‘up-regulated’ and values below zero are ‘down-regulated’.

Tumor Suppressor						
TP53	1 hr	6 hr	12 hr	24 hr	48 hr	72 hr
0.005 Gy	0.37	4.17	5.62	0.06	0.08	0.09
0.05 Gy	0.16	0.08	0.12	3.17	-0.01	-4.43
0.5 Gy	0.04	0.06	0.04	5.46	0.08	4.44
Bcl-2 Family Pro and Anti-apoptotic						
Bax	1 hr	6 hr	12 hr	24 hr	48 hr	72 hr
0.005 Gy	1.49	2.02	0.88	-0.44	0.37	-0.29
0.05 Gy	1.69	1.19	-0.89	0.3	0.29	-0.12
0.5 Gy	1.47	0.67	-1.56	0.06	-0.44	-0.78
Bcl-2	1 hr	6 hr	12 hr	24 hr	48 hr	72 hr
0.005 Gy	3.75	-2	-3.95	-1.73	1.02	0.27
0.05 Gy	4.54	-1.18	-3.4	-0.65	0.34	0.12
0.5 Gy	2.9	-1.6	-0.65	-3.05	-0.39	-1.45
Stress Activated Protein Kinases						
ERK	1 hr	6 hr	12 hr	24 hr	48 hr	72 hr
0.005 Gy	-2.7	0.84	3.77	1.35	-1.42	4.8
0.05 Gy	-2.96	0.11	3.43	0.86	-0.36	-0.22
0.5 Gy	-1.11	0.73	2.33	1.54	-0.18	1.24
Initiator Caspases						
Caspase 2	1 hr	6 hr	12 hr	24 hr	48 hr	72 hr
0.005 Gy	-3.75	3.96	0.81	0.79	0.06	5.67
0.05 Gy	2.96	1.63	2.17	0.56	0.07	0.05
0.5 Gy	-1.52	1.3	1.26	1.29	0.08	0.74
Caspase 9	1 hr	6 hr	12 hr	24 hr	48 hr	72 hr
0.005 Gy	-3.98	3.62	2.15	0.018	-0.13	1.44
0.05 Gy	3.74	1.61	2.09	0.97	0.97	0.05
0.5 Gy	-1.46	0.3	0.4	-0.36	-0.16	2.34
Effector Caspases						
Caspase 6	1 hr	6 hr	12 hr	24 hr	48 hr	72 hr
0.005 Gy	-0.16	2.03	4.1	1.41	-1.9	-0.03
0.05 Gy	2.32	0.86	0.1	1.17	-0.78	0.3
0.5 Gy	-0.3	1.07	0.61	1.98	-0.59	1.32
Caspase 7	1 hr	6 hr	12 hr	24 hr	48 hr	72 hr
0.005 Gy	-3.85	5.43	-1.14	1.21	-0.19	-0.12
0.05 Gy	-2.92	-2.89	-2.01	-0.04	-0.01	-0.03
0.5 Gy	-1.16	2.43	-0.69	0.04	0.4	1.11

Table 4.3: Statistical values for Real-Time PCR gene expression analysis data are presented below. Statistically significant differences in gene expression changes were determined with Two-way Anova analysis of variance, whereby the mean values of target genes (for each dose and time-point) were compared for significant variability in data. Statistical analysis are represented as  $P > 0.05$  (ns),  $P \leq 0.01$  (\*\*) and  $P \leq 0.05$  (\*).

	Two-way Anova							
	TP53	Bax	Bcl-2	ERK	Casp 2	Casp 9	Casp 6	Casp 7
<b>0.005 Gy</b>								
1 hr vs 6 hr	ns	ns	*	ns	ns	ns	ns	*
1 hr vs 12 hr	**	ns	**	*	ns	ns	ns	ns
1 hr vs 24 hr	ns	ns	*	ns	ns	ns	ns	ns
1 hr vs 48 hr	ns	ns	ns	ns	ns	ns	ns	ns
1 hr vs 72 hr	ns	ns	ns	**	*	ns	ns	ns
6 hr vs 12 hr	ns	ns	ns	ns	ns	ns	ns	*
6 hr vs 24 hr	ns	*	ns	ns	ns	ns	ns	ns
6 hr vs 48 hr	ns	*	ns	ns	ns	ns	ns	ns
6 hr vs 72 hr	ns	*	ns	*	ns	ns	ns	ns
12 hr vs 24 hr	**	ns	ns	ns	ns	ns	ns	ns
12 hr vs 48 hr	**	ns	*	*	ns	ns	*	ns
12 hr vs 72 hr	**	ns	ns	ns	*	ns	ns	ns
24 hr vs 48 hr	ns	ns	ns	ns	ns	ns	ns	ns
24 hr vs 72 hr	ns	ns	ns	*	*	ns	ns	ns
48 hr vs 72 hr	ns	ns	ns	*	*	ns	ns	ns
<b>0.05 Gy</b>								
	TP53	Bax	Bcl-2	ERK	Casp 2	Casp 9	Casp 6	Casp 7
1 hr vs 6 hr	ns	ns	*	ns	ns	ns	ns	ns
1 hr vs 12 hr	ns	ns	**	*	ns	ns	ns	ns
1 hr vs 24 hr	ns	ns	*	ns	ns	ns	ns	ns
1 hr vs 48 hr	ns	ns	ns	ns	ns	ns	ns	ns
1 hr vs 72 hr	ns	ns	ns	ns	ns	ns	ns	ns
6 hr vs 12 hr	ns	ns	ns	ns	ns	ns	ns	ns
6 hr vs 24 hr	ns	ns	ns	ns	ns	ns	ns	ns
6 hr vs 48 hr	ns	ns	ns	ns	ns	ns	ns	ns
6 hr vs 72 hr	ns	ns	ns	ns	ns	ns	ns	ns
12 hr vs 24 hr	ns	ns	ns	ns	ns	ns	ns	ns
12 hr vs 48 hr	ns	ns	*	ns	ns	ns	ns	ns
12 hr vs 72 hr	ns	ns	ns	ns	ns	ns	ns	ns
24 hr vs 48 hr	ns	ns	ns	ns	ns	ns	ns	ns
24 hr vs 72 hr	*	ns	ns	ns	ns	ns	ns	ns
48 hr vs 72 hr	ns	ns	ns	ns	ns	ns	ns	ns
<b>0.5 Gy</b>								
	TP53	Bax	Bcl-2	ERK	Casp 2	Casp 9	Casp 6	Casp 7
1 hr vs 6 hr	ns	ns	ns	ns	ns	ns	ns	ns
1 hr vs 12 hr	ns	ns	ns	ns	ns	ns	ns	ns
1 hr vs 24 hr	ns	ns	ns	ns	ns	ns	ns	ns
1 hr vs 48 hr	ns	ns	ns	ns	ns	ns	ns	ns
1 hr vs 72 hr	ns	ns	ns	ns	ns	ns	ns	ns
6 hr vs 12 hr	ns	ns	ns	ns	ns	ns	ns	ns
6 hr vs 24 hr	ns	ns	ns	ns	ns	ns	ns	ns
6 hr vs 48 hr	ns	ns	ns	ns	ns	ns	ns	ns
6 hr vs 72 hr	ns	ns	ns	ns	ns	ns	ns	ns
12 hr vs 24 hr	ns	ns	ns	ns	ns	ns	ns	ns
12 hr vs 48 hr	ns	ns	ns	ns	ns	ns	ns	ns
12 hr vs 72 hr	ns	ns	ns	ns	ns	ns	ns	ns
24 hr vs 48 hr	ns	ns	ns	ns	ns	ns	ns	ns
24 hr vs 72 hr	ns	ns	ns	ns	ns	ns	ns	ns
48 hr vs 72 hr	ns	ns	ns	ns	ns	ns	ns	ns

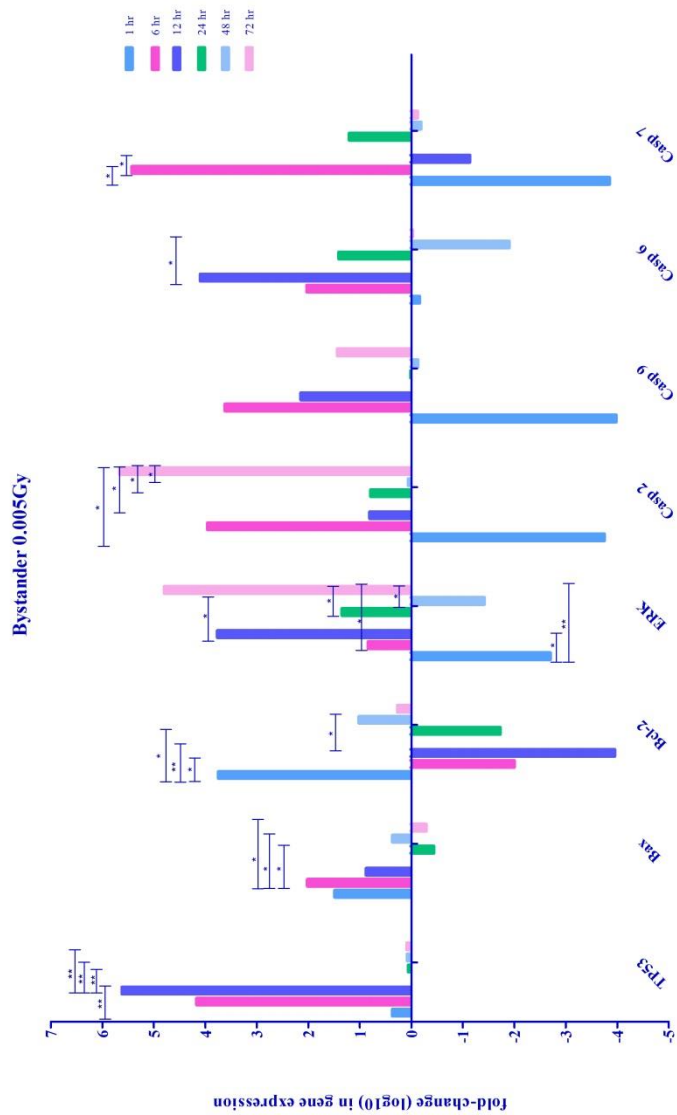


Figure 4.1: Comparison of gene expression patterns of TP53, Bax, Bcl-2, ERK, caspase 2, caspase 9, caspase 6 and caspase 7 in HaCaT cells, following 1 hr, 6 hr, 12 hr, 24 hr, 48 hr and 72 hr exposures to 0.005 Gy indirect (bystander) gamma irradiation, presented as fold-changes of gene expression ( $n = 3$ ). Statistical analysis are represented as  $P \leq 0.01$  (\*\*) and  $P \leq 0.05$  (\*).

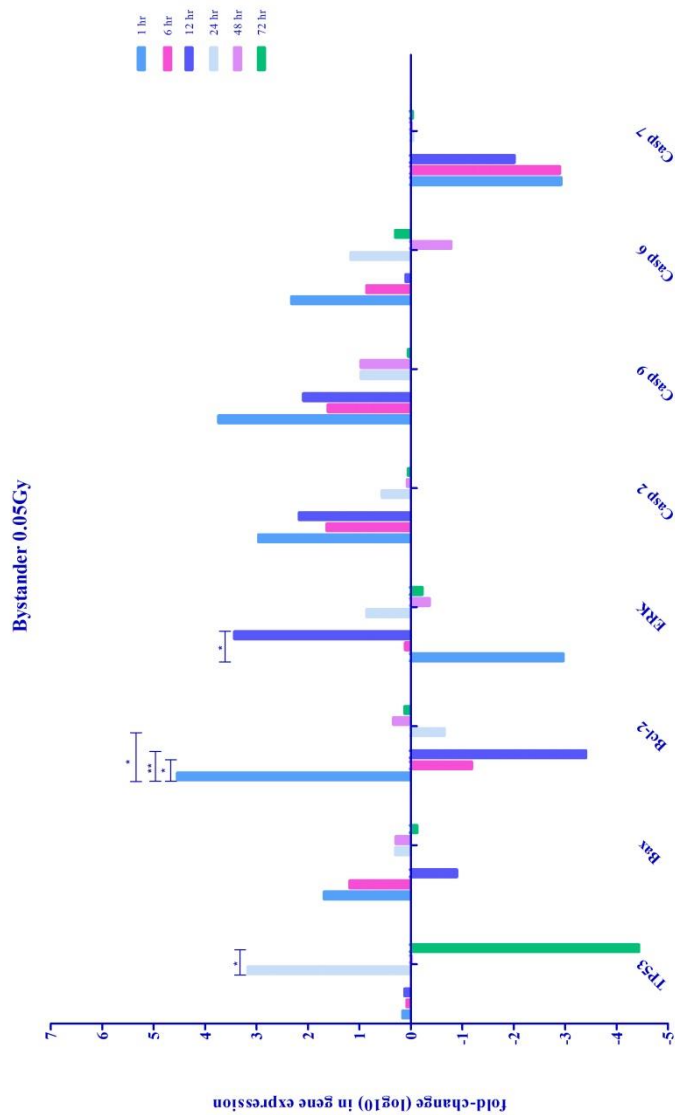


Figure 4.2: Comparison of gene expression patterns of TP53, Bax, Bcl-2, ERK, caspase 2, caspase 9, caspase 6 and caspase 7 in HaCaT cells, following 1 hr, 6 hr, 12 hr, 24 hr, 48 hr and 72 hr exposures to 0.05 Gy indirect (bystander) gamma irradiation, presented as fold-changes of gene expression ( $n = 3$ ). Statistical analysis are represented as  $P \leq 0.01$  (\*\*) and  $P \leq 0.05$  (\*).

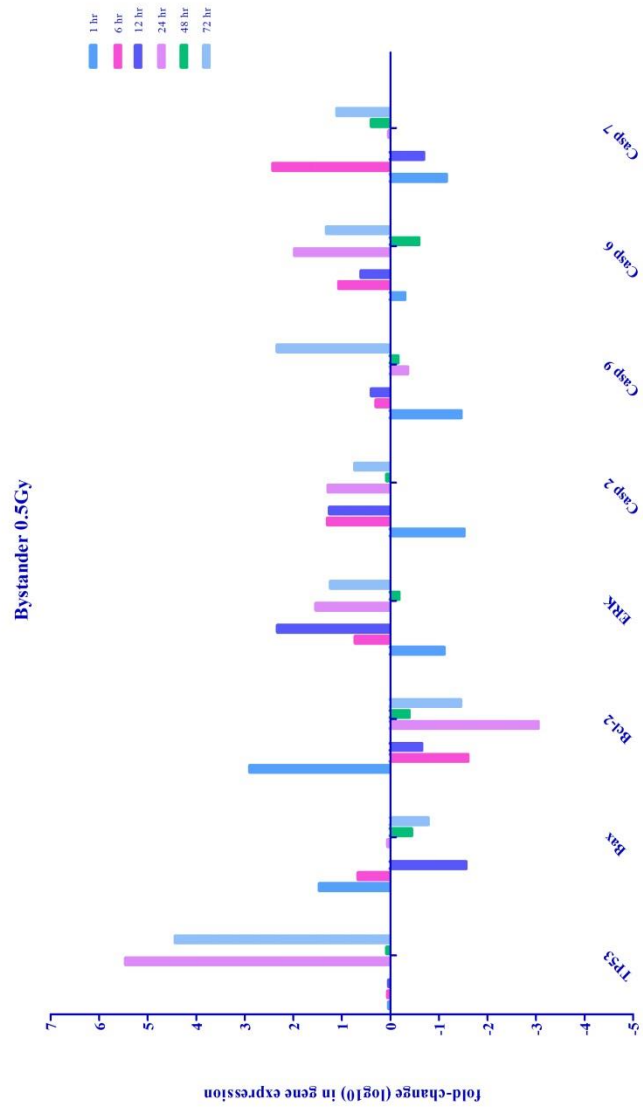


Figure 4.3: Comparison of gene expression patterns of TP53, Bax, Bcl-2, ERK, caspase 2, caspase 9, caspase 6 and caspase 7 in HaCaT cells, following 1 hr, 6 hr, 12 hr, 24 hr, 48 hr and 72 hr exposures to 0.5 Gy indirect (bystander) gamma irradiation, presented as fold-changes of gene expression ( $n = 3$ ). Statistical analysis are represented as  $P \leq 0.01$  (\*\*) and  $P \leq 0.05$  (\*).

#### 4.4 Discussion

The current study further investigated the role for apoptosis in directly (See Appendix C3.3 for the direct-irradiation gene expression figures) and indirectly irradiated HaCaT cells *in vitro* with additional low doses of IR and additional time points reflecting early and much later RIBE responses. The study specifically focused on the bystander gene responses of the apoptotic intrinsic pathway including mitochondrial genes and caspases, at a range of low doses, 0.005 Gy, 0.05 Gy and 0.5 Gy and very specific time points 1, 6, 12, 24, 48 and 72 hr. Gene expression changes were monitored over the extensive timescale and revealed approximate times of expression for each gene, justifying that a substantial timescale is essential for fine tuning specific gene expression responses. While the doses were all low, they did elucidate unique gene expression patterns that can be compared and contrasted to one another. As expected the role for apoptosis was complex for bystander cells and this time the apoptotic gene expression changes in bystander cells were isolated to specific times allowing construction of distinctive apoptotic gene expression patterns in bystander cells.

Overall the cells exposed to indirect doses of 0.005 Gy instigated a greater level of statistically significant changes in gene expression and appeared more sensitive. It appears from the data that Bax was attempting to instigate permeability of the mitochondrial membrane as seen from early up-regulation but did not persist over time. In fact it appears that both anti-apoptotic Bcl-2 and ERK, known for modulation of apoptosis via MAPK pathways and is anti-apoptotic was expressed and up-regulated early in the response, possibly attempting to compete with pro-apoptotic properties of Bax. Something that was common to all caspases was the pattern of up-regulation after 6 hr exposure. Maybe this is a key signalling time point of the intrinsic pathway and is

suggestive of cross-talk signalling with other modes of cell death such as necrosis and mitotic catastrophe.

Interestingly, there were common expression patterns between caspase 2, 9, 6 and 7 with respect to time and up-regulation/down-regulation of genes in 0.005 and 0.5 Gy exposed cells. The data suggests similar gene response signalling between the two low doses and possible cross-talk with other modes of cell death. Mitotic death has been suggested in studies as a signalling response of RIBE and may be potentially cross-signalling in the final execution stages of apoptotic cell death that are unclear in the data 0.005 Gy and 0.5 Gy data (Jella *et al.* 2013). For the 0.05 Gy dose-responses, apoptosis is clearly proceeding to final stages of cell death. The data revealed an initiation of apoptosis, through Bax signalling but also an induction of anti-apoptotic signalling of Bcl-2 and ERK, the caspases were initiated but later on (6 hr) and there were very small up-regulations of the caspases to drive the process. It must be noted that there were differences in gene expression changes between the current study and in Chapter 3 which is probably due to the fact that experiments were carried out at different times, and naturally introduces sample-to-sample variation. Also, the data was calculated following the  $\Delta\Delta$  CT method, but in the current study the data was presented as Log values, which clearly represents fold-changes in a different manner, so the two studies cannot be direct comparisons of each other by just looking at the figures.

For the 0.5 Gy dose-responses, bystander signalling was instigated in HaCaT cells, most likely resulting in inflow of calcium ions into the cells from the outside (Lyng *et al.* 2002; Lyng *et al.* 2006) followed by recruitment of mitochondrial associated genes Bax and Bcl-2. Bax is responsible for triggering the release of cytochrome c from the mitochondria and recruitment of caspase 2 followed by activation of caspase 9. Significant changes in gene expression were noted around 6 hr exposure for the 0.005

Gy and 0.5 Gy doses and remarkably, production of reactive oxygen species has been recognised by our research group in radiation-induced bystander effects at 6 hr (Lyng *et al.* 2002) which may be significant time-point for the cell in deciding its fate.

The requirement for more complex time course gene expression analysis was established by the exact points of expression elucidated. Extremely specific differences in gene expression changes between low doses of bystander radiation were uncovered which implies that there may be long term consequences of low dose RIBE if the cell cannot carry out final stages of apoptosis, particularly 0.5 Gy doses or perhaps the cells are inducing a protective mechanism at 0.5 Gy and higher doses.



# **Chapter 5**

**Identification of Key Proteins Signalled in Response to  
Radiation-Induced Bystander Effects in Human Skin Cells  
and a Gene Expression Investigation**

## 5.1 Introduction

There are fundamental cellular events central to the overall process of RIBE including chromosomal rearrangements, gene mutations, apoptosis and genomic instability (Morgan & Sowa 2007). The experimental evidence for RIBE has been well documented and associated responses include generation of reactive oxygen species (ROS), reactive nitrogen species (RNS) and  $\text{Ca}^{2+}$  signalling in bystander cells after exposure to radiation-induced bystander medium (Narayanan *et al.* 1997; Lyng *et al.* 2000; Azzam *et al.* 2012). However, the specific molecular events and signalling entities are still not completely understood and must be investigated further.

To date a lot of work investigating RIBE has been carried out *in vitro*. The design and development of tissue explant techniques specifically for radiobiological experiments (Mothersill *et al.* 1990; Mothersill 1998; Mothersill *et al.* 2001) has progressed the *in vivo* bystander research. Tissue can be irradiated *in vivo* or *ex vivo*, followed by harvest of the media and transfer to either un-irradiated tissue or to a reporter cell line (Mothersill *et al.* 2001; Mothersill *et al.* 2005). Measurement of specific endpoints such as cell survival, cell death or various biochemical parameters allows identification of the key cellular mechanisms.

An extensive amount of studies to determine whether irradiation induced bystander signalling can occur between fish and mammals have been achieved. Bystander signals can be passed from irradiated rainbow trout (*Oncorhynchus mykiss*) to neighbouring fish, possibly through release of a chemical component into the water surrounding the fish, representative of bystander factor(s). Studies involving zebrafish (*Danio rerio*) (Mothersill *et al.* 2007) revealed that they are also capable of producing bystander signals, which are not held in the water for long periods of time. The same study

demonstrated that various sensitivity levels exist among the individual fish and between different cell lines. Experiments involving Japanese Medaka (*Oryzias latipes*) recognised that bystander signals are stronger when emitted or received by repair deficient cell, as these are more sensitive (Mothersill *et al.* 2009). Additionally a role for serotonin in the bystander signaling response has been investigated, and may be a potential contender in bystander signalling (Mothersill *et al.* 2010; Lyng *et al.* 2012; Fazzari *et al.* 2012) particularly in zebrafish (*Danio rerio*) (Saroya *et al.* 2009). Further examinations have established fish cell lines for bystander studies (O'Neill-Mehlenbacher *et al.* 2007). The same study revealed that bystander signal production and cellular response varied depending on the cell line, and that the production of a signal and the response are actually independent from one another.

Consequently, the current study developed a Fish model to study human cell responses, which was a novel and somewhat controversial approach. The reasoning behind this was that the previous Fish studies (discussed above) showed that RIBE can be passed between fish and different species of fish, and this was further confirmed with extensive clonogenic assays with human cells. So, if the bystander factor was being transmitted into the media and then inducing reduced clonogenicity, then how so? If investigated this could reveal some major inducers of key bystander molecular mechanism.

Proteomic tools have been very successful in radiobiological research examining RIBE and their sensitivity has been reported by Smith and colleagues (Smith *et al.* 2007). Analysis of bystander signals emitted by rainbow trout (*Oncorhynchus mykiss*) with proteomic techniques demonstrated a novel functional protein profile in fish. In particular Annexin II (ANXA2) expression has been found to be increased in directly irradiated fish and hemopexin-like protein, RhoGDI2 and PDH expression have been

increased in bystander fish. Increased expression of ANXA2 is associated with radiation induced cancers, it is associated with reduced levels of apoptosis (Singh 2007). RhoGDI2 expression is associated with normal cell functions although aberrant signaling of these molecules can facilitate the development of tumours (Zhang 2006). The multifunctional gill proteome of medaka (*Oryzias latipes*) has also been examined following exposure to both direct and indirect X-irradiations (Smith *et al.* 2011). In the directly irradiated fish there was an increase in expression of Annexin max 3, creatine 3 kinase (CK) and lactate dehydrogenase (LDH) and a decrease in expression of annexin 4 (A4). Indirectly irradiated (bystander) fish revealed an increase in expression of proteins CK and LDH, annexin max 3 and A4. The proteins expressed were an implication of an immediate protective function and suggestive of long-term adaption to any consequent radiation exposures.

Using the same reliable reporter cell line (HaCaT) (Mothersill & Seymour 1997; Furlong *et al.* 2013), the objective of the study was to see if they induced a similar proteome in response to fish signals as that induced in the live fish. Therefore, HaCaT cells were exposed to ICCM harvested from explants taken from irradiated fish and investigated using 2-D difference gel electrophoresis (2-D DIGE) coupled with Mass Spectroscopy (MS) for emerging novel proteins. This is the first study to investigate whether common proteins are induced in both fish and human reporter cells through proteomic analysis.

## 5.2 Materials and Methods

### 5.2.1 X- Irradiations, Tissue Collection and Tissue Explant Technique

All rainbow trout (*Oncorhynchus mykiss*) fish were sourced from Humber Springs Trout Farm (Orangeville, ON) and housed at McMaster University, Hamilton, ON, Canada. Conditions and details of animal husbandry are specified by Mothersill *et al.*, (2006). Briefly, the rainbow trout were acclimated to laboratory conditions at McMaster for a minimum of 21 days before exposure to radiation. The fish were housed at a density of 1g mass 10L<sup>-1</sup> and supplied with flow-through dechlorinated, temperature-controlled water from the city (Hamilton, Ontario Canada) which consisted of; [Na<sup>+</sup> = 0.6; Cl<sup>-</sup> = 0.7; K<sup>+</sup> = 0.05; Ca<sup>2+</sup> = 0.5; Mg<sup>2+</sup> = 0.1; titration alkalinity (to pH 4.0) = 1.9 meq L<sup>-1</sup>; total hardness = 140mgL<sup>-1</sup> as CaCO<sub>3</sub>; pH 8.0]. In addition, the fish were supplied with commercial fish food (Martin Mills, ON, Canada) at a 2% of body mass ration on a daily basis.

A portable X-ray unit (Faxitron X-ray Corporation cabinet X-ray system, Wheeling, IL, USA) was used to deliver a mean dose of 0.1 Gy and 0.5 Gy to the fish, and was previously calibrated using thermoluminescence discs (TLDs). The fish weighed approximately 20 – 25 g. It was not possible to aerate the water or control temperature during irradiation time. Therefore, for irradiation the fish were placed in groups of two in 2L water in covered containers and the irradiation process took 5 min. Following irradiations, the fish were placed in containers that were aerated during the entire experiment and maintained at 19 °C (different containers for different doses). The fish were left for a 4 hr period to allow for signals to accumulate, after which they were killed humanely by a blow to the head and dissected. Skin epidermis was excised and collected immediately after death for subsequent tissue explant culture. Additional

controls of untreated fish (i.e., un-irradiated rainbow fish from same facility) were also included. All control fish skin excision (non-irradiated) and collection was carried out exactly as described above.

The fish tissue explants were set up using the technique as described and improved by Mothersill and colleagues (Mothersill *et al.* 1988). The excised tissue was transported immediately in RPMI-1640 medium supplemented with 10% FBS, 5ml of 200mM L-glutamine, 0.5µg/ml hydrocortisone and 12.2 ml of HEPES buffer (See appendix A8 for tissue explant culture medium recipe). The supplemented RPMI-1640 medium was used throughout the experiments. Each piece of skin was carefully poured into a petri dish and cut into smaller pieces of approximately 2-3 mm<sup>2</sup>. Tissue culture flasks (T25) were prepared with 2ml RPMI and each one labelled accordingly. The prepared explants were placed into flasks containing 2 ml RPMI complete medium. Flasks were stacked in an incubator at 19°C for 2 days to allow explants to attach and start to grow. Tissue culture flasks were set up as follows; 6 untreated control fish (0 Gy, n = 6), 6 fish treated with 0.1 Gy (n = 6) and 6 fish treated with 0.5 Gy (n = 6). Nine explants were prepared per fish, so a total of 162 explants/flasks were prepared in total for this experiment. Tissue explants were closely monitored for 2 days. All tissue was obtained and handled according to guidelines at McMaster University and the procedures were also covered by AUP 06-21-01. Refer to Appendix B13.1 for complete tissue explant culturing details.

### 5.2.2 Cell Culture, Medium Transfer and Protein Extraction

Prior to irradiations  $5 \times 10^4$  HaCaT cells were seeded in each well of a sterile 6-well plate (BD, Oakville, ON) covered with 3ml of RPMI-1640 supplemented media and allowed to grow for 2 - 3 days and incubated at 37°C with 5% CO<sub>2</sub> air. The plates were set up in triplicate, one plate per dose (0 Gy, 0.1 Gy and 0.5 Gy) and one well per dose administered. Cells were monitored on a daily basis and allowed to reach approximately 70 – 80% confluency, so that enough protein could be extracted post-exposure.

Media from tissue explants (ICCM) was carefully harvested from tissue explant flasks after 2 days incubation, making sure not to disrupt intact tissue explant, and the ICCM was filter sterilised through 0.22µm<sup>2</sup> filters. The explants from which the media was harvested were replaced with fresh RPMI-1640 and tissue explants were re-incubated at 19°C and after 10 days incubation fixed in 10% formalin (See Appendix A9 for the 10% Formalin recipe). Throughout the 10 day incubation period, flasks were observed under a microscope to ensure explant outgrowth. Refer to Appendix B13.2 for details of the media (ICCM) harvest.

Once the HaCaT cells had reached 70 – 80% confluency, media was poured off the cells and cells were washed with PBS (Gibco, Burlington, ON). The filter sterilised ICCM harvested from tissue explants was poured onto the ‘recipient’ HaCaT cells grown in 6 well plates (0 Gy, 0.1 Gy and 0.5 Gy) and re-incubated at 37°C for 4 hrs to allow for bystander signal transmission from media to cells. After the exposure period, ICCM was poured off the cells and the cells were washed in ice cold PBS. Protein lysis buffer (recorded in Appendix A10) described by Smith *et al.*, (Smith *et al.* 2005) containing 8 M urea containing 10% (v/v) 0.5 M Tris–HCl (pH 7.4), 0.02 EDTA, 0.05M dithiothreitol (DTT), 10% (v/v) glycerol, 6% (v/v) ampholytes (Resolyte, pH 3.5–10;

Merck-BDH), 2% (v/v) 3-[(3-cholamidopropyl) dimethylammonio]-1-propanesulfonate (CHAPS), 0.2 mg ml<sup>-1</sup> RNase and 0.2 mg ml<sup>-1</sup> DNase, was added to the cells and cells were scraped from the wells and the remaining cell lysates were stored in tubes on ice. Cell lysates were refined by centrifugation (10,000 x g for 5 min at 4°C) and desalted using a commercially available kit (see Appendix B14) to produce a better recovery of high quality protein for 2D electrophoresis. Total protein content was measured with a standard Bradford Assay kit (Bio rad, Mississauga, ON) and it was calculated that 45µg from each sample was sufficient for subsequent 2D gel electrophoresis (see Appendix B15 for the protein assay method and A10 for a full list of protein assay reagents).

### **5.2.3 2-D electrophoresis**

The HaCaT cell preparations were analysed by 2D gel electrophoresis. All electrophoresis was carried out using Protean® IEF system (Biorad), following the manufacturer's instructions and using rehydration/solubilisation, equilibration and running buffers supplied by Biorad.

The soluble protein extracts from cell lysates were mixed with re-swelling buffer: 7M urea, 2M thiourea, 4% (w/v) CHAPS, 0.3% (w/v) DTT to give a final volume of 140 µl. 125 µl of this mixture was then used to re-hydrate a pH 4–7 immobilised pH gradient (IPG) strip (Biorad). IPG strips were rehydrated overnight, at room temperature, with rehydration/solubilisation buffer (10 ml or 8 M urea, 2% CHAPS, 50 mM dithiothreitol-DTT, 0.2 % (w/v) Biolyte® and bromophenol blue). Isoelectric focusing (IEF) was then carried out using the Biorad IEF instrument. A ramped voltage change, was delivered



over three steps, up to a maximum of 20,000 V. Specifically, rapid ramping was applied first, a conditioning voltage of 4,000 V and final focusing of 4,000 V (max current limit=50  $\mu$ A/IPG strip). After IPG strip equilibration (2 x 10 min equilibration in buffer I, followed by 1 x 10 min equilibration in buffer II), Each IPG strip was then laid onto a 10–15% gradient polyacrylamide slab gel (8 x 7 cm) for the second dimension electrophoresis. The second dimension was resolved on a 1x Tris/glycine gel (Biorad) and separated by size (molecular weight) in a direction perpendicular to the first dimension run on the Protean 2-D casting and running apparatus, using 25 mM Tris, 192 mM glycine, 0.1% SDS buffers in the upper and lower tank, respectively; max voltage = 200 V, running time = 45 min. After electrophoresis the gels were fixed with 10 % methanol, 7 % acetic acid and water (in accordance with the instructions provided with the gel stain) and then stained with SYPRO-ruby stain (Biorad) and de-stained in 10 % ethanol. Images of the stained gels were captured using the Biorad 4.2.1 Fluor-S™ MultiImager system using top illumination fluorescence. Prior to image capture the charged coupled device (CCD) camera was calibrated, with a single frame image of the flat field emission filter (400–550 nm). Gel image analysis was achieved using Phoretix 2D™ analytical software version v2004 (Nonlinear Dynamics), as a “blind” study, with each gel image being assigned a random number prior to analysis. Therefore, to fully accommodate any background variation across the 2-D gels, all images were background corrected by the “average on boundary” background subtraction option. This calculates the background for each spot separately from the grey scale intensity immediately adjacent to that spot. Protein expression was then quantified as normalised spot volume, a parameter offered by the Phoretix software which combines spot area and peak height to give an overall expression index, and which has been used previously in fish proteomics (Smith *et al.* 2007 & 2011). Normalised spot volumes

were expressed as mean  $\pm$  SD (Figure 5.2 A - H) and compared by one-way ANOVA followed by least square difference using the StatistiX statistical analysis programme; a  $p \leq 0.05$  was considered statistically significant and individual  $p$  values are displayed on graphs. Each individual HaCaT cell lysate was resolved on a separate 2D gel. The data presented here are from the gels of HaCaT cells exposed to ICCM of 0 Gy, 0.1 Gy and 0.5 Gy X-ray generated *in vivo*. Selected protein spots (refer to reference gel Figure 5.1) were cut from the gel and the gel plugs containing these spots were preserved in 2% glycerol at 4°C ready for Mass Spectroscopy (MS) analysis. The spot chosen had to be consistently expressed or consistently absent on all gels within HaCaT genotype/treatment combination.

Spot volumes were expressed as mean  $\pm$  SD (Figure 5.2 A - H) and compared by one-way ANOVA followed by least square difference using GraphPad Prism statistical analysis software; a  $p < 0.05$  was considered statistically significant and individual  $p$  values are displayed on graphs. Statistical analysis is represented as  $P \leq 0.05$  (\*). Each individual HaCaT cell lysate was resolved on a separate 2D gel. The data presented here are from the gels of HaCaT cells exposed to ICCM of 0 Gy, 0.1 Gy and 0.5 Gy X-ray generated *in vivo*. Selected protein spots (refer to reference gel Figure 5.1) were cut from the gel (see Appendix B17) and the gel plugs containing these spots were preserved in 2% glycerol at 4°C ready for Mass Spectroscopy (MS) analysis. The spot chosen had to be consistently expressed or consistently absent on all gels within HaCaT genotype/treatment combination.

#### 5.2.4 Mass Spectroscopy Analysis and Protein Identification

This analysis was carried out as previously described by Smith *et al.*, (Smith *et al.* 2007 & 2011) at Queen's Mass Spectrometry and Proteomics Unit, Ontario, Canada. About 331 protein spot-features per sample gel were detected. Eight proteins exhibiting significant expression changes at any time of the irradiation time-course were then identified using MS and database searches (refer to Appendix B18 for the full mass spectroscopy analysis and protein identification method). Selected protein spots (refer to reference gel Figure 5.1) were cut from the gel with a scalpel and the gel plugs containing these spots were preserved in 2% glycerol at 4°C. The proteins cut out from the gel were first treated with ammonium bicarbonate, dehydrated with acetonitrile (ACN), and subjected to in-gel trypsin digestion. The digested proteins were concentrated in formic acid, using Millipore C18 ZipTips and analysed using a quadrupole time of flight (Q-TOF) Global Ultima (Waters, Micromass) with nanoES source; capillary voltage of 1.2–1.6 kV, cone voltage of 50–100 V. Mass spectra in TOF mass spectrometry (MS) and mass spectrometry/mass spectrometry (MS/MS) mode were in a mass range of 50–1800 m/e with a resolution of 8000 full width at half maximum height. Argon was used as the collision gas. MS/MS data were searched using online MASCOT (Matrix Science, UK) against the National Centre for Biotechnology and Information (NCBI) and the MS protein sequence database (MSDB). Search criteria were as follows: monoisotopic masses, one missed cleavage, tolerances set for 0.3 kDa for peptides matches, and 0.2 kDa for MS/MS fragment matches. All peptide fragments that were obtained for each digest were submitted to online protein database UniProt for searching.

## **5.2.5 Gene Expression Study**

### **5.2.5.1 Direct and Bystander Irradiation Experiments *in vitro***

HaCaT were routinely cultured in DMEM cell culture media and a full description of routine cell culture, maintenance and cell counting is described in Chapter 2 (section 2.2.1).  $2 \times 10^5$  cells were plated into T25 flasks. A set of flasks was set up for direct irradiation and for harvesting of bystander media for each of the dose points (0 Gy, 0.05 Gy and 0.5 Gy) in triplicate. Another set of flasks was set up as bystander recipients in triplicate. Full experimental details of the direct irradiation exposure, the irradiated cell conditioned media (ICCM) harvest and exposure for bystander HaCaT cells are provided in Chapter 2 (section 2.2.2). The media (ICCM) was harvested and pooled per triplicate flask for the directly irradiated flasks at each of the time points (1, 4, 8 and 24 hr) and each of the dose points (0, 0.05 and 0.5 Gy). RNA was extracted following the technique described in Chapter 3 (section 2.1) and Chapter 4 (section 4.2.1)

### **5.2.5.2 Real-Time PCR with SYBR Green Technology**

ANXA2 was designed and optimised following the same procedure as described in Chapter 3 (section 2.2) and Chapter 4 (section 4.2.2) and a list of forward and reverse sequences for ANXA2 and housekeeper gene (Actin) are displayed in Table 5.2. Actin was chosen as it was deemed to be a more reliable endogenous control for the extent of the study involved and this was confirmed with careful analysis of raw data. Relative quantification analysis was used to determine the ANXA2 gene expression levels, previously discussed in Chapter 3 (Section 2.2.3) and Chapter 4 (section 4.2.2). Gene expression changes were measured for ANXA2 normalised to Actin (housekeeper gene)

monitored at 0.05 Gy and 0.5 Gy for 1, 4, 8 and 24 hr and relative to the expression at 0 Gy (control). The value of the mean-fold change at 0 Gy (control) was fixed to zero and mean-fold changes in gene expression of each target gene were plotted in Microsoft Excel. The figures illustrate up-regulation (above zero) and down-regulation (below zero) of target genes.

### **5.2.5.3 Statistical Data Analysis**

Significance of variances were determined, for each specific gene targeted, applying the statistical one-way analysis of variance (ANOVA) test with the aid of GraphPad Prism software. For ANXA2 the control (0 Gy) samples were compared to each dose to determine overall significant changes. Significance is marked on Figure 5.3 with  $*p < 0.05$ .

## **5.3. Results**

### **5.3.1 Mass Spectroscopy Analysis and Protein Identifications**

Rainbow trout (*Oncorhynchus mykiss*) were exposed to low doses (0.1 Gy and 0.5 Gy) of X-ray radiation *in vivo* and *in vitro* explant cultures were generated from the skin. The ICCM was harvested from all explant cultures and placed on recipient HaCaT bystander reporter cells. Two-dimensional gel electrophoresis and mass spectroscopy (MS) were employed to screen for novel proteins which were significantly over or under-expressed in the recipient HaCaT cells exposed to the ICCM. It was also of particular interest of this study to see if common proteins were induced in the fish and

human reporter cells. Table 5.1 illustrates the protein identifications marked with an arrow on the reference gel. The most statistically significant induced proteins were analysed with and identified with MS. The protein identifications along with sequence numbers are listed in Table 5.1.

ANXA2 (Figure 5.2-A) was significantly up-regulated ( $p = 0.0161$ ) after exposure to 0.1 Gy and 0.5 Gy ICCM, the change of expression between ANXA2 was much greater with exposure to 0.5 Gy, almost twice of protein expression as in the control samples. Rho-GDI2 (Figure 5.2-B) was significantly reduced in expression ( $p = 0.0497$ ) when exposed to 0.1 Gy and 0.5 Gy ICCM. There was a similar reduction of expression of the protein in the HaCaT cells in exposure to both 0.1 and 0.5 Gy doses. MMS19 nucleotide excision repair protein (MMS19-like protein) displayed in Figure 5.2-C was significantly reduced in expression ( $p = 0.0343$ ) in HaCaT cells exposed to 0.1 Gy. The protein was reduced to less than half the amount of expression as in the control, and there was a very slight reduction in expression as a result of 0.5 Gy exposures. F-actin capping protein (Figure 5.2-D) was significantly reduced in expression ( $p = 0.0366$ ), almost half of the expression levels of the control sample in cells exposed to 0.1 Gy, and the protein was further reduced in expression in cells exposed to 0.5 Gy. Microtubule-associated protein RP/EB family member 1 (EB1) displayed in Figure 5.2E was significantly reduced in expression ( $p = 0.0021$ ) very slightly in the 0.1 Gy samples. The protein was reduced to a greater extent in the 0.5 Gy samples, less than half of the expression levels of the protein in the control. 14-3-3 expression is displayed in Figure 5.2-F and significantly increased in expression ( $p = 0.0269$ ) in the 0.1 Gy samples whereas exposure to 0.5 Gy induced a significant reduction in expression of the protein to half of the expression amount in control samples. Cingulin (Figure 5.2-G) was significantly increased ( $p = 0.0001$ ) in expression to exposure of both 0.1 and 0.5

Gy ICCM. Although the 0.5 Gy dose induced a greater increase in expression to almost five times higher than the control samples. Figure 5.2-H displays the expression differences of APC 1. There was a reduced expression of the protein in both 0.1 and 0.5 Gy doses, but consequently it was not statistically significant ( $p = 0.114$ ).

Table 5.1: Peptide ion identification information for proteins indicated in spot volumes

Spot Number	Protein description	Species	Database/accession no.	Peptide sequence	Analysis
168	Annexin II	Bos taurus (Bovine)	P04272	136-TNQELQEINR-145	MS/MS
299	Rho-GDP	Homo sapiens (Human)	P52566	51-TLLGDGPVVTDPK-63	MS/MS
53	MM519 nucleotide excision repair protein homolog	Danio rerio (Zebrafish)	E7FBU4	380-ASLIGIQAVIPALLDQYBBR-399	MS/MS
254	F - actin capping protein subunit beta	Pongo abelii (Sumatran orangutan)	Q5R507	96-LEVEANNAFDQYR-108	MS/MS
256	Microtubule - associated protein RP/EB family member 1	Homo sapiens (Human)	Q15691	183-NPGVGNDDDEAAELMQQVNVLK-204	MS/MS
269	14-3-3 protein beta/alpha	Homo sapiens (Human)	P31946	141-QITVSNQQAYQEAFEISK-159	MS/MS
290	Cingulin	Callicebus moloch (Dusky titi monkey)	B1MTG4	653-DRELEKQLAGLR-664	MS/MS
313	Anaphase - promoting complex subunit 1	Mus musculus (Mouse)	P53995	544-LLGSMDEVVLLSPVELRDSsK-565	MS/MS



Figure 5.1 Representative 2D gel from HaCaT cells: Protein ID's are identified with an arrow on the gel.

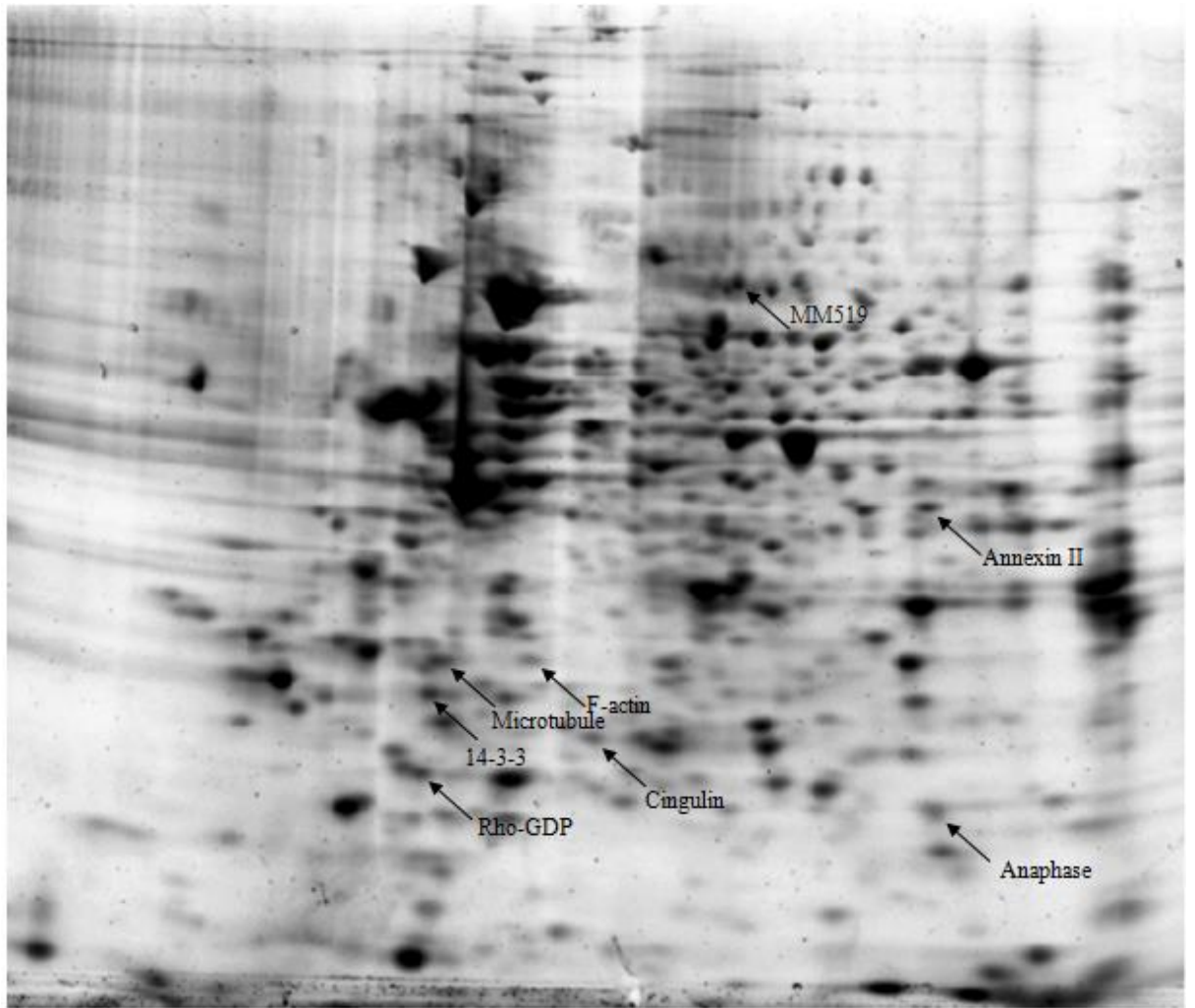
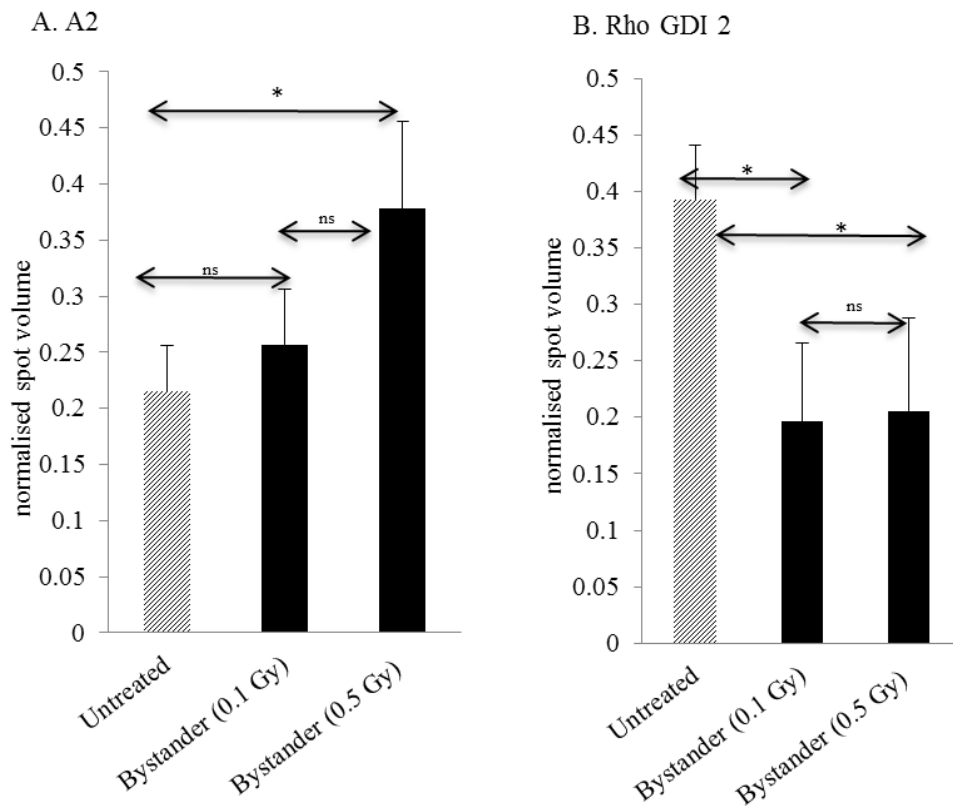
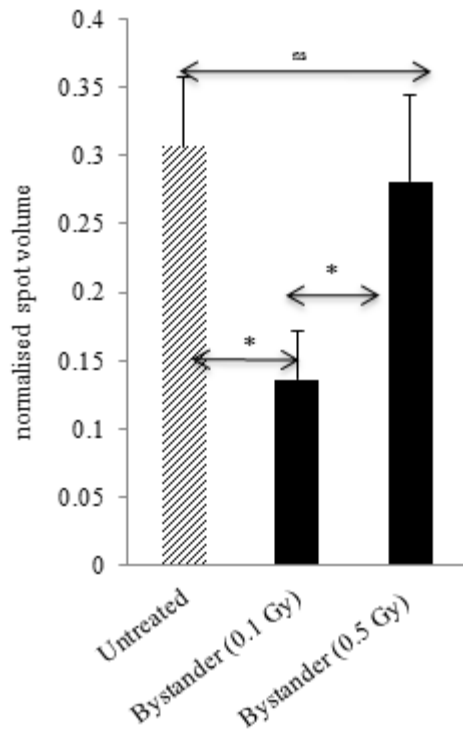


Figure 5.2: (A - H) Increased and decreased expression of proteins (revealed through MS) by HaCaT cells exposed to media borne signals from directly irradiated fish skin.

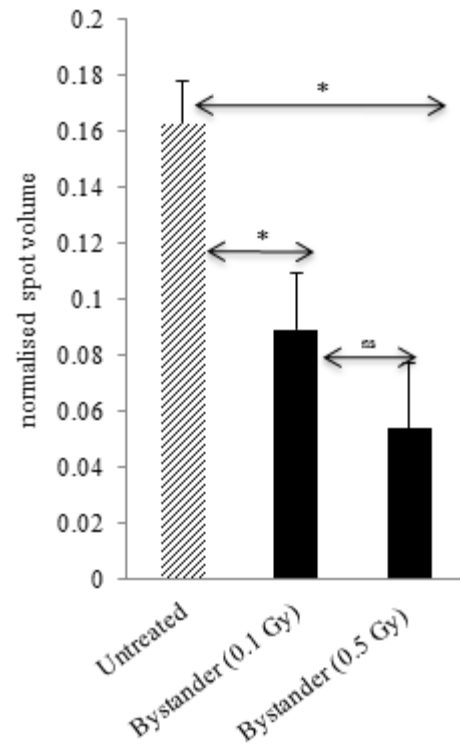
Refer to Appendix C4.1 for the raw data.



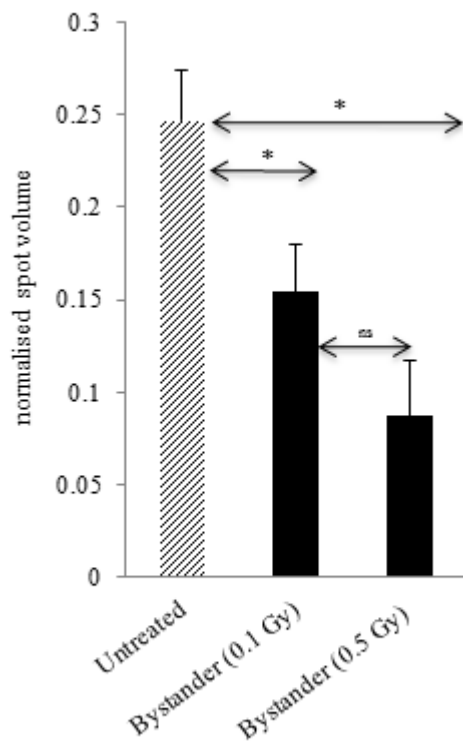
C. MMS19



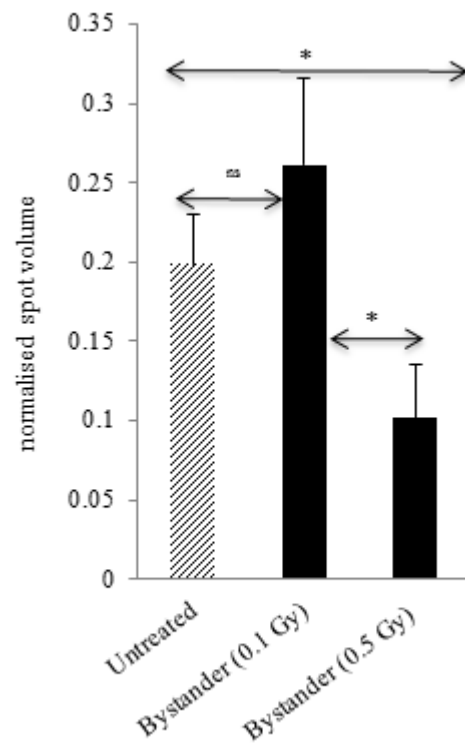
D. F-actin capping protein



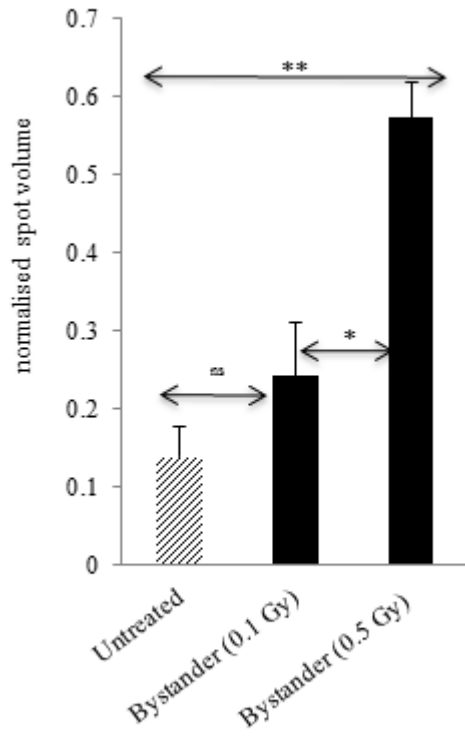
E. EB1



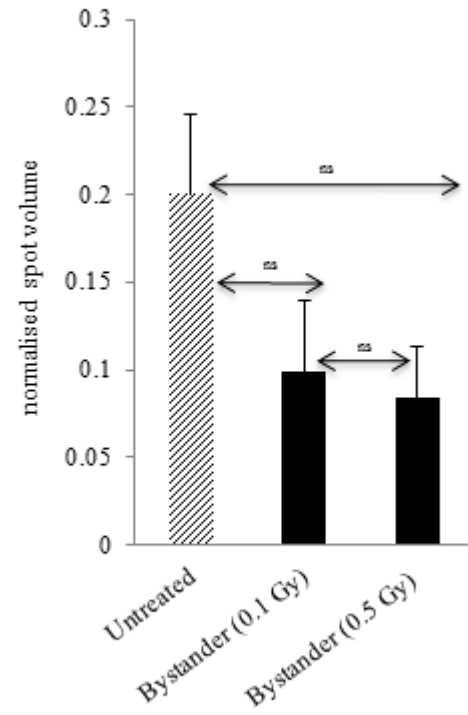
F. 14-3-3



G. Cingulin



H. APC1



### 5.3.2 RT-PCR Gene expression Study

Figure 5.3 displays the mean-fold changes in gene expression of ANXA2 in both directly and indirectly irradiated (0 Gy, 0.05 Gy and 0.5 Gy) HaCaT cells exposed for 1, 4, 8 and 24 hr.

The 0.05 Gy direct exposures revealed an up-regulation of ANXA2 that increased between 1 and 4 hr exposure, and up-regulated almost 6-fold after 24 hr exposure. In comparison, the 0.05 Gy indirect exposure revealed minor changes in ANXA2 expression. The gene was only slightly up-regulated after 4 hr exposure.

The 0.5 Gy direct exposure revealed an up-regulation of ANXA2, similar to the 0.05 Gy direct pattern of expression, but to a lesser extent. After 24 hr exposure to direct 0.5 Gy exposure, ANXA2 was up-regulated almost 5-fold more than the control. In the indirect 0.5 Gy HaCaT cells, ANXA2 expression displayed a similar pattern of expression to the 0.5 Gy direct response. It was up-regulated after 8 hr exposure and possibly earlier. Interestingly, ANXA2 was reduced after 24 hr exposure to indirect 0.5 Gy. Unfortunately, the changes in ANXA2 expression were not statistically significant.

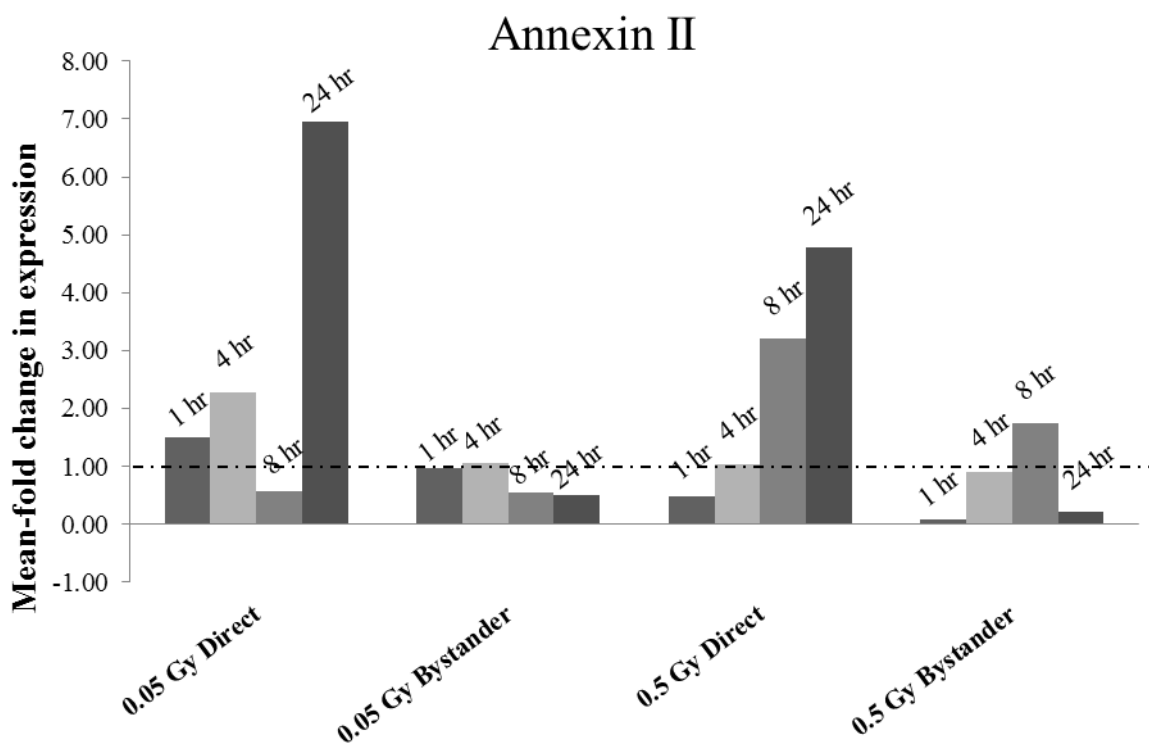


Figure 5.3 The mean-fold changes of ANXA2 expression in HaCaT cells directly and indirectly exposed to 0.05 Gy and 0.5 Gy irradiation for 1, 4, 8 and 24 hr. The dotted line represents the control samples. See Appendix C4.2 for raw data.

Gene	Forward Oligo Sequence	Reverse Oligo Sequence
ANXA2	5'ACAGCCATCAAGACCAAAGG'3	5'CAAATCACCGTCTCCAGGT'3
Actin	5'ACTCTTCCAGCCTTCCTTCC'3	5'GTTGGCGTACAGGTCTTTGC'3

Table 5.2 List of forward and reverse oligo sequences of ANXA2 and Actin.

## 5.4 Discussion

The aim of this study was to further investigate the key molecular signalling events in RIBE and contribute to an improved modelling of bystander signalling. HaCaT cells were exposed to indirect low doses of X-irradiation using the well-established medium transfer technique. Four hours exposure to ICCM induced very interesting biological changes to specific proteins in the cells. These proteins were identified and analysed according to the changes in their expression. The proteins were chosen based on statistically significant changes discovered between control (0 Gy) and exposed cells (0.1 Gy and 0.5 Gy).

This study required the HaCaT reporter system to determine the quantitative strength of the bystander signal and because the experimental assay involved the transfer of irradiated fish explant media to a human HaCaT cell cultures, it was of interest to see if there were significant common proteins induced in both the fish and human reporter cells. The reasoning for this model was the complex molecular mechanisms associated with bystander HaCaT cells could be compared previous studies thus creating a better understanding of RIBE. Previous studies have demonstrated that this irradiation procedure is capable of instigating both direct and bystander radiation effects through reporter cell survival experiments in rainbow trout (*Onchorhynchus mykiss*) (O'Dowd *et al.* 2006), zebrafish (*Danio rerio*) (Mothersill *et al.* 2007) and medaka (*Oryzias latipes*) (Mothersill *et al.* 2009). It has also been shown to induce direct and bystander proteomic changes in rainbow trout (*Oncorhynchus mykiss*) gills (Mothersill *et al.* 2006) therefore the present study can be compared.

A similar protein expression pattern in HaCaT cells was discovered between the low doses of ICCM (0.1 Gy and 0.5 Gy). Overall, there was a greater increase in protein

expression in HaCaT cells exposed to 0.5 Gy ICCM. So although the mechanism of signalling may have revealed a similar pattern, the 0.5 Gy dose seems to induce greater quantitative changes to the proteins expressed, and quite possibly more sensitive. The only exception was that the 14-3-3 protein increased more with a dose of 0.1 Gy ICCM.

Cingulin is important for the formation and regulation of tight junctions (TJ's) in cells and the protein is found at the surfaces of TJ's (He *et al.* 2007). It is recruited to cell-cell junctions and responsible for gene expression regulation, cell proliferation and cell density via a RhoA activator GDP/GTP-exchange factor signalling pathway (Guillemot & Citi 2006). Cingulin protein expression was increased in exposure to 0.1 Gy ICMM and increased twice that in exposure to 0.5 Gy ICCM, possibly marking epithelial differentiation (Figure 5.2-G). *In vitro* studies have revealed that cingulin interacts with various components of TJ's including F-actin suggesting a role for cingulin as a linker between the tight junction membrane and F-actin cytoskeleton re-organisation (Bazzoni *et al.* 2000; Ohnishi *et al.* 2004). The presence of Cingulin in epithelia tissues was previously measured and the level of cingulin present in four adenocarcinomas was higher than that of the normal tissue and was not detected in non-epithelial tissues and tumors. Cingulin is absent from non-epithelial human tissues and neoplasias but is expressed in metastatic colon neoplasms and in inflammatory bowel disease and so suggests that cingulin may be a useful 'marker' in the characterisation of epithelial neoplasias (Citi *et al.* 1991).

Furthermore, MMS19 protein expression decreased 2.5-fold in exposure to 0.1 Gy ICCM (Figure 5.2-C). MMS19-like protein usually functions as a platform to facilitate other proteins responsible for repair and replication (Seroz 2000). The protein interacts with a mitotic spindle-associated complex that is important in chromosome segregation



(Ito *et al.* 2010). Perhaps the ability of MMS19 to repair the damage to the cell or be responsible for DNA replication was hindered. EB1 proteins bind to the plus end of microtubules and regulate the dynamics of the microtubule cytoskeleton. EB1 specifically promotes cytoplasmic microtubule nucleation and elongation. It may be involved in spindle function by stabilising microtubules and anchoring them at centrosomes and is responsible for cell migration (Askham *et al.* 2002; Hayashi *et al.* 2005; Honnappa *et al.* 2009; van der Vaart *et al.* 2011). Reduced protein expression of EB1 was observed in HaCaT's exposed to 0.1 Gy ICCM almost 2-fold and reduced almost 4-fold in exposure to 0.5 Gy ICCM (Figure 5.2-E). Interestingly, EB1 interacts with tumour suppressor Adenomatous polyposis coli protein (APC) and maybe the reduced expression of EB1 exerts an effect on the actin cytoskeletal network. APC1 is known for its role in the movement of chromosomes to opposite poles of the cell during cell division. There was a 2-fold decrease in expression of the protein in 0.1 Gy and 0.5 Gy doses (Figure 5.2-H). Component of the anaphase promoting complex/cyclosome (APC/C), a cell cycle-regulated E3 ubiquitin ligase that controls progression through mitosis and the G1 phase of the cell cycle (Jin *et al.* 2008). It is possible that cell cycle progression was affected by the reduced expression of APC1, but the changes were not statistically significant.

Rho- GDP dissociation inhibitor 2 (GDI's) protein expression was decreased 2-fold in HaCaT cells exposed to 0.1 Gy ICCM and similarly to 0.5 Gy ICCM (Figure 5.2-B). Rho-GDI's are the regulators of Rho-GTPases. The Rho GTPases are involved in the regulation of a diverse array of cellular processes including actin dynamics, gene transcription, and motility (Bishop & Hall 2000) they escort GTPases to specific membrane signalling complexes, also protecting them from degradation (Zhang 2006). The role of RhoGDI as a regulator of epithelial apical/basolateral polarity via the

regulation of GTPase activity is well established (Fukata *et al.* 2003). They are responsible for normal cell growth and malignant transformation. One of the regulators in particular, Rho GDP dissociation inhibitor 2 (RhoGDI2), has been shown to act as a metastasis suppressor gene in cancer and reduced levels of RhoGDI2 have been shown to be associated with reduced survival rate for patients with human bladder cancer (Theodorescu *et al.* 2004). Thus not protecting the GTPases from degradation by caspases (apoptotic associated proteins). RhoGDI2 expression is deregulated in various cancers (Dovas & Couchman 2005; DerMardirossian & Bokoch 2005; Ellenbroek & Collard 2007). And the pattern of expression in this present study suggests an overall damaging effect of low dose bystander signal exposure in the HaCaT cells. GDP dissociation inhibitors (GDI's) are central to the fundamental processes of intercellular signalling and transport (Seabra & Wasmeier 2004). A decrease in expression of Rho-GDI observed in our samples contrasts with the fish study in which Rho-GDI was increased in response to bystander x-radiation (Smith *et al.* 2007). Decreased expression of their activity may potentially impact a large number of processes, including cell migration. Perhaps the HaCaT cells are more tolerant of the damaging signal. Some of the 14-3-3 binding proteins are involved in the regulation of the GTPase function (Jin *et al.* 2004). 14-3-3 binding antagonises the pro-apoptotic activity of Bad (Bcl-2 family) and possibly competes with pro-apoptotic proteins important for cell death signalling processes. Our research group recently documented some of the pro- and anti-apoptotic radiation-induced bystander gene expression changes in HaCaT cells in Chapter 3 and Chapter 4 (Furlong *et al.* 2013). Remarkably the isoform, 14-3-3 $\sigma$  is directly linked to cancer and becomes induced in association with p21 by p53 (apoptotic-associated proteins) after irradiation. It has been documented that a loss of 14-3-3 $\sigma$  expression lowers the controlled regulation of multiple pathways and is an early event in neoplastic

transformation, carcinogenesis (Nakajima *et al.* 2003; Mhawech 2005) and is also present in many carcinomas increasing their radiosensitivity. Inhibition of this protein could be a positive marker in sensitising human cancers to radiation. 14-3-3 $\sigma$  expression has been observed in the keratinocytes of skin (Nakajima *et al.* 2003). In the current study increased expression of 14-3-3 was observed in HaCaT exposed to 0.1 Gy ICCM and protein expression decreased when exposed to 0.5 Gy ICCM (Figure 5.2-F). 14-3-3 may be responsible for modulating the cell death pathway and may work differently with different dose-exposures. Finally, there was reduced expression pattern of F-actin capping protein, which is responsible for cell morphology and cytoskeletal organisation (Maruyama *et al.* 1990). It is a type of cytoskeletal protein that binds in a Ca<sup>2+</sup> - independent manner to the ends of actin filaments (barbed end) therefore, blocking the exchange of subunits at these ends. F-actin capping protein expression was decreased approximately 2-fold in response to 0.1 Gy doses and about 3-fold in response to 0.5 Gy (Figure 5.2-D) and possibly characteristic of apoptotic morphological changes?

There is evidence that a protective mechanism may be induced reflective in the increased protein expression of ANXA2 which is intriguing as reports have shown that it may be tumour-related and participate in several types of cancer (Olwill *et al.* 2005). The annexins are a group of cytosolic proteins that bind to phospholipids in a calcium-dependent manner. ANXA2 is composed of two domains, the first is the NH<sub>2</sub>-terminal head and secondly the COOH- terminal protein core, which harbours the Ca<sup>2+</sup> and membrane binding sites (Gerke & Moss 2002; Debret *et al.* 2003). Annexins may therefore have roles as effectors, regulators, and mediators of Ca<sup>2+</sup> signals (Gerke & Moss 2002). Although the full biological functions of annexins are not well defined, previous studies have established ANXA2 as a radioresponsive protein associated with anchorage independent growth (Waters *et al.* 2013; Weber *et al.* 2005). ANXA2

accumulates in the nucleus in response to DNA damaging agents (X-ray) suggesting that ANXA2 may play a role in protecting DNA from oxidation by ROS (Waters *et al.* 2013). Interestingly ANXA2 can bind RNA impacting on RNA stability and subsequent protein expression in cells, which may impact on the overall fate of the cells (mRNA stability) (Filipenko *et al.* 2004). A recent study showed that ANXA2 can contribute to radiation-dependent regulation of transcription and cell fate, whereby ‘silencing’ A2 can lead to an increase in cell death, perhaps suggesting a possible role for protection of the cell from damage such as radiation as discussed by Waters and colleagues in 2013 (Waters *et al.* 2013). The same research group revealed that cells depleted of annexin ANXA2 have more oxidative DNA damage than control cells in response to IR. It has been demonstrated that ANXA2 is secreted into the medium by irradiated cells and can bind to non-irradiated neighbouring cells in the vicinity, inducing anchorage-independent growth (Weber *et al.* 2005; Weber *et al.* 2009). As previously mentioned, direct DNA damage may not be necessary to cause a bystander effect, as Smith *et al* showed in 2007 (Smith *et al.* 2007). The proteomics study by Smith *et al* 2007 showed increased levels of ANXA2 in directly X-radiated fish but not in bystander fish, regardless of the source of bystander signalling, and confirming the ‘stability’ of the bystander ‘molecule’ in a 4 hr time frame. Additional studies with bystanders to irradiated medaka (*Oryzias latipes*) illustrated increased proteins of the Annexin family also (Smith *et al.* 2011). Previous studies consolidating the role of apoptosis in both a direct and bystander response revealed that bystander irradiation instigated an apoptotic pathway in HaCaT cells exposed to low doses (0.05 and 0.5 Gy) (Mothersill & Seymour 1997) and there as evidence to suggest that the apoptotic pathway was modulated in the bystander response, and that it is unique in comparison to directly irradiated cells. It appeared that the apoptotic cell death pathway was not fully executed by the caspases

but that it had indeed been initiated and possibly reached a point of no return. This was evident from the involvement of pro-apoptotic Bax (Bcl-2 family). It is therefore interesting to see that in the HaCaT cells in this study instigated increased expression of ANXA2 which is associated with reduced amounts of apoptosis through modulating the Bcl-2 family of proteins.

There was an increase in protein expression of ANXA2 in exposure to 0.1 and 0.5 Gy ICCM (Figure 5.2-A), possibly a protective mechanism stimulated by the cell from oxidation caused by ROS. ANXA2 is capable of reducing the level of apoptosis through control of pro-apoptotic proteins. It is apparent that ANXA2 has a role to play in radiation-induced bystander effects, protecting DNA from genotoxic damage/stress, specifically at low doses. The *ex vivo* generated ICCM was analysed using the MTT assay (Appendix B19) and the data demonstrated that there was individual variation in the RIBE in HaCaT cell cultures receiving this ICCM. See Appendix C4.3 for the raw data and Appendix C4.4 for the figure showing the surviving fractions of HaCaT cells exposed to ICCM harvested from irradiated fish explants (0 Gy, 0.1 Gy and 0.5 Gy). The assay illustrated a substantial increase in the surviving fraction of ICCM (0.1 and 0.5 Gy) exposed HaCaT cell cultures in comparison to HaCaT cell cultures exposed to 0 Gy ICCM. This is suggestive of a proliferative effect in turn triggered by RIBE. This unusual response could be attributed to a well-known cellular response, hormesis which has been defined as “the stimulation of a system by low doses of substances that are toxic at high doses” (Ryan *et al.* 2008).

A further investigation was carried out to discover how ANXA2 gene expression changed in HaCaT cells both directly and indirectly (ICCM) exposed to 0.05 and 0.5 Gy IR for 1, 4, 8 and 24 hr. and compare with the protein expression levels obtained using

the *ex vivo* fish model The gene expression study revealed that exposure to both direct and indirect (ICCM) 0.05 Gy and 0.5 Gy, stimulated increased expression of ANXA2. ANXA2 was up-regulated more so in the direct samples. Remarkably, the data uncovered an up-regulation in an increasing fashion of ANXA2 in HaCaT cell cultures between 4 – 8 hr exposures to 0.5 Gy ICCM. This correlates with the current protein study, whereby 4 hr exposure to ICCM also instigated an increase in ANXA2 in the HaCaT cells exposed to 0.5 Gy ICCM from irradiated Fish. Nonetheless, the changes were not statistically significant.

Overall the bystander signalling initiated a ‘protective’ mechanism to the DNA from oxidation by ROS in bystander cells through expression of ANXA2 but the reduction of RhoGDI2 expression may have permitted the recruitment action of apoptotic caspases in the cells. Remarkably, the increase in 14-3-3 expression under 0.1 Gy conditions may be responsible for regulation of cell proliferation and differentiation, and modulate the cell death pathways.

The remaining identified proteins were decreased in expression levels in response to signalling of bystander factors in the cells. Many of the identified proteins were associated with cell cycle control and so it is anticipated from the data that the normal functioning of the cell cycle in HaCaT cells was deregulated by the response to bystander signalling. The proteins identified were novel and also common to proteins induced RIBE in previous proteomic fish studies. This has contributed to a better understanding of RIBE studies that investigate key molecular signalling pathways and could even be considered as biological ‘markers’ in cells/tissues undergoing indirect low-dose radiation exposures. Currently a lot of on-going research is dedicated to proteomics and is continually evolving and developing. Advances in the field of

proteomics for radiobiological studies have and will further improve our understanding and regard of the remarkable bystander phenomena. It is important to appreciate the signalling events both transcriptionally and post-transnationally as some genes are not always translated into a functional protein complex.

### **Acknowledgments**

H.F. thanks the Dublin Institute of Technology, Ireland for the *International Student Internship Award* to fund the project at McMaster University, Hamilton, Ontario, Canada.

# **Chapter 6**

## **Discussion**



## 6. Discussion

Over recent years unusual data has emerged from radiobiological studies suggesting that irradiated cellular damage does not always depend on direct DNA damage and these occurrences are due to radiation-induced non-targeted effects (NTE). Further investigations into this phenomenon have revealed that complex responses exist for what are now known as bystander effects. The radiation-induced bystander effects (RIBE) occur as a result of transmission of damage signals from directly irradiated cells to non-irradiated neighbouring cells, either via cell-to-cell communication or by gap-junction intercellular communication. To date the bystander ‘factor’ responsible for transmission of the signal has not yet been identified but some characteristics has been discovered. The ‘factor’ is believed to be a protein of some sort as it can freeze thaw once and stored at  $-80^{\circ}\text{C}$ , it is denatured at  $70^{\circ}\text{C}$  and is a small and transient molecule.

It is evident that *in vitro*, *in vivo*, and *ex vivo* experimental models produce a high variability in RIBE responses. Genetic factors can influence this variability in responses which poses difficulties as there is no degree of consistency. However, the molecular mechanisms of RIBE are slowly being unveiled with the use of radiobiological molecular techniques *in vivo* and *in vitro*. There has created a lot of controversy surrounding the potential clinical implications for RIBE and further translational research studies are essential to address this question for patients undergoing radiotherapy in the future. The aim of the current study was to further elucidate the cellular and molecular signalling mechanisms associated with RIBE, which will hopefully contribute to the development of non-targeted human radiation risk assessments and thus improve radiotherapy methods.

The first part of this study consolidated a HaCaT cell test model and proved it to be a good reporter for RIBE and therefore it was used for the subsequent studies. This was followed by investigations of the unique pathways involved in RIBE to discover significant targets for the intercellular and intracellular signalling events. One of the initial intercellular signalling events discovered Annexin II signalling on the surface of the cell membrane. A unique role of intrinsic apoptosis events part of the intracellular signalling was elucidated. As a result of the data generated, two pathways dependent on dose are proposed and are illustrated in Figure 6.1 and Figure 6.2. For the 0.05 Gy dose gene expression data unveiled an induction of pro-apoptotic genes and an induction of initiator caspases, to drive the cell death process forward in HaCaT cells exposed to ICCM. The Annexin II gene was shown to be down-regulated which is suggestive of increased apoptosis, and thus at this dose the HaCaT cells are experiencing intrinsic-apoptosis leading to cell death.

With respect to the 0.5 Gy dose, the MTT cell viability assay suggested a reduction in cell viability in HaCaT cells in response to ICCM, indicative of increased cell death. However, apoptotic gene expression changes were minor and occurred at later times of 6 hr as well as increased anti-apoptotic signalling. The proteomic data demonstrated an increase of Annexin II at this dose (4 hr), and the gene expression data showed an up-regulation of the Annexin II gene 8 hr post-exposure, both suggestive of reduced apoptosis. Together with the apoptotic gene data generated, it is clear that either the cell death process is delayed or other modes of cell death are involved in the bystander process for the 0.5 Gy dose. Overall, the proposed pathways demonstrate clearly that bystander responses in HaCaT cells can be dose-specific, causing unique bystander effects in response to different low-doses of non-targeted irradiation which is a key discovery of this project.

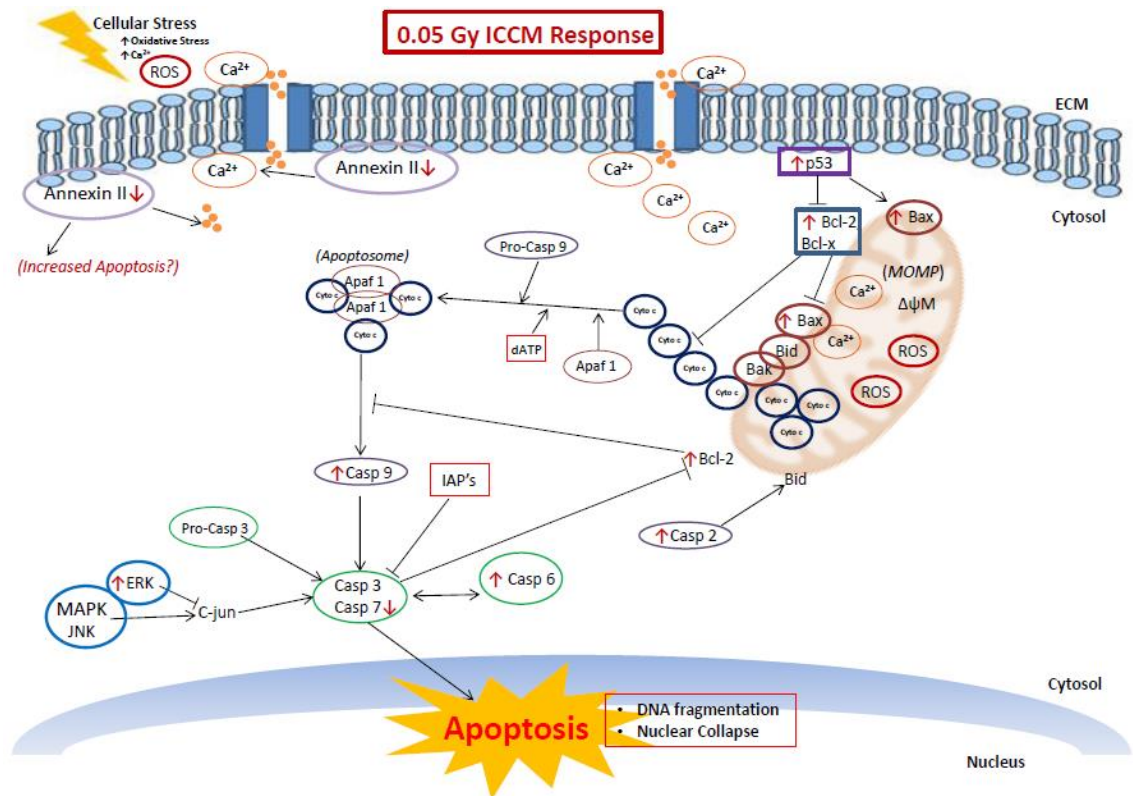


Figure 6.1: The proposed radiation-induced bystander apoptotic signalling pathway response for HaCaT cells exposed to irradiated cell-conditioned medium at a dose of 0.05 Gy.

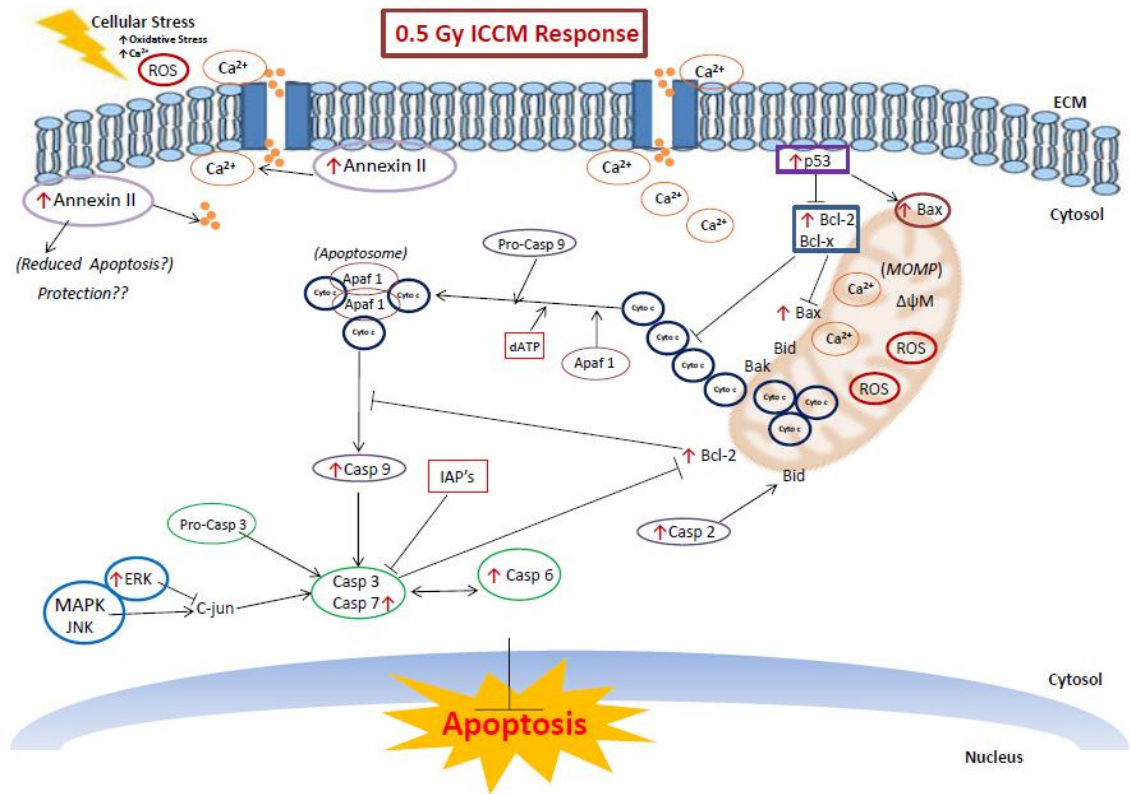


Figure 6.2: The proposed radiation-induced bystander apoptotic signalling pathway response for HaCaT cells exposed to irradiated cell-conditioned medium at a dose of 0.5 Gy.

## References

- Aldridge, D. R., Arends, M. J., & Radford, I. R. (1995). Increasing the susceptibility of the rat 208F fibroblast cell line to radiation-induced apoptosis does not alter its clonogenic survival dose-response. *British journal of cancer*, *71*, 571–7.
- Alexander, P., & Bacq, Z. M. (1961). The nature of the initial radiation damage at the subcellular level. In *The Initial Effects of Ionizing Radiations on Cells* (pp. 3–19). RJC Harris.
- Amundson, S. A. (2008). Functional genomics in radiation biology: a gateway to cellular systems-level studies. *Radiation and environmental biophysics*, *47*, 25–31.
- Amundson, S. A., Do, K. T., Shahab, S., Bittner, M., Meltzer, P., et al. (2000). Identification of potential mRNA biomarkers in peripheral blood lymphocytes for human exposure to ionizing radiation. *Radiation research*, *154*, 342–6.
- Anoopkumar-Dukie, S., Carey, J. B., Conere, T., O'sullivan, E., van Pelt, F. N., et al. (2005). Resazurin assay of radiation response in cultured cells. *The British journal of radiology*, *78*, 945–7.
- Askham, J. M., Vaughan, K. T., Goodson, H. V., & Morrison, E. E. (2002). Evidence that an interaction between EB1 and p150 (Glued) is required for the formation and maintenance of a radial microtubule array anchored at the centrosome. *Molecular biology of the cell*, *13*, 3627–45.

- Assefa, Z., Garmyn, M., Vantieghem, A., Declercq, W., Vandenabeele, P., et al. (2003). Ultraviolet B radiation-induced apoptosis in human keratinocytes: cytosolic activation of procaspase-8 and the role of Bcl-2. *FEBS Letters*, 540, 125–132.
- Assefa, Z., Van Laethem, A., Garmyn, M., & Agostinis, P. (2005). Ultraviolet radiation-induced apoptosis in keratinocytes: on the role of cytosolic factors. *Biochimica et biophysica acta*, 1755, 90–106.
- Assefa, Z., Vantieghem, a, Garmyn, M., Declercq, W., Vandenabeele, P., et al. (2000). p38 mitogen-activated protein kinase regulates a novel, caspase-independent pathway for the mitochondrial cytochrome c release in ultraviolet B radiation-induced apoptosis. *The Journal of biological chemistry*, 275, 21416–21.
- Asur, R., Balasubramaniam, M., Marples, B., Thomas, R. a, & Tucker, J. D. (2010). Involvement of MAPK proteins in bystander effects induced by chemicals and ionizing radiation. *Mutation research*, 686, 15–29.
- Asur, R., Balasubramaniam, M., Marples, B., Thomas, R. a, & Tucker, J. D. (2010b). Involvement of MAPK proteins in bystander effects induced by chemicals and ionizing radiation. *Mutation research*, 686, 15–29.
- Asur, R., Balasubramaniam, M., Marples, B., Thomas, R. A., & Tucker, J. D. (2010a). Bystander effects induced by chemicals and ionizing radiation: evaluation of changes in gene expression of downstream MAPK targets. *Mutagenesis*, 25, 271–9.

- Audette-Stuart, M., Kim, S. B., McMullin, D., Festarini, a, Yankovich, T. L., et al. (2011). Adaptive response in frogs chronically exposed to low doses of ionizing radiation in the environment. *Journal of environmental radioactivity*, 102, 566–73.
- Aypar, U., Morgan, W. F., & Baulch, J. E. (2011). Radiation-induced genomic instability: are epigenetic mechanisms the missing link? *International journal of radiation biology*, 87, 179–91.
- Azzam, E. I., de Toledo, S. M., & Little, J. B. (2001). Direct evidence for the participation of gap junction-mediated intercellular communication in the transmission of damage signals from alpha -particle irradiated to nonirradiated cells. *Proceedings of the National Academy of Sciences of the United States of America*, 98, 473–8.
- Azzam, E. I., de Toledo, S. M., & Little, J. B. (2003). Oxidative metabolism, gap junctions and the ionizing radiation-induced bystander effect. *Oncogene*, 22, 7050–7.
- Azzam, E. I., De Toledo, S. M., Gooding, T., & Little, J. B. (1998). Intercellular communication is involved in the bystander regulation of gene expression in human cells exposed to very low fluences of alpha particles. *Radiation Research*, 150, 497–504.
- Azzam, E. I., de Toledo, S. M., Waker, A. J., & Little, J. B. (2000). High and Low Fluences of alpha Particles Induce a G1 Checkpoint in Human Diploid Fibroblasts. *Cancer Res.*, 60, 2623–2631.

- Azzam, E. I., Jay-Gerin, J.-P., & Pain, D. (2012). Ionizing radiation-induced metabolic oxidative stress and prolonged cell injury. *Cancer letters*, 327, 48–60.
- Azzam, E. I., Toledo, S. M. De, & Spitz, D. R. (2002). Oxidative Metabolism Modulates Signal Transduction and Micronucleus Formation in Bystander Cells from  $\alpha$  -Particle-irradiated Normal Human Fibroblast Cultures. *Cancer Research*, 5436–5442.
- Balduzzi, M., Saporita, O., Matteucci, A., & Paradisi, S. (2010). Modulation of the bystander effects induced by soluble factors in HaCaT cells by different exposure strategies. *Radiation research*, 173, 779–88.
- Barcellos-Hoff, M. H., & Brooks, a L. (2001). Extracellular signaling through the microenvironment: a hypothesis relating carcinogenesis, bystander effects, and genomic instability. *Radiation research*, 156, 618–27.
- Baskar, R. (2010). Emerging role of radiation induced bystander effects: Cell communications and carcinogenesis. *Genome integrity*, 1, 13.
- Baskar, R., Balajee, A. S., & Geard, C. R. (2007). Effects of low and high LET radiations on bystander human lung fibroblast cell survival. *International journal of radiation biology*, 83, 551–9.
- Baskar, R., Lee, K. A., Yeo, R., & Yeoh, K.-W. (2012). Cancer and radiation therapy: current advances and future directions. *International journal of medical sciences*, 9, 193–9.



- Bazzoni, G., Martinez-Estrada, O. M., Orsenigo, F., Cordenonsi, M., Citi, S., et al. (2000). Interaction of junctional adhesion molecule with the tight junction components ZO-1, cingulin, and occludin. *The Journal of biological chemistry*, 275, 20520–6.
- Belyakov, O. V, Folkard, M., Mothersill, C., Prise, K. M., & Michael, B. D. (2003). A proliferation-dependent bystander effect in primary porcine and human urothelial explants in response to targeted irradiation. *British journal of cancer*, 88, 767–74.
- Belyakov, O. V, Folkard, M., Mothersill, C., Prise, K. M., & Michael, B. D. (2006). Bystander-induced differentiation: a major response to targeted irradiation of a urothelial explant model. *Mutation research*, 597, 43–9.
- Belyakov, O. V, Malcolmson, a M., Folkard, M., Prise, K. M., & Michael, B. D. (2001). Direct evidence for a bystander effect of ionizing radiation in primary human fibroblasts. *British journal of cancer*, 84, 674–9.
- Belyakov, O. V, Mitchell, S. a, Parikh, D., Randers-Pehrson, G., Marino, S. a, et al. (2005). Biological effects in unirradiated human tissue induced by radiation damage up to 1 mm away. *Proceedings of the National Academy of Sciences of the United States of America*, 102, 14203–8.
- Belyakov, O. V. (2005). Non-targeted effects of ionising radiation. In *Proceedings of the RISC-RAD specialised training course “Non-targeted effects of ionising radiation”*. (pp. 13–46).

- Bernier, J., Hall, E. J., & Giaccia, A. (2004). Radiation oncology: a century of achievements. *Nature reviews. Cancer*, 4, 737–47.
- Berridge, M. V., & Tan, A. S. (1993). Characterization of the Cellular Reduction of 3-(4,5-dimethylthiazol-2-yl)-2,5-diphenyltetrazolium bromide (MTT): Subcellular Localization, Substrate Dependence, and Involvement of Mitochondrial Electron Transport in MTT Reduction. *Archives of Biochemistry and Biophysics*, 303, 474–482.
- Beyzadeoglu, M. (2011). *Basic Radiation Oncology*.
- Bishop, A. L., & Hall, A. (2000). Rho GTPases and their effector proteins. *The Biochemical journal*, 348 Pt 2, 241–55.
- Blyth, B. J., & Sykes, P. J. (2011). Radiation-Induced Bystander Effects : What Are They , and How Relevant Are They to Human Radiation Exposures ? *Radiation Research*, 176, 139–157.
- Boukamp, P., Petrussevska, R. T., Breitkreutz, D., Hornung, J., Markham, A., et al. (1988). Normal Keratinization in a Spontaneously Immortalized Aneuploid Human Keratinocyte Cell Line. *The Journal of Cell Biology*, 106, 761–771.
- Boukamp, P., Stanbridge, E. J., Foo, D. Y., Cerutti, P. A., & Fusenig, N. E. (1990). c-Ha-ras Oncogene Expression in Immortalized Human Keratinocytes ( HaCaT ) Alters Growth Potential in Vivo but Lacks Correlation with Malignancy c-Ha-ras Oncogene Expression in Immortalized Human Keratinocytes ( HaCaT ) Alters Growth Potential in Vivo bu. *Cancer*, 50, 2840–2847.

- Boukamp, P., Stanbridge, E. J., Foo, D. Y., Cerutti, P. A., & Fusenig, N. E. (1990). c-Ha-ras Oncogene Expression in Immortalized Human Keratinocytes (HaCaT) Alters Growth Potential in Vivo but Lacks Correlation with Malignancy. *Cancer Res.*, 50, 2840–2847.
- Brentnall, M., Rodriguez-Menocal, L., De Guevara, R. L., Cepero, E., & Boise, L. H. (2013). Caspase-9, caspase-3 and caspase-7 have distinct roles during intrinsic apoptosis. *BMC cell biology*, 14, 32.
- Burdak-Rothkamm, S., & Prise, K. M. (2009). New molecular targets in radiotherapy: DNA damage signalling and repair in targeted and non-targeted cells. *European journal of pharmacology*, 625, 151–5.
- Cain, K., Bratton, S. B., & Cohen, G. M. (2002). The Apaf-1 apoptosome: a large caspase-activating complex. *Biochimie*, 84, 203–14.
- Calabrese, E. J., Stanek, E. J., & Nascarella, M. a. (2011). Evidence for hormesis in mutagenicity dose-response relationships. *Mutation research*, 726, 91–7.
- Camphausen, K., Moses, M. A., Ménard, C., Me, C., Sproull, M., et al. (2003). Radiation Abscopal Antitumor Effect Is Mediated through p53. *Cancer Res.*, 63, 1990–1993.
- Campos, M. S., Rodini, C. O., Pinto-Júnior, D. S., & Nunes, F. D. (2009). GAPD and tubulin are suitable internal controls for qPCR analysis of oral squamous cell carcinoma cell lines. *Oral oncology*, 45, 121–6.

- Cerella, C., Diederich, M., & Ghibelli, L. (2010). The dual role of calcium as messenger and stressor in cell damage, death, and survival. *International journal of cell biology*, 2010, 546163.
- Chaudhry, M. A. (2006). Bystander effect: biological endpoints and microarray analysis. *Mutation research*, 597, 98–112.
- Chen, S., Zhao, Y., Zhao, G., Han, W., Bao, L., et al. (2009). Up-regulation of ROS by mitochondria-dependent bystander signaling contributes to genotoxicity of bystander effects. *Mutation research*, 666, 68–73.
- Chipuk, J. E., Bouchier-Hayes, L., & Green, D. R. (2006). Mitochondrial outer membrane permeabilization during apoptosis: the innocent bystander scenario. *Cell death and differentiation*, 13, 1396–402.
- Chomczynski, P., & Sacchi, N. (1987). Single-step method of RNA isolation by acid guanidinium thiocyanate-phenol-chloroform extraction. *Analytical Biochemistry*, 162, 156–159.
- Chowdhury, I., Tharakan, B., & Bhat, G. K. (2008). Caspases - an update. *Comparative biochemistry and physiology. Part B, Biochemistry & molecular biology*, 151, 10–27.
- Citi, S., Amorosi, A., Franconi, F., & Giotti, A. (1991). Cingulin , a Specific Protein Component of Tight Junctions , Is Expressed in Normal and Neoplastic human Epithelial Tissues. 138, 781–789.

- Clutton, S. M., Townsend, K. M., Walker, C., Ansell, J. D., & Wright, E. G. (1996). Radiation-induced genomic instability and persisting oxidative stress in primary bone marrow cultures. *Carcinogenesis*, 17, 1633–9.
- Coates, P. J., Lorimore, S. a, & Wright, E. G. (2004). Damaging and protective cell signalling in the untargeted effects of ionizing radiation. *Mutation research*, 568, 5–20.
- Coates, P. J., Rundle, J. K., Lorimore, S. A., & Wright, E. G. (2008). Indirect macrophage responses to ionizing radiation: implications for genotype-dependent bystander signaling. *Cancer research*, 68, 450–6.
- Coleman, M. a, Yin, E., Peterson, L. E., Nelson, D., Sorensen, K., et al. (2005). Low-dose irradiation alters the transcript profiles of human lymphoblastoid cells including genes associated with cytogenetic radioadaptive response. *Radiation research*, 164, 369–82.
- Crowther, J. a. (1924). Some Considerations Relative to the Action of X-Rays on Tissue Cells. *Proceedings of the Royal Society B: Biological Sciences*, 96, 207–211.
- Debret, R., El Btaouri, H., Duca, L., Rahman, I., Radke, S., et al. (2003). Annexin A1 processing is associated with caspase-dependent apoptosis in BZR cells. *FEBS Letters*, 546, 195–202.
- Demoise, C. F., & Conard, R. A. (1972). Effects of Age and Radiation Exposure on Chromosomes in a Marshall Island Population. *Journal of Gerontology*, 27, 197–201.

- DerMardirossian, C., & Bokoch, G. M. (2005). GDIs: central regulatory molecules in Rho GTPase activation. *Trends in cell biology*, 15, 356–63.
- Deshpande, A., Goodwin, E. H., Bailey, S. M., Marrone, B. L., & Lehnert, B. E. (1996). Alpha-particle-induced sister chromatid exchange in normal human lung fibroblasts: evidence for an extranuclear target. *Radiation research*, 145, 260–7.
- Deyrieux, A. F., & Wilson, V. G. (2007). In vitro culture conditions to study keratinocyte differentiation using the HaCaT cell line. *Cytotechnology*, 54(2), 77–83. doi:10.1007/s10616-007-9076-1
- Dovas, A., & Couchman, J. R. (2005). RhoGDI: multiple functions in the regulation of Rho family GTPase activities. *The Biochemical journal*, 390, 1–9.
- Doyle, A., & Griffiths, J. B. (1997). *Mammalian cell culture*.
- Efeyan, A., & Serrano, M. (2007). p53: Guardian of the Genome and Policeman of the Oncogenes. *Cell Cycle*, 1006–1010.
- Ellenbroek, S. I. J., & Collard, J. G. (2007). Rho GTPases: functions and association with cancer. *Clinical & experimental metastasis*, 24, 657–72.
- Elmore, S. (2007). *Apoptosis: A Review of Programmed Cell Death* Susan Elmore. *Apoptosis*, 35, 495–516.
- Emerit, I. (1981). Clastogenic Activity from Bloom Syndrome Fibroblast Cultures. *Proceedings of the National Academy of Sciences*, 78, 1868–1872.

- Emerit, I. (1994). Reactive oxygen species, chromosome mutation, and cancer: possible role of clastogenic factors in carcinogenesis. *Free Radical Biology and Medicine*, 16, 99–109.
- Emerit, I., Arutyunyan, R., Oganessian, N., Levy, A., Cernjavsky, L., et al. (1995). Radiation-induced clastogenic factors: Anticlastogenic effect of ginkgo biloba extract. *Free Radical Biology and Medicine*, 18, 985–991.
- Emerit, I., Levy, A., & S.Khan. (1991). Superoxide Generation by Clastogenic Factors. In *Free Radicals, Lipoproteins, and Membrane Lipids* (pp. 99–104).
- Eriksson, D., & Stigbrand, T. (2010). Radiation-induced cell death mechanisms. *Tumour Biology*, 31, 363–72.
- Faguet, G. B., Reichard, S. M., & Welter, D. A. (1984). Radiation-induced clastogenic plasma factors. *Cancer genetics and cytogenetics*, 12, 73–83.
- Fazzari, J., Mersov, A., Smith, R., Seymour, C., & Mothersill, C. (2012). Effect of 5-hydroxytryptamine (serotonin) receptor inhibitors on the radiation-induced bystander effect. *International journal of radiation biology*, 88, 786–90.
- Feinendegen, L., Hahnfeldt, P., Schadt, E. E., Stumpf, M., & Voit, E. O. (2008). Systems biology and its potential role in radiobiology. *Radiation and environmental biophysics*, 47, 5–23.
- Filipenko, N. R., MacLeod, T. J., Yoon, C.-S., & Waisman, D. M. (2004). Annexin A2 is a novel RNA-binding protein. *The Journal of biological chemistry*, 279, 8723–31.

- Fleckenstein, A., Janke, J., Döring, H. J., & Leder, O. (1974). Myocardial fiber necrosis due to intracellular Ca overload-a new principle in cardiac pathophysiology. *Recent advances in studies on cardiac structure and metabolism*, 4, 563–80.
- Fournier, C., Barberet, P., Pouthier, T., Ritter, S., Fischer, B., et al. (2009). No evidence for DNA and early cytogenetic damage in bystander cells after heavy-ion microirradiation at two facilities. *Radiation research*, 171, 530–40.
- Fukata, M., Nakagawa, M., & Kaibuchi, K. (2003). Roles of Rho-family GTPases in cell polarisation and directional migration. *Current Opinion in Cell Biology*, 15, 590–597.
- Fulda, S., & Debatin, K.-M. (2006). Extrinsic versus intrinsic apoptosis pathways in anticancer chemotherapy. *Oncogene*, 25, 4798–811.
- Furlong, H., Mothersill, C., Lyng, F. M., & Howe, O. (2013). Apoptosis is signalled early by low doses of ionising radiation in a radiation-induced bystander effect. *Mutation research. Fundamental and molecular mechanisms of mutagenesis*, 741-742, 35–43.
- Galluzzi, L., Vitale, I., Abrams, J. M., Alnemri, E. S., Baehrecke, E. H., et al. (2012). Molecular definitions of cell death subroutines: recommendations of the Nomenclature Committee on Cell Death 2012. *Cell death and differentiation*, 19, 107–20.
- Ganesan, V., & Colombini, M. (2010). Regulation of ceramide channels by Bcl-2 family proteins. *FEBS letters*, 584, 2128–34.



- Gerber, H. P., Dixit, V., & Ferrara, N. (1998). Vascular endothelial growth factor induces expression of the antiapoptotic proteins Bcl-2 and A1 in vascular endothelial cells. *The Journal of biological chemistry*, 273, 13313–6.
- Gerke, V., & Moss, S. E. (2002). Annexins: from structure to function. *Physiological reviews*, 82, 331–71.
- Ghandhi, S. a, Yaghoubian, B., & Amundson, S. a. (2008). Global gene expression analyses of bystander and alpha particle irradiated normal human lung fibroblasts: synchronous and differential responses. *BMC medical genomics*, 1, 63.
- Goh, K., & Sumner, H. (1968). Breaks in normal human chromosomes: are they induced by a transferable substance in the plasma of persons exposed to total-body irradiation? *Radiation research*, 35, 171–174.
- Gow, M. D., Seymour, C. B., Ryan, L. a, & Mothersill, C. E. (2010). Induction of bystander response in human glioma cells using high-energy electrons: a role for TGF-beta1. *Radiation research*, 173, 769–78.
- Graves, J. D., Gotoh, Y., Draves, K. E., Ambrose, D., Han, D. K., et al. (1998). Caspase-mediated activation and induction of apoptosis by the mammalian Ste20-like kinase Mst1. *The EMBO journal*, 17, 2224–34.
- Groesser, T., Cooper, B., & Rydberg, B. (2008). Lack of bystander effects from high-LET radiation for early cytogenetic end points. *Radiation research*, 170, 794–802.

- Grubbe, E. H. (1946). X-ray treatment; its introduction to medicine. *Journal of the American Institute of Homeopathy*, 39, 419–22.
- Grubbe, E. H. (1947). The origin and birth of x-ray therapy. *The Urologic and cutaneous review*, 51, 375–9.
- Grütter, M. G. (2000). Caspases: key players in programmed cell death. *Current opinion in structural biology*, 10, 649–55.
- Guillemot, L., & Citi, S. (2006). Cingulin Regulates Claudin-2 Expression and Cell Proliferation through the Small GTPase RhoA. *Molecular Biology of the Cell*, 17, 3569–3577.
- Guo, Y., Srinivasula, S. M., Druilhe, A., Fernandes-Alnemri, T., & Alnemri, E. S. (2002). Caspase-2 induces apoptosis by releasing proapoptotic proteins from mitochondria. *The Journal of biological chemistry*, 277, 13430–7.
- Halazonetis, T. D., Gorgoulis, V. G., & Bartek, J. (2008). An oncogene-induced DNA damage model for cancer development. *Science (New York, N.Y.)*, 319, 1352–5.
- Hall, E. J. (2007). Cancer caused by x-rays-a random event? *The lancet oncology*, 8, 369–70.
- Hall, E. J., & Giaccia, A. J. (2012). *Radiobiology for the Radiologist*. Lippincott Williams & Wilkins.

- Hamada, N., Ni, M., Funayama, T., Sakashita, T., & Kobayashi, Y. (2008). Temporally distinct response of irradiated normal human fibroblasts and their bystander cells to energetic heavy ions. *Mutation research*, 639, 35–44.
- Harris, S. L., & Levine, A. J. (2005). The p53 pathway: positive and negative feedback loops. *Oncogene*, 24, 2899–908.
- Hayashi, I., Wilde, A., Mal, T. K., & Ikura, M. (2005). Structural Basis for the Activation of Microtubule Assembly by the EB1 and p150Glued Complex. *Molecular Cell*, 19, 449–460.
- He, J., Liu, Y., He, S., Wang, Q., Pu, H., et al. (2007). Proteomic Analysis of a Membrane Skeleton Fraction from Human Liver research articles. *Journal of proteome research*, 3509–3518.
- He, M., Zhao, M., Shen, B., Prise, K. M., & Shao, C. (2011). Radiation-induced intercellular signaling mediated by cytochrome-c via a p53-dependent pathway in hepatoma cells. *Oncogene*, 30, 1947–1955.
- Hei, T. K., Zhou, H., Chai, Y., Ponnaiya, B., & Ivanov, V. N. (2011). Radiation Induced Non-targeted Response: Mechanism and Potential Clinical Implications. *Current molecular pharmacology*, 4, 96–105.
- Hei, T. K., Zhou, H., Ivanov, V. N., Hong, M., Lieberman, H. B., et al. (2008). Mechanism of radiation-induced bystander effects: a unifying model. *The Journal of pharmacy and pharmacology*, 60, 943–50.

- Hollowell, J. G. J., & Littlefield, L. G. (1967). Chromosome Aberrations Induced by Plasma from Irradiated Patients: A Brief Report. *J. S. C. Med. Ass.*, 63: 437-442(Dec. 19, 1967).
- Hollowell, J. G., & Littlefield, L. G. (1968). Chromosome Damage Induced by Plasma of X-Rayed Patients: An Indirect Effect of X-Ray. *Experimental Biology and Medicine*, 129, 240–244.
- Honnappa, S., Gouveia, S. M., Weisbrich, A., Damberger, F. F., Bhavesh, N. S., et al. (2009). An EB1-Binding Motif Acts as a Microtubule Tip Localization Signal. *Cell*, 138, 366–376.
- Hosokawa, Y., Sakakura, Y., Tanaka, L., Okumura, K., Yajima, T., et al. (2005). Radiation-induced apoptosis is independent of caspase-8 but dependent on cytochrome c and the caspase-9 cascade in human leukemia HL60 cells. *Journal of radiation research*, 46, 293–303.
- Howe, O., Malley, K. O., Lavin, M., Gardner, R. A., Seymour, C., et al. (2005). Cell Death Mechanisms Associated with G<sub>2</sub> Radiosensitivity in Patients with Prostate Cancer and Benign Prostatic Hyperplasia. *Radiation Research*, 634, 627–634.
- Howe, O., O’Sullivan, J., Nolan, B., Vaughan, J., Gorman, S., et al. (2009). Do radiation-induced bystander effects correlate to the intrinsic radiosensitivity of individuals and have clinical significance? *Radiation research*, 171, 521–9.

- Hwang, J., Kim, Y.-Y., Huh, S., Shim, J., Park, C., et al. (2005). The Time-Dependent Serial Gene Response to Zeocin Treatment Involves Caspase-Dependent Apoptosis in HeLa Cells. *Microbiology and immunology*, 49, 331–342.
- Igney, F. H., & Krammer, P. H. (2002). Death and anti-death: tumour resistance to apoptosis. *Nature reviews. Cancer*, 2, 277–88.
- Ilnytsky, Y., Koturbash, I., & Kovalchuk, O. (2009). Radiation-Induced Bystander Effects In Vivo are Epigenetically Regulated in a Tissue-Specific Manner. *Mutation Research*, 113, 105–13.
- Inoue, S., Browne, G., Melino, G., & Cohen, G. M. (2009). Ordering of caspases in cells undergoing apoptosis by the intrinsic pathway. *Cell death and differentiation*, 16, 1053–61.
- Internal Atomic Energy Agency Publications. (2004). *Radiation, People and the Environment*.
- Irons, S. L., Serra, V., Bowler, D., Chapman, K., Militi, S., et al. (2012). The effect of genetic background and dose on non-targeted effects of radiation. *International journal of radiation biology*, 88, 735–42.
- Ito, S., Tan, L. J., Andoh, D., Narita, T., Seki, M., et al. (2010). MMXD, a TFIIF-Independent XPD-MMS19 Protein Complex Involved in Chromosome Segregation.

- Ivanov, V. N., Zhou, H., Ghandhi, S. a, Karasic, T. B., Yaghoubian, B., et al. (2010). Radiation-induced bystander signaling pathways in human fibroblasts: a role for interleukin-33 in the signal transmission. *Cellular signalling*, 22, 1076–87.
- Iyer, R., & Lehnert, B. . (2002). Low dose, low-LET ionizing radiation-induced radioadaptation and associated early responses in unirradiated cells. *Mutation research*, 503, 1–9.
- Iyer, R., & Lehnert, B. E. (2002a). Alpha-particle-induced increases in the radioresistance of normal human bystander cells. *Radiation research*, 157, 3–7.
- Iyer, R., Lehnert, B. E., & Svensson, R. (2000). Factors underlying the cell growth-related bystander responses to alpha particles. *Cancer Research*, 60, 1290–1298.
- Jain, M. R., Li, M., Chen, W., Liu, T., Toledo, S. M. De, et al. (2012). In Vivo Space Radiation-Induced Non-Targeted Responses: Late Effects On Molecular Signaling In Mitochondria. *Current molecular pharmacology*, 4, 106–114
- Jella, K. K., Garcia, A., McClean, B., Byrne, H. J., & Lyng, F. M. (2013). Cell death pathways in directly irradiated cells and cells exposed to medium from irradiated cells. *International journal of radiation biology*, 89, 182–190.
- Jella, K. K., Rani, S., O’Driscoll, L., McClean, B., Byrne, H. J., et al. (2014). Exosomes are involved in mediating radiation induced bystander signaling in human keratinocyte cells. *Radiation research*, 181, 138–45.

- Jen, K.-Y., & Cheung, V. G. (2005). Identification of novel p53 target genes in ionizing radiation response. *Cancer research*, 65, 7666–73.
- Jimbo, a, Fujita, E., Kouroku, Y., Ohnishi, J., Inohara, N., et al. (2003). ER stress induces caspase-8 activation, stimulating cytochrome c release and caspase-9 activation. *Experimental Cell Research*, 283, 156–166.
- Jin, J., Smith, F. D., Stark, C., Wells, C. D., Fawcett, J. P., et al. (2004). Proteomic , Functional , and Domain-Based Analysis of In Vivo 14-3-3 Binding Proteins Involved in Cytoskeletal Regulation and Cellular Organization. *Current Biology*, 14, 1436–1450.
- Jin, L., Williamson, A., Banerjee, S., Philipp, I., & Rape, M. (2008). Mechanism of Ubiquitin-Chain Formation by the Human Anaphase-Promoting Complex. *Cell*, 133, 653–665.
- Jin, Z., & El-Deiry, W. S. (2005). Overview of Cell Death Signaling Pathways. *Cancer Biology and Therapy*, 139–163.
- Joiner, M. C., Marples, B., Lambin, P., Short, S. C., & Turesson, I. (2001). Low-dose hypersensitivity: current status and possible mechanisms. *International Journal of Radiation Oncology\*Biology\*Physics*, 49, 379–389.
- Joiner, M., & Kogel, A. van de. (2009). *Basic Clinical Radiobiology* (fourth edition).
- Kadhim, M. A., MacDonald, D. A., Goodhead, D. T., Lorimore, S. A., Marsden, S. J., et al. (1992). Transmission of chromosomal instability after plutonium  $\alpha$ -particle irradiation. *Nature*, 355, 738–740.

- Kaminski, J. M., Shinohara, E., Summers, J. B., Niermann, K. J., Morimoto, A., et al. (2005). The controversial abscopal effect. *Cancer treatment reviews*, 31, 159–72.
- Kang, M. H., & Reynolds, and C. P. (2009). Bcl-2 inhibitors: targeting mitochondrial apoptotic pathways in cancer therapy. *Clinical Cancer Research*, 15, 1126–1132.
- Kashino, G., Prise, K. M., Suzuki, K., Matsuda, N., Kodama, S., et al. (2007). Effective Suppression of Bystander Effects by DMSO Treatment of Irradiated CHO Cells. *Journal of Radiation Research*, 48, 327–333.
- Kashino, G., Suzuki, K., Matsuda, N., Kodama, S., & Ono, K. (2010). Radiation induced bystander signals are independent of DNA damage and DNA repair capacity of the irradiated cells. *Mutation research. Fundamental and molecular mechanisms of mutagenesis*, 619, 134–138.
- Kaufmann, S. H., Lee, S.-H., Meng, X. W., Loegering, D. a, Kottke, T. J., et al. (2008). Apoptosis-associated caspase activation assays. *Methods (San Diego, Calif.)*, 44, 262–72.
- Kaup, S., Grandjean, V., Mukherjee, R., Kapoor, A., Keyes, E., et al. (2006). Radiation-induced genomic instability is associated with DNA methylation changes in cultured human keratinocytes. *Mutation research*, 597, 87–97.
- Kelly, S. A., Havrillal, C. M., Brady, T. C., Abramo, K. H., & Levin, E. D. (1998). Oxidative Stress in Toxicology: Established Mammalian and Emerging Piscine Model Systems. *Environmental Health Perspectives*, 106, 375–384.



- Kerr, J. F., Wyllie, A. H., & Currie, A. R. (1972). Apoptosis: a basic biological phenomenon with wide-ranging implications in tissue kinetics. *British journal of cancer*, 26, 239–57.
- Khan, M. A., Hill, R. P., & Dyk, J. Van. (1998). Partial volume rat lung irradiation: an evaluation of early DNA damage. *International Journal of Radiation Oncology*, 40, 467–476.
- Khan, S. H., & Emerit, I. (1985). Lipid peroxidation products and clastogenic material in culture media of human leukocytes exposed to the tumor promoter phorbol-myristate-acetate. *Journal of Free Radicals in Biology & Medicine*, 1, 443–449.
- Kim, C., Ryu, Ho-Cheol., & Kim, Jae-Hong. (2010). Low-dose UVB irradiation stimulates matrix metalloproteinase-1 expression via a BLT2-linked pathway in HaCaT cells. *Experimental & molecular medicine*, 42, 833–841.
- Kondo, Y., Kanzawa, T., Sawaya, R., & Kondo, S. (2005). The role of autophagy in cancer development and response to therapy. *Nature reviews. Cancer*, 5, 726–34.
- Koturbash, I., Boyko, A., Rodriguez-Juarez, R., McDonald, R. J., Tryndyak, V. P., et al. (2007). Role of epigenetic effectors in maintenance of the long-term persistent bystander effect in spleen in vivo. *Carcinogenesis*, 28, 1831–8.
- Koturbash, I., Loree, J., Kutanzi, K., Koganow, C., Pogribny, I., et al. (2008). In vivo bystander effect: cranial X-irradiation leads to elevated DNA damage, altered cellular proliferation and apoptosis, and increased p53 levels in

shielded spleen. *International journal of radiation oncology, biology, physics*, 70, 554–62.

Koturbash, I., Rugo, R. E., Hendricks, C. a, Loree, J., Thibault, B., et al. (2006). Irradiation induces DNA damage and modulates epigenetic effectors in distant bystander tissue in vivo. *Oncogene*, 25, 4267–75.

Kroemer, G., El-Deiry, W. S., Golstein, P., Peter, M. E., Vaux, D., et al. (2005). Classification of cell death: recommendations of the Nomenclature Committee on Cell Death. *Cell death and differentiation*, 12 Suppl 2, 1463–7.4

Kroemer, G., Galluzzi, L., Vandenabeele, P., Abrams, J., Alnemri, E., et al. (2009). Classification of cell death: recommendations of the Nomenclature Committee on Cell Death 2009. *Cell death and differentiation*, 16, 3–11.

Krysko, D. V, Vanden Berghe, T., D’Herde, K., & Vandenabeele, P. (2008). Apoptosis and necrosis: detection, discrimination and phagocytosis. *Methods (San Diego, Calif.)*, 44, 205–21.

Kryston, T. B., Georgiev, A. B., Pissis, P., & Georgakilas, A. G. (2011). Role of oxidative stress and DNA damage in human carcinogenesis. *Mutation research*, 711, 193–201.

Kuo, W.-H., Chen, J.-H., Lin, H.-H., Chen, B.-C., Hsu, J.-D., et al. (2005). Induction of apoptosis in the lung tissue from rats exposed to cigarette smoke involves p38/JNK MAPK pathway. *Chemico-biological interactions*, 155, 31–42.

- Launay, S., Hermine, O., Fontenay, M., Kroemer, G., Solary, E., et al. (2005). Vital functions for lethal caspases. *Oncogene*, 24, 5137–48.
- LeBlanc, A. C. (2003). Natural cellular inhibitors of caspases. *Progress in neuro-psychopharmacology & biological psychiatry*, 27, 215–29.
- Lehman, T. a, Modali, R., Boukamp, P., Stanek, J., Bennett, W. P., et al. (1993). P53 Mutations in Human Immortalized Epithelial Cell Lines. *Carcinogenesis*, 14, 833–9.
- Lehnert, B. E., & Goodwin, E. H. (1997). A new mechanism for DNA alterations induced by alpha particles such as those emitted by radon and radon progeny. *Environmental health perspectives*, 105 Suppl , 1095–101.
- Lehnert, B. E., Goodwin, E. H., & Deshpande, a. (1997). Extracellular factor(s) following exposure to alpha particles can cause sister chromatid exchanges in normal human cells. *Cancer research*, 57, 2164–71.
- Lemaître, G., Lamartine, J., Pitaval, A., Vaigot, P., Garin, J., Bouet, S., ... Waksman, G. (2004). Expression profiling of genes and proteins in HaCaT keratinocytes: proliferating versus differentiated state. *Journal of Cellular Biochemistry*, 93(5), 1048-1062
- Lewis, D. A, Mayhugh, B. M., Qin, Y., Trott, K., & Mendonca, M. S. (2001). Production of delayed death and neoplastic transformation in CGL1 cells by radiation-induced bystander effects. *Radiation research*, 156, 251–8.

- Li, L., Yan, Y., Xu, H., Qu, T., & Wang, B. (2011). Selection of reference genes for gene expression studies in ultraviolet B-irradiated human skin fibroblasts using quantitative real-time PCR. *BMC molecular biology*, 12, 8–10.
- Lieschke, G. J., & Currie, P. D. (2007). Animal models of human disease: zebrafish swim into view. *Nature reviews. Genetics*, 8, 353–67.
- Lindsay, J., Esposti, M. D., & Gilmore, A. P. (2011). Bcl-2 proteins and mitochondria--specificity in membrane targeting for death. *Biochimica et biophysica acta*, 1813, 532–9.
- Little, J. B., Azzam, E. I., de Toledo, S. M., & Nagasawa, H. (2002). Bystander effects: intercellular transmission of radiation damage signals. *Radiation protection dosimetry*, 99, 159–62.
- Littlefield, L. G., Hollowell, J. G., & Pool, W. H. (1969). Chromosomal Aberrations Induced by Plasma from Irradiated Patients: An Indirect Effect of X Radiation. *Radiology*, 93, 879–886.
- Liu, Z., Mothersill, C. E., McNeill, F. E., Lyng, F. M., Byun, S. H., et al. (2006). A dose threshold for a medium transfer bystander effect for a human skin cell line. *Radiation research*, 166, 19–23.
- Logue, S. E., & Martin, S. J. (2008). Caspase activation cascades in apoptosis. *Biochemical Society transactions*, 36, 1–9.
- Lomonosova, E., & Chinnadurai, G. (2008). BH3-only proteins in apoptosis and beyond: an overview. *Oncogene*, 27, S2 – S19.

- Lorimore, S. a, Chrystal, J. a, Robinson, J. I., Coates, P. J., & Wright, E. G. (2008). Chromosomal instability in unirradiated hemaopoietic cells induced by macrophages exposed in vivo to ionizing radiation. *Cancer research*, 68, 8122–6.
- Lyng, F. M., Desplanques, M., Jella, K. K., Garcia, A., & McClean, B. (2012). The importance of serum serotonin levels in the measurement of radiation-induced bystander cell death in HaCaT cells. *International journal of radiation biology*, 88, 770–2.
- Lyng, F. M., Howe, O. L., & McClean, B. (2011). Reactive oxygen species-induced release of signalling factors in irradiated cells triggers membrane signalling and calcium influx in bystander cells. *International journal of radiation biology*, 87, 683–95.
- Lyng, F. M., Maguire, P., Kilmurray, N., Mothersill, C., Shao, C., et al. (2006). Apoptosis is initiated in human keratinocytes exposed to signalling factors from microbeam irradiated cells. *International journal of radiation biology*, 82, 393–9.
- Lyng, F. M., Maguire, P., McClean, B., Seymour, C., & Mothersill, C. (2005). Signalling pathways induced in cells exposed to medium from irradiated cells.
- Lyng, F. M., Maguire, P., McClean, B., Seymour, C., & Mothersill, C. (2006). The involvement of calcium and MAP kinase signaling pathways in the production of radiation-induced bystander effects. *Radiation research*, 165, 400–9.

- Lyng, F. M., Seymour, C. B., & Mothersill, C. (2000). Production of a signal by irradiated cells which leads to a response in unirradiated cells characteristic of initiation of apoptosis. *British journal of cancer*, 83, 1223–30.
- Lyng, F. M., Seymour, C. B., & Mothersill, C. (2001). Oxidative stress in cells exposed to low levels of ionizing radiation. *Biochemical Society transactions*, 29, 350–3.
- Lyng, F. M., Seymour, C. B., & Mothersill, C. (2002). Early events in the apoptotic cascade initiated in cells treated with medium from the progeny of irradiated cells. *Radiation protection dosimetry*, 99, 169–172.
- Lyng, F. M., Seymour, C. B., & Mothersill, C. (2002). Initiation of apoptosis in cells exposed to medium from the progeny of irradiated cells: a possible mechanism for bystander-induced genomic instability? *Radiation research*, 157, 365–70.
- Lyng, F. M., Seymour, C. B., & Mothersill, C. (2002a). Early events in the apoptotic cascade initiated in cells treated with medium from the progeny of irradiated cells. *Radiation protection dosimetry*, 99, 169–172.
- Lyng, F. M., Seymour, C. B., & Mothersill, C. (2002b). Initiation of apoptosis in cells exposed to medium from the progeny of irradiated cells: a possible mechanism for bystander-induced genomic instability? *Radiation research*, 157, 365–70.
- Maguire, P., Mothersill, C., Seymour, C., & Lyng, F. M. (2005). Medium from irradiated cells induces dose-dependent mitochondrial changes and BCL2

responses in unirradiated human keratinocytes. *Radiation research*, 163, 384–90.

Martin, R., & Haseltine, W. (1981). Range of radiochemical damage to DNA with decay of iodine-125. *Science*, 213, 896–898.

Maruyama, K., Kurokawa, H., Oosawa, M., Shimaoka, S., Yamamoto, H., et al. (1990). Beta-actinin is equivalent to Cap Z protein. *The Journal of biological chemistry*, 265, 8712–5.

Matsumoto, H., Hamada, N., Takahashi, A., Kobayashi, Y., & Ohnishi, T. (2007). *Vanguards of Paradigm Shift in Radiation Biology: Radiation-Induced Adaptive and Bystander Responses*. *Journal of Radiation Research*, 48, 97–106.

Mattson, M. P., & Chan, S. L. (2003). Calcium orchestrates apoptosis. *Nature cell biology*, 5, 1041–3.

Mhawech, P. (2005). 14-3-3 Proteins--an Update. *Cell research*, 15, 228–36.

Micallef, L., Belaubre, F., Pinon, A., Jayat-Vignoles, C., Delage, C., Charveron, M., & Simon, A. (2009). Effects of extracellular calcium on the growth-differentiation switch in immortalized keratinocyte HaCaT cells compared with normal human keratinocytes. *Experimental Dermatology*, 18(2), 143–51.

Mitchell, S. a., Marino, S. a., Brenner, D. J., & Hall, E. J. (2004). Bystander effect and adaptive response in C3H 10T½ cells. *International Journal of Radiation Biology*, 80, 465–472.

- Montour, J. L. (1971). Abscopal radiation damage to chick thymus and bursa of Fabricius. *Acta radiologica: therapy, physics, biology*, 10, 150–60.
- Morgan, W. F. (2003). Non-targeted and Delayed Effects of Exposure to Ionizing Radiation : I . Radiation-Induced Genomic Instability and Bystander Effects In Vitro. *Radiation Research*, 159, 223–236.
- Morgan, W. F. (2012). Non-targeted and Delayed Effects of Exposure to Ionizing Radiation : I . Radiation-Induced Genomic Instability and Bystander Effects In Vitro. *Radiation Research*, 236, 223–236.
- Morgan, W. F., & Sowa, M. B. (2007). Non-targeted bystander effects induced by ionizing radiation. *Mutation research*, 616, 159–64.
- Mosmann, T. (1983). Rapid colorimetric assay for cellular growth and survival: application to proliferation and cytotoxicity assays. *Journal of immunological methods*, 65, 55–63.
- Mothersill, C. (1998). Development of Primary Tissue Culture Techniques for Use in Radiobiology. *Radiation Research*, 150, 121–125.
- Mothersill, C. E., & Seymour, C. B. (1997). Medium from irradiated human epithelial cells but not human fibroblasts reduces the clonogenic survival of unirradiated cells. 71.
- Mothersill, C. E., & Seymour, C. B. (1997a). Medium from irradiated human epithelial cells but not human fibroblasts reduces the clonogenic survival of unirradiated cells. 71.



- Mothersill, C. E., Malley, K. J. O., Murphy, D. M., Seymour, C. B., Lorimore, S. A., et al. (1999). Identification and characterization of three subtypes of radiation response in normal human urothelial cultures exposed to ionizing radiation variation in human responses to radiation exposure , exposure to a range of doses of  $^{60}\text{Co}$  . *Carcinogenesis*, 20, 2273–2278.
- Mothersill, C., & Seymour, C. (1997). Medium from irradiated human epithelial cells but not human fibroblasts reduces the clonogenic survival of unirradiated cells. *International Journal of Radiation Biology*, 71, 421–427.
- Mothersill, C., & Seymour, C. (1997). Survival of human epithelial cells irradiated with cobalt 60 as microcolonies or single cells. *International journal of radiation biology*, 72, 597–606.
- Mothersill, C., & Seymour, C. (1997b). Medium from irradiated human epithelial cells but not human fibroblasts reduces the clonogenic survival of unirradiated cells. *International Journal of Radiation Biology*, 71, 421–427.
- Mothersill, C., & Seymour, C. (2009). Communication of ionising radiation signals--a tale of two fish. *International journal of radiation biology*, 85, 909–19.
- Mothersill, C., & Seymour, C. (2012). Changing paradigms in radiobiology. *Mutation research. Reviews in mutation research*, 750, 85–95.
- Mothersill, C., & Seymour, C. B. (1998). Cell-Cell Contact during Gamma Irradiation Is Not Required to Induce a Bystander Effect in Normal Human Keratinocytes: Evidence for Release during Irradiation of a Signal Controlling Survival into the Medium. *Radiation Research*, 149, 256–262.

- Mothersill, C., & Seymour, C. B. (2002). Bystander and delayed effects after fractionated radiation exposure. *Radiation research*, 158, 626–33.
- Mothersill, C., & Seymour, C. B. (2004). Radiation-induced bystander effects--implications for cancer. *Nature reviews. Cancer*, 4, 158–64.
- Mothersill, C., Bristow, R. G., Harding, S. M., Smith, R. W., Mersov, A., et al. (2011). A role for p53 in the response of bystander cells to receipt of medium borne signals from irradiated cells. *International journal of radiation biology*, 87, 1120–5.
- Mothersill, C., Bucking, C., Smith, R. W., Agnihotri, N., Oneill, a, et al. (2006). Communication of radiation-induced stress or bystander signals between fish in vivo. *Environmental science & technology*, 40, 6859–64.
- Mothersill, C., Cusack, a, MacDonnell, M., Hennessy, T. P., & Seymour, C. B. (1988). Differential response of normal and tumour oesophageal explant cultures to radiation. *Acta oncologica (Stockholm, Sweden)*, 27, 275–80.
- Mothersill, C., Lyng, F., Seymour, C., Maguire, P., & Wright, E. (2005). Genetic Factors Influencing Bystander Signaling in Murine Bladder Epithelium after Low-Dose Irradiation In Vivo. *Radiation Research*, 399, 391–399.
- Mothersill, C., O'Brien, a, & Seymour, C. B. (1990). The effect of radiation in combination with carcinogens on the growth of normal urothelium in explant culture. *Radiation and environmental biophysics*, 29, 213–23.
- Mothersill, C., Rea, D., Wright, E. G., Lorimore, S. A., Murphy, D., et al. (2001). Individual variation in the production of a “ bystander signal ” following

irradiation of primary cultures of normal human urothelium. *Carcinogenesis*, 22, 1465–1471.

Mothersill, C., Saroya, R., Smith, R. W., Singh, H., & Seymour, C. B. (2010). Serum serotonin levels determine the magnitude and type of bystander effects in medium transfer experiments. *Radiation research*, 174, 119–23.

Mothersill, C., Seymour, C. B., & Joiner, M. C. (2002). Relationship between radiation-induced low-dose hypersensitivity and the bystander effect. *Radiation research*, 157, 526–32.

Mothersill, C., Seymour, R. J., & Seymour, C. B. (2004). Bystander effects in repair-deficient cell lines. *Radiation research*, 161, 256–63.

Mothersill, C., Smith, R. W., Hinton, T. G., Aizawa, K., & Seymour, C. B. (2009). Communication of radiation-induced signals in vivo between DNA repair deficient and proficient medaka (*Oryzias latipes*). *Environmental science & technology*, 43, 3335–42.

Mothersill, C., Smith, R. W., Saroya, R., Denbeigh, J., Rowe, B., et al. (2010). Irradiation of rainbow trout at early life stages results in legacy effects in adults. *International journal of radiation biology*, 86, 817–28.

Mothersill, C., Smith, R., Agnihotri, N., & Seymour, C. (2007). Characterization of a Radiation-Induced Stress Response Communicated in Vivo between Zebrafish. *Environ. Sci. Technol*, 41, 3382–3387.

- Mothersill, C., Stamato, T. D., Perez, M. L., Cummins, R., Mooney, R., et al. (2000). Involvement of energy metabolism in the production of “bystander effects” by radiation. *British journal of cancer*, 82, 1740–6.
- Muller, H. J. (1930). Radiation and Genetics. *The American Society of Naturalists*, 64, 220–251.
- Muñoz-Pinedo, C. (2012). Signaling pathways that regulate life and cell death: evolution of apoptosis in the context of self-defense. In *Self and Nonself* (pp. 124–143).
- Muroya, Y., Plante, I., Azzam, E. I., Meesungnoen, J., Jay-gerin, J., et al. (2006). High-LET Ion Radiolysis of Water : Visualization of the Formation and Evolution of Ion Tracks and Relevance to the Radiation-Induced Bystander Effect. *Radiation Research*, 491, 485–491.
- Murphy, J. B., & Norton, J. J. (1915). The Effect of X-Ray on the Resistance To Cancer in Mice. *Science (New York, N.Y.)*, 42, 842–3.
- Nagasawa, H., & Little, J. B. (1992). Induction of sister chromatid exchanges by extremely low doses of alpha-particles. *Cancer Research*, 52, 6394–6396.
- Nagasawa, H., & Little, J. B. (1992a). Induction of sister chromatid exchanges by extremely low doses of alpha-particles. *Cancer Research*, 52, 6394–6396.
- Nagasawa, H., & Little, J. B. (1992b). Induction of Sister Chromatid Exchanges by Extremely Low Doses of  $\alpha$  -Particles. *Cancer Research*, 6394–6396.

- Nakajima, T., Shimooka, H., Weixa, P., Segawa, A., Motegi, A., et al. (2003). Immunohistochemical demonstration of 14-3-3 sigma protein in normal human tissues and lung cancers, and the preponderance of its strong expression in epithelial cells of squamous cell lineage. *Pathology international*, 53, 353–60.
- Narayanan, P. K., Goodwin, E. H., Lehnert, B. E., & Goodwin Lehnert. (1997). Alpha particles initiate biological production of superoxide anions and hydrogen peroxide in human cells. *Cancer research*, 57, 3963–71.
- Narayanan, P. K., LaRue, K. E. A., Goodwin, E. H., & Lehnert, B. E. (1999). Alpha Particles Induce the Production of Interleukin-8 by Human Cells. *Radiation Research*, 152, 57–63.
- Nitta, M., Kobayashi, O., Honda, S., Hirota, T., Kuninaka, S., et al. (2004). Spindle checkpoint function is required for mitotic catastrophe induced by DNA-damaging agents. *Oncogene*, 23, 6548–58.
- Nobler, M. P. (1969). The Abscopal Effect in Malignant Lymphoma and Its Relationship to Lymphocyte Circulation<sup>1</sup>. *Radiology*, 410–412.
- O'Brien, J., Wilson, I., Orton, T., & Pognan, F. (2000). Investigation of the Alamar Blue (resazurin) fluorescent dye for the assessment of mammalian cell cytotoxicity. *European journal of biochemistry / FEBS*, 267, 5421–6.
- O'Dowd, C., Mothersill, C. E., Cairns, M. T., Austin, B., McClean, B., et al. (2006). The release of bystander factor(s) from tissue explant cultures of rainbow

trout (*Onchorhynchus mykiss*) after exposure to gamma radiation. *Radiation research*, 166, 611–7.

O'Neill-Mehlenbacher, A., Kilemade, M., Elliott, A., Mothersill, C., & Seymour, C. (2007). Comparison of direct and bystander effects induced by ionizing radiation in eight fish cell lines. *International journal of radiation biology*, 83, 593–602.

Oberst, A., Bender, C., & Green, D. R. (2008). Living with death: the evolution of the mitochondrial pathway of apoptosis. *Cell death and differentiation*, 15, 1139–1146.

Ohnishi, H., Nakahara, T., Furuse, K., Sasaki, H., Tsukita, S., et al. (2004). JACOP, a novel plaque protein localizing at the apical junctional complex with sequence similarity to cingulin. *The Journal of biological chemistry*, 279, 46014–22.

Olive, P. L. (1998). The Role of DNA Single- and Double-Strand Breaks in Cell Killing by Ionizing Radiation. *Radiation Research*, 150, 42–51.

Oliver, L., & Vallette, F. M. (2005). The role of caspases in cell death and differentiation. *Drug resistance updates: reviews and commentaries in antimicrobial and anticancer chemotherapy*, 8, 163–70.

Olwill, S. A., McGlynn, H., Gilmore, W. S., & Alexander, H. D. (2005). Annexin II cell surface and mRNA expression in human acute myeloid leukaemia cell lines. *Thrombosis research*, 115, 109–14.

- Orrenius, S., Zhivotovsky, B., & Nicotera, P. (2003). Regulation of cell death: the calcium-apoptosis link. *Nature reviews. Molecular cell biology*, 4, 552–65.
- Paglin, S., Hollister, T., Delohery, T., Hackett, N., McMahon, M., et al. (2001). A Novel Response of Cancer Cells to Radiation Involves Autophagy and Formation of Acidic Vesicles Advances in Brief A Novel Response of Cancer Cells to Radiation Involves Autophagy and Formation of Acidic Vesicles 1. *Electrophoresis*, 439–444.
- Pant, G. S., & Kamada, N. (1977). Chromosome aberrations in normal leukocytes induced by the plasma of exposed individuals. *Hiroshima journal of medical sciences*, 26, 149–54.
- Papp, H., Czifra, G., Bodó, E., Lázár, J., Kovács, I., et al. (2004). Opposite roles of protein kinase C isoforms in proliferation, differentiation, apoptosis, and tumorigenicity of human HaCaT keratinocytes. *Cellular and molecular life sciences : CMLS*, 61, 1095–105
- Parsons, W. B., Watkins, C. ., Pease, G. ., & Donalds, C. (1954). Changes in sternal bone marrow following roentgen-ray therapy to the spleen in chronic granulocytic leukaemia. *Cancer*.
- Pfaffl, M. W. (2001). A new mathematical model for relative quantification in real-time RT-PCR. *Nucleic Acids Research*, 29, e45.
- Poon, R. C. C., Agnihotri, N., Seymour, C., & Mothersill, C. (2007). Bystander effects of ionizing radiation can be modulated by signaling amines. *Environmental research*, 105, 200–11.

- Portess, D. I., Bauer, G., Hill, M. a, & O'Neill, P. (2007). Low-dose irradiation of nontransformed cells stimulates the selective removal of precancerous cells via intercellular induction of apoptosis. *Cancer research*, 67, 1246–53.
- Pradelli, L. a, Bénétteau, M., & Ricci, J.-E. (2010). Mitochondrial control of caspase-dependent and -independent cell death. *Cellular and molecular life sciences : CMLS*, 67, 1589–97.
- Prise, K. M., & O'Sullivan, J. M. (2009). Radiation-induced bystander signalling in cancer therapy. *Nature reviews. Cancer*, 9, 351–60.
- Prise, K. M., Belyakov, O. V., FOLKARD, M., & Michael, B. D. (1998). Studies of bystander effects in human fibroblasts using a charged particle microbeam. *International Journal of Radiation Biology*, 74, 793–798.
- Prise, K. M., Burdak-Rothkamm, S., Folkard, M., Kashino, G., Shao, C., et al. (2007). New insights on radiation-induced bystander signalling and its relationship to DNA repair. *International Congress Series*, 1299, 121–127.
- Prise, K. M., Folkard, M., & Michael, B. D. (2003). A review of the bystander effect and its implications for low-dose exposure. *Radiation protection dosimetry*, 104, 347–355.
- Prise, K. M., Schettino, G., Folkard, M., & Held, K. D. (2005). New insights on cell death from radiation exposure. *The lancet oncology*, 6, 520–8.
- Przybyszewski, W. M., Widel, M., Szurko, A., Lubecka, B., Matulewicz, L., et al. (2004). Multiple bystander effect of irradiated megacolonies of melanoma cells on non-irradiated neighbours. *Cancer letters*, 214, 91–102.



- Puck, T., & Marcus, P. (1956). Action of X-rays on Mammalian Cells. *Journal of Experimental Medicine*, 103, 653–666.
- Qian, L., Shen, J., Chuai, Y., & Cai, J. (2013). Hydrogen as a New Class of Radioprotective Agent. *International journal of biological sciences*, 9, 887–894.
- Radiological Protection Institute of Ireland. (2012). Annual Report & Accounts 2012 “To ensure that people in Ireland are protected from the harmful effects of radiation”.
- Rashi-Elkeles, S., Elkon, R., Shavit, S., Lerenthal, Y., Linhart, C., et al. (2011). Transcriptional modulation induced by ionizing radiation: p53 remains a central player. *Molecular oncology*, 5, 336–48.
- Rastogi, S., Boylan, M., Wright, E. G., & Coates, P. J. (2013). Interactions of apoptotic cells with macrophages in radiation-induced bystander signaling. *Radiation research*, 179, 135–45.
- Reed, J. C. (1998). Bcl-2 family proteins. *Oncogene*, 17, 3225–36.
- Rodriguez, J., & Lazebnik, Y. (1999). Caspase-9 and APAF-1 form an active holoenzyme. *Genes & development*, 13, 3179–84.
- Ryan, L. a, Seymour, C. B., Joiner, M. C., & Mothersill, C. E. (2009). Radiation-induced adaptive response is not seen in cell lines showing a bystander effect but is seen in lines showing HRS/IRR response. *International journal of radiation biology*, 85, 87–95.

- Ryan, L. a, Smith, R. W., Seymour, C. B., & Mothersill, C. E. (2008). Dilution of irradiated cell conditioned medium and the bystander effect. *Radiation research*, 169, 188–96.
- Rzeszowska-Wolny, J., Herok, R., Widel, M., & Hancock, R. (2009). X-irradiation and bystander effects induce similar changes of transcript profiles in most functional pathways in human melanoma cells. *DNA repair*, 8, 732–8.
- Saroya, R., Smith, R., Seymour, C., & Mothersill, C. (2009). Injection of reserpine into zebrafish, prevents fish to fish communication of radiation-induced bystander signals: confirmation in vivo of a role for serotonin in the mechanism. *Dose-response: a publication of International Hormesis Society*, 8, 317–30.
- Sawant, S. G., Randers-Pehrson, G., Metting, N. F., & Hall, E. J. (2001). Adaptive response and the bystander effect induced by radiation in C3H 10T(1/2) cells in culture. *Radiation research*, 156, 177–80.
- Schmittgen, T. D., & Livak, K. J. (2008). Analyzing real-time PCR data by the comparative C(T) method. *Nature protocols*, 3, 1101–8.
- Scott, D. (1969). The Effect of Irradiated Plasma on Normal Human Chromosomes and Its Relevance to the Long-Lived Lymphocyte Hypothesis. *Cell Proliferation*, 2, 295–305.
- Seabra, M. C., & Wasmeier, C. (2004). Controlling the location and activation of Rab GTPases. *Current opinion in cell biology*, 16, 451–7.

- Seltzer, S. M. (2011). ICRU Report No. 85: Fundamental Quantities and Units for Ionizing Radiation. *Journal of the ICRU*, 11.
- Seroz, T. (2000). Cloning of a human homolog of the yeast nucleotide excision repair gene MMS19 and interaction with transcription repair factor TFIIH via the XPB and XPD helicases. *Nucleic Acids Research*, 28, 4506–4513.
- Seymour, C. B., & Mothersill, C. (2000). Relative contribution of bystander and targeted cell killing to the low-dose region of the radiation dose-response curve. *Radiation research*, 153, 508–11.
- Seymour, C. B., Mothersill, C., & Alper, T. (1986). High yields of lethal mutations in somatic mammalian cells that survive ionizing radiation. *International journal of radiation biology and related studies in physics, chemistry, and medicine*, 50, 167–79.
- Shao, C., Aoki, M., & Furusawa, Y. (2003). Bystander effect on cell growth stimulation in neoplastic HSGc cells induced by heavy-ion irradiation. *Radiation and environmental biophysics*, 42, 183–7.
- Shao, C., Folkard, M., & Prise, K. M. (2008). Role of TGF-  $\beta$  1 and nitric oxide in the bystander response of irradiated glioma cells. *Oncogene*, 27, 434–440.
- Shao, C., Lyng, F. M., Folkard, M., & Prise, K. M. (2006). Calcium fluxes modulate the radiation-induced bystander responses in targeted glioma and fibroblast cells. *Radiation research*, 166, 479–87.

- Shao, C., Stewart, V., Folkard, M., Michael, B. D., & Prise, K. M. (2003). Nitric oxide-mediated signaling in the bystander response of individually targeted glioma cells. *Cancer Research*, 63, 8437–8442.
- Singh, P. (2007). Role of Annexin-II in GI cancers: Interaction with Gastrins/Progastrins. *Cancer Letters*, 252, 19–35.
- Sitailo, L. a, Tibudan, S. S., & Denning, M. F. (2002). Activation of caspase-9 is required for UV-induced apoptosis of human keratinocytes. *The Journal of biological chemistry*, 277, 19346–52.
- Slee, E. a, Adrain, C., & Martin, S. J. (2001). Executioner caspase-3, -6, and -7 perform distinct, non-redundant roles during the demolition phase of apoptosis. *The Journal of biological chemistry*, 276, 7320–6.
- Smith, R. W., Wang, J., Bucking, C. P., Mothersill, C. E., & Seymour, C. B. (2007). Evidence for a protective response by the gill proteome of rainbow trout exposed to X-ray induced bystander signals. *Proteomics*, 7, 4171–80.
- Smith, R. W., Wang, J., Mothersill, C. E., Hinton, T. G., Aizawa, K., et al. (2011). Proteomic changes in the gills of wild-type and transgenic radiosensitive medaka following exposure to direct irradiation and to X-ray induced bystander signals. *Biochimica et biophysica acta*, 1814, 290–8.
- Smith, R. W., Wood, C. M., Cash, P., Diao, L., & Prt, P. (2005). Apolipoprotein AI could be a significant determinant of epithelial integrity in rainbow trout gill cell cultures : A study in functional proteomics. *Biochimica et biophysica acta*, 1749, 81–93.

- Souto, J. (1962). Tumour Development in the Rat Induced by Blood of Irradiated Animals. *Nature*, 195, 1317–1318.
- Sowa, M. B., Goetz, W., Baulch, J. E., Pyles, D. N., Dziegielewski, J., et al. (2010). Lack of evidence for low-LET radiation induced bystander response in normal human fibroblasts and colon carcinoma cells. *International journal of radiation biology*, 86, 102–113.
- Sugihara, T., Murano, H., Nakamura, M., & Tanaka, K. (2013). In Vivo Partial Bystander Study in a Mouse Model by Chronic Medium-Dose-Rate  $\gamma$ -Ray Irradiation. *Radiation research*, 179, 221–231.
- Surinov, B. P., Isaeva, V. G., & Tokarev, O. (2001). Allelopathic activity of volatile secretions in irradiated animals. *Radiats Biol Radioecol*, 41, 645–649.
- Suzuki, M., Youle, R. J., & Tjandra, N. (2000). Structure of Bax: coregulation of dimer formation and intracellular localization. *Cell*, 103, 645–654.
- Taghiyev, A. F., Rokhlin, O. W., & Glover, R. B. (2011). Caspase-2-Based Regulation of the Androgen Receptor and Cell Cycle in the Prostate Cancer Cell Line LNCaP. *Genes & cancer*, 2, 745–752.
- Tait, S. W. G., & Green, D. R. (2010). Mitochondria and cell death: outer membrane permeabilization and beyond. *Nature reviews. Molecular cell biology*, 11, 621–632.
- Taylor, R. C., Cullen, S. P., & Martin, S. J. (2008). Apoptosis: controlled demolition at the cellular level. *Nature reviews. Molecular cell biology*, 9, 231–241.

- Theodorescu, D., Sapinoso, L. M., Conaway, M. R., Oxford, G., & Hampton, G. M. (2004). Reduced Expression of Metastasis Suppressor RhoGDI2 Is Associated with Decreased Survival for Patients with Bladder Cancer. *Clinical Cancer Research*, 10, 3800–3806.
- Tinel, A., & Tschopp, J. (2004). The PIDDosome, a protein complex implicated in activation of caspase-2 in response to genotoxic stress. *Science*, 304, 843–846.
- Vakifahmetoglu, H., Olsson, M., & Zhivotovsky, B. (2008). Death through a tragedy: mitotic catastrophe. *Cell death and differentiation*, 15, 1153–62.
- Vakifahmetoglu-Norberg, H., & Zhivotovsky, B. (2010). The unpredictable caspase-2: what can it do? *Trends in cell biology*, 20, 150–9.
- Van der Vaart, B., Manatschal, C., Grigoriev, I., Olieric, V., Gouveia, S. M., et al. (2011). SLAIN2 links microtubule plus end-tracking proteins and controls microtubule growth in interphase. *The Journal of cell biology*, 193, 1083–99.
- Vandenabeele, P., Galluzzi, L., Vanden Berghe, T., & Kroemer, G. (2010). Molecular mechanisms of necroptosis: an ordered cellular explosion. *Nature reviews. Molecular cell biology*, 11, 700–14.
- Vines, a M., Lyng, F. M., McClean, B., Seymour, C., & Mothersill, C. E. (2009). Bystander effect induced changes in apoptosis related proteins and terminal differentiation in in vitro murine bladder cultures. *International journal of radiation biology*, 85, 48–56.

- Vines, A. M., Lyng, F. M., McClean, B., Seymour, C., & Mothersill, C. E. (2008). Bystander signal production and response are independent processes which are cell line dependent. *International journal of radiation biology*, 84, 83–90.
- Vitale, I., Galluzzi, L., Castedo, M., & Kroemer, G. (2011). Mitotic catastrophe: a mechanism for avoiding genomic instability. *Nature reviews. Molecular cell biology*, 12, 385–92.
- Vujosevic, B., & Bokorov, B. (2010). Radiotherapy: Past and present. *Archive of oncology*, 18, 140–142.
- Waters, K. M., Stenoiien, D. L., Sowa, M. B., von Neubeck, C., Chrisler, W. B., et al. (2013). Annexin A2 modulates radiation-sensitive transcriptional programming and cell fate. *Radiation research*, 179, 53–61.
- Weber, T. J., Opresko, L. K., Waisman, D. M., Newton, G. J., Quesenberry, R. D., et al. (2009). Regulation of the low-dose radiation paracrine-specific anchorage-independent growth response by annexin A2. *Radiation research*, 172, 96–105.
- Weber, T. J., Siegel, R. W., Markillie, L. M., Chrisler, W. B., Lei, X. C., et al. (2005). A paracrine signal mediates the cell transformation response to low dose gamma radiation in JB6 cells. *Molecular carcinogenesis*, 43, 31–7.
- Wei, M. C., Zong, W. X., Cheng, E. H., Lindsten, T., Panoutsakopoulou, V., et al. (2001). Proapoptotic BAX and BAK: a requisite gateway to mitochondrial dysfunction and death. *Science (New York, N.Y.)*, 292, 727–30.
- Whiting, P. W. (1929). X-rays and parasitic wasps. *J. Hered.*, 20, 269–276.

- Wilson, V. G. (2014). Growth and Differentiation of HaCaT Keratinocytes. *Methods in molecular biology* (Clifton, N.J.), 1195, 33–41.
- Wilson, M. R., Close, T. W., & Trosko, J. E. (2000). Cell population dynamics (apoptosis, mitosis, and cell-cell communication) during disruption of homeostasis. *Experimental cell research*, 254, 257–68.
- Wright, E. G. (2010). Manifestations and mechanisms of non-targeted effects of ionizing radiation. *Mutation research*, 687, 28–33.
- Xue, L. Y., Butler, N. J., Makrigiorgos, G. M., Adelstein, S. J., & Kassis, A. I. (2002). Bystander effect produced by radiolabeled tumor cells in vivo. *Proceedings of the National Academy of Sciences of the United States of America*, 99, 13765–70.
- Zhang, B. (2006). Rho GDP dissociation inhibitors as potential targets for anticancer treatment. *Drug resistance updates: reviews and commentaries in antimicrobial and anticancer chemotherapy*, 9, 134–41.
- Zhang, K., & Kaufman, R. J. (2008). From endoplasmic-reticulum stress to the inflammatory response. *Nature*, 454, 455–462.
- Zheng, T. S., Hunot, S., Kuida, K., Momoi, T., Srinivasan, A., et al. (2000). Deficiency in caspase-9 or caspase-3 induces compensatory caspase activation. *Nature medicine*, 6, 1241–7.
- Zhou, H., Ivanov, V. N., Gillespie, J., Geard, C. R., Amundson, S. A., et al. (2005). Mechanism of radiation-induced bystander effect: role of the



cyclooxygenase-2 signaling pathway. *Proceedings of the National Academy of Sciences of the United States of America*, 102, 14641–6.

Zhou, H., Suzuki, M., Geard, C. R., & Hei, T. K. (2002). Effects of irradiated medium with or without cells on bystander cell responses. *Mutation research*, 499, 135–41.

Zirkle, R. E., & Bloom, W. (1953). Irradiation of Parts of Individual Cells. *Science*, 117, 487–493.

